



UNIVERSIDADE ESTADUAL DE CAMPINAS

FACULDADE DE ENGENHARIA DE ALIMENTOS

**RICARDO ABEL DEL CASTILLO TORRES**

**IMPLEMENTATION OF A PSEUDOCONTINUOUS PROCESS OF  
SUPERCritical FLUID FRACTIONATION WITH SUBSEQUENT  
PURIFICATION AND RECYCLING OF SOLVENT IN PILOT SCALE**

***IMPLEMENTAÇÃO DE UM PROCESSO PSEUDOCONTÍNUO DE  
FRACIONAMENTO COM FLUIDO SUPERCRÍTICO COM SUBSEQUENTE  
PURIFICAÇÃO E RECICLO EM ESCALA PILOTO***

CAMPINAS

2019

**RICARDO ABEL DEL CASTILLO TORRES**

**IMPLEMENTATION OF A PSEUDOCONTINUOUS PROCESS OF  
SUPERCritical FLUID FRACTIONATION WITH SUBSEQUENT  
PURIFICATION AND RECYCLING OF SOLVENT IN PILOT SCALE**

***IMPLEMENTAÇÃO DE UM PROCESSO PSEUDOCONTÍNUO DE  
FRACIONAMENTO COM FLUIDO SUPERCRÍTICO COM SUBSEQUENTE  
PURIFICAÇÃO E RECICLO EM ESCALA PILOTO***

Thesis presented to the School of Food Engineering from University of Campinas in partial fulfillment of the requirements for the degree of Doctor in Food Engineering.

Tese de doutorado apresentada à Faculdade de Engenharia de Alimentos da Universidade Estadual de Campinas como parte dos requisitos exigidos para a obtenção do título de Doutor em Engenharia de Alimentos.

*Supervisor/Orientadora:* Prof<sup>a</sup>. Dr<sup>a</sup>. Maria Angela de Almeida Meireles Petenate

ESTE EXEMPLAR CORRESPONDE À VERSÃO FINAL DE TESE DEFENDIDA PELO ALUNO RICARDO ABEL DEL CASTILLO TORRES, E ORIENTADO PELA PROF<sup>a</sup>. DR<sup>a</sup>. MARIA ANGELA DE ALMEIDA MEIRELES PETENATE

CAMPINAS

2019

Ficha catalográfica  
Universidade Estadual de Campinas  
Biblioteca da Faculdade de Engenharia de Alimentos  
Claudia Aparecida Romano - CRB 8/5816

C278i Castillo Torres, Ricardo Abel del, 1974-  
Implementation of a pseudocontinuous process of supercritical fluid fractionation with subsequent purification and recycling of solvent in pilot scale / Ricardo Abel del Castillo Torres. – Campinas, SP : [s.n.], 2019.

Orientador: Maria Angela de Almeida Meireles Petenate.  
Tese (doutorado) – Universidade Estadual de Campinas, Faculdade de Engenharia de Alimentos.

1. Urucum. 2. Curcuma. 3. Adsorção. 4. Farelo de aveia. 5. Extração com fluido supercrítico. I. Petenate, Maria Angela de Almeida Meireles. II. Universidade Estadual de Campinas. Faculdade de Engenharia de Alimentos. III. Título.

Informações para Biblioteca Digital

**Título em outro idioma:** Implementação de um processo pseudocontínuo de fracionamento com fluido supercrítico com subsequente purificação e reciclo em escala piloto

**Palavras-chave em inglês:**

Annatto  
Turmeric  
Adsorption  
Oat bran  
Supercritical fluid extraction

**Área de concentração:** Engenharia de Alimentos

**Titulação:** Doutor em Engenharia de Alimentos

**Banca examinadora:**

Maria Angela de Almeida Meireles Petenate [Orientador]  
Fernando Antonio Cabral  
Maria Teresa Pedrosa Silva Clerici  
Maria Thereza de Moraes Gomes Rosa  
Philippe dos Santos

**Data de defesa:** 09-04-2019

**Programa de Pós-Graduação:** Engenharia de Alimentos

**Identificação e informações acadêmicas do(a) aluno(a)**

- ORCID do autor: <https://orcid.org/0000-0001-6911-6392>
- Currículo Lattes do autor: <http://lattes.cnpq.br/5578795665056448>

## **BANCA EXAMINADORA**

Prof<sup>a</sup> Dr<sup>a</sup> Maria Angela de Almeida Meireles Petenate

(ORIENTADORA) DEA/FEA/Unicamp

Prof. Dr. Fernando Antonio Cabral

(MEMBRO) DEA/FEA/Unicamp

Prof<sup>a</sup> Dr<sup>a</sup>. Maria Teresa Pedrosa Silva Clerici

(MEMBRO) DTA/FEA/Unicamp

Prof<sup>a</sup>. Dr<sup>a</sup>. Maria Thereza de Moraes Gomes Rosa

(MEMBRO) Mackenzie

Dr. Philipe dos Santos

(MEMBRO) Rubian Extratos

A Ata da defesa com as respectivas assinaturas dos membros encontra-se no SIGA/Sistema de Fluxo de Dissertação/Tese e na Secretaria do Programa da Unidade.

## **AGRADECIMENTOS**

Graças Deus por ter me conduzido pelo caminho do aprendizado e por haver me trazido até este momento, momento na qual tenho que lembrar de todas as pessoas que de uma e outra forma contribuíram para a conclusão do meu doutorado.

Minha esposa Cecilia leva a minha gratidão infinita pelo convívio diário e que junto com a responsabilidade de ela ser estudante de doutorado na FCM da UNICAMP também é a mãe de nossos três amados filhos Bruce Stefano, Christopher Giovanni e Briana Sophia. Obrigado pelo apoio e a fortaleza que me brindas.

A minha mãe Juanita pelo eterno amor e carinho, quem desde quase um ano pese a ter comprometida a sua saúde com uma neoplasia maligna, mostra-se animada para continuar com as suas atividades diárias e continua dando exemplo de ter um grande espírito de luta e perseverança.

À Professora Maria Angela, pela oportunidade, credibilidade, orientação e conselhos, mais ainda neste duro último ano de doutorado que possibilitaram a realização e culminação da minha tese. Por ter sugerido a parceria com a Ádina no momento certo.

Aos meus amigos Diego, Juliana e Ádina pelas orientações e contribuições no documento da tese. Agradeço muito em especial a Ádina pelo suporte para melhorar a qualidade da minha tese segundo recomendações da banca.

Aos professores e funcionários da Universidade Estadual de Campinas, muito em especial aos integrantes da Faculdade de Engenharia de Alimentos, por disponibilizarem a estrutura necessária para a realização das atividades de pós-graduação, assim como pelos diversos ensinamentos, dentro e fora das salas de aula.

“O presente trabalho foi realizado com apoio da Coordenação de Aperfeiçoamento de Pessoal de Nível Superior - Brasil (CAPES) - Código de Financiamento 001”.

A meu amigo Éder Valdir do LDPC/FEQ

A meu amigo Éder Valdir do LDPC/FEQ e aos amigos e colegas do LASEFI, Pedro, Julio, Tahmas, Graziele, Eric, Renata, Gislaine, Isabel e Monique pelo ânimo, disponibilidade e os bons momentos de trabalho no laboratório. Agradeço muito em especial ao meu amigo Pedro por me compartilhar o seu conhecimento e a sua experiência na área da Tecnologia Supercrítica durante os incontáveis momentos de troca de ideias durante a execução do trabalho e fora dele. O meu amigo Julio, merece também um agradecimento especial por se disponibilizar para a impressão do boneco e encaminhamento à secretaria da pós-graduação da minha tese enquanto eu estava dando atenção à saúde da minha mãe.

Gostaria de expressar minha profunda gratidão aos integrantes da banca que contribuíram para melhorar a qualidade do trabalho.

Ao Ariovaldo Astini, técnico do LASEFI, pela disponibilidade, auxílio e amizade.

A meus amigos Fernando e Antonio da Universidade Nacional da Amazônia Peruana pela confiança, amizade e orientações.

Aos amigos e colegas da pós-graduação do DEA/FEA/UNICAMP, Rúbner, Daniel, Manuel, Renata, Juliane, José, Paulo e Ariel pelos gratos momentos.

Aos membros do Departamento de Engenharia de Alimentos da Faculdade de Indústrias de Alimentos da Universidade Nacional da Amazônia Peruana pela aprovação da minha permissão para a realização de meu doutorado.

A minha sogra Marthita pelo carinho, conselhos e pelo suporte por me representar frente aos diversos escritórios no Peru.

Aos meus irmãos Homero, Winston, Rosário e Rosa pelo carinho e amor sem limites.

## RESUMO

Alguns dos aspectos de tecnologias sustentáveis constam na obtenção de produtos variados dotados de valor agregado, associada à redução do número de etapas de processamento, bem como de rejeitos ambientais. A utilização dessas técnicas vem ganhando força na indústria e na comunidade científica. Neste trabalho o foco principal foi dado ao processo de extração com fluido supercrítico (SFE) de matrizes vegetais, combinada com subsequente fracionamento, por ser uma forma versátil de se conseguir produtos variados de alta qualidade, por conta da redução do número de etapas de processamento. A primeira parte experimental desta tese consistiu na validação do sistema de recirculação de CO<sub>2</sub>. Para tal, foram comparados rendimentos de extrações aplicadas às sementes inteiras de urucum (material modelo), realizadas em equipamentos em escala de bancada e em escala piloto. No equipamento em escala de bancada foi realizada apenas SFE das sementes com o objetivo de se atingir valores máximos de razão solvente/alimentação (S/F), pois em escala de bancada a quantidade de CO<sub>2</sub> gasta e liberada ao ambiente é mínima, enquanto que máximos valores de S/F atingidos em escala piloto resultariam em grandes quantidades de CO<sub>2</sub> que seriam liberadas ao ambiente, considerando-se ausência de reciclo. Enquanto que no equipamento em escala piloto foram realizadas SFE combinada com fracionamento dos extratos em três vasos de separação e uma coluna empacotada com algodão ou celite® para adsorção em condições subcríticas. A segunda parte experimental da tese consistiu na validação da SFE em modo pseudocontínuo representada pela reprodução de 4 ciclos de extração por processo em escala piloto, a partir de duas matérias-primas modelo (urucum e cúrcuma). Visando a otimização do processo de extração+fracionamento, a adição de um adsorvente natural (farelo de aveia) foi vista como uma opção atrativa para purificação do CO<sub>2</sub>. Para tal, novamente a unidade em escala de bancada foi utilizada para avaliar os efeitos da vazão do solvente CO<sub>2</sub> sobre a adsorção dos extratos de urucum no farelo de aveia, partindo de uma coluna de extração SFE de  $25 \times 10^{-3}$ L, seguida de um vaso de separação de extratos e de uma coluna de adsorção, ambas de  $5 \times 10^{-3}$ L. A partir dos resultados de adsorção em escala de bancada, o sistema de purificação e reciclo do CO<sub>2</sub> (Purification and Recycling System of CO<sub>2</sub> – PRSCO<sub>2</sub>) foi aplicado para o urucum em uma unidade em escala piloto (UP) com coluna de extração de 5 L, três vasos de separação de extratos de 1 L e duas colunas de adsorção de 0.65 L (AdC1) e 0.40 L (AdC2), com aproximadamente 2.8 kg de CO<sub>2</sub> sendo continuamente purificado e reciclado em condições subcríticas. Através da reprodução deste processo, partindo do uso de uma segunda matéria prima (cúrcuma) o processamento pseudocontínuo a escala piloto foi validado. Com isso, além

de se obter extratos separados segundo a sua composição dentro dos três vasos de separação e obter a matriz vegetal sem extratos alvos em C1 e C2 após o processamento, foram obtidos mais dois tipos de subprodutos por cada matéria-prima, que se trata do farelo de aveia enriquecido. Assim, da AdC1 se obteve o primeiro subproduto enriquecido, para isso o extrato que não precipitou no terceiro vaso de separação a 6.5 MPa foi adsorvido na AdC1 a 5.5 MPa permitindo a purificação do CO<sub>2</sub> em condições subcríticas em quanto imediatamente prossegue com a recirculação. O segundo subproduto enriquecido se obteve a partir da despressurização da C1 e C2. Para isso, finalizado o tempo de extração dinâmica da C1 o extrato ainda solubilizado no seu interior foi despressurização desde 20 MPa (urucum) ou 25 MPa (cúrcuma) até a pressão ambiente dentro da AdC2, enquanto mais um ciclo inicia seu processamento numa segunda coluna de extração C2 com subsequente adsorção em AdC1. Com isso, foram obtidos o máximo aproveitamento do extrato e a diversificação dos produto dentro da mesma linha de processamento, junto às análises químicas dos extratos e a caraterização do material adsorvente.

## ABSTRACT

Some aspects of emerging technologies consist on the obtaining of value-added products, associated with the decreasing of processing steps and generation of wastes. Recently the use of emerging extraction technologies has increased in industry and in scientific communities. This work focused on the combination of supercritical fluid extraction (SFE) of plant matrices combined with fractionation of extracts. Combination of processes is a versatile alternative for the obtaining of several products with enhanced quality, because of reduction of processing procedures. The first experimental part of this thesis consisted on the validation of a recycling CO<sub>2</sub> system. Comparisons of global yield of extractions applied to whole annatto seeds (standard raw material) were established between the assays performed in bench and pilot scale. In the bench-scale unit only SFE was performed for the obtaining of maximum solvent to feed (S/F) ratios, because in bench-scale unit, the quantity of CO<sub>2</sub> spent and released to the atmosphere is minimal, while the maximum values of S/F reached in pilot-scale would result in huge quantities of CO<sub>2</sub> released to atmosphere, considering a process with absence of recycling system. In the pilot-scale unit SFE was performed combined with fractionation of the extracts in three separation vessels and a column packed with cotton or celite® for adsorption under subcritical conditions. The second experimental part of this thesis consisted on the validation of a pseudocontinuous SFE process represented by the reproduction of 4 extraction cycles per process in pilot scale using two standard raw materials (annatto and turmeric). In order to optimize the extraction + fractionation process, the addition of a natural adsorbent (oat bran) was considered as an attractive option for purification of CO<sub>2</sub>. In this case, again the bench scale unit was used to evaluate the effects of the CO<sub>2</sub> flow on the adsorption of annatto extracts in oat bran, starting from a  $25 \times 10^{-3}$  L SFE column, followed by one separation vessel and one adsorption column, both  $5 \times 10^{-3}$  L. From the adsorption results on bench scale, the Purification and Recycling System of CO<sub>2</sub> (PRSCO<sub>2</sub>) was applied to the annatto in a pilot scale unit (UP) with two 5 L extraction columns, three 1 L extract separation vessels and two adsorption columns of 0.65 L (AdC1) and 0.40 L (AdC2), with approximately 2.8 kg of CO<sub>2</sub> being continuously purified and recycled under subcritical conditions. For the validation of the pseudocontinuous process, its reproduction was performed with the use of a second raw material (turmeric). In this context, in addition to obtaining separate extracts according to their composition within the three separation vessels and obtaining the vegetable matrix without extracts at C1 and C2 after processing, two types of by-products were obtained for each raw material, i.e., oat bran enriched with the adsorbed extracts.

In this way, the first enriched by-product was obtained from the AdC1. The extract that did not precipitate in the third separation vessel (6.5 MPa) was adsorbed on AdC1 at 5.5 MPa, allowing the purification of CO<sub>2</sub> under subcritical conditions, and subsequently the recirculation started. The second enriched by-product was obtained with the depressurization of C1 and C2. For this, after the dynamic extraction time of C1 the extract still solubilized inside C1 was depressurized from 20 MPa (annatto) or 25 MPa (turmeric) to 1 atm, inside the AdC2, while another cycle of extraction begins in a second extraction column C2 with subsequent adsorption in AdC1. In this case, the maximum utilization of the extract and the diversification of the products within the same processing line were obtained, together with the chemical composition of the extracts and of the adsorbent material.

## SUMÁRIO

- CAPÍTULO 1 – <i>Introdução e objetivos</i> .....	15
1 INTRODUÇÃO .....	16
1.1 JUSTIFICATIVA .....	17
2 OBJETIVOS .....	17
2.1 OBJETIVO GERAL .....	17
2.2 OBJETIVOS ESPECÍFICOS .....	17
3 ESTRUTURA DO TRABALHO .....	18
4 REFERÊNCIAS BIBLIOGRÁFICAS .....	23
- CAPÍTULO 2 – <i>Perspectives on the application of supercritical antisolvent fractionation process for the purification of plant extracts: effects of operating parameter and patent survey</i> .....	25
1 INTRODUCTION .....	26
2 SUPERCRITICAL ANTISOLVENT FRACTIONATION (SAF) PROCESS .....	27
2.1 Description of a SAF Unit and Experimental Procedure .....	27
2.2 Effects of saf operating parameters .....	29
3 APPLICATIONS OF SAF FOR THE PURIFICATION OF BIOACTIVE COMPOUNDS ...	32
4 RECENT PATENTS ON BIOACTIVE COMPOUNDS OBTAINING USING SAF .....	33
5 CONCLUSION & FUTURE DEVELOPMENTS .....	34
ACKNOWLEDGEMENTS .....	34
REFERENCES .....	34
- CAPÍTULO 3 – <i>Construction and Validation of an Online Subcritical Adsorption-based Device for Assisting CO<sub>2</sub> Recycling during a Supercritical Fluid Extraction Process</i> .....	36
1 INTRODUCTION .....	37
2 MATERIAL AND METHODS.....	38
2.1 Raw Material Characterization .....	38
2.2 Description of Supercritical Fluid Extraction Units.....	39
2.2.1 SFE Bench-scale Unit .....	39
2.2.2 SFE Pilot scale Unit Description .....	39
2.3 Supercritical Fluid Extraction Experiments .....	40
2.3.1 SFE Bench-scale Unit Experiments.....	40
2.3.2 SFE Pilot-scale Unit Experiments .....	41
2.4 Description of SFE Pilot-scale Modifications.....	42
3 RESULTS AND DISCUSSION.....	44

3.1 Effects of the Ratio of Solvent Mass to Feed Mass on the Extraction Yield Using the SFE Bench-scale Unit .....	44
3.2 Preliminary Tests of the Developed Online Subcritical Adsorption-based Device for Assisting CO <sub>2</sub> Recycling in an SFE Pilot-scale Unit .....	45
3.3 Effects of the Ratio of Solvent Mass to Feed Mass on the Extraction Yield Using the SFE Pilot-scale Unit Coupled with the Online Subcritical Adsorption-based Device .....	47
3.4 Estimated Cost of the Constructed Online Subcritical Adsorption-based Device .....	48
CONCLUSION & FUTURE DEVELOPMENTS .....	49
ACKNOWLEDGEMENTS.....	50
REFERENCES .....	50
<b>- CAPÍTULO 4 – A novel process for CO<sub>2</sub> purification and recycling based on subcritical adsorption in oat bran .....</b>	<b>53</b>
Graphical abstract .....	55
Abstract.....	56
1 INTRODUCTION .....	56
2 MATERIALS AND METHODS .....	58
2.1 RAW MATERIAL.....	58
2.2 EXPERIMENTAL.....	58
2.3 BENCH SCALE UNIT .....	58
2.3.1 Preliminary section: obtainining of overall extraction curves .....	58
2.3.2 Adsorption in bench-scale unit .....	59
2.4 PILOT SCALE UNIT: INTRODUCTION OF PURIFICATION AND RECYCLING SYSTEM CO <sub>2</sub> (PRSCO <sub>2</sub> ) .....	60
2.4.1 Process parameters .....	65
2.4.2 S/F calculation in pilot scale experiments.....	65
2.5 EXTRACTS COMPOSITION.....	66
2.5.1 Annatto.....	66
2.5.2 Turmeric.....	67
2.6 CHARACTERIZATION OF THE ADSORBENT.....	67
2.6.1 Adsorbent (Oat bran) .....	67
2.6.2 Differential scanning calorimetry (DSC) .....	68
2.6.3 X-ray diffraction (XRD) .....	68
2.6.4 Thermogravimetric analysis.....	68
2.6.5 Scanning electron microscopy (SEM) .....	68
2.7 PROCESS MODELING AND SIMULATION DESCRIPTION.....	69
2.7.1 Mass and energy flows using Aspen Plus.....	69
2.7.2 Economic model and economic performance indicators.....	70

<b>3 RESULTS AND DISCUSSION.....</b>	<b>72</b>
<b>3.1 RAW MATERIAL AND ADSORBENT CHARACTERIZATION.....</b>	<b>72</b>
<b>3.2 ADSORPTION IN BENCH SCALE UNIT.....</b>	<b>73</b>
<b>3.3 VALIDATION OF PSEUDOCONTINUOUS PROCESS RECYCLING SYSTEM .....</b>	<b>76</b>
<b>3.4 COMPOSITION OF EXTRACTS.....</b>	<b>80</b>
<b>3.5 ADSORBENT COMPOSITION .....</b>	<b>82</b>
<b>3.5.1 Differential Scanning calorimetry.....</b>	<b>82</b>
<b>3.5.2 X-ray diffraction (XRD) .....</b>	<b>83</b>
<b>3.5.3 Thermogravimetric analysis.....</b>	<b>83</b>
<b>3.5.4 Scanning electron microscopy (SEM) .....</b>	<b>84</b>
<b>3.6 PROCESS EVALUATION USING SIMULATION TOOLS.....</b>	<b>85</b>
<b>4 CONCLUSIONS .....</b>	<b>89</b>
<b>ACKNOWLEDGMENTS .....</b>	<b>89</b>
<b>REFERENCES .....</b>	<b>89</b>
Suplementary material .....	92
<b>- CAPÍTULO 5 – <i>Discussão geral</i> .....</b>	<b>95</b>
<b>DISCUSSÃO GERAL.....</b>	<b>96</b>
<b>- CAPÍTULO 6 – <i>Conclusões gerais e sugestões para trabalhos futuros .....</i></b>	<b>98</b>
<b>CONCLUSÕES GERAIS .....</b>	<b>99</b>
<b>SUGESTÕES PARA TRABALHOS FUTUROS .....</b>	<b>100</b>
<b>Memórias do doutorado .....</b>	<b>101</b>
<b>MEMÓRIAS DO DOUTORADO.....</b>	<b>102</b>
<b>REFERÊNCIAS .....</b>	<b>104</b>
<b>Apêndice .....</b>	<b>117</b>
<b>APÊNDICE A .....</b>	<b>118</b>
A.1 Diâmetro médio para sementes de urucum <i>in natura</i> .....	118
A.2 Estado inicial da UP.....	119
A.3 Estado inicial do sistema de reciclo da UP .....	123
A.4 Dados das cinéticas de extração e determinação do valor médio de $X_0$ .....	125
A.5 Curvas de extração de urucum.....	128
A.6 Características do leito.....	134
<b>APÊNDICE B .....</b>	<b>136</b>
B.1 Massa de CO <sub>2</sub> calculada durante a despressurização do leito com urucum. ....	136
B.2 Massa de CO <sub>2</sub> calculada durante a despressurização dos vasos de fracionamento.....	137
B.3 Massa de CO <sub>2</sub> calculada durante a despressurização do leito com cúrcuma. ....	138

B.4 Orientação para a limpeza das válvulas backpressure. ....	139
B.5 Coluna utilizada durante os testes de adsorção. ....	140
B.6 Diâmetro médio geométrico das partículas de cúrcuma. ....	141
B.7 Diâmetro médio geométrico das partículas de farelo de aveia.....	143
<b>APÊNDICE C</b> .....	145
C.1 Dados da cinética de extração e determinação de $X_0$ da cúrcuma. ....	145
<b>APÊNDICE D</b> .....	146
Procedimentos operacionais de unidade piloto Thar Technologies junto a PRSCO <sub>2</sub> .....	146
D.1 Etapa 1: Pré-extração .....	146
D.2 Etapa 2: Pressurização do tanque pulmão (TP) .....	147
D.3 Etapa 3: Condicionamento das colunas AdC1 e AdC2 .....	151
D.4 Etapa 4: Extração SFE .....	152
D.5 Etapa 5: Procedimento alternativo a partir do passo 19 da D.4 Etapa 4.....	159
D.6. Etapa 6: Limpeza da unidade piloto .....	160
D.7. Etapa 7: Limpeza do tanque pulmão.....	162
D.8 Etapa 8: Limpeza de AdC1 e AdC2.....	163
<b>APÊNDICE E</b> .....	165
E.1 Tampa e interior da AdC1 .....	165
E.2 Desmontagem da tampa da AdC1 e farelo de aveia após processo pseudocontínuo .....	166
E.3 Extrato adsorvido no farelo de aveia e mistura das frações de farelo de aveia .....	167
E.4 Extrato à saída da AdC2 durante a despressurização das C1 e C2 e coluna de adsorção 2 (AdC2) com e sem farelo de aveia .....	168
E.5 Válvula de purga do Tanque pulmão .....	169
E.6 Limpeza das válvulas backpressure .....	169
<i>Anexos</i> .....	170
<b>ANEXO A</b> .....	171
A.1 Laudo Técnico - Cúrcuma moída. ....	171
<b>ANEXO B</b> .....	172
B.1 Determinação da densidade por picnometria de gás hélio - Urucum e Cúrcuma. ....	172
B.2 Determinação da densidade por picnometria de gás hélio - Pérola de vidro e Farelo de aveia ..	174

## - CAPÍTULO 1 – *Introdução e objetivos*

Este capítulo aborda as circunstâncias que encadearam o desenvolvimento desta tese. Está inserida uma breve contextualização bibliográfica de itens justificativos da pesquisa, seguida da estruturação do trabalho.

## 1 INTRODUÇÃO

Atualmente, a redução de etapas de processamento, bem como o reaproveitamento de insumos (solvente, matéria-prima) e a combinação de processos são fortes tendências descritas pela comunidade científica para a otimização das tecnologias de fluidos supercríticos para fins sustentáveis.

A maioria dos processos de separação de gases pode ser realizada por meio de técnicas de adsorção, tais como adsorção por oscilação de pressão (PSA), adsorção por oscilação de temperatura (TSA) e adsorção por oscilação a vácuo (VSA). Estes são frequentemente realizados com adsorventes comercialmente disponíveis, como zeólitas, carvão ativado e aluminofosfatos, embora o uso de outras substâncias também tenha sido sugerido, como óxido de cálcio, carbonatos, uréia, amônia e fosfatos de cálcio (Souza et al., 2019).

Adsorção é um fenômeno de superfície, que consiste na adesão de moléculas de um fluido (adsorvato ou adsorvido) a uma superfície sólida (adsorvente ou substrato). A adsorção varia em função da temperatura, da pressão, da área da superfície, bem como das forças que atuam entre o adsorvato e o adsorvente, que podem ser químicas ou físicas.

No grupo dos cereais, a aveia oferece uma particularidade única em termos de composição química e teor de fibras dietéticas. Os componentes básicos da aveia são carboidratos não amiláceos como as  $\beta$ -glucanas (Górecka & Stachowiak, 2002). Como material adsorvente, possui vantagens de não ser tóxico e ter capacidade de remoção de cromo maior que 80% (Gardea-Torresdey et al., 2000). Porém, não há relatos de aplicação deste material para ensaio realizados como material adsorvente em meio subcrítico ou supercrítico.

Até o presente momento também não há relatos disponíveis relacionados a implementação de processos em escala piloto visando a purificação com subsequente reciclo do solvente CO<sub>2</sub> (oriundo de etapa de extração em estado supercrítico combinado com fracionamento do extrato) para ser destinado a posteriores ciclos de extração/fracionamento. O que se tem disponível da aplicação da adsorção em fluidos supercríticos, consta na remoção do CO<sub>2</sub> para purificação de gases, por ser visto como contaminante na linha de produção (Abdul Kareem et al., 2018). Em relação ao reciclo, existe apenas uma pesquisa recente que mostra por simulação o reciclo de CO<sub>2</sub> nas linhas de compressores centrífugos (Budinis & Thornhill, 2016).

Diante desse contexto, a extração supercrítica (SFE) combinada com fracionamento de extrato (coletadas em três vasos de separação + adsorção em meio subcrítico) com

consequente purificação e reciclo de CO<sub>2</sub>, pode ser uma alternativa vantajosa para aquisição de produtos diversificados obtidas a partir de uma mesma matriz vegetal utilizando um único equipamento. Além do mínimo impacto no meio ambiente, economia de solvente e redução do número de etapas no processo. Nesta tese, farelo de aveia foi aplicado como material adsorvente. Assim, uma primeira coluna de adsorção (AdC1) foi colocada a continuação do terceiro vaso coletor de extrato (VS3) para adsorver a fração de extrato não precipitado nos VS1, VS2 e VS3. Uma segunda coluna de adsorção (AdC2) foi colocada para adsorver a fração de extrato ainda solubilizado no CO<sub>2</sub> no interior de C1 e C2 ao final do período de extração dinâmica através da despressurização. Desta forma o processo de fracionamento de extrato do processo foi maximizado combinando a separação de extrato (nos VS1, VS2 e VS3) + adsorção (nas AdC1 e AdC2). Nesse sentido, o processo proposto, foi validado em unidade piloto (UP) comercial.

## **1.1 JUSTIFICATIVA**

Atualmente é crescente a demanda por tecnologias sustentáveis com o aproveitamento máximo dos insumos, redução de etapas e tempos de processamento. Portanto, esta tese tem como objetivo investigar a possibilidade de reciclo de CO<sub>2</sub> em processo de extração e fracionamento através da combinação deste processo com a operação de adsorção em meio subcrítico, a fim de purificar o referido solvente e viabilizar sua reutilização em etapas de extração e fracionamento posteriores, dentro de uma mesma linha de produção.

## **2 OBJETIVOS**

### **2.1 OBJETIVO GERAL**

Modificação das configurações do sistema de reciclo de uma unidade piloto (UP) comercial (Thar Technologies, CL 1373, Pittsburg, EUA) para purificação e reciclo de CO<sub>2</sub> durante tempos que permitam esgotamento do leito de extração em batelada, seguido de validação do procedimento em modo de extração pseudocontínua com sub etapas otimizadas.

### **2.2 OBJETIVOS ESPECÍFICOS**

- Modificar a Unidade Piloto (UP) comercial através de instalação de válvulas, conectores e tubulações junto à coluna de adsorção 1 (AdC1) de 0.65 L, para purificar e recircular o CO<sub>2</sub>.
- Validar os procedimentos de purificação e recirculação de CO<sub>2</sub> em escala piloto durante intervalos que permitam esgotamento da matriz vegetal utilizando reduzida massa de CO<sub>2</sub>.

- Construir as curvas globais de extração (OEC) em escala comercial de bancada (unidade Spe-ed) das SFE de urucum e cúrcuma para determinar os três períodos característicos: taxa de extração constante (CER), taxa de extração decrescente (FER) e período difusional (DC); visando otimizar as etapas em escala piloto, onde a SFE+fracionamento (coleta nos três vasos de separação + uma coluna de adsorção AdC1) acontecem;
- Validar o processo pseudocontínuo em escala piloto utilizando urucum e cúrcuma como materiais-modelo de extração e farelo de aveia como material modelo de adsorção. Para isso, os tempos das etapas (carga, pressurização, período estático, extração, despressurização e descarga) do ciclo foram otimizados;
- Maximizar a coleta de frações de extrato. Para tal, finalizado o período dinâmico de extração da C1, o extrato ainda solubilizado no CO<sub>2</sub> é expandido no farelo de aveia no interior da AdC2, produzindo-se mais um subproduto;
- Caracterizar os extratos (dos vasos de separação e das frações adsorvidas em AdC1 e AdC2) e o material adsorvente da AdC1 e AdC2;
- Avaliar a economia do processo em escala piloto;
- Comparar os rendimentos globais de SFE, acompanhado do balanço de massa dos extratos recolhidos da limpeza dos componentes da UP;

### 3 ESTRUTURA DO TRABALHO

A tese está dividida em 6 capítulos, nos quais estão registrados os resultados obtidos das distintas etapas. Nestes capítulos estão inclusos o levantamento bibliográfico, artigos publicados e artigos submetidos para publicação. No **Capítulo 1 – Introdução e objetivos** – foram apresentados sucintamente os objetivos pretendidos neste trabalho e as etapas envolvidas para a sua realização. As atividades cumpridas neste trabalho são exibidas na Figura 1.

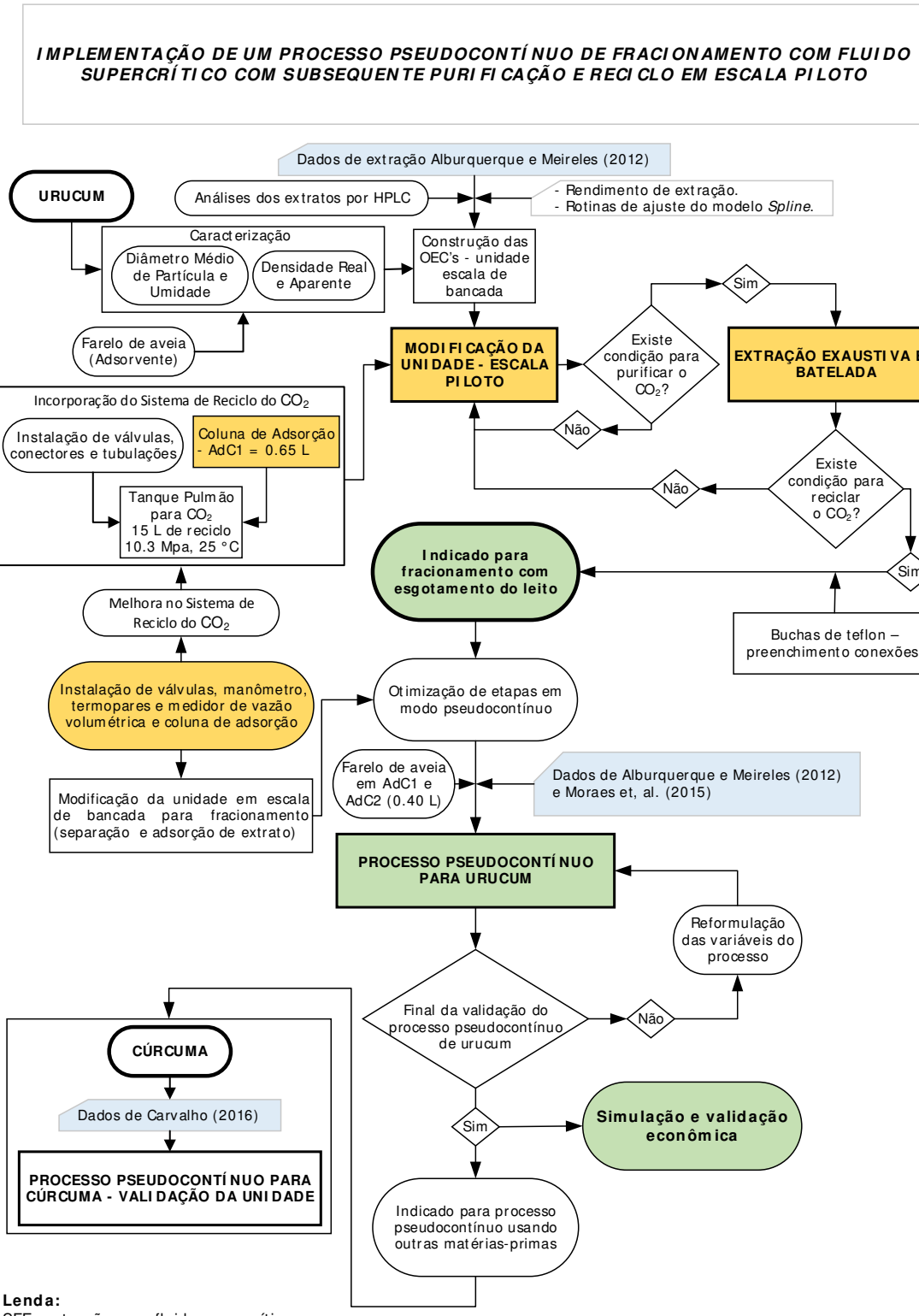


**Figura 1.** Estrutura do trabalho.

Uma revisão da literatura no que diz respeito ao fracionamento de extratos vegetais em meio supercrítico foi realizada no **capítulo 2**. Ainda que este capítulo trate do uso do CO<sub>2</sub>

supercrítico para obtenção de extratos fracionados em forma de partículas, esta bibliografia nos serviu para termos maior clareza no que diz respeito ao fracionamento de extratos para obtenção de produtos de composição diversificada, e na adaptação dos componentes de uma unidade de processamento, tais como características de um vaso de fracionamento e bico injetor visando sua otimização, seja em escala de bancada, seja em escala piloto.

Segundo King and List (1996), a adsorção é um processo de fracionamento competitivo que forma as bases de um processo de separação. Isso pode ser observado no **Capítulo 4** na seção de Resultados, que mostra o efetivo fracionamento dos extratos de urucum e cúrcuma durante a purificação do CO<sub>2</sub> para recirculação e na saída do sistema durante o processo de despressurização da coluna de extração (C1 ou C2) e cuja corrente é expandida dentro da coluna de adsorção 2 (AdC2) onde entra em contato com o material adsorvente (farelo de aveia). A combinação, extração supercrítica com sistema de purificação e recirculação de CO<sub>2</sub> (SCPRSCO<sub>2</sub>), consiste na extração com fluido supercrítico (SFE) da matriz vegetal, seguida de fracionamento do extrato, tanto nos vasos de separação quanto nas colunas de adsorção para purificação do solvente CO<sub>2</sub>, onde a adsorção acontece em meio subcrítico com uso do farelo de aveia como material adsorvente.

Este processo combinado proposto nesta tese foi comprovadamente capaz de produzir três tipos de extratos diferentes (uma por cada vaso de separação) e de um subproduto de alto valor agregado, que se trata do farelo de aveia enriquecido com compostos bioativos de frações de extratos que não precipitaram no interior dos vasos de separação e que foram carregadas pelo CO<sub>2</sub> até a coluna de adsorção 1 (AdC1). E após o tempo dinâmico de extração da C1, ocorre a despressurização, em que o extrato ainda solubilizado no interior dela são transportados para a coluna de adsorção 2 (AdC2), desde a pressão de processamento (20 MPa) até pressão ambiente.

Para atingir tais fins, neste trabalho foram utilizadas duas unidades comerciais de extração supercrítica, sendo uma em escala de bancada (unidade Spe-ed, Applied Separations, Allentown, EUA) e a outra, em escala piloto (Unidade Piloto -UP, Thar Technologies, CL 1373, Pittsburgh, EUA).

Este trabalho foi iniciado com informações descritas no **Capítulo 3**, a partir da construção das curvas globais de extração (OECs) referentes às cinéticas SFE do urucum, realizadas em escala de bancada (unidade Spe-ed) a fim de determinar as condições ótimas de extração em termos de rendimento global e determinação dos parâmetros cinéticos obtidos através do modelo spline de três retas. Os tempos obtidos pelo spline referentes à taxa de

extração constante ( $t_{CER}$ ) e taxa decrescente de extração ( $t_{FER}$ ) serviram como base para determinar os tempos de extração SFE em escala piloto, realizados no **Capítulo 4**.

Também no **Capítulo 3** foi validado o processo de extração com reduzida massa de CO<sub>2</sub> sobre recirculação (realimentada no sistema) por longos períodos de tempo com o intuito de esgotar o leito de extração. Porém, para mostrar o impacto e a importância da incorporação do sistema de recirculação em escala piloto, a massa de CO<sub>2</sub> reciclada foi contabilizada como nova massa ingressando ao processo. Com isso, o cálculo mostrou elevada massa de CO<sub>2</sub>, multiplicando a vazão do solvente pelo tempo dinâmico de extração. O resultado da multiplicação é o valor S na relação S/F que é Solvente/Alimentação (massa de solvente/massa de matéria-prima), pelas siglas em inglês, Solvent/Feed. Sob essa consideração a relação S/F atingiu altos valores quando a unidade em escala piloto foi operada por longos períodos de tempo. O sistema de recirculação mostrou que o armazenamento de CO<sub>2</sub> no tanque pulmão pode ser posteriormente reaproveitado para o processamento de novas matérias-primas, pois este sistema foi otimizada a partir da inclusão de uma coluna de adsorção (AdC) para purificação de CO<sub>2</sub>, utilizando-se como adsorventes-modelo a celite e o algodão. O CO<sub>2</sub> a ser purificado continha extratos SFE que foram arrastados desde os vasos de separação.

O **Capítulo 4** consiste em apresentar o processo de adsorção em meio subcrítico em escala de bancada para reprodução em escala piloto, afim de se estudar o comportamento do farelo de aveia como material adsorvente, tendo como variáveis investigadas a massa de farelo de aveia e a vazão de solvente (primeira parte). Os ensaios de adsorção reproduzidos em escala piloto servirão para a validação do sistema de purificação e reciclo em modo pseudocontínuo proposto neste mesmo capítulo (segunda parte).

Para execução dos experimentos da primeira parte, foram realizadas modificações na unidade Spe-ed (unidade de bancada), que consistiram de incorporação de acessórios (conexões, válvulas, manômetro e tubulações), indicador de temperatura, e colunas de fracionamento (um vaso de separação de extratos + uma coluna de adsorção). Nos ensaios de escala bancada não foi realizada a recirculação de solvente.

De posse das informações obtidas em escala de bancada, foi feita tomada de decisão em utilizar uma quantidade fixa de farelo de aveia na coluna de adsorção em escala piloto, pois foi observado que uma quantidade elevada de adsorvente não teve aumento significativo de material adsorvido.

A validação da unidade em escala piloto em modo pseudocontínuo, detalhada ainda no **Capítulo 4** foi feita tendo como base as informações do **Capítulo 3** referentes à validação do sistema de purificação e reciclo de CO<sub>2</sub>. A validação foi feita utilizando-se como materiais-

modelo de extração o urucum e a cúrcuma e o farelo de aveia como material adsorvente, desenvolvendo dois processos pseudocontínuos por cada matéria-prima para a validação da unidade. Cada processo consistiu de 4 ciclos (Figura 2). Cada ciclo compreendia as etapas de carregamento de matéria-prima, pressurização da coluna de extração, período estático (iniciado após atingida a pressão de processo dentro da coluna de extração, que consiste no intervalo de tempo no qual está ocorrendo a extração da matéria-prima em estado estacionário), período dinâmico (extração com coleta de extrato), despressurização e descarregamento da matéria-prima. Enquanto o período dinâmico de extração está sendo executado, um novo ciclo está sendo iniciado na segunda coluna de extração.

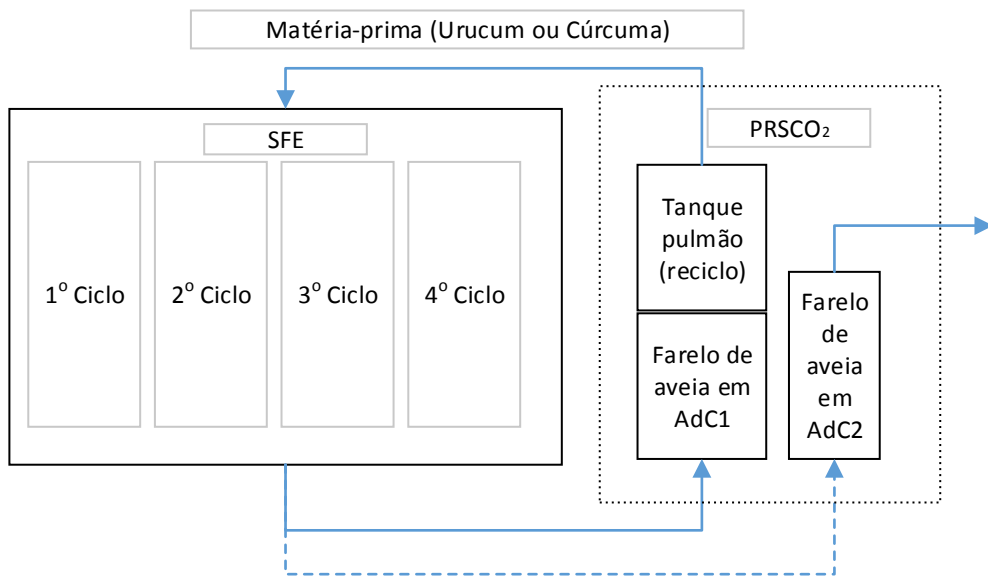


**Figura 2.** Diagrama esquemático do sistema de extração/fracionamento em meio supercrítico (generalizado por ‘‘SFE’’), seguido de purificação (AdC1) e reciclo de CO<sub>2</sub> por adsorção em meio subcrítico e a etapa de despressurização em AdC2 (identificado por PRSCO<sub>2</sub>).

Nos 4 ciclos, ocorre a purificação de solvente na primeira coluna de adsorção (AdC1). Enquanto o período dinâmico de cada ciclo finaliza, imediatamente ocorre a despressurização da coluna de extração na segunda coluna de adsorção (AdC2).

Estes processos resultaram na obtenção de três extratos fracionados (uma por cada vaso de separação), e de um subproduto, que se trata do farelo de aveia enriquecido com compostos bioativos dos extratos em diferentes concentrações, por serem originados de colunas de adsorção distintas (AdC1 e AdC2), sendo que uma das colunas foi usada para recirculação de CO<sub>2</sub>, e a outra, para a despressurização das colunas de extração. Além dos extratos e do

farelo de aveia, outro subproduto do processo consta nas sementes de urucum com teor lipídico reduzido, ou nos rizomas desaromatizados de cúrcuma.

No fracionamento em condições supercríticas, por exemplo a partir de uma mistura de compostos dissolvidos em etanol durante o processamento SAS (estudado no **Capítulo 2**), quando o etanol e o CO<sub>2</sub> entram em contato acontece a liberação e precipitação dos compostos de interesse. Mas uma fração da mistura dos compostos inicialmente dissolvidos no etanol ainda é arrastrado junto aos efluentes fora da unidade de processamento. Assim, por analogia, no processamento em escala piloto utilizando o PRSCO<sub>2</sub> durante o fracionamento nos vasos de separação uma fração dos compostos é arrastrado fora deles até a AdC1 onde são retidos, permitindo a purificação e reciclo do CO<sub>2</sub> e ainda enriquecer o material adsorvente com a fração de extratos.

Assim também no **Capítulo 2**, uma análise dos componentes (características de uma coluna de fracionamento e bico injetor) utilizados nas unidades de processamento para fracionar e obter partículas purificadas foi feita, o que certamente serviu para ter maior clareza no que diz respeito da modificação na configuração da unidade Spe-ed para estudos prévios de adsorção e a adaptação de colunas de adsorção em escala piloto feitas nos **Capítulos 3 e 4**.

A separação dos compostos oriundos dos extratos obtidos em várias frações e a adaptação dos componentes de uma unidade de processamento visando sua otimização mantiveram o vínculo entre o **Capítulo 2** junto aos outros precedentes.

#### **4 REFERÊNCIAS BIBLIOGRÁFICAS**

- F. A. Abdul Kareem, A. M. Shariff, S. Ullah, F. Dreisbach, L. K. Keong, N. Mellon, S. Garg, Experimental measurements and modeling of supercritical CO<sub>2</sub> adsorption on 13X and 5A zeolites. *Journal of Natural Gas Science and Engineering*, 50 (2018)115-127.
- S. Budinis, N. F. Thornhill, Supercritical fluid recycle for surge control of CO<sub>2</sub> centrifugal compressors, *Computers & Chemical Engineering*, 91(2016) 329-342.
- J. L. Gardea-Torresdey, K. J. Tiemann, V. Armendariz, L. Bess-Oberto, R. R. Chianelli, J. Rios, J.G. Parsons, G. Gamez, Characterization of Cr(VI) binding and reduction to Cr(III) by the agricultural byproducts of Avena monida (Oat) biomass. *Journal of Hazardous Materials*, 80(1) (2000) 175-188.
- D. Górecka, J. Stachowiak, Sorption of copper, zinc and cobalt by oat and oat products. *Food / Nahrung*, 46(2) (2002) 96-99.
- J. W. King, G. R. List, *Supercritical fluid technology in oil and lipid chemistry*. The American Oil Chemists Society, 1996. ISBN 0935315713.

F. S. Souza, M. J. S. Matos, B. R. L. Galvão, A. F. C. Arapiraca, S. N. da Silva, I. P. Pinheiro, Adsorption of CO<sub>2</sub> on biphasic and amorphous calcium phosphates: An experimental and theoretical analysis. *Chemical Physics Letters*, 714 (2019) 143-148.

- CAPÍTULO 2 –*Perspectives on the application of supercritical antisolvent fractionation process for the purification of plant extracts: effects of operating parameter and patent survey*

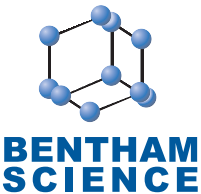
Este capítulo trata de uma revisão bibliográfica a respeito de um processo intitulado “fracionamento por antisolvante supercrítico” para obtenção de extratos vegetais concentrados e elevada pureza, porém na forma de partículas. Estão descritas as condições de processamento e as características detalhadas dos equipamentos e seus componentes responsáveis pelo fracionamento.

*Artigo publicado no periódico de acesso aberto*

*Recent Patents in Engineering, 2016; v. 10, n°. 2, p. 1-10*

ISSN: 2212-4047 DOI: 10.2174/1872212110666160311201756.

## REVIEW ARTICLE



## Perspectives on the Application of Supercritical Antisolvent Fractionation Process for the Purification of Plant Extracts: Effects of Operating Parameters and Patent Survey

Abel R.C. Torres, Ádina L. Santana, Diego T. Santos and M. Angela A. Meireles\*

LASEFI/DEA/FEA (School of Food Engineering)/UNICAMP (University of Campinas), R. Monteiro Lobato, 80; 13083-862, Campinas, SP, Brazil

**Abstract:** **Background:** A recently developed process entitled Supercritical Antisolvent Fractionation (SAF) was recently described for the fractionation of plant extract solutions using supercritical fluids to give two or more fractions containing bioactive compounds with widely differing polarities. An updated overview of SAF of natural products is presented in this article.

### ARTICLE HISTORY

Received: October 21, 2015

Revised: January 15, 2016

Accepted: February 09, 2016

DOI:  
10.2174/18722121106661603112017  
56

**Objective:** The goal of this work is to show some perspectives about the use of supercritical CO<sub>2</sub> (SC-CO<sub>2</sub>) applied to the fractionation of plant extract compounds, such as phenolic compounds, lipids, and carotenoids; among other components, those extracted from seeds, leaves, stems, roots and other parts of the plants are described. The main features and mechanisms of antisolvent techniques that contribute to the understanding of the fundamentals of the supercritical antisolvent fractionation (SAF) process are also described.

**Method:** The influence of various operating parameters, such as, CO<sub>2</sub> temperature and pressure, CO<sub>2</sub> flow rate, among others, during SAF process on the purification efficiency and particle morphology and the main differences about the patented SAF processes are reviewed.

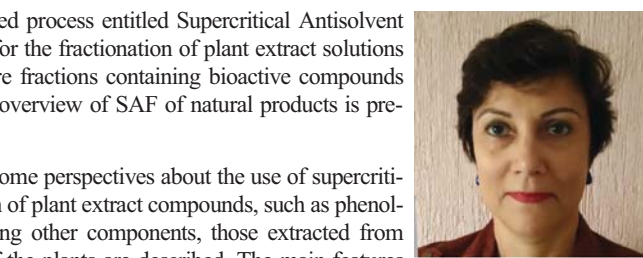
**Results:** The various experimental works intend to optimize their processes through adaptations or modifications of equipments that constitute the SAF unit, as the study of process parameters.

**Conclusion:** SAF process is a technique to produce particles with high yield and purity of bioactive compounds. On the other hand, patents developed using this type of process are very scarce, less attention being given be given to the potential of this technique to purify plant extracts with a very complex content of bioactive compounds.

**Keywords:** Fractionation methods, plant extracts, precipitation of bioactive compounds, SAF, supercritical antisolvent processes, Supercritical CO<sub>2</sub>.

### 1. INTRODUCTION

Nowadays, there is a growing requirement for environmentally friendly separation technologies of valuable compounds from vegetable raw materials that cause little or no damage to the plant material in order to maximize its usability, generating new tradeable products free from harmful solvents and therefore, decrease the amount of waste. Most conventional separation techniques suffer from several drawbacks such as lack of selectivity, the need for large amounts of organic solvent, high temperatures, and long processing times [1]. Supercritical fluid technology that uses carbon dioxide meets these requirements and is constituted of several processes. Supercritical CO<sub>2</sub> (SC-CO<sub>2</sub>) is the most widely used supercritical fluid because of its relatively low critical conditions (T<sub>c</sub> = 305K, P<sub>c</sub> = 7.38MPa), nontoxicity,



M. Angela  
A. Meireles

no flammability, and low price [2-4]. The transport properties of supercritical fluids are intermediate between the properties of gas and liquid, being very useful for several processing applications [5].

The supercritical fluid-based particle formation application, in particular, is one of the most explored applications and is present in several industrial fields such as the chemical, pharmaceutical and food industries [6]. When a supercritical fluid is used for this application, setting optimized process parameters, it is possible to produce particles with controlled size with well defined characteristics in terms of crystallinity, purity and morphology [7].

The synthesis of fine particles with controlled particle size distributions, ranging from submicrons to hundreds of microns, has found considerable interest in the scientific and industrial sectors with applications for advanced materials, catalysts, coatings, polymer industries, and for the formulation of injectables, inhalables and controlled release pharmaceuticals [8]. According to the scientific literature, some

\*Address correspondence to this author at the LASEFI/DEA/FEA (School of Food Engineering)/UNICAMP (University of Campinas), CEP 13083-862, Campinas, SP, Brazil; Tel: +55 1935210100;  
E-mail: meireles@fea.unicamp.br

from the well-known techniques for particle formation using supercritical carbon dioxide are Gas Antisolvent, GAS and Supercritical Antisolvent, SAS, in which SC-CO<sub>2</sub> acts as an antisolvent, in batch and in a semi-continuous way [9], Supercritical Assisted Atomization, SAA, in which SC-CO<sub>2</sub> acts as a propeller [10], Rapid Expansion of Supercritical Solutions, RESS, in which SC-CO<sub>2</sub> acts as a solvent [11], and Particles from Gas Saturated Solutions, PGSS, in which SC-CO<sub>2</sub> acts as a solute [12]. At the same time within each of these subvariants it is possible to identify other subvariants with their own characteristics. Fig. (1) presents a schematic diagram of these processes for a better understanding of their particularities and differences. SAS (Supercritical Antisolvent) process was indicated in order to introduce the process that is the main focus of this review, the Supercritical Antisolvent Fractionation (SAF) process, which is a subvariant of SAS process.

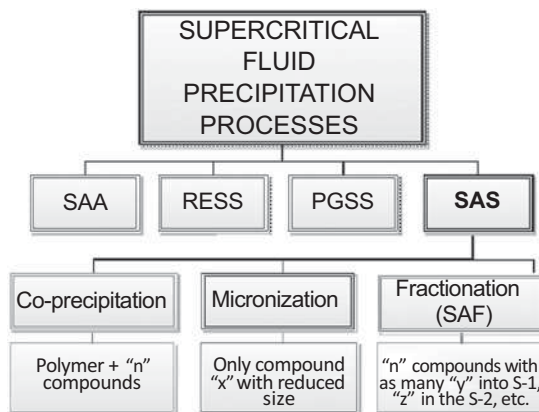


**Fig. (1).** Schematic diagram of the main supercritical fluid-based precipitation processes.

SAS process is a technique relatively simple, cost effective and easy to scale-up [13]. In this process the solute, dissolved in a liquid organic solvent, is injected through a nozzle into a compressed gas which has a low affinity for the solute and a high affinity for the organic solvent [7]. Upon contact, CO<sub>2</sub>, the most widely used fluid, removes the organic solvent from the liquid mixture, leaving a dry solute behind. Precipitation is dictated among other things by the phase behavior of the system, which is a reflection of solute-solvent-antisolvent interactions [14].

As shows in Fig. (1), exists in SAS process the subvariants co-precipitation, micronization and fractionation.

What distinguishes a case from another is that in co-precipitation the objective is to encapsulate the compound(s), using a wall material which is mixed with an organic solution formed by an organic solvent and the compound(s) [15]. In micronization, an organic solvent is generally mixed in a pure compound in order to reduce the particle size [16]. In Supercritical Antisolvent Fractionation (SAF) process an organic solvent is used in combination with a mixture of various compounds in order to fractionate the compounds present in the mixture. The configuration of the elements that constitute a SAS unit is the same as for the co-precipitation, micronization and fractionation processes. Probably this is the reason why some authors refer these processes using SAS acronyms to refer to some of these processes. In addi-

tion, these processes might differ in terms of the contact mode between the two phases, in the flows direction and/or in the operational mode (continuous or batch).

In some cases the SAF process is also called Supercritical Antisolvent Precipitation, SASP [15]. SAF is an interesting alternative to fractionate bioactive compounds extracted from vegetable materials, such as rutin from amaranth leaves extract [17], flavonoids from propolis tincture [18], curcumin from turmeric rhizomes [13], polyphenols from eucalyptus [19] and olive leaves [1], carotenoids from microalgae [20], and anthocyanins from grape by-products [21].

SAF process can also be used as a stage prior to other processes, as in the case of quercetin encapsulation [22].

In the following sections the SAF process is detailed in terms of main characteristics, advantages and future perspectives.

## 2. SUPERCRITICAL ANTISOLVENT FRACTIONATION (SAF) PROCESS

SAF process is achieved by the contact between the supercritical carbon dioxide (SC-CO<sub>2</sub>) and a liquid mixture at pressurized conditions. Under these conditions, the SC-CO<sub>2</sub> is able to dissolve the organic solvent and the non-polar compounds in the mixture SC-CO<sub>2</sub> + organic solvent, selectively precipitating heavier, more polar compounds that are not soluble in the fractionation medium [17].

With regard to the SAF processing parameters applied to fractionate bioactive compounds extracted from vegetable materials, usually the temperature conditions during the fractionation steps are maintained at or close to the temperature conditions that were done in the previous extraction step.

The mixing of solvents, *e.g.*, ethanol and CO<sub>2</sub>, for example, in supercritical conditions contribute to the dissolution of the impurities present in the bioactive compounds by dragging them together with the effluents [23]. Thus, it is possible to obtain enriched particles precipitated in a particular bioactive compound, probably due to the fact that the other bioactive compounds are further diluted in the supercritical solution.

### 2.1. Description of a SAF Unit and Experimental Procedure

All fractionation processes that employ supercritical technology result in the total or partial separation of the liquid mixture containing the bioactive compounds in two or more fractions of compounds. It is expected that the studied fraction of compounds is free of liquids and presents particle characteristics (powder) with size from 0.1 to 5 μm [24].

In this work, the liquid mixture containing the organic solvent and the bioactive compounds obtained from vegetable raw parts (flowers, leaves, seeds, husks, *etc.*) is designated as Bioactives Solution (BS). In all situations when solvent extraction is used as preparative step, post-processing steps are required to fractionate or to purify the more desirable compounds from the undesirable co-extracted compounds, and to eliminate the organic solvent [25]. In the case of SAF process, the antisolvent fractionation can also be used as a preparative step for further encapsulation (co-precipitation)

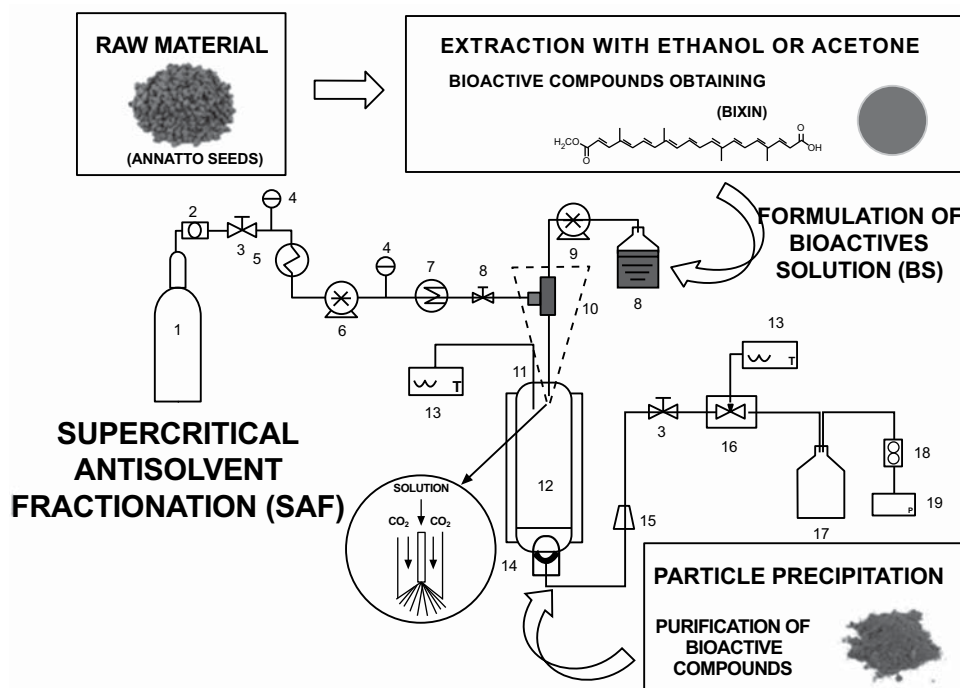


**Fig. (2).** Schematic steps for bioactive compounds fractionation using Supercritical Antisolvent Fractionation (SAF) process.

step, which may be applied using the same antisolvent precipitation unit. In literature, alternative nomenclatures are used according to the quantity of precipitation columns in each precipitation unit, *i.e.*, if the unit is provided by one column, the possible names that are normally used are purification or concentration [26, 23], precipitation [15, 27, 28] and extraction [29]. If the unit is provided by two or more precipitation columns, the process is designated simply as fractionation [24, 30, 31] to obtain a specific type of bioactive compound in great quantity as the pressure inside each column reduces. Independent of the number of columns, the SAF process is carried out normally by the continuous contact between the fluids.

In particular, SC-CO<sub>2</sub> is a model of anti-solvent fluid while another fluid used to obtain the BS is commonly an organic solvent. In SAF both fluids enter in the previously pressurized column in which precipitation is carried out. It is expected that with an appropriate selection of the process conditions, the solvent presented in the BS is extracted by SC-CO<sub>2</sub> at the same time the solid particles precipitate in the inferior part of the column [29].

A schematic diagram of a SAF unit is shown in Fig. (2), which represents an equipment built and performed by our research group (LASEFI/Unicamp/Brazil) [32]. The annatto seeds were adopted as illustration example, because our research group extensively studied this raw material [33, 34].

In the CO<sub>2</sub> cylinder (1) exit, the SAF apparatus configuration recommends the use of a cooling bath (5) [26, 4, 31, 15] in order to control the temperature of CO<sub>2</sub> at the moment it is pumped by an HPLC pump (6), in order to avoid cavitation [35]. This pump guarantees the maintenance of pressure conditions above the critical point of the SC-CO<sub>2</sub>-organic solvent mixture meanwhile SC-CO<sub>2</sub> flows through a heat exchanger (7) to increase the temperature also above the

critical point. In the same way, inside a recipient (8) the BS is pumped through an HPLC pump (9), which enters in contact with SC-CO<sub>2</sub>. These fluids are mixed through an injection system (10) which is in some cases constituted by an adaption of stainless steel tubes and connectors which facilitates the fractionation of the compounds of interest [36]. In other cases the injection system is defined as a three-step fractionation column [31], whose operational detail is described in the following section. Inside this injection system, complete solubility of the organic solvent is reached in SC-CO<sub>2</sub> phase (depending on the injector dimensions, a previous fractionation process is possible), following its passage into the precipitation column (12), when the atomization or expansion of fluids occurs, resulting in the fractionation of the mixture through the precipitation of the purified compounds.

A stainless steel filter (14), with porosity usually ranging from 0.1-1.0 µm is situated in the inferior part of the precipitation column [26, 31], in order to recover the highest proportion of powder solids [26, 31, 37]. Leaving the column is the mixture (organic solvent+SC-CO<sub>2</sub>+non-precipitated compounds). A line filter (15) can help retain part of the solids that were not precipitated into the precipitation column [32].

Afterwards, the mixture is depressurized through a micrometering valve (16) and collected in a liquid separator tank (17), while the gaseous CO<sub>2</sub> continues its passage through a relief valve, a rotameter (18) and finally a mass flow meter [30]. The other installed parts in the unit are a filter (2), blocking valves (3), manometers (4), a thermocouple (11) and a temperature controller (13) [32].

Basically, the differential of any unit that uses the SAF process is the injection system, which can be a nozzle or a fractionation column. The nozzle is a pipe that promotes the contact between the bioactive solution and the antisolvent

fluid, accelerating the mass transfer between them in order to generate the fractionation products with reduced particle diameter. The fractionation column is used to separate mixtures into different parts, based on the differences in volatilities. In the case of the unit built by our research group, the adaptation is correspondent to the nozzle in the form of a T-tube (item number 10 in Fig. 2), which is succeeded by decreasing the pipe length from 8 to 6 cm in order to increase the purification of solid precipitates [38]. Regardless the configuration of the injection system, the goal is the same for all SAF units, *i.e.*, to obtain maximum purified precipitates.

## 2.2. Effects of SAF Operating Parameters

The process parameters that influence the performance of a SAF process are temperature, pressure, flow of antisolvent and BS, type of organic solvent, characteristics of the nozzle, the concentration of the bioactive compound in the BS, time of processing and characteristic of the separator(s). The influence of these operating parameters on the purification of bioactive compounds is presented in Table 1.

Before conducting SAF process, it is necessary to have solubility data of the studied organic solvents that obviously will permit the reliable choice of some process parameters. Beside these, the knowledge of the thermodynamics restrictions and the mass transfer mechanisms is important [26, 29]. When SC-CO<sub>2</sub> is in contact with the organic solvent present in the BS it can induce an increase in the solubility of the solid bioactive compounds. By increasing the solubility, the organic solvent acts as a co-solvent, retaining the solid compounds in the fluid phase during SAF, which afterwards recover the solid particles inside the recipient vase in which SC-CO<sub>2</sub> is circulated under its supercritical conditions. In this case, the selective fractionation process inside a precipitation vessel is possible after appropriate selection of process parameters [26].

The concentration of solids in the BS is a considerable factor that should also be analyzed [26]. Generally, in the SAF process the same temperature (or near) conditions are employed that were used in the previous extraction step. Haimer *et al.* [24] used 424 K in the previous extraction step and in the posterior precipitation and purification of hemicellulose from dimethylsulfoxide (DMSO) and DMSO/water mixtures.

In cases, in which BS is constituted by more than one solvent, the knowledge of the polarity and solubility of each component is necessary. During SAF the solvent power of a polar liquid solvent in which the substrate (bioactive compound of interest) is dissolved is reduced by saturating it with CO<sub>2</sub> at supercritical conditions, causing the substrate precipitation or recrystallization [39].

Extracts of amaranth leaves containing 70% water: 30% ethanol were mixed with supercritical CO<sub>2</sub> and separated successfully into two fractions according to the molecular mass and solubility of the contained compounds depending on the BS polarity [17].

Thermodynamics has the role to indicate the preliminary conditions for a successful antisolvent precipitation process. The effect of the phase region decreasing is the decreasing of the particle size. According to the phase diagram of the sys-

tem CO<sub>2</sub>+ethanol studied by [40], each process that employs this system can be performed in a monophasic zone (314K and 10MPa) and biphasic zone (324K and 10MPa). Considering the fact that BS can be constituted of ethanol and it will be in contact with the antisolvent SC-CO<sub>2</sub>, this information is useful before performing SAF processes.

Solubility parameters are also used to choose the most suitable organic solvent for a given application [41]. In order to fractionate ryanodol from *Persea indica* [26], vapor liquid equilibria (VLE) data of the system CO<sub>2</sub>+ethanol under pressure was investigated from the literature, with the aim to select SAF conditions that allow working in homogeneous supercritical phase [42].

The recovery of 84% of five lignans from *Schisandra chinensis* fruit by SAF was reached as a function of the highest condition of temperature (334K) [23].

Nano-sized curcumin particles with oral bioavailability were obtained by inserting its BS into a reacting vessel through a capillary nozzle (internal diameter of 100 μm) employing the conditions of 14MPa, 313k, CO<sub>2</sub> flow rate at 40 g/min, solution flow rate at 0.5 mL/min, and solution concentration at 0.5% [43].

When higher levels of pressure were employed associated to lower levels of temperature for the precipitation of rosemary particles, a reduced quantity of compounds is recovered. However, the combination of high levels of pressure and temperature can double the recovery of compounds, when compared to the initial antioxidant content on the BS, before fractionation [15].

Continuous antisolvent production of drug nanoparticles with a static mixer using six mixing elements was sufficient to precipitate particles with the submicron range by employing the total flow rate ranging from 1.0 to 3.0 L/min, while the flow rate ratio of solvent to antisolvent was maintained at 1:9 [44].

High purification levels of lignans from BS composed of ethanol and flaxseed (associated to the minor presence of organic solvent) was reached by employing high pressure and high solvent flow levels of SC-CO<sub>2</sub> and BS [31].

The increase in the precipitation yield and recovery of bioactive compounds with high purity from a BS composed of rosemary extracts diluted in ethanol was obtained by partial evaporation of ethanol in vacuous and modification of the nozzle configuration through the connecting of a 7 mm x 0.13 mm stainless steel tube with diameter of 1.59 mm [15].

Fractionation of BS composed of rosemary oleoresin diluted in ethanol was successfully performed by the use of a specially designed nozzle to improve the mixing of the viscous BS with the SC-CO<sub>2</sub>, attaining effective separation and purification of compounds adopting the conditions of 324K and 30 MPa [36].

The increasing of recovered ryanodol was reached after the adoption of a cooling cyclone separator, which minimized the contact with liquid CO<sub>2</sub>, reducing the drag of the solution out from the flow of gas exiting the top of the separator when the mixture is decompressed [27]. Some particularities from fractionation units that use the SAF technique are summarized in Table 2.

**Table 1.** Recent applications of supercritical antisolvent fractionation (SAF).

Bioactive Compounds Source	Bioactive Compounds (%), w/w Before SAF Processing	Extraction Solvent to Obtain the Bioactive Compounds	SAF Fractionation Solvent	Operating Parameters*	Products Characteristic	Bioactive Compounds (%), w/w After SAF Processing	Purification Yield Increase (%), w/w**	References
Hemicelluloses from oat, birch and spruce *** 1-5mg.mL <sup>-1</sup>	Oat xylan = 4.6 Birch xylan = 10.6 Spruce mannan = 4.0	DMSO	DMSO	P = 15; T = 424; Q <sub>CO<sub>2</sub></sub> = 5; V <sub>BS</sub> = 20; Q <sub>BS</sub> = 2; t = 100	S-1= products brighter. Reduced the lignin content by 49 and 85%, respectively for Oat xylan and Birch xylan	Oat xylan = 9.5 Birch xylan = 24.4 Spruce mannan = 8.0	Oat xylan = 107 Birch xylan = 130 Spruce mannan = 100	[24]
Grilled <i>Schisandra chinensis</i> , 206 mg.g <sup>-1</sup>	Schisandrol B = 20.58 Schisandrin A = 9.39 γ-Schisandrin = 12.6 Gomisin N = 12.6 Schisandrin C = 10.1	Ethanol	Ethanol	P = 13; T = 333; Q <sub>CO<sub>2</sub></sub> = 0.108; V <sub>BS</sub> = 4; Q <sub>BS</sub> = 0.1; t = 40	S-1=quadruple purification in a PS100 columns	Schisandrol B = 58.92 Schisandrin A = 22.94 γ-Schisandrin = 26.943 Gomisin N = 108.132 Schisandrin C = 18.95	Schisandrol B = 286.36 Schisandrin A = 244.15 γ-Schisandrin = 213.3 Gomisin N = 228.57 Schisandrin C = 187.3	[23]
laxseeds (100g)	Lignans = 100	Acetic acid (sodium) buffer solution at pH=6.0	Ethanol	P = 30; T = 313, 323, 333; Q <sub>CO<sub>2</sub></sub> = 15; V <sub>BS</sub> = 350; Q <sub>BS</sub> = 1.94; t = 180	Residual fraction content of ethanol with a decrease in value from 60 to 92%	206-781	106-681	[31]
Lyophilized grape residues (1000g)	Polyphenols, considering only the majoritary compound, malvin cumarate (0.926)	Tartaric acid (sodium) buffer solution at pH=3.2	Methanol	P = 11; T = 313; Q <sub>CO<sub>2</sub></sub> = 1.028; Q <sub>BS</sub> = 0.7	S-1= powders with particle size greater of 1μm S-2= residual methanol	99.53 2.79	Non identified Non identified	[35]
Rosemary (extract with a mean solid content of 2.7 %)	Rosmarinic acid = 3.4 Carnosic acid = 5.8	Ethanol	Ethanol	T = 323; P = 10; Q <sub>CO<sub>2</sub></sub> = 0.7; Q <sub>BS</sub> = 1.0	Non identified	Rosmarinic acid = 7.4 Carnosic acid = 18.1	Rosmarinic acid = 117.6 Carnosic acid = 212	[15]
Rosemary (48 % oleoresins)	Carnosic acid in crude extract = 0.033	Ethanol	Ethanol	P = 30; Q <sub>BS</sub> = 4.3; T = 323; P = 10; Q <sub>CO<sub>2</sub></sub> = 4.3; T = 323	S-1= insoluble dark green powder S-2: orange colored resinous extract	Carnosic acid in S-1: 5.51 Carnosic acid in S-2: 33.0	16597 99900	[36]
Persea indica Liquid Extract (approximately 3% of solids)	Ryanodol = 7.5	Ethanol	Ethanol	P = 15; Q <sub>CO<sub>2</sub></sub> = 2.38; Q <sub>BS</sub> = 5.7; T = 308	Non identified	37.7	402	[26]
Grape seeds Liquid Extract (approximately 3% of solids)	Polyphenols = 23.4	Ethanol	Ethanol	P = 15; T = 314	Non identified	63.9	173	[45]
Oat flakes (1000 g)	polar lipids = 35	Ethanol	Ethanol	P = 23; Q <sub>CO<sub>2</sub></sub> = 10.585; Q <sub>BS</sub> = 7.1; T = 344	Non identified	Up to 59	68	[46; 47]

\*T = Temperature (K); P = Pressure (MPa); Q<sub>CO<sub>2</sub></sub> = Carbon dioxide mass flow rate (kg.h<sup>-1</sup>); V<sub>BS</sub> = Volume of bioactive compounds solution (mL); Q<sub>BS</sub> = Bioactive compounds solution flow rate (mL.min<sup>-1</sup>); t = Time of treatment (min); S-1 = Precipitation chamber [30] or precipitator vessel [35]; S-2 = cylindrical separator [30, 31, 35] and S-3 = Term related to the 1<sup>st</sup>, 2<sup>nd</sup> and 3<sup>rd</sup> cylindrical separators, respectively [30, 31];

\*\* Purification yield increase (%), w/w = [Bioactive compounds (%), w/w after SAF processing - Bioactive compounds (%), w/w before SAF processing]/Bioactive compounds (%), w/w before SAF processing

\*\*\* calculated from the cumulated relative peak areas of polysaccharide and lignin derived pyrolysis products obtained by Curiepoint pyrolysis of three different hemicelluloses samples prior and after anti-solventprecipitation from DMSO

Table 2. Injection systems commonly used for supercritical antisolvent fractionation (SAF).

Type	Specification	Benefits	Mixing		Precipitation Column Characteristics	Solvent Recovery Dispositive	References
			Design				
Three-stage fractionation column	Length=3 m, Diameter =3 cm, Internal volume= 2 L	The temperatures preserve the ethanol evaporation, save energy and explore the behavior at the related densities. This determined a density gradient in the solvent stream, with SC-CO <sub>2</sub> densities varying along the column.		S-1: cylindrical separator of 1 L S-2 and S-3: separator fraction (trace lignan)	Vacuum separation, distillation and membrane techniques	[31]	
T-tube nozzle	Internal diameter=0.4mm External diameter=0.6mm Mixing chamber	Proper mixing between two fluid streams		S-1=2.5L S-2=0,5L	[36]		
Concentric tubes nozzle	Tube-in-tube injection system in which CO <sub>2</sub> flowed in the external annulus. The two tubes had external diameters of 6.35 mm and 1.59 mm, respectively. The internal hole had a diameter of 120 μm.	Maximizes the surface between the liquid and the antisolvent and to favor the solubilization of the liquid in the fluid phase.		S-1: precipitator (internal volume 470mL, internal diameter 45mm) heated by a circulation heater. A stainless steel filter with a porosity of 1 μm was located at the bottom of the precipitator, to collect the powders. S-2: separator (internal volume of 500 mL) and was used to collect the liquid discharged from the precipitator.	[45]		
				Cyclonic separator	Conventional separator	[35]	
	d <sub>INTERNAL</sub> =1mm for BS d <sub>EXTERNAL</sub> =3.2mm for CO <sub>2</sub>	Particle size = 1μm. Agglomeration particles = 200μm		S1=1.5L	Separator flash.	[15]	

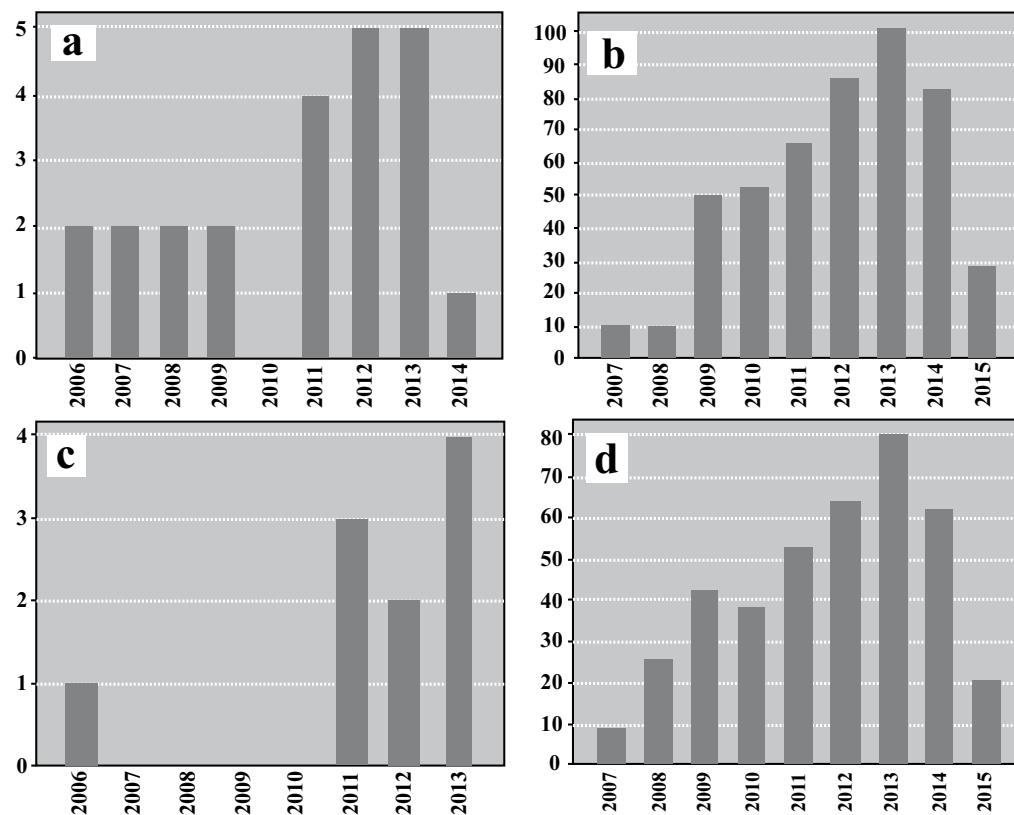


**Fig. (3).** Results for the search using the keywords “Antisolvent Supercritical Fractionation” in Web of Science database. 3.a. and 3.c. show the number of published articles per year and 3.b and 3.d. show the number of times these articles were cited from the first (using the keywords “Supercritical Antisolvent Fractionation”, 23 items found) and second (“Supercritical Antisolvent Fractionation”, ‘Vegetable Materials’ and/or “Phase Equilibrium”, 10 items found) search.

The injection system is defined as a three stages fractionation column, SC-CO<sub>2</sub> enters the column at the bottom and the BS is introduced from an upper part of the column. As the two fluids are mixed, the heavier solid compounds from BS are precipitated due to the solubility of the organic solvent in SC-CO<sub>2</sub> dragging along with the fluid stream of lighter compounds. Reaching this model of the injection system, the fractionation process appears to become efficient in terms purification of bioactive compounds through the simple insertion of stainless steel rings (10mm x 10mm) in the column in order to saturate the SC-CO<sub>2</sub> with the organic solvent by increasing the mass transfer between these solvents prior its expansion in the precipitation vessel. Since the interface between the two fluids is increased by the presence of these rings, a small portion of the organic solvent in the liquid drops of BS is lost [31].

Depending on the scale of the operational unit, some considerations can contribute to improving and increasing the efficiency of the process itself. For example, the use of operational laboratory scale unit can be used with flexibility and operational variables including the addition or modification of the elements or constituent parts of the operational unit, without incurring large investments of time, manpower, material resources and financial resources.

### 3. APPLICATIONS OF SAF FOR THE PURIFICATION OF BIOACTIVE COMPOUNDS

The Web of Science database [48] was used in this research to obtain data for the implementation of this review

article using the keywords “Supercritical Antisolvent Fractionation”. This research showed 38 results (including articles and patents) from 1992 until 2015. It was found that in 2006, the first published review article that addressed, the theme was from the authorship of E. Reverchon and I. De Marco [29]. Thus we proceeded to refine the search from 2006, resulting in 23 found items. From those 23 items, Fig. (3a) shows the number of published articles per year and Fig. (3b) shows the number of times these articles were cited. Afterwards another refining of the research was done focusing the attention on the relationship of the terms “Supercritical Antisolvent Fractionation”, ‘Vegetable Materials’ and/or “Phase Equilibrium”, resulting in the reduction from 23 to 10 items. Given this new classification, Figs. (3a and 3b) were replotted originating Figs. (3c and 3d), respectively.

It was observed that published works in an interval of four years do not exist, when employing the term “Supercritical Antisolvent Fractionation”. However it is possible to observe the impact that these items had, which is manifested by the number of citations they had with the passing of time.

In this section, some particularities of the 10 items are described (Table 3). The article published by Reverchon and De Marco [29], that possesses 368 citations, presents a review with information of the last 10 years about supercritical extraction using with or without cosolvent of volatile oils, pesticides, pharmaceuticals, colorants, antioxidants and the fractionation of liquid mixtures by SAF. In the 2006-2015 period, this work maintained per year the citation average of 36.8.

**Table 3.** Scientific publications and number of citations per year according to the term Supercritical Antisolvent Fractionation.

Title	Publication Date	Total Citations	Average Citations Per Year	2006	2007	2008	2009	2010	2011	2012	2013	2014	2015	References
Supercritical fluid extraction and fractionation of natural matter	SEP 2006	368	36.80	0	9	26	43	39	52	57	68	58	16	[29]
Supercritical CO <sub>2</sub> fractionation of rosemary ethanolic oleoresins as a method to improve carnosic acid recovery	APR 2011	11	2.20	-	-	-	-	-	0	5	5	0	1	[36]
Supercritical antisolvent fractionation of ryanodol from <i>Persea indica</i>	DEC 2011	5	1.00	-	-	-	-	-	0	2	3	0	0	[26]
Supercritical antisolvent extraction of antioxidants from grape seeds after vinification	OCT 2013	4	1.33	-	-	-	-	-	-	-	0	1	3	[45]
Supercritical antisolvent fractionation of lignans from the ethanol extract of flax-seed	MAR 2013	3	1.00	-	-	-	-	-	-	-	1	2	0	[31]
Phase equilibrium data for the ternary system (propane plus chloroform plus oryzanol)	JAN 2011	3	0.60	-	-	-	-	-	1	0	1	0	1	[49]
The utilization of oat polar lipids produced by supercritical fluid technologies in the encapsulation of probiotics	OCT 2013	1	0.33	-	-	-	-	-	-	-	0	1	0	[47]
Purification of lignans from <i>Schisandra chinensis</i> fruit by using column fractionation and supercritical antisolvent precipitation	MAR 2013	1	0.33	-	-	-	-	-	-	-	0	1	0	[23]
Supercritical extraction and supercritical antisolvent fractionation of natural products from plant material: comparative results on <i>Persea indica</i>	DEC 2012	1	0.25	-	-	-	-	-	-	0	1	0	0	[52]
Supercritical methodologies applied to the production of biopesticides: a review	DEC 2012	1	0.25	-	-	-	-	-	-	0	1	0	0	[53]

From this period of publication (2006-2015), our review article proposes to show detailed information about the use of SAF process for the purification of vegetable extracts solutions. SAF was used to obtain antioxidant compound, mainly carnosic acid, from high viscosity oleoresins, derived from rosemary dried leaves, extracted with ethanol [36], to purify a insecticide compound from *Persea indica* leaves, and to obtain phenolic compounds with antioxidant properties from grape wastes [45].

Phase equilibrium measurements for the system (gamma-oryzanol + cloroform) in compresses propane were performed to study the previous conditions to oryzanol fractionation [49]. A previous extraction step of oat flakes was performed for afterwards precipitate 35% of polar lipids using SAF [47].

#### 4. RECENT PATENTS ON BIOACTIVE COMPOUNDS OBTAINING USING SAF

On Web of Science database [48] few patents were found that hinder SAF recovery of bioactive substances through SAF process. Bioactive compounds purified by using SAF

revealed that it is A method for purifying schizadrin from schisandra fruit using 95% ethanol as solvent extraction assisted by ultrasound. From this effluent with total 20.3% schizadrin content an ethanolic extract was obtained with a recovery rate of 82%. Pressure range of 20-50 bar and 303 K [50].

A method for preparing a pure beta-carotene nanopowder from *dunaliella salina*, is comprised of the following steps: majorly extracting a *dunaliella salina* powder from tetrahydrofuran (THF) solvent by ultrasonic wave; purifying 3-cm column; and using supercritical carbon dioxide antisolvent tetrahydrofuran (THF) solution to obtain a crystalline deposit is registered on patent TW201300157-A, in which conditions of pressure and temperature are not specified [51].

#### 5. CURRENT & FUTURE DEVELOPMENTS

There is currently a growing interest for the elaboration of new products with commercial value through separation and purification of bioactive compounds from plant extracts. Supercritical anti-solvent fractionation (SAF) process is con-

sidered to be a clean technology suitable to attend these requirements.

One of the key challenges in the successful operation of a particle formation involving supercritical fluids is the monitoring and the control of the system. Different processing parameters that can govern the mean particle size and size distribution of nanoparticles were well investigated by manipulating the types of solvents, mixing vessel pressure, mixing vessel temperature, CO<sub>2</sub> flow rate, solution flow rate and solution concentration.

Various experimental works intended to optimize their processes through adaptations or modifications of equipments that constitute the SAF unit, as the study of process parameters.

SAF process is a technique to produce particles of bioactive compounds with high yield and purity. On the other hand, patents developed using this type of process are very scarce, less attention being given to the potential of this technique to purify plant extracts with a very complex content of bioactive compounds. Otherwise, we can conclude that this research topic is very promising since it can produce fractions of bioactive compounds in a continuous way with high purity, that can be used to prepare products with refined attributes, which gives it a greater commercial value.

## CONFLICT OF INTEREST

The authors confirm that this article content has no conflict of interest.

## ACKNOWLEDGEMENTS

R. Abel C. Torres and Ádina L. Santana thank Capes for their doctorate assistantship. Diego T. Santos thanks CAPES (7545-15-0) for the postdoctoral fellowship. M. Angela A. Meireles thanks CNPq for the productivity grant (301301/2010-7). The authors acknowledge CNPq (560914/2010-5) and FAPESP (2012/10685-8; 2015/13299-0) for financial support.

## REFERENCES

- [1] C. Chinnarasu, A. Montes, M. T. F. Ponce, L. Casas, C. Mantell, C. Pereyra, and E. J. M. de la Ossa, "Precipitation of antioxidant fine particles from Olea europaea leaves using supercritical antisolvent process", *J. Supercrit. Fluids*, Vol. 97, no. pp. 125-132, 2015.
- [2] G. Brunner, "Supercritical fluids: technology and application to food processing", *J. Food Eng.*, Vol. 67, no. 1-2, pp. 21-33, 2005.
- [3] G. Brunner, "Gas extraction: an introduction to fundamentals of supercritical fluids and the application to separation processes", Steinkopff ; Springer, Darmstadt: New York., 1994.
- [4] F. Miguel, A. Martin, T. Gamse, and M. J. Cocco, "Supercritical anti solvent precipitation of lycopene - Effect of the operating parameters", *J. Supercrit. Fluids*, Vol. 36, no. 3, pp. 225-235, 2006.
- [5] T. Bruno, C. A. Nieto de Castro, J. F. P. Hamel, and A. M. F. Palavra, "Supercritical Fluid Extraction of Biological Products", John Wiley & Sons, 1993.
- [6] A. Montes, N. Kin, M. D. Gordillo, C. Pereyra, and E. J. M. de la Ossa, "Polymer-naproxen precipitation by supercritical antisolvent (SAS) process", *J. Supercrit. Fluids*, Vol. 89, pp. 58-67, 2014.
- [7] P. Imsanguan, S. Pongamphai, S. Douglas, W. Teppaitoon, and P. L. Douglas, "Supercritical antisolvent precipitation of andrographolide from Andrographis paniculata extracts: Effect of pressure, temperature and CO<sub>2</sub> flow rate", *Powder Technol.*, Vol. 200, no. 3, pp. 246-253, 2010.
- [8] Y. Bakhtbakhshi, S. Alfadul, and A. Ajbar, "Precipitation of Ibuprofen Sodium using compressed carbon dioxide as antisolvent", *Eur. J. Pharmaceut. Sci.*, Vol. 48, no. 1-2, pp. 30-39, 2013.
- [9] A. Bertucco, M. Lora, and I. Kikic, "Fractional crystallization by gas antisolvent technique: Theory and experiments", *Aiche J.*, Vol. 44, no. 10, pp. 2149-2158, 1998.
- [10] E. Reverchon, G. Caputo, and I. De Marco, "Role of phase behavior and atomization in the supercritical antisolvent precipitation", *Indus. Eng. Chem. Res.*, Vol. 42, pp. 6406-6414, 2003.
- [11] P. G. Debenedetti, J. W. Tom, and S. D. Yeo, "Rapid expansion of supercritical solutions (RESS): fundamentals and applications", *Fluid Phase Equilibria*, Vol. 82, pp. 311-318, 1993.
- [12] E. Weidner, Z. Knez, and Z. Novak, "Method for Producing a Powder Product from a Liquid Substance or Mixture of Substances", WO Patent 9521688, 1995.
- [13] D. Yadav, and N. Kumar, "Nanonization of curcumin by antisolvent precipitation: Process development, characterization, freeze drying and stability performance", *Int. J. Pharmaceut.*, Vol. 477, no. 1-2, pp. 564-577, 2014.
- [14] D. Villanueva Bermejo, E. Ibáñez, G. Reglero, C. Turner, T. Fornari, and I. Rodriguez-Meizoso, "High catechins/low caffeine powder from green tea leaves by pressurized liquid extraction and supercritical antisolvent precipitation", *Separat. Purif. Technol.*, Vol. 148, pp. 49-56, 2015.
- [15] A. Visentin, S. Rodríguez-Rojo, A. Navarrete, D. Maestri, and M. J. Cocco, "Precipitation and encapsulation of rosemary antioxidants by supercritical antisolvent process", *J. Food Eng.*, Vol. 109, no. 1, pp. 9-15, 2012.
- [16] R. Adami, E. Reverchon, E. Jarvenpaa, R. Huopalahti, "Supercritical Antisolvent micronization of naloxone HCl on laboratory and pilot scale", *Powder Technol.*, Vol. 182, pp. 105-112, 2008.
- [17] P. Kraujalis, P. R. Venskutonis, E. Ibáñez, and M. Herrero, "Optimization of rutin isolation from Amaranthus paniculatus leaves by high pressure extraction and fractionation techniques", *J. Supercrit. Fluids*, Vol. 104, pp. 234-242, 2015.
- [18] O. J. Catchpole, J. B. Grey, K. A. Mitchell, and J. S. Lan, "Supercritical antisolvent fractionation of propolis tincture", *J. Supercrit. Fluids*, Vol. 29, no. 1-2, pp. 97-106, 2004.
- [19] C. Chinnarasu, A. Montes, M. T. Fernandez-Ponce, L. Casas, C. Mantell, C. Pereyra, E. J. M. de la Ossa, and S. Patabhi, "Natural antioxidant fine particles recovery from Eucalyptus globulus leaves using supercritical carbon dioxide assisted processes", *J. Supercrit. Fluids*, Vol. 101, pp. 161-169, 2015.
- [20] B.-C. Liu, C.-T. Shen, F.-P. Liang, S.-E. Hong, S.-L. Hsu, T.-T. Jong, and C.-M. J. Chang, "Supercritical fluids extraction and antisolvent purification of carotenoids from microalgae and associated bioactivity", *J. Supercrit. Fluids*, Vol. 55, no. 1, pp. 169-175, 2010.
- [21] J. L. Marqués, G. D. Porta, E. Reverchon, J. A. R. Renuncio, and A. M. Mainar, "Supercritical antisolvent extraction of antioxidants from grape seeds after vinification", *J. Supercrit. Fluids*, Vol. 82, pp. 238-243, 2013.
- [22] E. de Paz, Á. Martín, H. Every, and M. J. Cocco, "Production of water-soluble quercetin formulations by antisolvent precipitation and supercritical drying", *J. Supercrit. Fluids*, Vol. 104, pp. 281-290, 2015.
- [23] T.-L. Huang, J. C.-T. Lin, C.-C. Chyau, K.-L. Lin, and C.-M. J. Chang, "Purification of lignans from Schisandra chinensis fruit by using column fractionation and supercritical antisolvent precipitation", *J. Chromatogr. A*, Vol. 1282, pp. 27-37, 2013.
- [24] E. Haimer, M. Wendland, A. Potthast, U. Henniges, T. Rosenau, and F. Liebner, "Controlled precipitation and purification of hemicellulose from DMSO and DMSO/water mixtures by carbon dioxide as anti-solvent", *J. Supercrit. Fluids*, Vol. 53, no. 1-3, pp. 121-130, 2010.
- [25] M. A. Meneses, G. Caputo, M. Scognamiglio, E. Reverchon, R. Adami, "Antioxidant phenolic compounds recovery from Mangifera indica L. by-products by supercritical antisolvent extraction", *J. Food Eng.*, Vol. 163, pp. 45-53, 2015.
- [26] L. Martin, A. Gonzalez-Coloma, R. Adami, M. Scognamiglio, E. Reverchon, G. Della Porta, J. S. Urieta, and A. M. Mainar, "Supercritical antisolvent fractionation of ryanodol from Persea indica", *J. Supercrit. Fluids*, Vol. 60, pp. 16-20, 2011.
- [27] C. Chinnarasu, A. Montes, M. T. Fernandez-Ponce, L. Casas, C. Mantell, C. Pereyra, and E. J. M. de la Ossa, "Precipitation of

- Perspectives on the Application of Supercritical Antisolvent Fractionation Process
- antioxidant fine particles from *Olea europaea* leaves using supercritical antisolvent process", *J. Supercrit. Fluids*, Vol. 97, pp. 125-132, 2015.
- [28] Y. Zhang, X. Zhao, W. Li, Y. Zu, Y. Li, and K. Wang, "Preparation, characterization, and dissolution rate *in vitro* evaluation of total panax notoginsenoside nanoparticles, typical multicomponent extracts from traditional chinese medicine, using supercritical antisolvent process", *J. Nanomater.*, Vol. 2015, pp. 12, 2015
- [29] E. Reverchon, and I. De Marco, "Supercritical fluid extraction and fractionation of natural matter", *J. Supercrit. Fluids*, Vol. 38, no. 2, pp. 146-166, 2006.
- [30] O. J. Catchpole, J. B. Grey, K. A. Mitchell, and J. S. Lan, "Supercritical antisolvent fractionation of propolis tincture", *J. Supercrit. Fluids*, Vol. 29, no.1-2, pp. 97-106, 2004.
- [31] G. Perretti, C. Virgili, A. Troilo, O. Marconi, G. F. Regnicoli, and P. Fantozzi, "Supercritical antisolvent fractionation of lignans from the ethanol extract of flaxseed", *J. Supercrit. Fluids*, Vol. 75, pp. 94-100, 2013.
- [32] D. T. Santos, M. A. A. Meireles, "Micronization and encapsulation of functional pigments using supercritical carbon dioxide", *J. Food Process Eng.*, Vol.36, no.1, pp.36-49, 2013.
- [33] R. A. C. Torres, D. T. Santos, M. A. A. Meireles, "Novel extraction method to produce active solutions from plant materials", *Food Public Health*, Vol.5, no.2, pp.38-46, 2015.
- [34] M. N. Moraes, G. L. Zabot, and M. A. A. Meireles, "Extraction of tocotrienols from annatto seeds by a pseudo continuously operated SFE process integrated with low-pressure solvent extraction for bixin production", *J. Supercrit. Fluids*, Vol. 96, pp. 262-271, 2015.
- [35] T. Floris, G. Filippino, S. Scrugli, M. B. Pinna, F. Argiolas, A. Argiolas, M. Murru, and E. Reverchon, "Antioxidant compounds recovery from grape residues by a supercritical antisolvent assisted process", *J. Supercrit. Fluids*, Vol. 54, no. 2, pp. 165-170, 2010.
- [36] A. Visentin, M. Cismondi, and D. Maestri, "Supercritical CO<sub>2</sub> fractionation of rosemary ethanolic oleoresins as a method to improve carnosic acid recovery", *Innov. Food Sci. Emerg. Technol.*, Vol. 12, no. 2, pp. 142-145, 2011.
- [37] A. Gonzalez-Coloma, L. Martin, A. M. Mainar, J. S. Urieta, B. M. Fraga, V. Rodriguez-Vallejo, C. E. Diaz, "Supercritical extraction and supercritical antisolvent fractionation of natural products from plant material: comparative results on *Persea indica*", *Phytochem. Rev.*, Vol.11, no.4, pp.433-446, 2012.
- [38] R. A. C. Torres, "Bixin particles purification by precipitation with supercritical CO<sub>2</sub> anti-solvent from active solution Obtained from the extraction of semi-defatted seeds of annatto (*Bixa orellana* L.) assisted by ultrasound", University of Campinas/School of Food Engineering, Campinas, 2015.
- [39] Ž. Knez, E. Markočić, M. Leitgeb, M. Primožič, M. Knez Hrnčić, and M. Škerget, "Industrial applications of supercritical fluids: A review", *Energy*, Vol.77, pp. 235-243, 2014.
- [40] H.-Y. Chin, M.-J. Lee, H.-m. Lin, "Vapor-liquid phase boundaries of binary mixtures of carbon dioxide with ethanol and acetone", *J. Chem. Eng. Data*, Vol. 53, no. 10, pp. 2393-2402, 2008.
- [41] V. J. Pereira, R. L. Matos, S. G. Cardoso, R. O. Soares, G. L. Santana, G. M. N. Costa, and S. A. B. Vieira de Melo, "A new approach to select solvents and operating conditions for supercritical antisolvent precipitation processes by using solubility parameter and group contribution methods", *J. Supercrit. Fluids*, Vol. 81, pp. 128-146, 2013.
- [42] C. Zu, X. Zhao, and X. Du, "Enhanced water-solubility of Licorice extract microparticle prepared by antisolvent precipitation process", *Adv. Powder Technol.*, Vol. 25, no. 2, pp. 787-794, 2014.
- [43] M. Anwar, I. Ahmad, M. H. Warsi, S. Mohapatra, N. Ahmad, S. Akhter, A. Ali, and F. J. Ahmad, "Experimental investigation and oral bioavailability enhancement of nano-sized curcumin by using supercritical anti-solvent process", *Eur. J. Pharmaceut. Biopharmaceut.*, Vol. 96, pp. 162-172, 2015.
- [44] Y. Dong, W. K. Ng, J. Hu, S. Shen, and R. B. H. Tan, "A continuous and highly effective static mixing process for antisolvent precipitation of nanoparticles of poorly water-soluble drugs", *Int. J. Pharmaceut.*, Vol. 386, no. 1-2, pp. 256-261, 2010.
- [45] J. L. Marques, G. Della Porta, E. Reverchon, J. A. R. Renuncio, A. M. Mainar, "Supercritical antisolvent extraction of antioxidants from grape seeds after vinification", *J. Supercrit. Fluids*, Vol. 82, pp. 238-243, 2013.
- [46] H. Aro, E. Jarvenpaa, K. Konko, R. Huopalahti, and V. Hietaniemi, "The characterisation of oat lipids produced by supercritical fluid technologies", *J. Cereal Sci.*, Vol. 45, no. 1, pp. 116-119, 2007.
- [47] H. Aro, E. Järvenpää, J. Mäkinen, M. Lauraeus, R. Huopalahti, and V. Hietaniemi, "The utilization of oat polar lipids produced by supercritical fluid technologies in the encapsulation of probiotics", *LWT - Food Sci. Technol.*, Vol. 53, no. 2, pp. 540-546, 2013.
- [48] "Citation Report: 23 (from All Databases)", Available online: [http://apps.webofknowledge.com/CitationReport.do?product=UA&search\\_mode=CitationReport&SID=3FXObzJRT9yFV8YHBPt&age=1&cr\\_pqid=1&viewType=summary](http://apps.webofknowledge.com/CitationReport.do?product=UA&search_mode=CitationReport&SID=3FXObzJRT9yFV8YHBPt&age=1&cr_pqid=1&viewType=summary), Web of Science™.
- [49] F. V. Correa, S. R. R. Comim, A. M. de Cesaro, A. A. Rigo, M. A. Mazutti, H. Hense, and J. V. Oliveira, "Phase equilibrium data for the ternary system (propane plus chloroform plus oryzanol)", *J. Chem. Thermodynam.*, Vol. 43, no. 1, pp. 34-38, 2011.
- [50] C. Chang, T. Huang, C. M. Chang, and T. L. Huang, "Method for extracting high-purity schizandrin from schisandra fruit, involves applying ethanol solvent to ultrasonically extract schisandra powder, purifying using column and precipitating supercritical carbon dioxide", China, 2014.
- [51] C. Chang, Y. Shen, C. M. Chang, and Y. C. Shen, "Method for preparing purity beta-carotene nano powder from dunaliella salina capable of recycling at least beta-carotene of 36% from dunaliella salina per unit and producing nano particles of beta-carotene of at least 72.9% purity2013.
- [52] A. Gonzalez-Coloma, Á. Martín, A. M. Mainar, J. S. Urieta, B. M. Fraga, and V. Rodrigues-Vallejo, "Supercritical extraction and supercritical antisolvent fractionation of natural products from plant material: comparative results on *Persea indica*", *Phytochem. Rev.*, Vol. 11, no. pp. 413-431, 2012.
- [53] L. Martin, J. L. Marques, A. Gonzalez-Coloma, A. M. Mainar, A. M. F. Palavra, and J. S. Urieta, "Supercritical methodologies applied to the production of biopesticides: a review", *Phytochem. Rev.*, Vol. 11, pp. 413-431, 2012.

- CAPÍTULO 3 – ***Construction and Validation  
of an Online Subcritical Adsorption-based  
Device for Assisting CO<sub>2</sub> Recycling during a  
Supercritical Fluid Extraction Process***

O objetivo deste trabalho foi descrever o desenvolvimento de uma modificação de uma unidade piloto de extração de fluido supercrítico comercial projetada para auxiliar na reciclagem de CO<sub>2</sub> com base na adsorção subcrítica em um material adsorvente. O dispositivo proposto demonstrou ser muito promissor para aplicação no SFE pseudocontínuo

*Artigo publicado no periódico de acesso aberto*

*The Open Food Science Journal, 2018; v. 10, n°. 1, p. 3-17*

ISSN: 1874-2564 DOI: BMS-TOFSJ-2018-HT1-322-1



## RESEARCH ARTICLE

# Construction and Validation of an Online Subcritical Adsorption-based Device for Assisting CO<sub>2</sub> Recycling during a Supercritical Fluid Extraction Process

R. Abel C. Torres, Diego T. Santos and M. Angela A. Meireles\*

LASEFI/DEA/FEA School of Food Engineering/UNICAMP University of Campinas, R. Monteiro Lobato, 80; 13083-862, Campinas, SP, Brazil

Received: August 14, 2018

Revised: October 16, 2018

Accepted: November 12, 2018

### Abstract:

#### Background:

An efficient process for extracting food ingredients from plant materials should demand the use of a reduced volume of extraction solvent to obtain a final product that is free of solvent and reduces both the processing time and the costs. In some cases, achieving a new efficient process requires the modification, reconfiguration or renewal of elements that are part of a processing unit.

#### Objective:

The goal of this work is to describe the development of a modification of a commercial supercritical fluid extraction pilot unit designed to assist CO<sub>2</sub> recycling based on subcritical adsorption on an adsorbent material. In addition to the construction and validation of the system, a cost survey was performed to estimate the cost of the homemade device developed to allow effective CO<sub>2</sub> recycling.

#### Methods:

The developed device was tested using cotton and Celite® as model adsorption materials and annatto seeds (*Bixa orellana L.*) as a model plant material. A 0.65 L adsorption column was installed with a set of connections and valves that complemented the unit's recycle system. The validation procedure consisted of defatting annatto seeds.

#### Results:

The proposed online subcritical adsorption-based device was technically validated using cotton as an adsorbent material. The cost survey showed that an estimated total cost of USD 5731.36 would be required to install the developed device in a Supercritical Fluid Extraction (SFE) unit similar to the one coupled here (5 L).

#### Conclusion:

The proposed device was demonstrated to be very promising for application in the pseudocontinuous SFE, recirculating the same amount of CO<sub>2</sub> mass exceeding the S/F values by 14 times, when compared to a process without a CO<sub>2</sub> recycling system.

**Keywords:** *Bixa orellana L.*, CO<sub>2</sub> recycle, Online coupling, Plant extracts, SFE, Supercritical CO<sub>2</sub>.

## 1. INTRODUCTION

Several substances that can confer or intensify color, such as carotenoids ( $\beta$ -carotene, lycopene, lutein and zeaxanthin),

\* Address correspondence to this author at the LASEFI/DEA/FEA (School of Food Engineering)/UNICAMP (University of Campinas), CEP 13083-862, Campinas, SP, Brazil; Tel: +55 19 35210100; E-mail: maameireles@lasefi.com

thin) [1, 2], are added to foods to confer an extensive range of colors, including shades of red, orange and yellow [3]. There is a growing interest in using natural pigments because they present a wide range of biological activities, including antioxidant, anti-inflammatory, and anticancer activity [4 - 6].

Annatto seeds contain several carotenoid derivatives (including bixin and norbixin), terpenoids, tocotrienols, aromatic hydrocarbons, and flavonoids [7]. According to Rosa *et al.* [8], annatto seed oil is rich in tocotrienols, especially  $\gamma$ - and  $\delta$ -tocotrienols.

To obtain these compounds from annatto seeds, some conventional extraction techniques have been studied, such as extraction in oil, alkaline aqueous solutions and organic solvents [9] and mechanical extraction [10].

However, applications whose processes are called clean extraction technologies have also been studied. For example, Supercritical Fluid Extraction (SFE) has been studied by Albuquerque & Meireles [11], Moraes *et al.* [12] and Johner & Meireles [13]; pressurized liquid extraction (PLE) has been studied by Rodrigues *et al.* [14]; and Supercritical Fluid Extraction of Emulsions (SFEE) and Supercritical Antisolvent Precipitation (SAS) have been studied by Matthea *et al.* [15] and Santos & Meireles [16], respectively.

Based on clean extraction technologies, an efficient process for extracting food ingredients from plant materials should require the use of a small volume of extraction solvent to obtain the product without the presence of the solvent in the extract, reducing both the processing time and production costs. At the same time, efficient extraction contributes to the reduction of CO<sub>2</sub> emissions, which represents an international concern [17], as well as the search to reduce CO<sub>2</sub> emissions in relation to the energy generated to achieve such a reduction [18]. In Brazil and Latin America, the extraction of bioactive compounds from vegetable matrices using CO<sub>2</sub> as a solvent represents an attractive field [12]. As far as is known, semi-industrial commercial units are provided with a recycling mechanism for CO<sub>2</sub> that is sometimes reported to have some limitations in terms of functionality, since part of the extract goes to the reservoir of the recycling system, which limits its permanent use. One reason for this limitation is the high CO<sub>2</sub> flow rate that causes an inefficient separation. Decreasing CO<sub>2</sub> flow rate can be a possible solution. However, it consequently increases the extraction duration. Another possible solution is employing an adsorption column. Achieving new and efficient adsorption processes requires, in some cases, the modification, reconfiguration or renewal of the elements that are part of the processing unit. Therefore, the present work is related to these adaptations and details the modification of a commercial supercritical fluid extraction pilot unit to assist CO<sub>2</sub> recycling based on subcritical adsorption on an adsorbent material. Cotton and Celite® 512 medium were used as model adsorption materials, and annatto seeds (*Bixa orellana L.*) were used as a model plant material. In this context, this study aims to describe the development of a modification of a commercial supercritical fluid extraction pilot unit designed to assist CO<sub>2</sub> recycling based on subcritical adsorption on an adsorbent material. In addition to process construction and validation, a cost survey was performed to estimate the cost of the homemade device developed to allow effective CO<sub>2</sub> recycling.

## 2. MATERIALS AND METHODS

### 2.1. Raw Material Characterization

Annatto seeds of the variety Piave (*Bixa orellana L.*) were donated by Urucum do Brasil Ltda, located in Santa Marta, Monte Castelo - SP, Brazil. The seeds were stored at 291 K in a freezer (VF55D, Metalfrio, São Paulo, Brazil). The mean diameter of the annatto seeds,  $3.82 \pm 0.09$  mm, was calculated by an adaptation of Silva *et al.* [19]. A total of 30 annatto seeds were removed from 3.5 kg of seeds for the measurement of the lengths of their axes. Then, to repeat the measurement of lengths, 30 seeds were placed back into the bag (which again weighed 3.5 kg), and after homogenization, the procedure was repeated.

The moisture content of the annatto seeds,  $11.61 \pm 0.02$  g/100 g, was analyzed as described by AOAC [20] and was determined in triplicate by drying at 378 K until reaching constant mass. The true density ( $1.35 \pm 0.01$  g/cm<sup>3</sup>) of the particles was measured by pycnometry with helium gas at the Central Analytical Laboratory of the Institute of Chemistry - UNICAMP (Campinas, Brazil). The apparent density ( $0.7609 \pm 0.0000$  g/cm<sup>3</sup>) in SFE bench-scale unit, of the bed was calculated by dividing the sample feed mass by the extractor volume. The porosity of the bed was calculated by equation 1.

$$\varepsilon = 1 - \frac{\rho_a}{\rho_r} \quad (1)$$

where  $\rho_r$  is the true density of the particles;  $\rho_a$  is the apparent density of the bed; and  $\varepsilon$ : is the porosity of the bed.

## 2.2. Description of Supercritical Fluid Extraction Units

Two commercial supercritical fluid extraction units were used in this study, a bench-scale unit and a pilot-scale unit. In the bench-scale unit, the extraction kinetics of annatto seeds was investigated. However, in the pilot-scale unit, several elements were changed and adapted to test the possibility of recycling CO<sub>2</sub> without creating drag or with the least amount of drag, which would prevent the CO<sub>2</sub> from entering the extraction column.

### 2.2.1. SFE Bench-scale Unit

The main elements that compose the commercial SFE bench-scale unit (Spe-ed model, Applied Separations, Allentown, USA) are represented in Fig. (1). The extraction column used in this study has a total volume of 25 mL, height of 83.5 mm, and diameter of 20.0 mm.

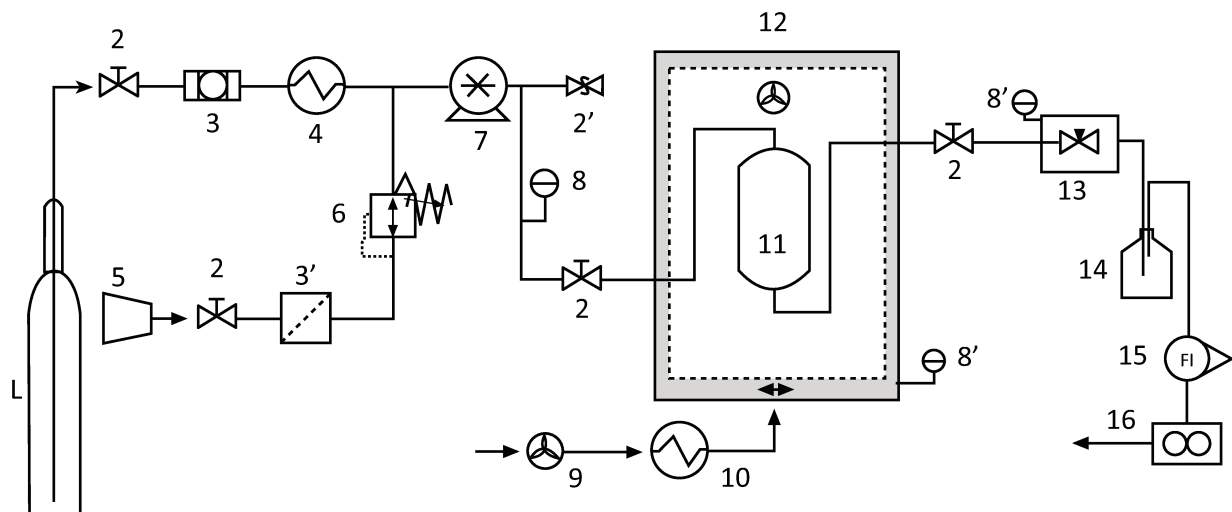


**Fig. (1).** SFE bench-scale unit. (1) CO<sub>2</sub> cylinder, (2) blocking valve, (2') safety valve, (3) line filter, (3') air filter, (4) cooling bath, (5) compressor, (6) air pressure regulator, (7) air-driven fluid pump, (8) manometer, (8') temperature indicator, (9) blow motor, (10) blow motor resistor, (11) extraction column, (12) oven module, (13) micrometric valve with heating system, (14) collection flask, (15) flow meter, (16) flow totalizer.

The operational sequence was as follows: CO<sub>2</sub> was cooled at 263 K by a cooling bath (Logen Scientific, LS-540, Diadema, Brazil) before reaching the pump. The desired temperature for CO<sub>2</sub> was obtained using hot air circulation by blow motor and blow motor resistor inside the oven module, which included the extraction column and the pipes connected to the inlet and outlet of the column. Accordingly, CO<sub>2</sub> transited a thermodynamic phase change from liquid state to supercritical state. Then, the extractor was kept at 20 MPa and 313 K for 20 min (static time) to get saturation of the solvent in the extractor before solvent pumping. After that, the outlet valve of extractor was opened, and the dynamic time of extraction was started. The extract was collected in a 100 mL glass vial immersed in an ice bath at ambient pressure. The total CO<sub>2</sub> was measured with a flow totalizer (Itron, model G1.0, Campinas, Brazil), and the mass flow for each process was calculated in an Excel spreadsheet, weighting the values of the density of the CO<sub>2</sub> found elsewhere [21] keeping the environment at a constant temperature; CO<sub>2</sub> was not recirculated. After the extraction, the glass vial was placed in a desiccator for thirty minutes to guarantee the complete elimination of CO<sub>2</sub>.

### 2.2.2. SFE Pilot-scale Unit Description

The commercial SFE pilot-scale unit (Thar Technologies, model SFE-2X5 LF-2-FMC, Pittsburgh, USA) used in this study was acquired in the framework of the PITE/FAPESP project (05/60948-1) in partnership with the company CENTROFLORA (Botucatu, SP) during the period 2006-2009.

The main elements that compose the initial state of the commercial SFE pilot-scale unit are represented in Fig. (2). The extraction column used in this study has a total volume of 5 L, height of 620 mm, and diameter of 106 mm. The open-closure sealing system is an internal thread with a depth of 7 threads x 39.0 mm and the cover is the external thread with a depth of 6 threads x 36.0 mm and sealing gasket (the maximum operating pressure and temperature are 68.95 MPa and 363 K, respectively).

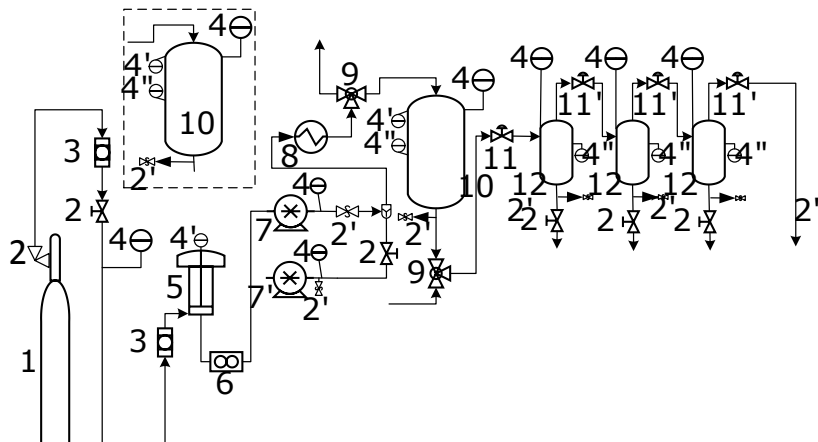


**Fig. (2).** Initial state of SFE pilot-scale unit. (1) CO<sub>2</sub> cylinder, (2) blocking valve, (2') safety valve, (3) line filter, (4) manometer, (4') internal temperature indicator, (4'') external temperature indicator, (5) heat exchanger with coiled tube for CO<sub>2</sub> cooling, (6) mass flow meter, (7) CO<sub>2</sub> pump, (7') cosolvent pump, (8) heat exchanger for CO<sub>2</sub> heating, (9) three-way valve, (10) extraction column, (11) automated backpressure valve, (11') manual backpressure valve, (12) separation vessel.

The operational sequence was as follows: CO<sub>2</sub> passed through the heat exchanger with coiled tube where it was cooled at 263 K by a cooling bath (Polyscience recirculator 6100T, Niles, Illinois, USA) and for the mass flow meter (Siemens Coriolis flowmeters SITRANS F C MASS 2100 Di 1.5), before reaching the pump (maximum flowrate of 350 mL/min, maximum operating pressure of 34.47 MPa). Then CO<sub>2</sub> passed through a heat exchanger, which raised the temperature and entered into the extraction column equipped with an electric heating jacket (Ogden Mighty-Miser CBE06A12A-02212, 2000 W, 240 V) kept to 313 K and 20 MPa for 20 min (static time) to get saturation of the solvent in the extractor before solvent pumping. After that, outlet three-way valve of extractor and the automated backpressure valve were opened, and the dynamic time of extraction was started. The extract was collected in three separators (Cyclone type, volume of 1 L, diameter of 74 mm, height of 275 mm. Each one with an electric heating jacket, Ogden Mighty-Miser CBE04J04A-02158, 500 W, 240 V). The total CO<sub>2</sub> was measured with a flow totalizer (Itron, model G1.6, Campinas, Brazil), and the mass flow for each process was calculated in an Excel spreadsheet, weighting the values of the density of the CO<sub>2</sub> found elsewhere [21] keeping the environment at a constant temperature. CO<sub>2</sub> was recirculated in 4 of 5 experiments (B, C, D and E). After the extraction, the extract was collected in glass bottles of 100 mL and placed in a desiccator for thirty minutes to guarantee the complete elimination of CO<sub>2</sub>.

### 2.3. Supercritical Fluid Extraction Experiments

#### 2.3.1. SFE Bench-scale Unit Experiments

CO<sub>2</sub> was used as the solvent (99.9% CO<sub>2</sub>, Gama Gases Especiais Ltd, São Bernardo do Campo, Brazil). The global extraction yield (X<sub>0</sub>) was obtained from kinetic curve data corresponding to the diffusion-controlled period [22]. The selected extraction conditions used in this study (313 K and 20 MPa) were set based on a previously optimized method for the recovery of tocotrienol-rich oil from annatto seeds by SFE developed by Albuquerque & Meireles [11] in an SFE bench-scale unit (290 mL). A 25 mL extractor was filled thoroughly with annatto seeds ( $15.4689 \pm 0.0001$  g (d.b.)), the CO<sub>2</sub> flow rate ( $11.10 \pm 0.04$  g/min) was kept constant. After that, the extraction bed was filled, and a plug of glass wool was placed on both the lower and upper ends of the extraction column. The relative yield (R, g extract/100 g of extractable) for the extraction was calculated using equation 2:

$$R \left( \frac{g \text{ extract}}{100 \text{ g of extractable}} \right) = \frac{\text{mass}_{\text{extract}} \left( \frac{S}{F} \right)}{\text{mass}_{\text{extract}} \left( \frac{S}{F} = 259 \right)} \times 100 \quad (2)$$

In our study, the global extraction yield ( $X_0$ ) was determined by the summation of the extract obtained from ethanol cleaning (after evaporation of the solvent) [23] and the extract obtained during the extraction kinetics experiment. Then, the glass vials were stored at 255 K until analysis. The  $X_0$  data obtained in this unit were compared with the data obtained in the pilot-scale unit.

The experimental overall extraction curve (OEC) data obtained using the bench unit were adjusted to fit a spline with three straight lines using the software SAS 9.2®. This software allowed the annatto oil extraction kinetic parameters to be determined, including the constant extraction rate (CER) period ( $t_{\text{CER}}$ ), the mass transfer rate for the CER period ( $M_{\text{CER}}$ ), the yield for the CER period ( $R_{\text{CER}}$ ), the mass ratio of solute in the fluid phase at the extractor outlet for the CER period ( $Y_{\text{CER}}$ ), the falling extraction rate (FER) period ( $t_{\text{FER}}$ ), the mass transfer rate for the FER period ( $M_{\text{FER}}$ ), the yield for the FER period ( $R_{\text{FER}}$ ) and the mass ratio of solute in the fluid phase at the extractor outlet for the FER period ( $Y_{\text{FER}}$ ).

Jesus *et al.* [24] describe the spline model adopted in this study with three periods using extraction kinetics data:

$$\begin{aligned} & \text{when } t \leq t_{\text{CER}}: \\ m_{\text{EXT}} &= b_0 + a_1 t \end{aligned} \quad (3)$$

$$\begin{aligned} & \text{when } t_{\text{CER}} < t \leq t_{\text{FER}}: \\ m_{\text{EXT}} &= b_0 + a_1 t + a_2(t - t_{\text{CER}}) \end{aligned} \quad (4)$$

$$\begin{aligned} & \text{when } t > t_{\text{FER}}: \\ m_{\text{EXT}} &= b_0 + a_1 t + a_2(t - t_{\text{CER}}) + a_3(t - t_{\text{FER}}) \end{aligned} \quad (5)$$

where  $t$  is the time of extraction (min);  $m_{\text{EXT}}$  is the mass of extract (g);  $b_0$  is the linear coefficient (zero-order term) of the CER straight line (g); and  $a_1$ ,  $a_2$  and  $a_3$  are the slope coefficients (first-order terms) of the CER, FER, and DC (diffusion-controlled) straight lines, respectively (g/min).

According to the results of Meireles [25] and Moraes *et al.* [26],  $t_{\text{CER}}$  is the intersection of the first straight line with the second, and  $t_{\text{FER}}$  is the intersection of the second straight line with the third (DC, diffusion-controlled) straight line.

Noticeably, this model is exclusively used for extractor, and it does not cover the adsorption column.

### 2.3.2. SFE Pilot-scale Unit Experiments

The extraction conditions (313 K and 20 MPa) set for the bench-scale unit for defatting annatto seeds were set for the SFE pilot-scale unit for 5 experimental runs. Based on previous studies performed in a pilot-scale unit, the automated backpressure valve was opened to flow CO<sub>2</sub> with the mass flow rate of 200 g/min [23]. The fractionation of the extracts by pressure and temperature reduction was also performed to obtain the heaviest fraction in the first separation vessel (SV), and the lighter fractions in the following separator vessels were as follows: SV1 (P = 8.0 MPa, T = 313 K), SV2 (P = 6.5 MPa, T = 303 K) and SV3 (P = 6.5 MPa, T = 313 K). These data were defined through detailed literature review. The use of a higher pressure reduces the cost of recompressing the solvent for recycling within the process [27]. Thus, Prado [23] inferred that a pressure of approximately 6 MPa may be economically interesting for use in separator vessels at an industrial level. Therefore, in this study, we chose to set the pressure of the last separator vessel (SV3) at 6.5 MPa.

There were 5 experimental runs carried out in the SFE pilot-scale unit. Experimental run A was developed according to the initial state just as the pilot-scale unit was found (in other words without any modification). The recycling and adsorption system was adapted to the pilot-scale unit to carry out the experimental runs from B to E. In the experimental runs, B and C, and, D and E, silicon dioxide (Celite® 512 medium) and cotton (in a uniform orthopedic blanket roll) (Hydrophilic Cotton, Medi House, São Paulo, Brazil), respectively, were tested as adsorbent materials for

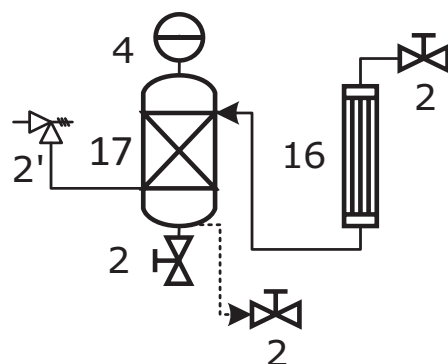
the validation of the developed online subcritical adsorption-based device for assisting CO<sub>2</sub> recycling during SFE. When using the Celite® 512 medium, the 0.65 L adsorption column was filled with 150 g of silicon dioxide inserted to the bottom part of the AdC, and a plain weave stainless steel disc filter (wire diameter 0.18 mm, aperture size 0.15 mm) was inserted on the top of silicon dioxide. The remaining part of AdC was filled with 0.43 kg of glass beads with a diameter of 0.3 mm, but when using cotton, only 100 g filled the adsorption column.

The tendency of the effect of three moments of pressurization/depressurization was studied in the experimental runs B and C, in that a single moment of pressurization/depressurization was applied for the experimental runs D and E.

#### 2.4. Description of SFE Pilot-scale Modifications

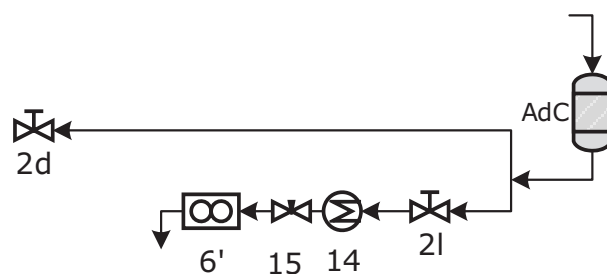
To recirculate CO<sub>2</sub> at purity conditions similar to those of the initial feed, an AdC was installed between the SV3 outlet and the CO<sub>2</sub> condenser, which was connected to what is here called the lung tank (LT). The capacity of LT is 15 L volume, having a maximum allowable working pressure of 10.34 MPa at 298 K, and it is made of 304 stainless steel.

Fig. (3) shows the initial step of the recycle system construction, as well as its main components.



**Fig. (3).** Initial step of the recycle system construction. (2) blocking valve, (2') safety valve, (4) manometer, (16) shell and tube heat exchanger, (17) lung tank (LT).

The purpose of installing an AdC (this column was maintained at an average room temperature of 295 K, it has no heating system) as part of the initial CO<sub>2</sub> recycle system was to keep the CO<sub>2</sub> mass in the same condition as if it were entering the system for the first time (*i.e.*, 99.9% purity). To this end, a 0.65 L (height of 22 cm and diameter of 12 cm) AdC was installed with a set of connections and valves that complemented the pilot-scale unit's recycle system. Fig. (4) shows the sequence of connections, valves, and piping that was installed in the final stage of the study, and Fig. (5) shows the final state of the SFE pilot-scale unit after the inclusion of the online subcritical adsorption-based device (shown in red).



**Fig. (4).** Final step of the recycle system construction. Adsorption column (AdC) and other components as part of the recycle system of the pilot-scale unit. (2) blocking valve, (6) diaphragm flow meter, (AdC) adsorption column, (14) heat exchanger with electric resistance to heat the micrometering valve, (15) micrometering valve.

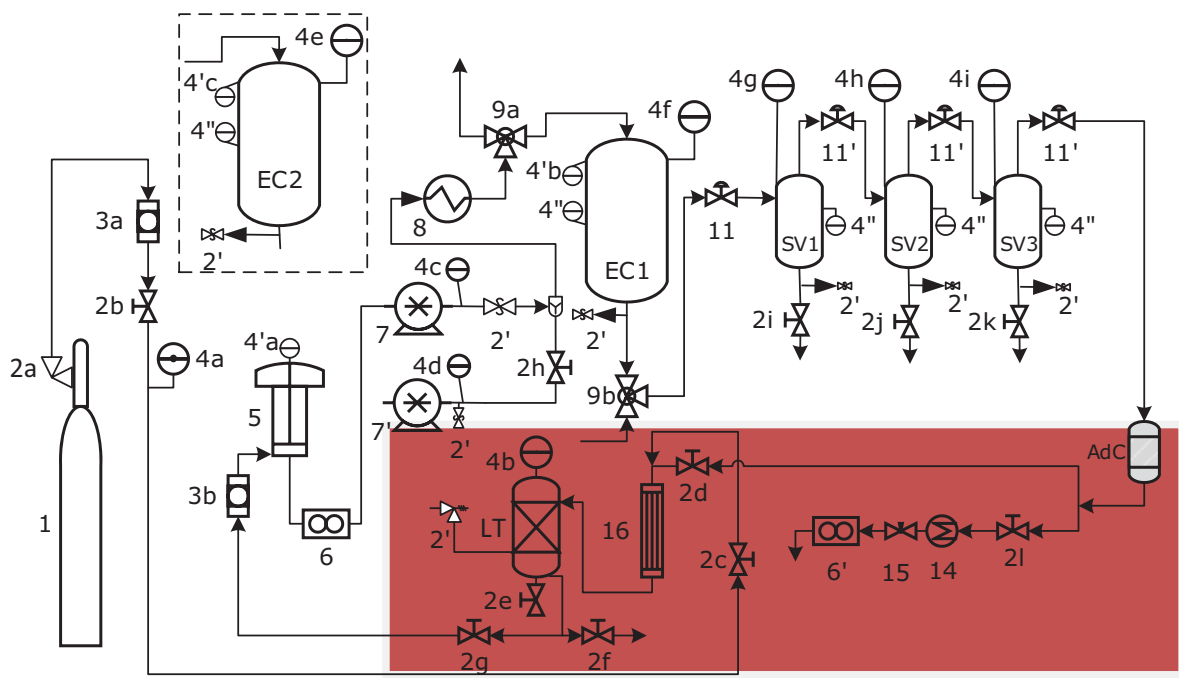


**Fig. (5).** Final state of SFE pilot-scale unit after online subcritical adsorption-based device inclusion. (1) CO<sub>2</sub> cylinder, (2) blocking valve, (2') safety valve, (3) line filter, (4) manometer, (4') internal temperature indicator, (4'') external temperature indicator, (5) heat exchanger with coiled tube for CO<sub>2</sub> cooling, (6) mass flow meter, (7) CO<sub>2</sub> pump, (7') cosolvent pump, (8) heat exchanger for CO<sub>2</sub> heating, (9) three-way valve, (10) extraction column, (11) automated backpressure valve, (11') manual backpressure valve, (12) separation vessel, (13) adsorption column (AdC), (14) heat exchanger with electric resistance, (15) micrometering valve, (16) shell and tube condenser, (17) lung tank (LT).

To facilitate cleaning and to understand in detail the parts that composed the developed recycle device, all the connections were disassembled to evaluate the possibility of avoiding dragging the extract toward the LT (17, in Fig. (3)). The blocking valve located at the inlet of the refrigeration heat exchanger (CO<sub>2</sub> condensing column) can operate at up to 41.37 MPa CWP (cold working pressure) and 311 K. The shell and tube heat exchanger used for refrigeration was of model # 00256-06 (Garden City, NY, USA), and the tube side pressure could withstand maximum conditions of 8.3 MPa [28]. The shell and tube heat exchanger contains 61 numbers of tubes with length and diameter of 51 cm, and 2.5 mm respectively. The cooling solution, composed of water + ethylene glycol (50:50 v/v), entered the side of the heat exchanger by applying pressure to the inner pipes of the exchanger. According to PolyScience [29], the maximum pressure exerted by the recirculating cooling bath (PolyScience recirculator 6100T - 230 V / 60 Hz / 12.2 A / 1 HP, Niles, Illinois, USA) that drives the refrigerant solution is 0.62 MPa. In addition, the minimum range of the flow rate alarm set point is 3 to 8 LPM (liters per minute), and the maximum flow rate at 0 MPa is 13.2 LPM [30].

With the modifications made in the recycling system, the experiments from B to E were developed as follows: the processes B and C are as follows: 1) The extractor was pressurized from 0.1 MPa to 20 MPa during 20 min. Then, the extractor remains in this condition for 20 min (static time). After that, the extractor was depressurized to 7 MPa. 2) The extractor was pressurized again from 7 MPa to 20 MPa during 10 min and remained in this condition for 20 min (static time). Then, the output valve of extractor was opened to start the dynamic extraction until reaching values of S/F ratio (g CO<sub>2</sub>/g annatto) 25, for B, and 10.36, for C. Next, the recycling valve (2d in Fig. (5)) was closed, and the ambient valve (2l in Fig. (5)) was opened to flow out the CO<sub>2</sub> to the ambient. After that, the extract was collected and weighted. 3) The same procedure of part 2 was repeated except that the pressurization occurs from 0.1 MPa to 20 MPa during 20 min.

In cases D and E, first the extractor was pressurized from 0.1 MPa to 20 MPa during 20 min. Then, the extractor remains in this condition for 20 min (static time). After that, the output valve of extractor was opened to start the dynamic extraction until reaching values of S/F 25.45, for D, and 55.98, for E. Next, the recycling valve (2d in Fig. (5))

was closed, and the ambient valve (2l in Fig. (5)) was opened to flow out the CO<sub>2</sub> to the ambient.

### 3. RESULTS AND DISCUSSION

#### 3.1. Effects of the Ratio of Solvent Mass to Feed Mass on the Extraction Yield Using the SFE Bench-scale Unit

The global extraction yield (X<sub>0</sub>) was obtained from kinetic curves corresponding to the diffusion-controlled period. In practical aspects, the global extraction yield (X<sub>0</sub>) represents the maximum amount of extract that can be recovered from a raw material at a given extraction pressure and temperature. In contrast to the bench-scale unit, in the pilot-scale unit, it is not possible to collect extracts continuously during kinetics experiments. It is necessary to interrupt the solvent flow and then depressurize the separators while keeping the extractor pressurized so that the extract can be collected, as is the case with experimental runs B and C. After this procedure, the extraction can be resumed until the next collection point. Interrupting the extraction at each point implies intermediary static periods in the extractor. Thus, in this study, we used the bench-scale unit to determine the overall extraction curve (OEC) and X<sub>0</sub> for annatto-seed extraction.

Fig. (6) shows the OEC obtained for annatto-seed SFE at the bench scale. The results are expressed in terms of the relative yield (R, g extract/100 g of extractable) of the extraction. The term extractable represents the maximum amount of extract that can be recovered from a raw material at a given extraction pressure and temperature within the diffusion-controlled period (S/F ratio of 259 g CO<sub>2</sub>/g annatto, which is in a good agreement with the value obtained by Moraes *et al.* [26]). The OEC presents a short CER (constant extraction rate) period of 26.17 min, which accounts for almost 60% of the total extract. A DC (diffusion controlled) period follows, with a rapid decrease in the extraction rate; this is the intermediary FER (falling extraction rate) period. The kinetic parameters calculated from the analysis performed using the software SAS 9.2® are in Table 1, where t<sub>CER</sub> is the time of the CER, M<sub>CER</sub> is the mass-transfer rate and R<sub>CER</sub> is the yield achieved during this period. The value of t<sub>CER</sub> roughly represents the minimum time an SFE cycle should last to keep the process economically viable [25]. Y<sub>CER</sub> is the mass ratio of solute in the supercritical phase at the bed outlet during the CER period.

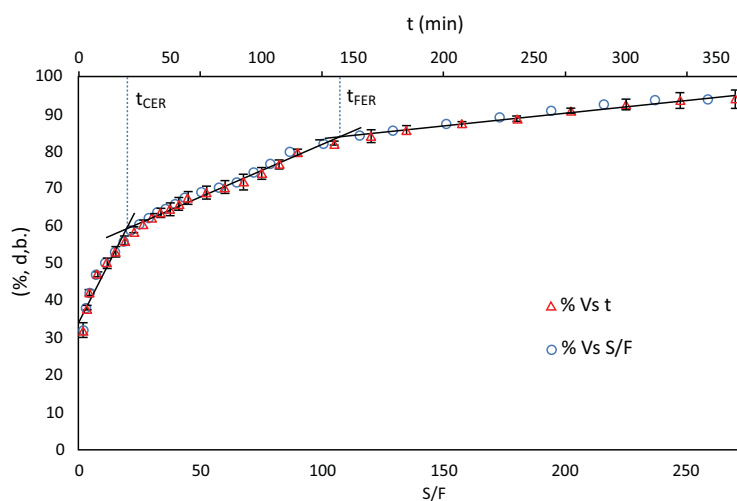


**Fig. (6).** Overall Extraction Curve (OEC) for annatto-seed extraction (313 K and 20 MPa) in the bench-scale unit; (—) indicates data fitted using SAS 9.2®.

**Table 1. Kinetic parameters of SFE from annatto seeds estimated using an SFE bench-scale unit\*.**

b0 ± SD	a1 ± SD	a2 ± SD	a3 ± SD
33.983 ± 0.578	0.997 ± 0.070	0.213 ± 0.006	0.050 ± 0.026
t <sub>CER</sub> (min) ± SD	M <sub>CER</sub> (g/min) × 10 <sup>3</sup> ± SD	R <sub>CER</sub> (%) ± SD	Y <sub>CER</sub> (g ext/g CO <sub>2</sub> ) × 10 <sup>4</sup> ± SD
24.83 ± 2.94	4.34 ± 0.35	58.58 ± 2.07	8.77 ± 1.09
t <sub>FER</sub> (min) ± SD	M <sub>FER</sub> (g/min) × 10 <sup>3</sup> ± SD	R <sub>FER</sub> (%) ± SD	Y <sub>FER</sub> (g ext/g CO <sub>2</sub> ) × 10 <sup>4</sup> ± SD
138.87 ± 20.98	2.27 ± 0.08	83.08 ± 3.43	2.23 ± 0.29

\*The parameters are presented with all digits from SD to avoid rounding errors in case of use of the model for simulating purposes.

Obtaining the CO<sub>2</sub> density as a function of ambient pressure (from [21]) together with the monitoring of both ambient pressure (measured through an aneroid barometer) and the volumetric flow of CO<sub>2</sub> (measured with the flow totalizer -16 of Fig. (1) and with a chronometer), allowed us to control CO<sub>2</sub> mass flow rate as accurate as possible. Accordingly, the error for CO<sub>2</sub> flow rate, 0.04 g/min, compared to the average of CO<sub>2</sub> flow rate, 11.10 g/min, indicates the infinitesimal impact of the precision of CO<sub>2</sub> flow rate on both the overall extraction curves and model parameters in this study.

Based on the OEC and kinetic parameters calculated, we also performed 3 runs in the SFE bench-scale system to ensure the reliability of experimental data using different solvent mass to feed mass (S/F) ratios which can be seen in Fig. (6). The Table 2 shows the results for the global extraction yield (X<sub>0</sub>) and residual extract indicators when S/F was varied. It can be observed that both the S/F ratio and the global extraction yield (X<sub>0</sub>) values had a coefficient of variation close to 1%, which represents a high reliability in the performed process. The Standard deviation reported in this table are related to the uncertainty of the experiments.

**Table 2. Percentage representation of the total extract and the residual extract for defatting annatto seeds using the bench-scale unit.**

Extraction	Annatto seeds (g) d.b.	S/F	Global extraction yield (X <sub>0</sub> )		Residual extract indicators		
			(g)	% [g extract/ 100 g annatto seeds]	(g)	% [g extract/ 100 g annatto seeds]	% [Percentage of residual extract]
1	15.4689	257.00	0.431	2.79	0.0382	0.25	8.23
2	15.4688	259.04	0.438	2.83	0.0229	0.15	5.04
3	15.4690	260.02	0.440	2.84	0.0186	0.12	4.05
Mean ± SD	15.4689 ± 0.0001	259 ± 2	0.436 ± 0.005	2.82 ± 0.03	0.027 ± 0.01	0.17 ± 0.07	6 ± 2
Coefficient of variation (%)	0.0006	0.60	1.040	1.04	38.7765	38.78	39.89

On the other hand, the process had a high variability with respect to the values obtained related to the extract collected during the cleaning of the unit (residual extract amount), which can be seen in terms of the standard deviation and coefficient of variation, indicating a strong correlation to the S/F ratio. The lower the S/F ratio is, the lower is the X<sub>0</sub> and the higher is the accumulation of extract inside the parts of the SFE bench-scale unit, and vice versa. In contrast, approximately 6% of the total amount of extract that can be extracted from the annatto seeds using the SFE conditions used here (313 K and 20 MPa) corresponds to the amount of extract lost from the retention of extract in the pieces of equipment used. The residence time of CO<sub>2</sub> in the extractor of bench unit was 0.08 s, while the residence time of pilot unit was from 8.03 to 19.60.

Santos *et al.* [31], using the same commercial equipment, observed a similar percentage of residual extract (7%) for annatto-seed extraction under different SFE conditions (31 MPa, 333 K). The authors also compared commercial equipment with a homemade system that had a similar volume capacity and observed that a significantly higher amount of residual extract was deposited in the tubing line when the homemade equipment was used compared with the amount of residual extract obtained using the commercial SFE apparatus; thus, when using the homemade modification that we applied to the pilot-scale unit, accounting for this loss of extract was a concern.

Before studying the effects of the ratio of solvent mass to feed mass on the extraction yield using the SFE pilot-scale unit, we performed preliminary tests with the developed online subcritical adsorption-based device coupled to the system to validate the device. Silicon dioxide (Celite® 512 medium) and cotton (in a uniform orthopedic blanket roll) (Hydrophilic Cotton, Medi House, São Paulo, Brazil) were tested as adsorbent materials. The technical viability validation criterion adopted, in addition to visual observation of the adsorbent material after the SFE process, consisted of monitoring the effects of the increased solvent mass to feed mass (S/F) ratio on the extraction yield and percentage of residual extract in the equipment parts and comparing the results for the SFE pilot-scale unit coupled with the online subcritical adsorption-based device with the results for the SFE bench-scale unit.

### 3.2. Preliminary Tests of the Developed Online Subcritical Adsorption-based Device for Assisting CO<sub>2</sub> Recycling in an SFE Pilot-scale Unit

Table 3 shows the results for extraction yield and residual extract percentage when solvent mass to feed mass ratio

(S/F) was varied. The term extraction yield is defined as the summation of mass of extract obtained in three separators per 100 g of raw material. Moreover, the term residual extract percentage in this table indicates the amount of residual extract retained inside the tubing system of the SFE unit. Based on this table, the Extraction yield was increased from 2.84, for B, to 3.09, for C. The residual extract was decreased from 8.12, for B, to 6.55, for C. The main reason for this drop of residual extract is the higher value of S/F for C compared to B that leads higher removal of extract available in the tube lines and connections. It can be observed that the values obtained related to the extract collected during the cleaning of the unit (residual extract percentage) presented a strong correlation to the values of S/F ratio.

**Table 3. Percentage representation of the total extract and the residual extract for defatting annatto seeds using a pilot-scale unit with a coupled subcritical adsorption-based device.**

Run	Annatto seeds (g) d.b.	S/F	Extraction yield				Residual extract indicators			
			(g) of extract in the 3 separation vessels	% [g extract/ 100 g annatto seeds]	(g) of extract/ 100 g of cotton present in the AdC	% [g extract/ 100 g annatto seeds]	Separator connections (g)	Others (g)	% [g extract/ 100 g annatto seeds]	% [Percentage of residual extract]
A	3111.33	3.69	44.31	1.42	without AdC	1.42	6.97	1.62	0.28	16.65
B	3239.23	25.00 19.38	44.37 88.93 3.05	91.98 2.75 0.09	2.84	---	2.84	7.55	0.58	0.25 8.12
C	3072.43	10.36 45.73	55.73 51.79 42.37	94.16 1.69 1.38	3.06	---	3.09	6.28	0.32	0.21 6.55
D	1326.66	25.45	24.14	1.82	1	1.89	2.85	0.17	0.23	10.73
E	1326.44	55.98	32.04	2.42	0.66	2.46	2.48	0.20	0.20	7.58

The higher the S/F ratio, the higher the extraction yield (measured by collecting the extracts in the 3 separation vessels), and the lower the accumulation of extract inside the parts of the SFE pilot scale unit (Residual Extract Percentage %). So, the use of silicon dioxide as adsorbent material for increasing extract recovery besides allow CO<sub>2</sub> recycling is an important issue to be addressed.

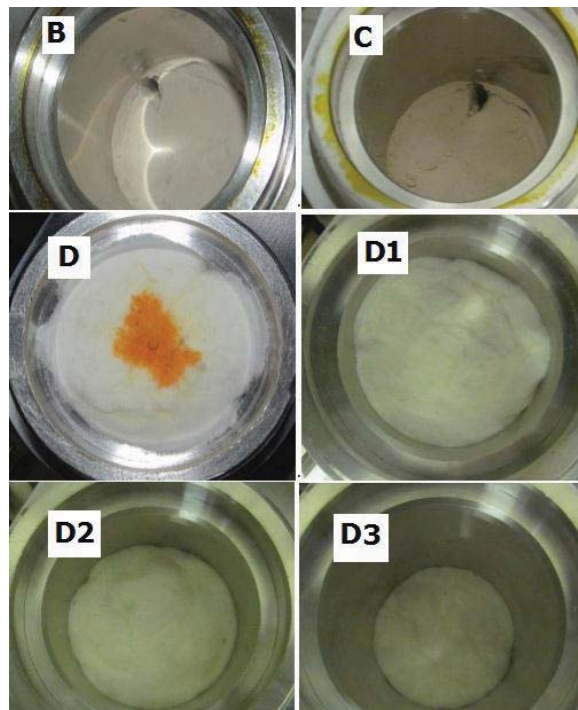


**Fig. (7).** Adsorbent materials used in the online subcritical adsorption-based device. B and C are Celite, and D is cotton. D1, D2 and D3 correspond to successive layers of cotton after removing the first layer seen in D.

The two adsorbent materials tested were compared in terms of operational aspects and cost. Because cotton is a soft-textured fibrous material, it facilitated the operability of the adsorption column at the time of packaging and unpacking. Almost 100 g (with a cost equivalent to approximately R\$ 25.00/kg, which is very cheap - approximately 10% of the cost of silicon dioxide (Celite® 512 medium, R\$ 263.00/kg)) was adequate to fill the 0.65 L volume of the adsorption column. In addition, other operational limitations (*i.e.*, the formation of preferred paths, as well as the loss of mass between the internal spaces of the adsorption column covers when collecting the Celite® 512 medium at the end of processing), made this product less preferable compared with cotton.

Another important conclusion regarding the operability of the proposed supercritical fluid extraction process concerned the cleaning step.

The need to reduce these cleaning times and the amount of cleaning solvents required led to the identification of empty spaces (Fig. 8) where the extracted material accumulated after each processing run. Studies performed by Torres [32] showed a similarity to this case, and therefore, the same strategies, such as the use of Teflon bushings, were applied to improve the equipment. Using Teflon bushings in the separators caused a dramatic drop in both cleaning time, from 40 h (after each experimental run, especially in cases of A, B and C) to 12 h (after each experimental run, D and E), and consumption solvent (essentially ethanol) volumes, from 14 L to 3 L.

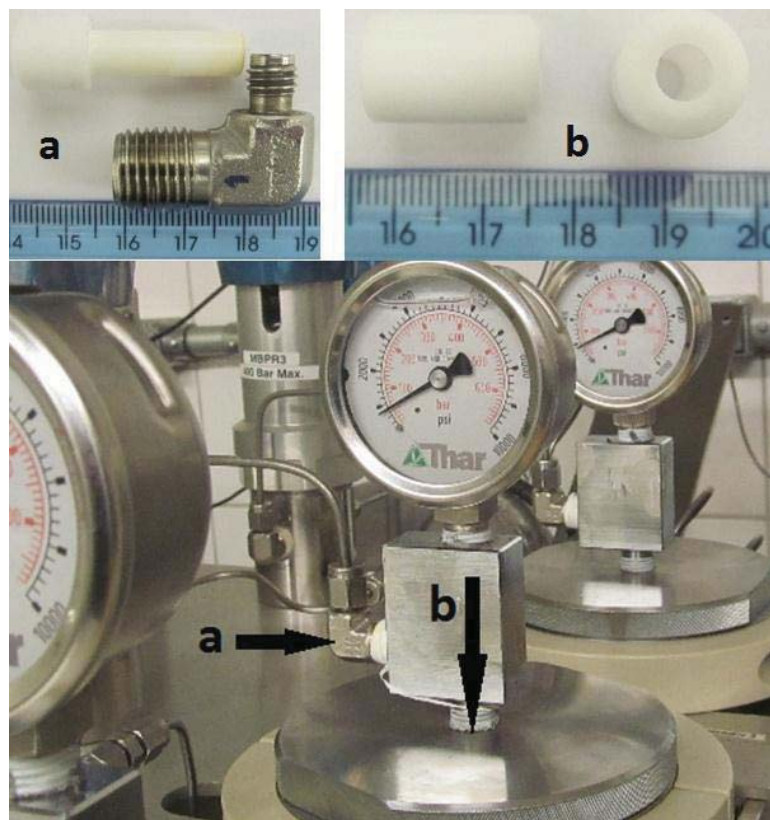


**Fig. (8).** Teflon bushings used to avoid the accumulation of extract in the SFE pilot-scale unit coupled with the developed online subcritical adsorption-based device.

### 3.3. Effects of the Ratio of Solvent Mass to Feed Mass on the Extraction Yield Using the SFE Pilot-scale Unit Coupled with the Online Subcritical Adsorption-based Device

After unit adjustments and the technical viability demonstration of the inclusion of the subcritical adsorption-based device in the SFE pilot-scale unit, 5 experimental runs (A-E) were performed to evaluate the effect of the solvent mass to feed mass (S/F) ratio on the extraction yield to validate the technical viability and better understand the process. Based on the OEC and kinetic parameters calculated using the data from defatting annatto seeds using the SFE bench-scale system, the extraction conditions were selected.

Run A was performed according to the initial state of the pilot-scale unit, *i.e.*, without any changes being made to the equipment. Thus, this extraction process served to allow data such as CO<sub>2</sub> consumption (approximately 13 kg) to be

surveyed under the processing conditions. In addition, Run A was performed to better compare the effects of the inclusion of the adsorption column and Lung Tank (LT) in assisting CO<sub>2</sub> recycling. Runs B and C correspond to the tests in which silicon dioxide (Celite® 512 medium) was used as an adsorbent material. Runs D and E correspond to the tests where the cotton (in a uniform orthopedic blanket roll) was used as an adsorbent material.

Table 3 shows the results for extraction yield and residual extract indicators when S/F was varied. It should be observed here that the extraction yield differs from the global extraction yield (X0) previously obtained in the bench-scale unit since the latter represents the maximum amount of extract that can be recovered from a raw material at a given extraction pressure and temperature (2.82% for annatto seeds for SFE at 313 K and 20 MPa). As observed for the bench-scale unit experiments, the values obtained related to the extract collected during the cleaning of the unit (residual extract amount) were strongly correlated to the S/F ratio. The higher the S/F ratio is, the higher is the extraction yield measured by collecting the extracts in the 3 separation vessels and the lower is the accumulation of extract inside the parts of the SFE pilot-scale unit. Comparing the percentages of residual extract obtained in the pilot-scale unit during runs A-E (7.58-16.65%) with those obtained previously in the bench-scale unit (4.05-8.23%), it can be observed that the pilot-scale unit retains more extract in its tubing (7.58-16.65%). Therefore, any gain related to an increase in the amount of extract collected would be interesting. Therefore, the use of cotton as an adsorbent material for increasing extract recovery in addition to allowing CO<sub>2</sub> recycling is a critical issue to be addressed.

In this context, we can see that an increase of 3.8 and 1.6% in the extraction yield was obtained using cotton inside the online subcritical adsorption-based device in runs D and E, respectively. In terms of the adsorbed extract amount (in grams) divided by 100 g of cotton, equivalent values of 1.02% and 0.67% were obtained, indicating that the amount of annatto-seed oil in the final adsorbent material is approximately 1% (see Fig. 7d, the colored cotton material with extract). Considering that in Run E, the S/F ratio was approximately double the value applied in Run D, we can infer that similarly to what occurred with the residual extract deposited in the tubing lines in both units tested here, the use of a higher S/F ratio is also preferred for reducing extract accumulation inside the adsorption column. In our case, when the S/F ratio was increased by 119.61%, the amount of adsorbed extract was reduced by 34.31%. Table 3 also shows the improvement in terms of the lower retention and accumulation of extracts obtained by the inclusion of Teflon bushings in the unit, comparing runs A, B and C (without unit adjustments) with runs D and E (with Teflon bushings and coupled with the developed online subcritical adsorption-based device).

Del Valle *et al.* [33] mentioned that one of the reasons for a low extraction yield compared with that obtained on an analytical (or laboratory) scale is the dispersion of the material extracted between the extraction column and the

separators. Corroborating these findings, in this study, we found that 92.54% and 94.37% of the total residual extract was provided by the separation-vessel cleaning step in runs B and C, respectively.

About the possibility of channeling in this study, it should be noted that the apparent density of the raw materials inside the extractor was the same for the whole runs, 0.7 g/cm<sup>3</sup>. According to the reference 33, the possibility of channeling is higher for a bed with height per diameter ratio of unity, which is far away from height per diameter ratio of 2.4 to 5.8 in the current study. Homogeneous color of the raw material at the end of the extraction is another reason that CO<sub>2</sub> distributed homogeneously inside the bed and channeling problem did not occur.

Table 3 shows that increasing S/F improves the extraction yield (g extract/ 100 g annatto seeds) due to higher CO<sub>2</sub> consumption. This table also reports the adsorbed mass of extract that is 1 g, for Run B with S/F of 25.45, and 0.66 g, for Run C with S/F of 55.98. One probable reason for lower amount of adsorbed mass of extract of Run C compared to run B is the higher amount of S/F in Run C that carries out higher amount of the extract available in the adsorption column. Accordingly, the total extraction yield, which includes the mass of extract inside the separators and the mass of extract in the adsorption column, determined to be 1.42, for Run A, 1.89, for Run B, and 2.46, for Run C. Moreover, as shown in the last column of this table, an increment of S/F from 3.69 to 55.98 reduces the amount of extract in the lines from 16.65% to 7.58%. This is mainly due to the employing adsorption-base device together with Teflon bushings in the separators that leads to recovering higher amount of extract and reducing the amount of extract in the lines.

### 3.4. Estimated Cost of the Constructed Online Subcritical Adsorption-based Device

Considering the need to perform tests in the pilot-scale unit to verify the possibility of recirculating CO<sub>2</sub> with the least amount of drag on the extract and without requiring a great initial investment, some components were borrowed from other units: a column that was used as adsorption column, a manometer and a micrometering valve (Fig. 9). Then, corrective maintenance of 4 valves that were previously in disuse was performed; these valves appear with a (\*) in

**Table 4.** In this sense, disregarding the cost calculation of items with (\*), we can say that an initial investment of only USD 461.36 was necessary.



**Fig. (9).** Components of the homemade online subcritical adsorption-based device developed to allow effective CO<sub>2</sub> recycling.

**Table 4. Estimated cost of the components of the homemade device developed to allow effective CO<sub>2</sub> recycling.**

Product Name	Qty	Price	Total (USD)
Adsorption column (AdC1)*	1	4,000.00	4,000.00
Recording manometer NS163 (Class A2 Ø150 mm, ABNT NBR-14105/98, São Paulo, Brazil)*	1	140.00	140.00
Blocking valve (Autoclave Engineers, 10V2071, PA, USA)*	4	166.00	664.00
Micrometering valve (Autoclave Engineers, 10VRM2812, PA, USA)*	1	466.53	466.53
Heat exchanger with electric resistance to heat the micrometric valve	1	70.00	70.00
Tubing 1/8" (6 m) (Fopil, ASTMA269S, Campinas, Brazil)	1	89.62	89.62
Ferrule 1/8" (Fopil, Campinas, Brazil)	5	3.24	16.2
Connector Tee OD 1/8" (Fopil, ASTMA276, Campinas, Brazil)	2	44.30	88.60
Connector Tee side NPT 1/4" (Fopil, A.276316, Campinas, Brazil)	2	20.13	40.26
Connector OD-NPT (Fopil, ASTMA269TP316S, Campinas, Brazil)	2	11.80	23.60
Silicone hose 14 x 8 x 3 mm (15 m) Ref. MS-207-KNR (Sinergia Científica, Campinas, Brazil)	1	57.74	57.74
Diaphragm gas meter Itron G1.6 DN20 x 110 mm (Hidrovolt, Campinas, Brazil)	1	75.34	75.34
		Total	5.731,53

On the other hand, an estimated total cost of USD 5731.36 would be required to build the developed device in an SFE unit like the one used here.

## CONCLUSION & FUTURE DEVELOPMENTS

The information obtained from the data used to construct the overall extraction curve (OEC) in the SFE bench-scale unit was of great use since it enabled a decision regarding the choice of the extraction time used in the pilot-scale unit for technical validation of the online subcritical adsorption-based device for assisting CO<sub>2</sub> recycling. The validation criterion adopted, in addition to visual observation of the adsorbent material after the SFE process, consisted of monitoring the effects of the increase in the solvent mass to feed mass (S/F) ratio on the extraction yield and percentage of residual extract in the equipment parts and comparing the results for the SFE pilot-scale unit coupled with the online subcritical adsorption-based device with the results obtained for the SFE bench-scale unit. In general, the higher the S/F ratio was, the higher was the extraction yield measured and the lower was the accumulation of extract inside the parts of the SFE unit used. Comparing the percentage of residual extract obtained in the pilot-scale unit during runs A-E (6.55-16.65%) with those obtained previously in the bench-scale unit (4.05-8.23%), it can be observed that the pilot-scale unit retained more extract in its tubing (6.55-16.65%).

The amount of extract in each of the parts of the SFE pilot-scale unit reported during the mass balance allowed the recognition of the loss of extract material caused by the existence of empty spaces between connections. This form of loss caused the accumulation of residual extract during the extraction process, and in addition to resulting in low

extraction yields, led to a higher consumption of solvents, energy and working hours during the cleaning of the equipment. In this sense, the detailed observation of the connections and various equipment parts suggested the use of an inert material (such as Teflon bushing) to fill these spaces.

The incorporation of an adsorption column along with valves and accessories allowed preliminary tests to be carried out to validate the reincorporation of the CO<sub>2</sub> recirculation system in the pilot-scale unit. The tests consisted of defatting annatto seeds, reaching S/F values of 25 and 55 with a mass flow rate of 200 g/min in all cases. This approach achieved the reasonable use of economic resources while at the same time achieving a major saving regarding the purchase of solvent. We could infer that similarl to what occurred with the residual extract deposited in the tubing line in both units tested here, the use of a higher S/F ratio is also preferred for reducing extract accumulation inside the adsorption column.

The cost survey showed that it would cost an estimated total of USD 5731.36 to install the developed device in an SFE unit like the one coupled here (5 L).

Since the proposed device was successfully technically validated using cotton as an adsorbent material, future developments will include the performance of the pseudocontinuous SFE of target compounds using supercritical CO<sub>2</sub> in the pilot-scale unit used in this study. Pseudocontinuous SFE is recommended because using n ( $n \geq 2$ ) extractor vessels, an industrial plant enables a pseudocontinuous operation to be simulated by intercalating the charge/extraction/discharge steps of each vessel.

Furthermore, the use of other adsorbent materials that in addition to allowing CO<sub>2</sub> recycling, can be further used directly as an adsorbent material enriched in bioactive compounds will be studied. For the case of cotton, the colored material (cotton with extract) is applicable in an extremely limited range of applications, and thus this material is unlikely to be pursued in the following steps.

## **ETHICS APPROVAL AND CONSENT TO PARTICIPATE**

Not applicable.

## **HUMAN AND ANIMAL RIGHTS**

No Animals/Humans were used for studies that are basis of this research.

## **CONSENT FOR PUBLICATION**

Not applicable.

## **CONFLICT OF INTEREST**

The authors declares no conflict of interest, financial or otherwise.

## **ACKNOWLEDGEMENTS**

This article was presented orally in the Brazilian Congress on Food Science and Technology - CBCTA 2018 (<http://cbcta2018.com.br/>). It received the Leopold Hartman Award as the best work among the 1000 works presented in this meeting. R. Abel C. Torres thanks Capes for their doctorate assistantship. Diego T. Santos thanks CNPq (processes 401109/2017-8 and 150745/2017-6) for the postdoctoral fellowship. M. Angela A. Meireles thanks CNPq for the productivity grant (302423/2015-0). The authors acknowledge the financial support from FAPESP (process 2015/13299-0).

## **REFERENCES**

- [1] Martin A, Mattea F, Gutierrez L, Miguel F, Cocero MJ. Co-precipitation of carotenoids and bio-polymers with the supercritical anti-solvent process. *J Supercrit Fluids* 2007; 41(1): 138-47.  
[<http://dx.doi.org/10.1016/j.supflu.2006.08.009>]
- [2] Tocchini L, Mercadante AZ. Extração e determinação, por clae, de bixina e norbixina em colorícos. *Food Sci Technol (Campinas)* 2001; 21: 310-3.  
[<http://dx.doi.org/10.1590/S0101-20612001000300010>]
- [3] Stahl W, Sies H. Antioxidant activity of carotenoids. *Mol Aspects Med* 2003; 24(6): 345-51.  
[[http://dx.doi.org/10.1016/S0098-2997\(03\)00030-X](http://dx.doi.org/10.1016/S0098-2997(03)00030-X)] [PMID: 14585305]

- [4] Santos DT, Albarelli JQ, Beppu MM, Meireles MAA. Stabilization of anthocyanin extract from jabuticaba skins by encapsulation using supercritical CO<sub>2</sub> as solvent. *Food Res Int* 2013; 50(2): 617-24.  
[<http://dx.doi.org/10.1016/j.foodres.2011.04.019>]
- [5] Shahid M, Shahid UI, Mohammad F. Recent advancements in natural dye applications: a review. *J Clean Prod* 2013; 53: 310-31.  
[<http://dx.doi.org/10.1016/j.jclepro.2013.03.031>]
- [6] Tapiero H, Townsend DM, Tew KD. The role of carotenoids in the prevention of human pathologies. *Biomed Pharmacother* 2004; 58(2): 100-10.  
[<http://dx.doi.org/10.1016/j.biopha.2003.12.006>] [PMID: 14992791]
- [7] Rodrigues SM, Soares VLF, de Oliveira TM, Gesteira AS, Otoni WC, Costa MGC. Isolation and purification of RNA from tissues rich in polyphenols, polysaccharides, and pigments of annatto (*Bixa orellana* L.). *Mol Biotechnol* 2007; 37(3): 220-4.  
[<http://dx.doi.org/10.1007/s12033-007-0070-9>] [PMID: 17952668]
- [8] Rosa MTMG, Silva EK, Santos DT, Petenate AJ, Meireles MAA. Obtaining annatto seed oil miniemulsions by ultrasonication using aqueous extract from Brazilian ginseng roots as a biosurfactant. *J Food Eng* 2016; 168: 68-78.  
[<http://dx.doi.org/10.1016/j.jfoodeng.2015.07.024>]
- [9] van Scheppingen WB, Boogers IALA, Duchateau ALL. Study on decomposition products of norbixin during bleaching with hydrogen peroxide and a peroxidase by means of UPLC-UV and mass spectrometry. *Food Chem* 2012; 132(3): 1354-9.  
[<http://dx.doi.org/10.1016/j.foodchem.2011.11.118>] [PMID: 29243622]
- [10] Barrozo MAS, Santos KG, Cunha FG. Mechanical extraction of natural dye extract from *Bixa orellana* seeds in spouted bed. *Ind Crops Prod* 2013; 45: 279-82.  
[<http://dx.doi.org/10.1016/j.indcrop.2012.12.052>]
- [11] Albuquerque CLC, Meireles MAA. Defatting of annatto seeds using supercritical carbon dioxide as a pretreatment for the production of bixin: Experimental, modeling and economic evaluation of the process. *J Supercrit Fluids* 2012; 66: 86-95.  
[<http://dx.doi.org/10.1016/j.supflu.2012.01.004>]
- [12] Moraes MN, Zabot GL, Meireles MAA. Applications of supercritical fluids in latin america: Past, present and future trends. *Food Public Health* 2014; 4(3): 162-79.  
[<http://dx.doi.org/10.5923/j.fph.20140403.11>]
- [13] Johner JCF, Meireles MAA. Construction of a supercritical fluid extraction (SFE) equipment: validation using annatto and fennel and extract analysis by thin layer chromatography coupled to image. *Food Sci Technol (Campinas)* 2016; 36(2): 210-47.  
[<http://dx.doi.org/10.1590/1678-457X.0027>]
- [14] Rodrigues LM, Alcázar-Alay SC, Petenate AJ, Meireles MAA. Bixin extraction from defatted annatto seeds. *C R Chim* 2014; 17(3): 268-83.  
[<http://dx.doi.org/10.1016/j.crci.2013.10.010>]
- [15] Mattea F, Martín Á, Matías-Gago A, Cocero MJ. Supercritical antisolvent precipitation from an emulsion: β-Carotene nanoparticle formation. *J Supercrit Fluids* 2009; 51(2): 238-47.  
[<http://dx.doi.org/10.1016/j.supflu.2009.08.013>]
- [16] Santos DT, Meireles MAA. Micronization and encapsulation of functional pigments using supercritical carbon dioxide. *J Food Process Eng* 2013; 36(1): 36-49.  
[<http://dx.doi.org/10.1111/j.1745-4530.2011.00651.x>]
- [17] Nong D, Siriwardana M. Environmental and economic impacts of a joint emissions trading scheme. *Int J Glob Energy Issues* 2017; 40(3-4): 184-206.  
[<http://dx.doi.org/10.1504/IJGEI.2017.086619>]
- [18] Royer-Adnot J, Le Gallo Y. Economic analysis of combined geothermal and CO<sub>2</sub> storage for small-size emitters. *Energy Procedia* 2017; 114: 7118-25.  
[<http://dx.doi.org/10.1016/j.egypro.2017.03.1853>]
- [19] Silva GF, Gamarra FMC, Oliveira AL, Cabral FA. Extraction of bixin from annatto seeds using supercritical carbon dioxide. *Braz J Chem Eng* 2008; 25: 419-26.  
[<http://dx.doi.org/10.1590/S0104-66322008000200019>]
- [20] AOAC. *Official Methods of Analysis* of AOAC International. 1997.
- [21] NIST. National Institute of Standards and Technology. 2017. Available at: <http://www.nist.gov>
- [22] Zabot GL, Moraes MN, Petenate AJ, Meireles MAA. Influence of the bed geometry on the kinetics of the extraction of clove bud oil with supercritical CO<sub>2</sub>. *J Supercrit Fluids* 2014; 93: 56-66.  
[<http://dx.doi.org/10.1016/j.supflu.2013.10.001>]
- [23] Prado JM. Estudo do aumento de escala do processo de extração supercrítica em leito fixo. Ph.D thesis, University of Campinas/School of Food Engineering, Campinas, Brazil, 2010.
- [24] Jesus SP, Calheiros MN, Hense H, Meireles MAA. A simplified model to describe the kinetic behavior of supercritical fluid extraction from a rice bran oil byproduct. *Food Public Health* 2013; 3: 215-22.  
[<http://dx.doi.org/10.5923/j.fph.20130304.05>]

- [25] Meireles MAA. Extraction of bioactive compounds from latim american plants. Supercritical Fluid Extraction of Nutraceuticals and Bioactive Compounds: CRC Press - Taylor & Francis Group, LLC. 2008; pp. 243-74.
- [26] Moraes MN, Zabot GL, Meireles MAA. Extraction of tocotrienols from annatto seeds by a pseudo continuously operated SFE process integrated with low-pressure solvent extraction for bixin production. J Supercrit Fluids 2015; 96: 262-71.  
[<http://dx.doi.org/10.1016/j.supflu.2014.09.007>]
- [27] Takeuchi TM, Leal PF, Favareto R, *et al.* Study of the phase equilibrium formed inside the flash tank used at the separation step of a supercritical fluid extraction unit. J Supercrit Fluids 2008; 43(3): 447-59.  
[<http://dx.doi.org/10.1016/j.supflu.2007.08.002>]
- [28] EXERGY-LLC. Model # 00256-06, Shell & Tube Heat Exchanger. USA, 17/05/2017 2017. Available at: <http://heat-exchangers.exergyllc.com/item/shell-tube-heat-exchangers/35-series-shell-tube-heat-exchangers/> 00256-06
- [29] POLYSCIENCE. Chillers and Coolers. USA, 2017. Available at: <https://polyscience.com/products/chillers/benchtop>
- [30] POLYSCIENCE. User Guide - Refrigerated Recirculating Chillers. USA: POLYSCIENCE 2016; p. 51.
- [31] Santos DT, Albuquerque CLC, Meireles MAA. Procedia Food Sci 2011; 1: 1581-8.  
[<http://dx.doi.org/10.1016/j.profoo.2011.09.234>]
- [32] Torres RADC. Purificação de partículas de bixina por precipitação com CO<sub>2</sub> supercrítico como antissolvente a partir de solução de ativos obtida da extração de sementes semi desengorduradas de urucum (*Bixa orellana* L.) assistida por ultrassom. Master thesis, University of Campinas/School of Food Engineering, Campinas, Brazil, 2015.
- [33] Del Valle JM, Rivera O, Mattea M, Ruetsch L, Daghero J, Flores A. Supercritical CO<sub>2</sub> processing of pretreated rosehip seeds: effect of process scale on oil extraction kinetics. J Supercrit Fluids 2004; 31(2): 159-74.  
[<http://dx.doi.org/10.1016/j.supflu.2003.11.005>]

© 2018 Torres *et al.*

This is an open access article distributed under the terms of the Creative Commons Attribution 4.0 International Public License (CC-BY 4.0), a copy of which is available at: (<https://creativecommons.org/licenses/by/4.0/legalcode>). This license permits unrestricted use, distribution, and reproduction in any medium, provided the original author and source are credited.

- CAPÍTULO 4 - ***A novel process for CO<sub>2</sub> purification and recycling based on subcritical adsorption in oat bran***

Este capítulo retrata a implementação de uma metodologia para purificação e reciclo de CO<sub>2</sub> em escala piloto utilizando-se farelo de aveia como adsorvente. A validação do procedimento foi realizada através da repetibilidade dos ensaios com mais uma matriz vegetal modelo, e a comparação com unidade comercial de escala de bancada mostrou a efetividade do processo para economia de solvente e obtenção de produtos diversificados dentro da mesma linha de processamento.

Artigo a ser submetido no periódico Journal of CO<sub>2</sub> Utilization (ISSN: 2212-9820)

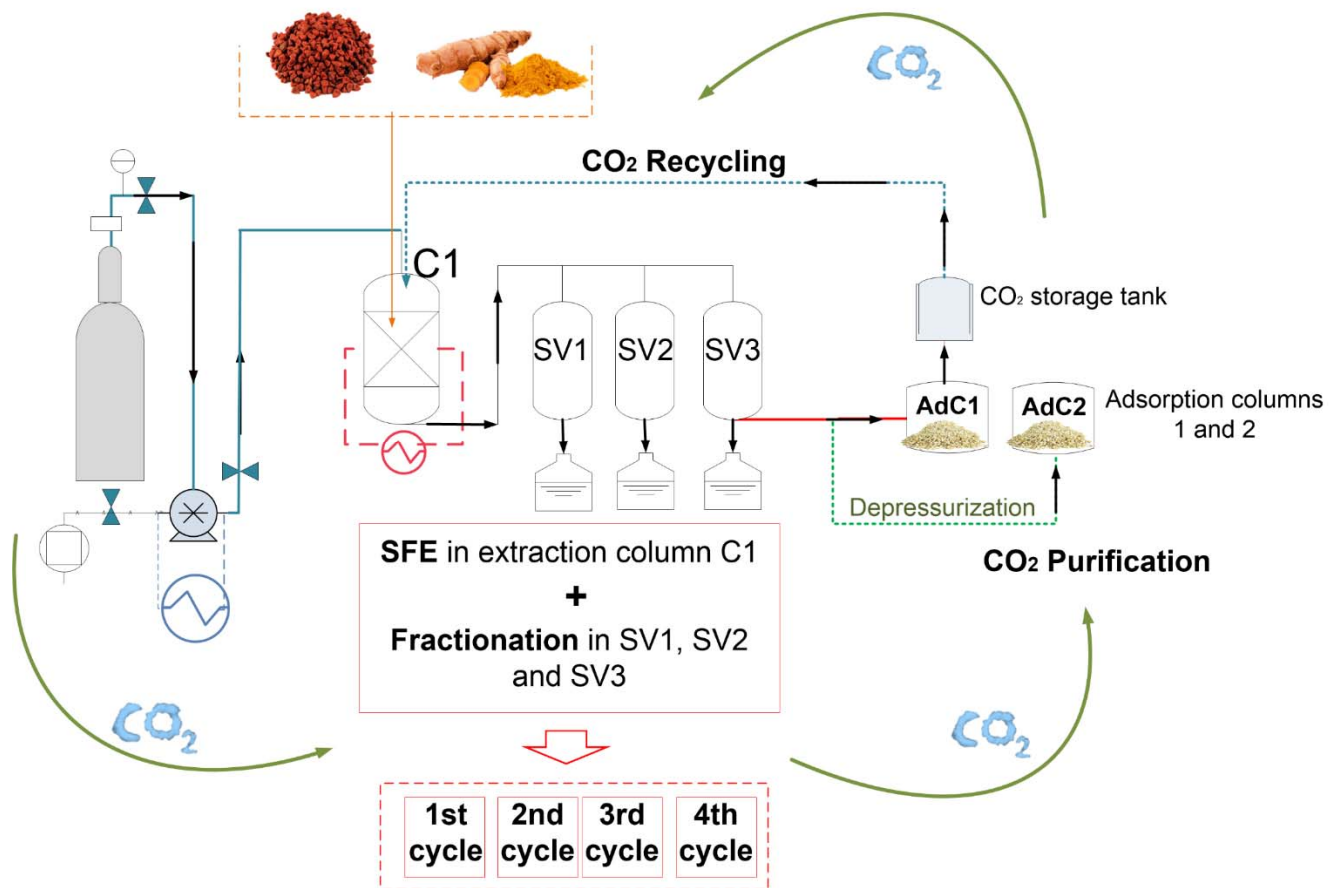
# A novel process for CO<sub>2</sub> purification and recycling based on subcritical adsorption in oat bran

R. Abel C. Torres<sup>a</sup>, Ádina L. Santana<sup>b</sup>, Diego T. Santos<sup>a</sup>, Juliana Q. Albarelli<sup>a</sup>, M.  
Angela A. Meireles<sup>a</sup>

<sup>a</sup>LASEFI/DEA/FEA (School of Food Engineering)/UNICAMP (University of Campinas), R. Monteiro Lobato, 80; 13083-862, Campinas, SP, Brazil

<sup>b</sup>Bioprocesses Laboratory/DEPAN/ FEA (School of Food Engineering)/UNICAMP (University of Campinas), R. Monteiro Lobato, 80; 13083-862, Campinas, SP, Brazil

*Corresponding authors:* [\(R. A. C. Torres\)](mailto:delcastilloabel18@gmail.com); [\(Á. L. Santana\)](mailto:adina.santana@gmail.com); [\(M. A. A. Meireles\)](mailto:maameireles@lasefi.com)

**Graphical abstract**

## Abstract

A system for the purification and recycling of CO<sub>2</sub>, namely PRCO<sub>2</sub> was validated in this work. The process consisted of on-line supercritical fluid extraction integrated with fractionation of the extracts in three separation vessels, followed by purification of CO<sub>2</sub> in adsorption columns in subcritical conditions, and subsequent recycling of CO<sub>2</sub>. Turmeric and annatto were the plant matrices used and oat bran was used as a low cost and biodegradable adsorbent. Considering a process consisted of 4 cycles, the extraction of 12 kg of annatto and 8 kg of turmeric with the presence of PRCO<sub>2</sub> reduced the consumption of CO<sub>2</sub> in 85.57% and 75.26%, respectively. Economical evaluation showed that the increasing of the number of cycles decreased the cost of manufacture. Besides fractionated extracts, this process generates byproducts that consists of an oat bran enriched with bioactive constituents from extract fraction dragged out the last separation vessel.

**Keywords:** CO<sub>2</sub> purification; CO<sub>2</sub> recycling; supercritical fluid extraction; subcritical adsorption; process intensification.

## 1 INTRODUCTION

The capture, utilization and storage of carbon dioxide (CO<sub>2</sub>) are considered crucial ways to meet the CO<sub>2</sub> emission reduction targets. Current demands for reutilization of materials for wastes reduction, besides global warming and climate change concerns have motivated scientific research on the development of clean technologies and optimization of process parameters to achieve sustainable production [1-3].

One promising option is purification and recycling of CO<sub>2</sub> indigenous to processes of extraction or fractionation with the use of adsorption.

Supercritical fluid extraction coupled with fractionation involves the continuous contact between the supercritical CO<sub>2</sub> (SC-CO<sub>2</sub>) and the extract in one or more

pressurized vessels (or columns) during separation of heavy and light fractions of extracts [4]. Its combination with subsequent adsorption and recycling would be an useful alternative for the purification and recirculation of CO<sub>2</sub>, which consequences include the reduction of costs with processing.

Adsorption is a surface phenomenon in which soluble particles from a solution are bonded onto a particular substrate (or adsorbent). The porous structure of adsorbent attracts and holds organic molecules as well as certain metal and inorganic molecules. Adsorption occurs because of: a) low solubility of target compounds in the CO<sub>2</sub>; b) the target compounds has greater affinity for the adsorbent than for the CO<sub>2</sub> and c) a combination of both [5].

Oats (*Avena sativa*) is a cereal grain and a good source of starch and soluble fiber β-glucan which were associated with technological properties as emulsion stabilizer and water binding, that justifies its inclusion in different food products to improve the textural and rheological properties [6, 7]. As an adsorbent, oat products have been considered as efficient and low costs. For instance, oat starch has been used for removal of water from butanol [8], and oat bran fiber β-glucan adsorbed the polyphenol epigallocatechin gallate [9]. Complexation of polysaccharides with polar molecules, like water and polyphenols, probably contributed to the adsorption efficiency of these compounds in oat bran.

To the best of our knowledge, this is the first study to propose a multi-stage process with the use of supercritical CO<sub>2</sub> for the obtaining of fractionated extracts, with subsequent purification and recycling with subcritical CO<sub>2</sub>.

It is expected that the results obtained will serve to support further researches to reduce the consumption of CO<sub>2</sub> in processes that uses supercritical technology, such as supercritical antisolvent (SAS) and rapid expansion from a saturated solution (RESS),

and also the subsequent obtaining of value added byproducts with potential application as functional foods, cosmetics and pharmaceuticals.

## 2 MATERIALS AND METHODS

### 2.1 RAW MATERIAL

Anatto (*Bixa Orellana* L.) seeds, variety Piave were donated by Urucum do Brasil Ltda., (Monte Castelo, Brazil). Turmeric (*Curcuma longa* L.) rhizomes were purchased from Oficina de Ervas Ltda (Ribeirão Preto, Brazil). The materials were stored at 255 K in the dark until further analysis. Moisture of annatto and turmeric were analyzed using official method from AOAC. Particle diameter was determined by sieving (W.S. Tyler, Wheeling, USA). All analyses were determined in triplicate.

### 2.2 EXPERIMENTAL

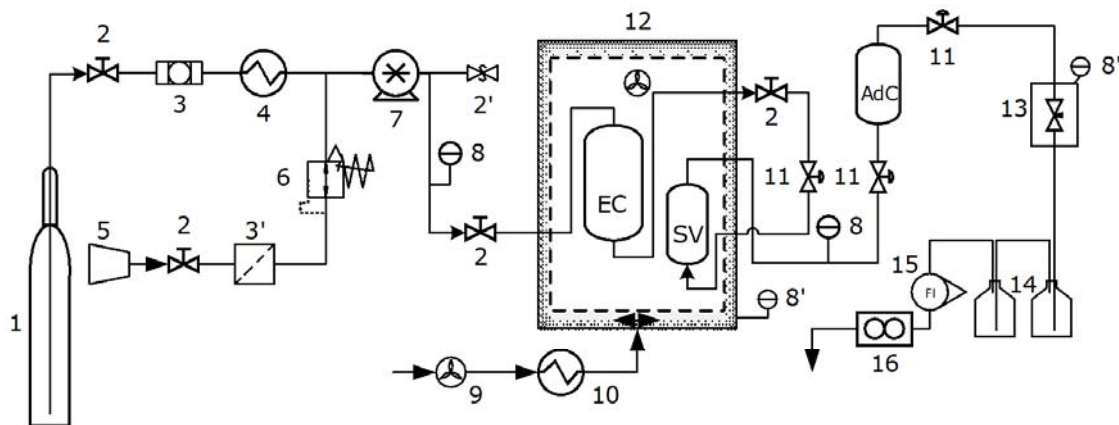
The extraction assays were performed with two commercial SFE equipment, which consisted of a bench scale unit (Spe-ed SFE Laboratory System, 7071, Applied Separations, Allentown, USA), and a pilot scale unit (Thar Designs, CL 1373, Pittsburg, USA). The solvent used was CO<sub>2</sub> (99.9%, White Martins, Campinas, Brazil).

### 2.3 BENCH SCALE UNIT

#### 2.3.1 Preliminary section: obtaining of overall extraction curves

Prior to extraction/adsorption experiments, exhaustive SFE of annatto (20 MPa and 313 K) and turmeric (25 MPa and 313 K) were performed in the equipment in bench scale using the extraction column C1 (Figure 1) in order to obtain the overall extraction curves (OECs) and subsequently calculate the time span of constant extraction rate ( $t_{CER}$ ) using three and two-straight lines spline for annatto and for turmeric with an algorithm implemented in MS Excel [10]. The  $t_{CER}$  values were used to estimate the optimal S/F values for further pilot scale assays and to optimize the periods of processing (Figure 3).

The OECs were not obtained in pilot scale because of impossibilities to collect extracts point by point. Extraction with annatto shows that modeled extraction curve with 3-straight lines spline resulted in time of constant extraction rate period,  $t_{CER}$  of 22 min. The modeling of turmeric OECs were made using a two-straight lines spline. For turmeric  $t_{CER}$  was 2 min. Results of experimental points of bench scale OECs and the remaining modeling parameters are available in the supplementary material.



(1) CO<sub>2</sub> cylinder, (2) blocking valve and (2') safety valve, (3) line filter, (3') air filter, (4) cooling bath, (5) compressor, (6) air pressure regulator, (7) air driven fluid pump, (8) manometer. (8') Internal temperature indicator, (9) blow motor, (10) blow motor resistor, (EC) extraction column, (SV) separation vessel, (11) backpressure valve, (12) oven module, (13) micrometric valve with heating system, (AdC) adsorption column, (14) collection flask, (15) flow meter, (16) flow totalizer.

**Figure 1.** Schematic diagram of bench scale unit.

### 2.3.2 Adsorption in bench-scale unit

Whole seeds of annatto were used as raw material model in bench scale unit. The process applied in bench scale unit consisted of a separation vessel, which was coupled with the extraction column packed with the raw material ( $17.5 \times 10^{-3}$  kg). Temperature was controlled with the aid of an oven, into which the extraction column and separation vessel were coupled (Figure 1).

On the outside of the oven, a valve system was coupled to an adsorption column previously packed with the adsorbent ( $2.5 \times 10^{-3}$  kg –  $3.5 \times 10^{-3}$  kg). Mass flow of CO<sub>2</sub> ranged between  $7.4\text{--}11.8 \times 10^{-3}$  kg/min. Temperature and pressure conditions were fixed

at 313 K and 20 MPa in the extraction column and 313K and 5.5 MPa in the separation vessel, and 298 K and 5.0 MPa in the adsorption column.

No periods of charging and pressurization (Figure 3) were considered, but the static time of 20 minutes only, which served as basis for the experiments in pilot scale. The static period consists of the time interval in which the extraction of the raw material in steady state is occurring.

Afterwards, the extractions were carried out for 30 minutes in a purposive way because this value was higher than the constant extraction rate period determined in the preliminary section under the justification of obtaining higher extraction yields in a scale-up [11, 12].

The first experimental assay was considered as control parameter, in comparison with further experiments, because it consisted of transference of extract from extraction column (20 MPa and 313 K) directly to adsorption column (5.0 MPa and 298 K) with further collecting of extract in a vial (Figure 1: number 14). This control experiment was carried out with the purpose to evaluate the capacity of oat bran to adsorb the extract.

Afterwards, 4 experimental assays were carried out, which extract was fractionated into collected extracts (after the inserting in separation vessels) and the fraction adsorbed in oat bran.

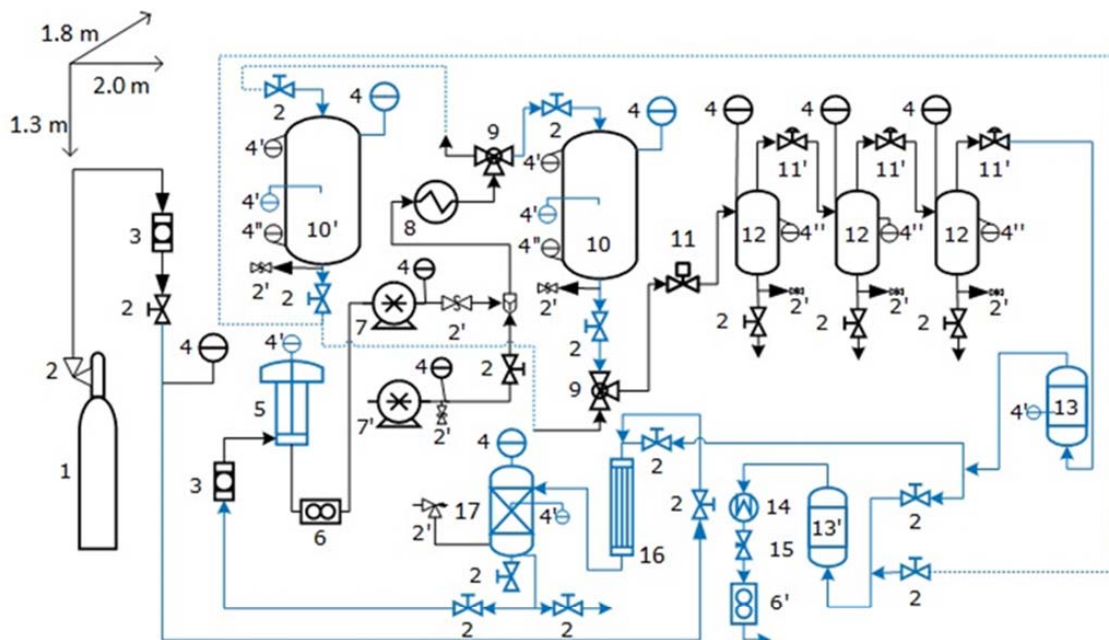
The amount of adsorbed extract was obtained by the differences between the mass of adsorbent material with the adsorbed extract obtained from experiment and the mass adsorbent prior the experiment.

## 2.4 PILOT SCALE UNIT: INTRODUCTION OF PURIFICATION AND RECYCLING SYSTEM CO<sub>2</sub> (PRSCO<sub>2</sub>)

The proposed PRSCO<sub>2</sub> was applied using a pilot scale unit coupled with a storage tank of CO<sub>2</sub>. The pilot scale unit consisted of two 2 L extraction columns, one adsorption

column of 0.65 L (AdC1) and another of 0.4 L (AdC2). Approximately 2.8 kg of CO<sub>2</sub> was continuously purified and recycled with the aid of a storage tank.

The recycle step consisted of coupling the storage tank (Figure 2: number 17) to the pilot unit. The CO<sub>2</sub> at 268 K was pumped gradually to the storage tank with gradual increasing of CO<sub>2</sub> flow until pressures up to 7 MPa, the limit pressure of storage tank. The CO<sub>2</sub> pumping to the storage tank was carried out in order to supply the CO<sub>2</sub> reservoir prior to the beginning of extraction procedures.



(1) CO<sub>2</sub> cylinder, (2) blocking valve and (2') safety valve, (3) line filter, (4) manometer. Temperature indicator: (4') internal and (4'') external, (5) heat exchanger with coiled tube for CO<sub>2</sub> cooling, (6) mass flow meter, (7) CO<sub>2</sub> pump, (7') Co-solvent pump, (8) heat exchanger for CO<sub>2</sub> heating, (9) three-way valve, (10) extraction column. Backpressure valve: (11) automated and (11') manual, (12) separation vessel = SV1, SV2 and SV3, (13) adsorption column 1 (AdC1 = 0.65 L), (13') adsorption column 2 (AdC2 = 0.4 L), (14) heat exchanger with electric resistance, (15) micrometering valve, (16) shell and tube condenser, (17) storage tank.

**Figure 2.** Schematic diagram of pilot scale unit.

Considering an one-cycle process, the recycling procedure occurred during the whole dynamic extraction period which started with SFE in the extraction column C1 (Figure 2: number 10, and Figure 3), from which extract was transferred to three separation vessels (Figure 2: number 12), and subsequently collected into three distinct fractions. The fraction of extracts that remained solubilized in CO<sub>2</sub> was adsorbed in the AdC1 (Figure 2: number 13) and CO<sub>2</sub> was purified.

Afterwards, the purified CO<sub>2</sub> was transferred to a condenser (Figure 2: number 16) and cooled with the aid of a cooling bath at 263 K, and transferred to the storage tank, from where it passes through the flow totalizer to thereby be pressurized and heated to be transported back to extraction column C1 (Figure 2).

The process applied in the pilot scale unit differs from the bench scale unit in considering the presence of a pseudocontinuous process constituted of 4 cycles.

Pseudocontinuous operation in SFE performed in pilot scale occurs with more than one extractor column, which plant is enabled by intercalating the charge/extraction/discharge steps for each vessel (Figure 3). As the process is pseudocontinuous, the finishing of dynamic period in extraction column C1 (considering one-cycle processing) occurs in parallel with the beginning of dynamic period in extraction column 2, which corresponds to the second cycle of the process.

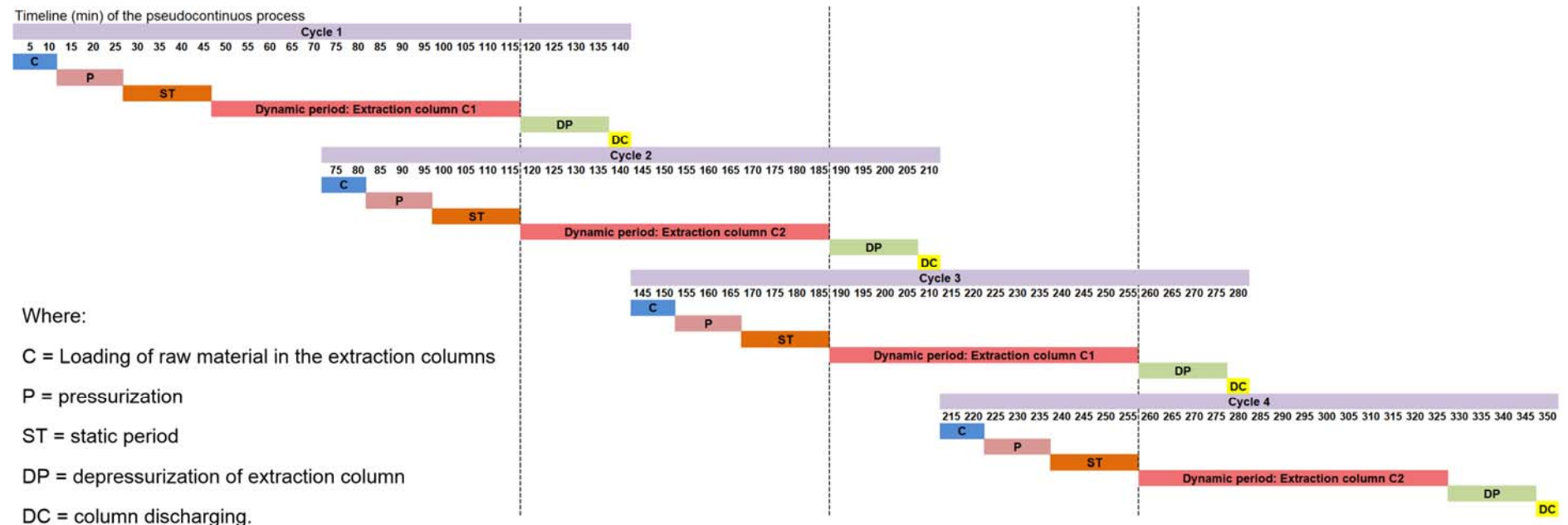


**Figure 3.** Optimized processing times of each processing stage. All cycles resulted in 350 min of process.

Each cycle consisted of charging of raw material in a 5 L extraction column for 10 min (Figure 2: numbers 10 and 10'; Figure 3: letters "C"), followed by pressurization of system for 15 min (Figure 3: letters "B") and static period for 20 min (Figure 3: letters "ST"). Static period is initiated after the process pressure has reached within the extraction column. Afterwards, the dynamic period begins. The dynamic period in a 1 cycle process is constituted of 70 minutes, which starts from the end of minute 45 until the end of minute 115 (Figure 3). In this procedure the extract are fractionated in three 1 L separation vessels with subsequent collecting (Figure 2: number 12), followed by purification of CO<sub>2</sub> through adsorption in a 0.6 L column (identified as AdC1, Figure 2: number "13") and finishes with the recycling of CO<sub>2</sub>.

Once finished the dynamic period, the depressurization of extraction column occurs during 20 min (Figure 3), through the passage of CO<sub>2</sub> from the second adsorption column (identified as AdC2, Figure 2: number "13") with subsequent discharging of depleted raw material (defatted annatto seeds/deflavored turmeric) for 5 min (Figure 3: DC), completing the first cycle. The second adsorption column AdC2 was applied in order to reuse the fraction of extract that was dragged out the third separation vessel by CO<sub>2</sub> previously solubilized in CO<sub>2</sub> for the obtaining of a second byproduct, which consists of adsorbent material enriched with extract with quality distinct from that used adsorbed in AdC1.

However, the dynamic extraction period is strongly dependent on the number of extraction vessels of the processing unit, and is also dependent of the CER interval, from which is possible to obtain approximately 70-90 % of extraction yields [13].

The addition of an extraction vessel would reduce the dynamic period from 70 to 22 minutes, and extractions performed on CER period would maximize the quantity of extracts obtained.

#### 2.4.1 Process parameters

The interstitial velocity ( $\bar{u}$ , m/min – Table 4) corresponds to the average velocity required by the solvent to flow through the extraction columns. This term is related to the performance of the process related to the acquisition of extracts, as well as the purification and recycling of CO<sub>2</sub>.

In order to calculate the interstitial velocity for bench and pilot scale processes, the following variables were necessary: mass flow of CO<sub>2</sub> (Q<sub>CO<sub>2</sub></sub>), real density of adsorbent (1350 kg/m<sup>3</sup>), the apparent density of column ( $\rho_a$ , kg/m<sup>3</sup>), which is the mass of raw material divided by the volume of the column, porosity of column ( $\epsilon$ , dimensionless) which corresponds to the filled fraction of column associated with its void fraction, the H<sub>B</sub>/D<sub>B</sub> (-), which is the ratio between the height of the column divided by its diameter (Table 4). The values of H<sub>B</sub> of adsorption columns for the bench and pilot units were 0.02 m, 0.17 m (AdC1) and 0.42 m (AdC2), respectively (Table 4).

The volume of the adsorption column of bench scale unit was  $5 \times 10^{-6}$  m<sup>3</sup> and the volumes of adsorption columns used in pilot scale experiments were  $6.5 \times 10^{-4}$  m<sup>3</sup> (AdC1) and  $4.0 \times 10^{-4}$  m<sup>3</sup> (AdC2). Density of CO<sub>2</sub> at 0.093 MPa and 295 K was 1.68 kg/m<sup>3</sup>.

For the calculations of adsorption efficiency in pilot scale, the fractions of adsorbent and adsorbent+adsorbed material were weighed separately (Table 5).

#### 2.4.2. S/F calculation in pilot scale experiments

The use of purification and recycling system of CO<sub>2</sub> (PRCO<sub>2</sub>) contributes to reduce solvent consumption. After purification, the CO<sub>2</sub> immediately flows through the storage tank, which subsequently allows the redistribution of CO<sub>2</sub> throughout the process.

Considering this concept, the amounts of CO<sub>2</sub> required for the pressurization of the separation vessels and the separation columns were estimated for the PRCO<sub>2</sub> process.

The general equation that we propose (Eq.1) shows the variables related to the consumption of CO<sub>2</sub> for process with the presence of PRCO<sub>2</sub> and with the absence of PRCO<sub>2</sub>. The Eq. 2 highlight the process parameters that compose the variable  $\lambda$ , which is a dimensionless term associated to the consumption of CO<sub>2</sub>, considering a process with absence of PRCO<sub>2</sub>,

$$\frac{S}{F} = \lim_{n \rightarrow \infty} \left[ \left( \frac{\phi n}{\delta n} + \frac{\kappa}{\delta n} \right) + \lambda \right] \quad (1)$$

$$\lambda = \frac{Q_{CO_2} t_{DIN} n}{\delta n} \quad (2)$$

Where n represent the number of cycles,  $\phi$  is the mass of CO<sub>2</sub> (kg) used to pressurize the extraction column,  $\kappa$  is the mass of CO<sub>2</sub> (kg) used to pressurize the separation vessels,  $\delta$  is the mass of raw material used to reach an on-cycle process.

In this work the values of variables were  $\phi=2.3$ ,  $\kappa=0.5$ ,  $\delta=3$  kg of annatto or 2 kg of turmeric,  $Q_{CO_2}=0.2$  kg/min for annatto and 0.1 kg/min for turmeric,  $t_{DIN}=70$  min.

## 2.5 COMPOSITION OF EXTRACTS

### 2.5.1 Annatto

Geranylgeraniol and bixin content in the annatto extracts were determined using high-performance liquid chromatography (HPLC). Chromatographic analyses were carried out using an HPLC-PDA (Waters, Alliance E2695, Milford, USA) system, consisting of a separation module with an integrated column heater, an autosampler and a photodiode array (PDA) detector. Separation of constituents was accomplished using a C18 column 150 × 4.6 nm, id., 2.6 μm (Phenomenex, Torrance, USA) at 323 K. A solution of methanol:ammonium acetate 50 mM (90:10, v/v) was the mobile phase to detect geranylgeraniol. The analysis were performed using a flow rate of 1 mL/min and elution gradient of mobile phase is available elsewhere [14].

Bixin was quantified using the mobile phases constituted of 2% formic acid in water (A) and 2% formic acid in acetonitrile (B). Temperature of column was 30°C. Elution with a flow rate of 0.9 mL/min was performed as follows: 0-5 min of 25-75% A in B; 6-18 min of 15-85% A in B; 19-20 min of 5-95% A in B; 20-20.20 min of 25-75% of A in B and 20.20-21 min of 25-75% A in B. The absorption spectra were obtained using the range between 210 and 600 nm. Bixin was detected at 459 nm.

### 2.5.2 Turmeric

Determination of curcumin was performed using the same HPLC equipment and column used to determine geranylgeraniol and bixin from annatto. The procedures of curcumin detection and quantification were based on the protocol validated elsewhere [15]. The mobile phases were 0.1% glacial acetic acid in water (v/v), and 0.1% glacial acetic acid in acetonitrile (v/v).

Ar-turmerone obtained from turmeric extracts was determined using a gas chromatographer with flame ionization, GC-FID (Shimadzu, CG 15, Kyoto, Japan) equipped with a fused-silica capillary column DB-5 (J&W Scientific, 5% phenyl 95% dimethylpolysiloxane, 30 mm × 0.25 mm i.d. × 0.25 µm, Folsom, USA), based on a previous method [16] with adaptations [17].

Extractions of crude raw material using ethanol (99%) at S/F=5 for 5 min were performed using a 13 mm ultrasonic probe (19 kHz, 800 W, Unique, Indaiatuba, Brazil), in order to establish comparisons of chemical constituents of turmeric and annatto extracts.

## 2.6 CHARACTERIZATION OF THE ADSORBENT

### 2.6.1 Adsorbent (Oat bran)

Moisture of oat bran was analyzed using official method from AOAC. Particle diameter was determined by sieving (W.S. Tyler, Wheeling, USA). The analysis was

determined in triplicate. Oat bran was purchased from Jasmine Alimentos (São Paulo, Brazil). Approximately 0.30 kg and 0.35 kg of oat bran was weighted using an analytical balance (BEL Engineering, São Paulo, Brazil) and loaded in the adsorption column 1 (AdC1) and for adsorption column 2 (AdC2) 0.20 kg and 0.25 kg was loaded in the adsorption column 2 (AdC2), to process annatto and turmeric, respectively.

#### 2.6.2. Differential scanning calorimetry (DSC)

Thermal properties were measured using a differential scanning calorimeter DSC 1 STARE System (Mettler Toledo, DSC1, Zurich, Switzerland). The lids of the pans were pierced. The initial temperature of the pans was 293 K, programmed to increase to 423 K by 283 K/min. Thermal decomposition parameters hydration temperature ( $T_{HD}$ ), pyrolysis temperature ( $T_P$ ), and carbonization temperature ( $T_C$ ) and total weight loss were recorded.

#### 2.6.3 X-ray diffraction (XRD)

X-ray diffractograms were obtained by X-ray diffractometer (X'Pert-MPD, Philips Analytical X Ray, New York, USA) at 30 kV, 30 mA, signals of the reflection of 2 $\theta$  angle varying from 5° to 40° at 1°/min scan, and copper irradiation at 298 K.

#### 2.6.4 Thermogravimetric analysis

The thermal decomposition analysis were performed using a thermogravimetric analyzer (Shimadzu Corporation, TGA-50, Japan) with a readability of 0.001 mg, temperature programing rate of 373 K/min at a temperature ranging between 293-1073 K. For the obtaining of an inert atmosphere, nitrogen (99.99%, 4.6 FID, White Martins, Brazil) was used. The flow rate of 50 mL/min was applied.

#### 2.6.5 Scanning electron microscopy (SEM)

The structure of adsorbent was examined using scanning electron microscopy (SEM). The samples were applied to circular aluminum stubs with double carbon sticky tape and coated with 200 Å of gold using a sputter coater (EMITECH, K450, Kent, United

Kingdom). The micrographs with magnification of 300 $\times$  were obtained using scanning electron microscope (Leo 440i, Cambridge, England) at an accelerating potential of 15 kV and current of 50 pA.

## 2.7 PROCESS MODELING AND SIMULATION DESCRIPTION

A flowsheet model of the process was developed using the commercial software Aspen Plus®. Matlab simulation software was used to perform thermal economic analysis of the evaluated process. In this study, the problem resolution was carried out following the steps:

1. Process data was gathered from the performed experiments.
2. Aspen Plus® flow sheeting software was used to model mass and energy flows of the process. The model was used to calculate the associated heat and power balances.
3. An economic model was developed using data obtained from the flowsheeting software Aspen Plus® and the results obtained by the thermal integration model.

### 2.7.1 Mass and energy flows using Aspen Plus

The thermodynamic model used to represent the process was the RK-ASPEN. SFE unit was simulated considering that the CO<sub>2</sub> sent to the process is initially cooled to 263 K and compressed to desired pressure. It is then heated to the extraction temperature, reaching the supercritical conditions. Later, the extraction vessel of 500 L is filled with the raw material and the supercritical fluid is passed through it. After the extraction process, the extract diluted in supercritical CO<sub>2</sub> is sent to a sequence of 3 separation vessels for fractionation of extracts. CO<sub>2</sub> obtained in third separation vessel is passed through an adsorption column containing oat bran. The final CO<sub>2</sub> is stored in a tank at 5.5 MPa and 30°C to be used in a new cycle. After the end of the number of cycles estipulated, the final depressurization occurred directly in the adsorption column. Table 1 presents the data considered for simulation. It was investigated two operating systems:

System A: Considering operation of one cycle before depressurization of the system.

System B: Considering operation of four cycles before depressurization of the system. In this process two different extractors are considered, each one operating while the other is being prepared for the new cycle.

**Table 1.** Data used on the process simulation based on the experimental data

	Turmeric	Annatto seed
<b>SFE process</b>		
Mass per cycle (kg)	200	300
Temperature (K)	333	313
Pressure (MPa)	25	20
S/F (-)	3.50	4.67
Yield (kg extract/100kg raw material)	5.81	1.69
Extraction column volume (L)	500	500
Extraction column preparation time (min)	45	45
Extraction time (min)	70	70
Extraction column unloading time (min)	25	25
N of system per year (System A) <sup>a</sup>	3394	3394
N of system per year (System B) <sup>b</sup>	1357	1357
<b>CO<sub>2</sub> decompression system</b>		
Separation vessel 1 temperature (K)	313	313
Separation vessel 1 pressure (MPa)	8	8
Separation vessel 2 temperature (K)	303	303
Separation vessel 2 pressure (MPa)	6.50	6.50
Separation vessel 3 temperature (K)	313	313
Separation vessel 3 pressure (MPa)	5.50	5.50
<b>Adsorption columns</b>		
AdC1 temperature (K)	305	303
AdC1 pressure (MPa)	5.50	5.50
AdC1 oat grain mass	35	30
AdC2 temperature (K)	270	270
AdC2 pressure (MPa)	0.10	0.10
AdC2 oat grain mass (kg)	25	20
<b>CO<sub>2</sub> storage tank</b>		
CO <sub>2</sub> tank temperature (K)	275	275
CO <sub>2</sub> tank pressure (MPa)	5.50	5.50

<sup>a</sup>operating 1 cycle before depressurization

<sup>b</sup>operating 4 cycles before depressurization

## 2.7.2 Economic model and economic performance indicators

The economic model was built in MatLab using information extracted from the Aspen Plus model. In order to accomplish an economic evaluation of the process viability

at industrial scale, lab results were scaled-up considering that the same performance would be obtained. This criterion, which has been used by other authors for supercritical fluid-based processes (Veggi et al., 2014; Cavalcanti et al., 2011), assumes that the process will have identical performance with respect to yield at the laboratory and industrial scales if the same process conditions are used (temperature, pressure, extraction time, etc.). To calculate the total investment cost, the major process equipment were roughly sized and their purchase cost were calculated and adjusted to account for specific process pressures and materials using correlations from literature [18, 19]. The total investment cost was then calculated using multiplication factors to take into account indirect expenses like installation costs, contingencies and auxiliary facilities. All costs were updated by using the Chemical Engineering Plant Cost Index.

Cost of manufacturing (COM) estimation for the proposed process was accomplished based on the methodology of Turton et al. (2009) in which variable cost (operational costs which are dependent on the production rate and consist in raw material costs, operational labor, utilities, among others), fixed costs (do not dependent on production rate and include territorial taxes, insurance, depreciation, etc.) and general expenses (cover business maintenance and include management, administrative sales, research and development costs) are calculated. These three components are estimated in terms of five main costs: fixed capital investment (FCI), cost of utilities (CUT), cost of operational labor (COL), cost of waste treatment (CWT) and cost of raw materials (CRM). Utility costs considered the electricity and the cooling requirements under 293 K. COM was calculated as presented in Eq.3.

$$\text{COM} = (\text{VC} + \text{FC} + \text{GE}) * (1 + 0.03\text{COM} + 0.11\text{COM} + 0.05\text{COM}) \quad (3)$$

In which 0.03COM represents the royalties; 0.11COM the distribution and selling and 0.05COM the research and development investments.

It was also evaluated the COM divided by the amount of product produced in a year as presented in Eq.4

$$COM_{prod} = \frac{COM}{m_{prod}} \quad (4)$$

Where m is the mass flow calculated per year, the sub-index *prod* is the product produced in each process. Table 2 shows the list of assumptions that support the economic assessment results.

**Table 2.** List of assumptions of the economic analysis of the proposed process.

Economic data	Value	Unit
<b>Days worked in a year</b>	330	(days/year)
<b>Raw materials prices</b>		
Annatto seeds	2.00	(USD/kg)
Turmeric	1.50	(USD/kg)
Oat bran	1.00	(USD/kg)
CO <sub>2</sub>	0.30 <sup>3</sup>	(USD/kg)
Electricity	0.05 <sup>4</sup>	(USD/kWh)
Cold demand under 293K	0.028 <sup>5</sup>	(USD/kWh)
Hot utility cost (steam low pressure)	0.052 <sup>5</sup>	(USD/kWh)

<sup>1</sup>calculated based on a medium value from different manufacturers; <sup>3</sup>data from Santos et al. (2014);

<sup>4</sup> data from Albarelli et al. (2014); <sup>5</sup>data from Pereira and Meireles (2010).

### 3 RESULTS AND DISCUSSION

#### 3.1 RAW MATERIAL AND ADSORBENT CHARACTERIZATION

Moisture of turmeric and annatto were 8.00±0.00 kg/100 kg raw material and 11.61±0.02 kg/100 kg, respectively, while the resulting particle diameters were 0.62±0.01 mm for turmeric and 3.82 ±0.09 mm for annatto. Moisture and particle diameter of oat bran were 9.00±0.01 kg/100 kg adsorbent and 0.89±0.001 mm, respectively.

### 3.2 ADSORPTION IN BENCH SCALE UNIT

The effects of CO<sub>2</sub> flow, mass of raw material and mass of adsorbent on the obtaining of extracts and adsorption efficiency on bench scale experiments are reported in Table 3 and comparisons of process performance with pilot scale tests are available in Table 4.

These results show that CO<sub>2</sub> flow ( $Q_{CO_2}$ ) and mass of adsorbent present strong correlation for the enhancement of adsorption efficiency, similarly to the assays performed in pilot scale (Table 4). This effect occurred because enhanced saturation of adsorbent by the extract. The enhancement of adsorbent saturation was attributed to the decreased porosity of column, attributed to the low proportion of void spaces inside the column. The decreased porosity of column was associated with the enhanced proportion of adsorbent used to fill the column (Table 3).

An excessive higher CO<sub>2</sub> flow rates would contribute to the dragging of extract out the adsorption column. Considering an equipment with PRCO<sub>2</sub>, the use of excessive higher CO<sub>2</sub> flow would result in pumping damaging.

Comparisons of the process parameters in bench and pilot scale are available in Table 4.

**Table 3.** Mass of adsorbed extract and calculation of adsorption efficiency in bench scale.

Process	Replica	$Q_{CO_2} \times 10^3$ (kg/min)	$F_0 (\times 10^3$ kg, d.b.)	$m_E (\times 10^3$ kg )	$m_{AE} (\times 10^3$ kg)	$m_{AD}$ (Oat bran $\times 10^3$ kg) (d.b.)	$A_E$ (kg adsorbed extract/100 kg oat bran, d.b.)
Control	1	11.78	15.47	0.26	0.09	3.19	2.98
	2	11.76	15.47	0.26	0.10	3.19	3.00
Mean $\pm$ amplitude		11.77 $\pm$ 0.01	15.47 $\pm$ 0.00	0.26 $\pm$ 0.00	0.10 $\pm$ 0.01	3.19 $\pm$ 0.00	2.99 $\pm$ 0.01
A*	1	11.78	15.47	0.26	0.02	3.19	0.53
	2	11.79	15.47	0.26	0.01	3.19	0.42
Mean $\pm$ amplitude		11.79 $\pm$ 0.01	15.47 $\pm$ 0.00	0.26 $\pm$ 0.00	0.02 $\pm$ 0.00	3.19 $\pm$ 0.00	0.47 $\pm$ 0.06
B*	1	11.81	15.47	0.26	0.02	2.28	0.80
	2	11.75	15.47	0.25	0.01	2.28	0.54
Mean $\pm$ amplitude		11.78 $\pm$ 0.03	15.47 $\pm$ 0.00	0.25 $\pm$ 0.00	0.02 $\pm$ 0.00	2.28 $\pm$ 0.00	0.67 $\pm$ 0.13
C*	1	7.56	15.47	0.23	0.01	2.28	0.34
	2	7.37	15.47	0.23	0.01	2.28	0.40
Mean $\pm$ amplitude		7.47 $\pm$ 0.09	15.47 $\pm$ 0.00	0.23 $\pm$ 0.00	0.01 $\pm$ 0.00	2.28 $\pm$ 0.00	0.37 $\pm$ 0.03
D*	1	10.07	15.47	0.24	0.01	2.28	0.54
	2	10.01	15.47	0.24	0.01	2.28	0.50
Mean $\pm$ amplitude		10.04 $\pm$ 0.03	15.47 $\pm$ 0.00	0.24 $\pm$ 0.00	0.01 $\pm$ 0.00	2.28 $\pm$ 0.00	0.52 $\pm$ 0.02

 $Q_{CO_2}$  = CO<sub>2</sub> mass flow $F_0$  = mass of annatto used in the packaging of extraction vessel $m_E$  = mass of extract $m_{AE}$  = mass of adsorbed extract $m_{AD}$  = mass of adsorbent material $A_E$  = Adsorption efficiency

\* Symbol that identifies experiments performed using annatto as raw material

**Table 4.** Interstitial velocity in adsorption columns in bench and pilot scale.

Process or Adsorption column	Replica	$m_{AD}$ (Oat bran $\times 10^3$ kg) (w..b.)	$\rho_a$ (kg/m <sup>3</sup> )	$\epsilon (-) = 1 - (\rho_a / \rho_r)$	$H_B/D_B (-)$	$\bar{u}$ (m/min)	$Q_{CO_2} \times 10^3$ (kg/min)
<b>BENCH SCALE</b>							
<b>Control</b>	1	3.50	700.32	0.48	1.05	46.49	11.78
	2	3.50	700.24	0.48	1.05	46.41	11.76
Mean ± amplitude		3.50 ± 0.00	700.28 ± 0.04	0.48 ± 0.00	1.05 ± 0.00	46.45 ± 0.04	11.77 ± 0.01
<b>A*</b>	1	3.50	700.32	0.48	1.05	46.49	11.78
	2	3.50	700.12	0.48	1.05	46.52	11.79
Mean ± amplitude		3.50 ± 0.00	700.22 ± 0.10	0.48 ± 0.00	1.05 ± 0.00	46.50 ± 0.01	11.79 ± 0.01
<b>B*</b>	1	2.50	500.14	0.63	1.05	35.63	11.81
	2	2.50	500.02	0.63	1.05	35.45	11.75
Mean ± amplitude		2.50 ± 0.00	500.08 ± 0.06	0.63 ± 0.00	1.05 ± 0.00	35.54 ± 0.09	11.78 ± 0.03
<b>C*</b>	1	2.50	500.04	0.63	1.05	22.81	7.56
	2	2.50	500.06	0.63	1.05	22.23	7.37
Mean ± amplitude		2.50 ± 0.00	500.05 ± 0.01	0.63 ± 0.00	1.05 ± 0.00	22.52 ± 0.29	7.47 ± 0.10
<b>D*</b>	1	2.50	500.06	0.63	1.05	30.38	10.07
	2	2.50	500.04	0.63	1.05	30.20	10.01
Mean ± amplitude		2.50 ± 0.00	500.05 ± 0.01	0.63 ± 0.00	1.05 ± 0.00	30.29 ± 0.09	10.04 ± 0.03
<b>PILOT SCALE</b>							
<b>AdC1*</b>	1	302.04	464.68	0.66	2.49	47.29	200.00
	2	300.98	463.05	0.66	2.49	47.20	200.00
Mean ± amplitude		301.51 ± 0.53	463.86 ± 0.82	0.66 ± 0.00	2.49 ± 0.00	47.24 ± 0.04	200.00 ± 0.00
<b>AdC2*</b>	1	201.00	502.50	0.63	12.35	120.39	115.00
	2	200.69	501.73	0.63	12.35	120.28	115.00
Mean ± amplitude		200.85 ± 0.16	502.11 ± 0.39	0.63 ± 0.00	12.35 ± 0.00	120.34 ± 0.06	115.00 ± 0.00
<b>AdC1**</b>	1	350.00	538.46	0.60	2.49	25.79	100.00
	2	350.00	538.46	0.60	2.49	25.79	100.00
Mean ± amplitude		350.00 ± 0.00	538.46 ± 0.00	0.60 ± 0.00	2.49 ± 0.00	25.79 ± 0.00	100.00 ± 0.00
<b>AdC2**</b>	1	250.00	625.00	0.54	12.35	140.73	115.00
	2	250.00	625.00	0.54	12.35	140.73	115.00
Mean ± amplitude		250.00 ± 0.00	625.00 ± 0.00	0.54 ± 0.00	12.35 ± 0.00	140.73 ± 0.00	115.00 ± 0.00

\* Experiments performed with annatto; \*\* Experiments performed with turmeric.

The enhancement of interstitial velocity is associated with the increase of the quantity of oat bran packed into the adsorption column. In bench-scale experiments, the interstitial velocity of experiment A\* was similar with that obtained in the control experiment, because of similarities between mass of adsorbent and mass flow of CO<sub>2</sub> used (Table 3 and 4).

The higher the quantity of oat bran used, the lower is the bed porosity ( $\varepsilon$ ), and subsequently, the reduction of preferred pathways by CO<sub>2</sub> (Table 3 and 4). In this case, CO<sub>2</sub> would have to travel many increasingly sinuous paths, which implied in the increasing of the distance traveled since entering until it leaves the adsorption column. The interstitial velocity also is enhanced due to the increasing of quantity of CO<sub>2</sub> passing through the adsorption column in a given unit of time. Among the experiments B\*, C\* and D\*, the flow of CO<sub>2</sub> exerted great influence for the interstitial velocity values (Table 3 and 4).

Differently from the bench scale tests, it was observed in pilot scale tests that despite increases in adsorbent amounts, there was a decrease in the interstitial velocity in AdC1 because of the reduction of the CO<sub>2</sub> flow, i.e., Q<sub>CO<sub>2</sub></sub> (Table 4).

In the second adsorption column, excessively high interstitial velocities were caused by the pressure variations ( $\Delta P=25$  MPa for annatto and  $\Delta P=20$  MPa for turmeric), which were caused by the depressurizing procedure.

### 3.3 VALIDATION OF PSEUDOCONTINUOUS PROCESS RECYCLING SYSTEM

Global mass balance of the replicates of pseudocontinuous extractions for turmeric and annatto are available in Table 5. It is observed that the values obtained between the parameters from each experimental replicate were next from each other. This behavior confirms the reliability of implemented pseudocontinuous system in pilot scale.

**Table 5.** Global mass balance of pseudocontinuous extraction process in pilot scale.

Replicate	Global mass balance: annatto					Global mass balance: turmeric				
	Annatto seeds (d.b.) (kg)	Extract (w.b.) (kg)	[kg extract/100 kg annatto seeds]	Extract adsorbed in Oat bran (kg)*	Turmeric (d.b.) (kg)	Extract (w.b.) (kg)	[kg extract/100 kg turmeric]	Extract adsorbed in Oat bran (kg)**		
1	10.61	0.18	1.70	<i>AdC1</i> *** $7 \times 10^{-3a}$	<i>AdC2</i> **** $3.20 \times 10^{-3b}$	7.36	0.41	5.57	<i>AdC1</i> *** $6.64 \times 10^{-3e}$	<i>AdC2</i> **** $1.10 \times 10^{-3f}$
2	10.61	0.18	1.68	$9 \times 10^{-3c}$	$4.86 \times 10^{-3d}$	7.36	0.45	6.06	$5.29 \times 10^{-3g}$	$2.26 \times 10^{-3h}$
Mean	-----	0.18	1.69	$8 \times 10^{-3}$	$4.03 \times 10^{-3}$	-----	0.43	5.81	$5.97 \times 10^{-3}$	$1.68 \times 10^{-3}$
+/-	-----	$2 \times 10^{-3}$	$2 \times 10^{-5}$	$2 \times 10^{-3}$	$1.66 \times 10^{-3}$	-----	0.03	$3.50 \times 10^{-4}$	$9.50 \times 10^{-4}$	$8.20 \times 10^{-4}$
[Amplitude]										

\* Total adsorbed mass of bixin and geranylgeraniol

\*\*Total adsorbed mass of ar-turmerone and curcumin adsorbed\*\*.

\*\*\*a, c, e and g correspond to the mass variation of extract adsorbed in the oat bran in AdC1, obtained by subtraction of oat bran with adsorbed extract and the initial mass of oat bran, i.e. 0.308.74g-302.04g (a), 309.99g-300.98g (c), 356.64g-350.00g (e) and 355.29g-350.00g (g).

\*\*\*\*b, d, f and h correspond to the mass variation of extract adsorbed in the oat bran in AdC2, obtained by subtraction of oat bran with adsorbed extract and the initial mass of oat bran, i.e. 197.80g-201.00g (b), 195.83g-200.69g (d), 248.90g-250.00g (f), and 247.74g-250.00g (h).

Comparative aspects of CO<sub>2</sub> consumption between the PRCO<sub>2</sub> system and the system with absence of PRCO<sub>2</sub> is shown in Table 6. The fourth column values in Table 6 were calculated considering a full 23 kg CO<sub>2</sub> cylinder, and represents the maximum quantity that would be used. In this case, for each cylinder approximately 12 kg CO<sub>2</sub> could be used.

With the use of PRCO<sub>2</sub>, the difference equivalent to 11 kg of remaining gas from the cylinder is applied to fill the storage tank, prior to extraction. That is, the PRCO<sub>2</sub> storage tank improves the economy of the use of gas for the initiation of further processes. In case of absence of storage tank, these 11 kg would not be reused and would represent an additional cost with acquisition of inputs.

Establishing comparisons between the mass of CO<sub>2</sub> to process a cycle of extraction without and with PRCO<sub>2</sub>, it is observed an expenditure of 250% more of mass of CO<sub>2</sub> which is equivalent to 7 kg of CO<sub>2</sub> spent more.

Comparing the amount of CO<sub>2</sub> spent in one cycle between the processes with absence (9.8 kg, from Table 6) and with the presence of PRCO<sub>2</sub> (2.8 kg, from Table 6), it is observed a CO<sub>2</sub> expense 250% higher for the system without PRCO<sub>2</sub>, i.e., 7 kg of CO<sub>2</sub> that was not reused, due to the absence of PRCO<sub>2</sub>.

Based on the calculations procedures applied in Table 6 associated with the definition of solvent to feed ratio (S/F) for n cycles in processes with PRCO<sub>2</sub>, according to the relation proposed in Eq. 1.

Considering this approach the range for S/F is a half-open interval from the left and equal to (0.77, 0.93] for annatto and (1.15, 1.40] for turmeric, which can consider the process as pseudocontinuous, with  $n \geq 2$ .

**Table 6.** Comparative aspects of CO<sub>2</sub> use in processes with and without PRSCO<sub>2</sub> applied to turmeric and annatto.

raw material	without PRSCO <sub>2</sub>							with PRSCO <sub>2</sub>				CO <sub>2</sub> saving aspects			
	n	raw material (kg)	*A (kg) = 2.3n+0.5	**B (kg) = Q <sub>CO<sub>2</sub></sub> × t <sub>DIN</sub> × n	Total (kg) = A+B	CO <sub>2</sub> cylinder (unit)	S/F	Total (kg) = A=2.3n+0.5	CO <sub>2</sub> cylinder (unit)	S/F	Cost of CO <sub>2</sub> cylinder (USD)	Monetary saving (USD)	CO <sub>2</sub> saving (%)		
								***Total/m <sub>CO<sub>2</sub>used</sub>	whole cylinder						
Turmeric	1	2	2.8	7	9.8	0.8	1	4.90	2.8	0.2	1	1.40	37.28	0.00	71.43
	2	4	5.1	14	19.1	1.6	2	4.78	5.1	0.4	1	1.28	74.55	37.28	73.30
	3	6	7.4	21	28.4	2.4	3	4.73	7.4	0.6	1	1.23	111.83	74.55	73.94
	4	8	9.7	28	37.7	3.1	4	4.71	9.7	0.8	1	1.21	149.11	111.83	74.27
Annatto	1	3	2.8	14	16.8	1.4	2	5.60	2.8	0.2	1	0.93	74.56	37.28	83.33
	2	6	5.1	28	33.1	2.8	3	5.52	5.1	0.4	1	0.85	111.84	74.56	84.59
	3	9	7.4	42	49.4	4.1	5	5.49	7.4	0.6	1	0.82	186.40	149.12	85.02
	4	12	9.7	56	65.7	5.5	6	5.48	9.7	0.8	1	0.81	223.68	186.40	85.24

n is the number of cycles (4 cycles, according to Figure 3).

\*A = (2.3n+0.5), is the sum between the minimum amount of CO<sub>2</sub> (in kg) required to pressurize the extraction column (2.3n) and the three separation vessels (0.5) in n cycles. For instance, in one cycle, 2.3 kg of CO<sub>2</sub> was used to pressurize the extraction column and 0.5 kg of CO<sub>2</sub> was used to pressurize the separation vessels.

\*\*B (Q<sub>CO<sub>2</sub></sub> × t<sub>DIN</sub> × n) is the amount of CO<sub>2</sub> associated with the number of cycles. Q<sub>CO<sub>2</sub></sub> (kg/min) is the mass flow of CO<sub>2</sub> and t<sub>DIN</sub> (min) is the dynamic period during 1 cycle, i.e., 70 min.

\*\*\* Total/m<sub>CO<sub>2</sub>used</sub> represents the ratio between the total mass of CO<sub>2</sub> used and the mass of CO<sub>2</sub> (12 kg) from a 23 kg cylinder that is able to be used for processing.

The remaining 11 kg from the cylinder cannot be used because of pumping limitations. Nevertheless, this quantity of CO<sub>2</sub> may be reused for further processes with the aid of a storage tank.

The S/F value for one cycle with 70 min of dynamic period with the absence of PR<sub>CO<sub>2</sub></sub> is 4.9 for turmeric and 5.6 for annatto, i.e., these values represent approximately 250-500% of non-reused CO<sub>2</sub> (7 kg and 14 kg, respectively). Considering a PR<sub>CO<sub>2</sub></sub> process with 4 cycles constituted of 70 min of dynamic period, S/F turns 0.81 for annatto and 1.21 for turmeric.

Considering a pseudo continuous process consisted of 4 cycles, the extraction of 12 kg of annatto seeds without and with the presence of PR<sub>CO<sub>2</sub></sub> requires 67.20 and 9.70 kg CO<sub>2</sub> respectively, which represents a saving equivalent to 85.57% for solvent consumption and the processing of 8 kg of turmeric 39.20 and 9.70 kg CO<sub>2</sub> considering processes without and with PR<sub>CO<sub>2</sub></sub>, which represents a saving of 75.26%.

### 3.4 COMPOSITION OF EXTRACTS

Bioactive constituents obtained are available in Table 7. Sesquiterpenes, like geranylgeraniol and ar-turmerone, are the major group of molecules found in the volatile oils of annatto [20] and turmeric [21].

The highest quantity of geranylgeraniol was obtained in AdC1, which was similar with that found in *Artemisia dracunculus* essential oil [22]. Bixin content in the crude and fractionated extracts were higher than those obtained previously [23], comparable than the extracts obtained using pressurized hot water [24] and lower than those extracts obtained with pressurized hot water extraction assisted with SC-CO<sub>2</sub> [25].

The adsorption capacity of target compounds are dependent on the accessibility of the organic molecules to the inner surface of the adsorbent, which depends on their size, as well as the solubility of the target compounds in CO<sub>2</sub> (Moreno-Castilla, 2004).

The lower quantity of adsorbed extracts in AdC2 is associated with losses of extract attributed to the depressurization of extraction columns after the dynamic pseudocontinuous extraction in 4 cycles (Table 7).

**Table 7.** Chemical composition of annatto and turmeric extracts (kg/100kg raw material, dry basis).

<b>Material</b>	<b>Process</b>	<b>Condition</b>	<b>Annatto</b>		<b>Turmeric</b>	
			<b>Geranylgeraniol</b>	<b>Bixin</b>	<b>Ar-turmerone</b>	<b>Curcumin</b>
Crude raw material	-	-	697.42±18.06	360.62±2.30	1.24±0.06	2.70±0.02
Deffatted annatto seeds/	1	4-cycle processing**	1204.42±13.55	512.37±5.76	0.52±0.15	4.02±0.37
Deflavored turmeric						
Oat bran + extract	1	AdC1	244.40±3.40	30.19±0.12	0.46±0.10	4.02±0.48
	2	AdC2	437.15±3.50	13.04±0.01	1.71±0.08	NI
	1	AdC1	496.97±6.02	40.60±0.10	3.57±0.19	0.72±0.09
	2	AdC2	228.62±5.34	4.47±0.03	3.95±0.15	NI
Fractionated extract	1	SV1	1.68±0.13	*	1.76±0.13	0.23±0.03
		SV2	0.33±0.02	*	10.78±0.36	0.02±0.00
		SV3	0.21±0.01	*	8.90±0.06	NI
	2	SV1	0.35±0.03	*	5.31±0.01	NI
		SV2	0.71±0.05	*	4.18±0.04	0.02±0.00
		SV3	2.54±0.18	*	4.03±0.17	0.00±0.00

AdC<sub>n</sub> – Adsorption column (n=1, 2, 3...); SV<sub>n</sub> – Separation vessels (n=1, 2, 3 ...). NI – non-identified, under detection limit for this methodology and equipment. \*Identified as traces, under detection limit for this methodology and equipment

\*\* Obtained from a process composed of 4 cycles

The solubility of the target compounds from turmeric and annatto in CO<sub>2</sub> probably contributed to the differences in adsorbed substances (Table 7). For instance, in comparison with crude raw materials used, 35% geranylgeraniol, 8.37% bixin, 37% of ar-turmerone and 148.89% of curcumin were adsorbed in AdC1 (first replicate).

Polyphenols like curcumin are poorly soluble in CO<sub>2</sub> and this factor justifies the highest adsorbed materials. This is in accordance with literature that states that adsorption increases with decrease in the solubility of the solvent. Greater the solubility, stronger the solute-solvent bond and the smaller the extent of adsorption [5].

### 3.5 ADSORBENT COMPOSITION

#### 3.5.1 Differential Scanning calorimetry

DSC gelatinization parameters of oat bran adsorbent (Table 8) showed similar trends, but in less intensity, which would reflect that the process for CO<sub>2</sub> purification and recycling based on subcritical adsorption did not alter the physical structure of the adsorbent. On set temperature data were comparable [26] and peak and conclusion temperatures were higher than those obtained in literature [27]. On the other hand, gelatinization enthalpy obtained was lower with those reported with oat starch [28, 29] which indicates that the adsorption conditions did not contribute to gelatinize the starchy structure of adsorbent (Table 8).

**Table 8.** Comparative thermal properties of crude oat bran and oat bran as adsorbent.

Sample	T <sub>O</sub> (K)	T <sub>PEAK</sub> (K)	T <sub>C</sub> (K)	ΔH <sub>GEL</sub> (J/g)
crude oat bran	324.56	377.03	458.15	2.06
adsorption in AdC1 + annatto extract	324.34	374.45	453.15	2.06
adsorption in AdC2 + annatto extract	326.27	379.20	456.15	1.96
adsorption in AdC1 + turmeric extract	325.44	377.03	456.15	1.98
adsorption in AdC2 + turmeric extract	336.18	376.35	453.15	2.03

### 3.5.2 X-ray diffraction (XRD)

The XRD patterns and the degree of crystallinity of adsorbent (Figure 4) was identified as an A-type polymorph with predominant characteristic peaks at Bragg angles ( $2\theta$ ) of 15, 17.0, 18.0, and 23°, similarly to oat bran [30], oat starch [28] and degraded oat glucan [6]. Neither conditions used were able to impart significant effects on the position of previously mentioned XR-D peaks, indicating that the crystalline structure characteristics of adsorbent remained intact after adsorption procedures.

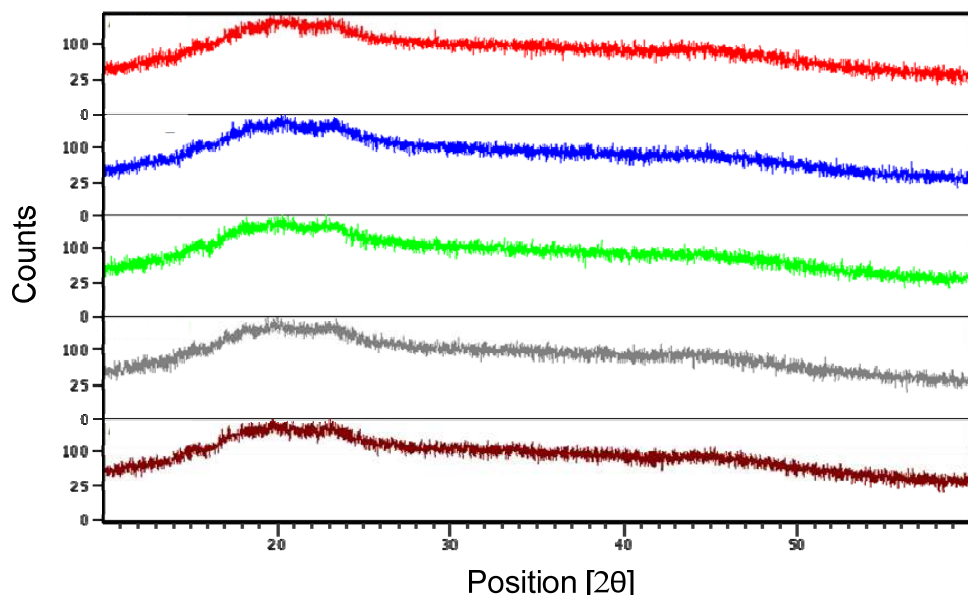


**Figure 4.** X-ray diffraction pattern of oat bran adsorbent: crude oat bran (red), adsorption in AdC1 + annatto extract (blue), adsorption in AdC2 + annatto extract (green), adsorption in AdC1 + turmeric extract (gray), adsorption in AdC2 + turmeric extract (brown).

### 3.5.3 Thermogravimetric analysis

Thermal decomposition behavior parameters of adsorbent (Table 9) were comparable with those detect to sugarcane straw [31]. The energy oat bran thermal decomposition was divided into three stages, such as dehydration ( $T_{HD}$ ), pyrolysis ( $T_p$ ),

and carbonization of the sample,  $T_c$ . Total weight loss correspond to 93.88-96.02% of adsorbent weight lost during analyses. Thermal decomposition parameters of oat bran showed slight similarity (Table 9), corroborating with the results obtained with DSC. In this case, the conditions used in PRCO<sub>2</sub> did not altered the structure of the adsorbent.

**Table 9.** Thermal decomposition of crude oat bran and oat bran as adsorbent.

<b>Sample</b>	<b><math>T_{START}</math> (K)</b>	<b><math>T_{DH}</math> (K)</b>	<b><math>T_p</math> (K)</b>	<b><math>T_c</math> (K)</b>	<b>Total weight loss (%)</b>
crude oat bran	298.81	373.20	642.30	881.00	-96.02
adsorption in AdC1 + annatto extract	299.31	369.86	639.75	870.85	-95.21
adsorption in AdC2 + annatto extract	301.15	370.11	639.15	876.75	-95.02
adsorption in AdC1 + turmeric extract	297.88	370.56	647.15	869.65	-93.88
adsorption in AdC2 + turmeric extract	298.79	370.61	643.15	858.95	-94.34

### 3.5.4 Scanning electron microscopy (SEM)

The SEM analysis of adsorbent is showed in Figure 5. In column A it can be observed two structures that characterize the particles of oat bran. In Figures 5.A2 and 5.A4 the magnitude was increased 500  $\times$ . In the Figure 5.A2, it is observed that the presence of porous and roughness visualized in oat bran suggest a tendency to retain substances originated from an adsorption process (Figure 5.A2). In this context an apparent accumulation of extracts of turmeric (Figure 5.B1 and 7.B2) and annatto (Figure 5.C1 and 6.C2) was observed.

In Figure 5.A4, oat bran presents smooth surface with presence of small particles deposited on the surfaces of larger ones. The effect of CO<sub>2</sub> on this material is reflected by the removal of particulate matter from the larger particles due to the drag

However, when high interstitial velocity is applied in the depressurization in the extraction and AdC2 columns, the presence of the microparticles is almost imperceptible (Figures 5.4B and 5.4C).

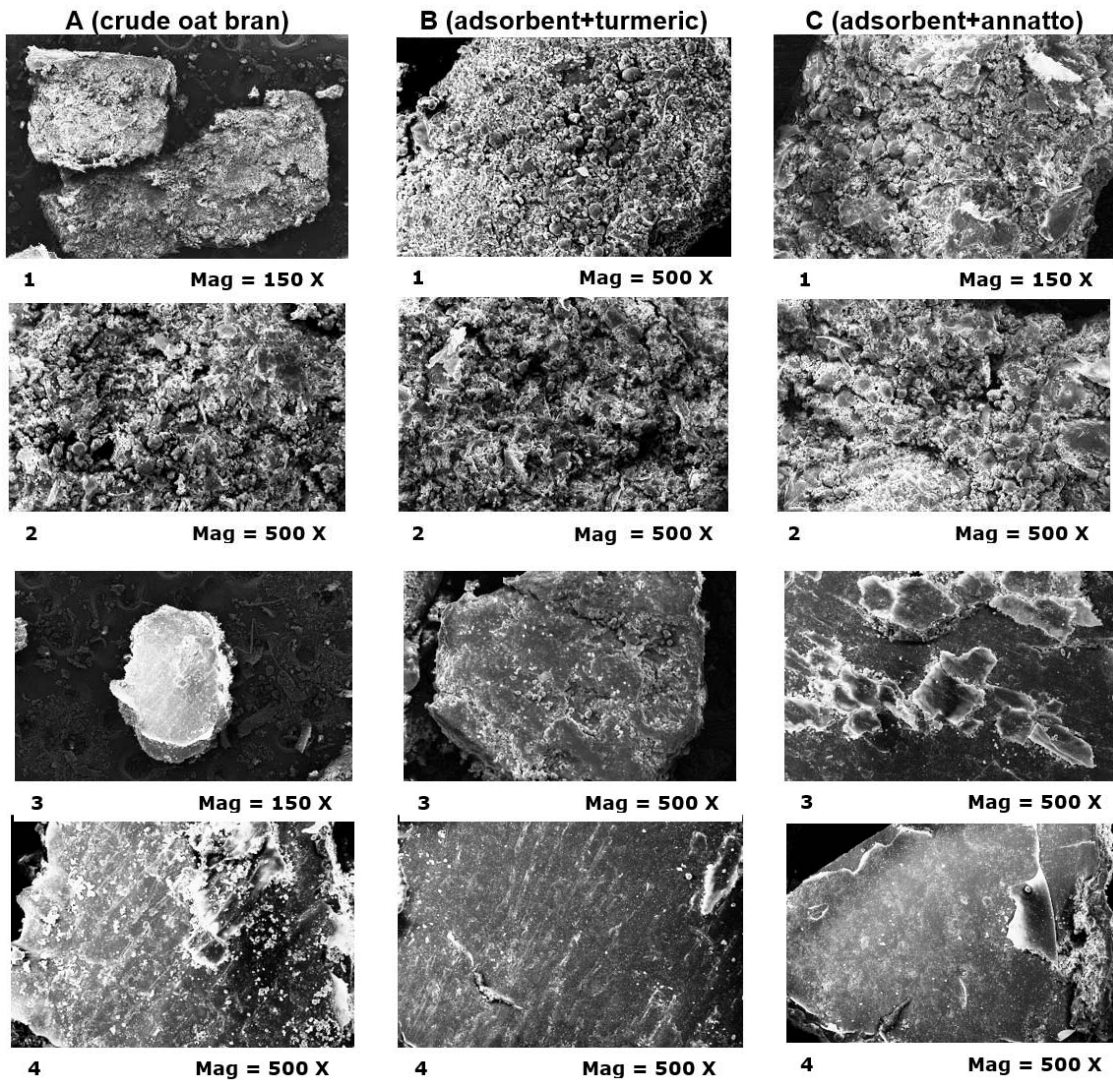


**Figure 5.** SEM of crude (A) and adsorbed oat bran in the extracts of turmeric (B) and annatto (C) in AdC1 (1 and 3) and AdC2 (2 and 4).

### 3.6 PROCESS EVALUATION USING SIMULATION TOOLS

Table 10 shows the investment necessary for each process. It was considered 2 SFE extractors working in parallel in order to enable multiple cycles before depressurization. Figure 6 shows the percentage contribution of each equipment to the total investment cost. In both cases the use of an adsorption column to CO<sub>2</sub> purification before recycle increases the investment in a extraction plant less than 5%. The main expenditure is the supercritical extractor vessel. Annatto seed extraction process presents higher investment

due to the higher S/F necessary for the process, increasing the CO<sub>2</sub> equipment related costs.

**Table 10.** Investment calculated for each SFE process studied.

	Turmeric	Annatto seeds	
SFE extractor	1.22	1.22	MUSD*
Separation vessel 1	0.42	0.55	MUSD
Separation vessel 2	0.18	0.29	MUSD
Separation vessel 3	0.14	0.23	MUSD
CO <sub>2</sub> storage tank	0.29	0.29	MUSD
Adsorption column	0.09	0.16	MUSD
CO <sub>2</sub> pump	0.26	0.29	MUSD
Heat exchange network	0.09	0.09	MUSD
<b>Total</b>	<b>2.68</b>	<b>3.11</b>	<b>MUSD</b>

\*MUSD – Million United States Dollars.

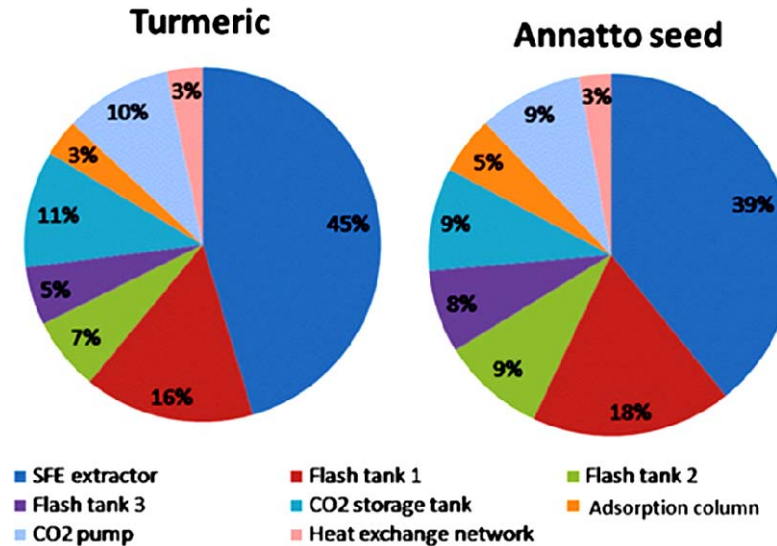


**Figure 6.** Contribution of each equipment to the total investment cost.

Table 11 shows the amount of extract produced at each process yearly and the amount of CO<sub>2</sub> consumption in a year necessary for reposition after each depressurization. Total extract produced increases with the increase of cycles without depressurization as less time is expended yearly with depressurization of the system. Less CO<sub>2</sub> consumption is necessary. For 8 and 12 cycles without depressurization it is necessary to check

experimentally if the same purity of CO<sub>2</sub> can be obtained without reposition of the oat adsorbent. One possibility would be to use both adsorption columns to work in parallel replacing the oat adsorbent when necessary. With the increase in the number of cycles without depressurization, the ratio of extract per mass of CO<sub>2</sub> consumed increases, representing a more efficient process. The impact of these factors on the economic indicators studied is presented in Table 12.

**Table 11.** Effects of impact of number of cycles on the economic indicators.

	System A	System B	Simulation extrapolation	
Number of cycles without depressurization	1	4	8	12
<b>Turmeric processing</b>				
Turmeric extract	36.30	58.00	64.50	67.00 t/year
CO <sub>2</sub> Consumption	2375.8	949.90	527.80	365.40 t/year
product/CO <sub>2</sub> consumption ratio	0.02	0.06	0.12	0.18
<b>Annatto seed processing</b>				
Annatto extract	15.80	25.30	28.10	29.20 t/year
CO <sub>2</sub> Consumption	4755	1901.20	1056.40	731.30 t/year
product/CO <sub>2</sub> consumption ratio	$3 \times 10^{-3}$	0.013	0.03	0.04

**Table 12.** Cost of manufacturing (COM) for the evaluated process.

	System A	System B	Simulation extrapolation		
Process time	2.3	5.8	10.5	15.2	h
Number of cycles without depressurization	1	4	8	12	
<b>Turmeric</b>					
total investment	2.07	2.68	2.68	2.68	MUSD
Variable cost	2.31	1.20	0.86	0.72	MUSD
Fix cost	0.46	0.56	0.56	0.56	MUSD
General production cost	0.02	0.02	0.02	0.02	MUSD
COM	3.31	2.12	1.72	1.56	MUSD
COM <sub>prod</sub>	91.31	36.56	26.61	23.29	USD/kg
<b>Annatto seeds</b>					
total investment	2.50	3.11	3.11	3.11	MUSD
Variable cost	4.10	1.95	1.30	1.05	MUSD
Fix cost	0.53	0.63	0.63	0.63	MUSD
General production cost	0.02	0.03	0.03	0.03	MUSD
COM	5.53	3.11	2.33	2.04	MUSD
COM <sub>prod</sub>	349.60	122.67	82.96	69.72	USD/kg

The process without the adsorption column for CO<sub>2</sub> recycle without depressurization would present around 0.8 to 0.9% lower COM<sub>prod</sub> than System A. The adsorption column facilitates the PRCO<sub>2</sub> without the need of depressurization, decreasing considerably the cost of manufacture of the product, COM (Table 12).

It is possible to envision that the higher the number of cycles without depressurization the higher is the economic benefit of the process. The use of oat as adsorbent enables the selling of a second product, the enriched oat, what increases the economic attractiveness of the process, because of the obtaining of three types of extracts,

and two types of different byproducts, which are the enriched oat bran of the adsorbed extracts, which have great potential of use for industry.

#### 4 CONCLUSIONS

The validation of a system for purification and recycling of CO<sub>2</sub> in pilot scale reduced the consumption of CO<sub>2</sub> to 85.24% on the processing of annatto, and 74.27% on the processing of turmeric. Process simulation and economic evaluation showed that the increasing of the number of cycles without increases the process feasibility, in the case the absence of depressurizing procedure. Besides the reusing of CO<sub>2</sub> and the production of extracts with different chemical compositions, the validated process contributed to the obtained of byproducts enriched with bioactive compounds.

#### ACKNOWLEDGMENTS

R. Abel C. Torres thanks Capes for his doctorate assistantship. Ádina L. Santana thanks Capes (88882.305824/2013-01) for her postdoctoral financial support. Diego T. Santos and Juliana Q. Albarelli thank CNPq (processes 401109/2017-8 and 150745/2017-6) and FAPESP (processes 2013/18114-2; 2015/06954-1) for the post-doctoral fellowships. M. Angela A. Meireles thanks CNPq for the productivity grant (302423/2015-0). The authors acknowledge the financial support from FAPESP (process 2015/13299-0)

#### REFERENCES

- [1] Á.L. Santana, D.T. Santos, M.A.A. Meireles, Perspectives on small-scale integrated biorefineries using supercritical CO<sub>2</sub> as a green solvent, Current Opinion in Green and Sustainable Chemistry 18 (2019) 1-12.
- [2] R.A.C. Torres, Á.L. Santana, D.T. Santos, M.A.A. Meireles, Perspectives on the Application of Supercritical Antisolvent Fractionation Process for the Purification of Plant Extracts: Effects of Operating Parameters and Patent Survey, Recent Advances in the Technologies of 10(2) (2016) 128.
- [3] X. Tang, N. Ripepi, High pressure supercritical carbon dioxide adsorption in coal: Adsorption model and thermodynamic characteristics, Journal of CO<sub>2</sub> Utilization 18 (2017) 189-197.
- [4] G. Perretti, C. Virgili, A. Troilo, O. Marconi, G.F. Regnicoli, P. Fantozzi, Supercritical antisolvent fractionation of lignans from the ethanol extract of flaxseed, The Journal of Supercritical Fluids 75 (2013) 94-100.

- [5] Shodhganga, Principles of adorption, 2019. [http://shodhganga.inflibnet.ac.in/bitstream/10603/22665/8/08\\_chapter3.pdf](http://shodhganga.inflibnet.ac.in/bitstream/10603/22665/8/08_chapter3.pdf). (Accessed 21.01.2019 2019).
- [6] P.R. Hussain, S.A. Rather, P.P. Suradkar, Structural characterization and evaluation of antioxidant, anticancer and hypoglycemic activity of radiation degraded oat (*Avena sativa*)  $\beta$ - glucan, *Radiation Physics and Chemistry* 144 (2018) 218-230.
- [7] K.S. Sandhu, P. Godara, M. Kaur, S. Punia, Effect of toasting on physical, functional and antioxidant properties of flour from oat (*Avena sativa L.*) cultivars, *Journal of the Saudi Society of Agricultural Sciences* 16(2) (2017) 197-203.
- [8] Q. Huang, C.H. Niu, A.K. Dalai, Production of anhydrous biobutanol using a biosorbent developed from oat hulls, *Chemical Engineering Journal* 356 (2019) 830-838.
- [9] R. Gao, H. Liu, Z. Peng, Z. Wu, Y. Wang, G. Zhao, Adsorption of (-)-epigallocatechin-3-gallate (EGCG) onto oat  $\beta$ -glucan, *Food Chemistry* 132(4) (2012) 1936-1943.
- [10] Á.L. Santana, J.Q. Albarelli, D.T. Santos, R. Souza, N.T. Machado, M.E. Araújo, M.A.A. Meireles, Kinetic behavior, mathematical modeling, and economic evaluation of extracts obtained by supercritical fluid extraction from defatted assaí waste, *Food Bioprod Process* 107 (2018) 25-35.
- [11] J.M. Prado, I. Dalmolin, N.D.D. Carareto, R.C. Basso, A.J.A. Meirelles, J. Vladimir Oliveira, E.A.C. Batista, M.A.A. Meireles, Supercritical fluid extraction of grape seed: Process scale-up, extract chemical composition and economic evaluation, *Journal of Food Engineering* 109(2) (2012) 249-257.
- [12] J.M. Prado, G.H.C. Prado, M.A.A. Meireles, Scale-up study of supercritical fluid extraction process for clove and sugarcane residue, *The Journal of Supercritical Fluids* 56(3) (2011) 231-237.
- [13] M.A.A. Meireles, Extraction of Bioactive Compounds from Latin American Plants, in: J.L. Martinez (Ed.), *Supercritical fluid extraction of nutraceuticals and bioactive compounds*, CRC Press-Taylor and Francis Group, Boca Raton, 2007.
- [14] E.K. Silva, G.L. Zabot, M.A. A. Meireles, Ultrasound-assisted encapsulation of annatto seed oil: Retention and release of a bioactive compound with functional activities, *Food Research International* 78 (2015) 159-168.
- [15] J.F. Osorio-Tobón, P.I.N. Carvalho, M.A. Rostagno, A.J. Petenate, M.A.A. Meireles, Extraction of curcuminoids from deflavored turmeric (*Curcuma longa L.*) using pressurized liquids: Process integration and economic evaluation, *J Supercrit Fluids* 95 (2014) 167-174.
- [16] M.E.M. Braga, P.F. Leal, J.E. Carvalho, M.A.A. Meireles, Comparison of Yield, Composition, and Antioxidant Activity of Turmeric (*Curcuma longa L.*) Extracts Obtained Using Various Techniques, *Journal of Agricultural and Food Chemistry* 51(22) (2003) 6604-6611.
- [17] P.I.N. Carvalho, J.F. Osorio-Tobón, M.A. Rostagno, A.J. Petenate, M.A.A. Meireles, Techno-economic evaluation of the extraction of turmeric (*Curcuma longa L.*) oil and ar-turmerone using supercritical carbon dioxide, *J. Supercrit. Fluids* 105 (2015) 44-54.
- [18] J.Q. Albarelli, A.V. Ensinas, M.A. Silva, Product diversification to enhance economic viability of second generation ethanol production in Brazil: the case of the sugar and ethanol joint production., *Chem. Eng. Res. Des.* 92 (2014) 1470–1481.
- [19] J.M. Prado, I. Dalmolin, N.D.D. Carareto, R.C. Basso, A.J.A. Meirelles, J. Vladimir Oliveira, E.A.C. Batista, M.A.A. Meireles, Supercritical fluid extraction of grape seed: process scale-up, extract chemical composition and economic evaluation, *J Food Eng* 109 (2012).

- [20] I. Shahid ul, L.J. Rather, F. Mohammad, Phytochemistry, biological activities and potential of annatto in natural colorant production for industrial applications – A review, *Journal of Advanced Research* 7(3) (2016) 499-514.
- [21] H. Xiang, L. Zhang, L. Xi, Y. Yang, X. Wang, D. Lei, X. Zheng, X. Liu, Phytochemical profiles and bioactivities of essential oils extracted from seven Curcuma herbs, *Industrial Crops and Products* 111 (2018) 298-305.
- [22] T. Liu, P. Lin, T. Bao, Y. Ding, Q. Lha, P. Nan, Y. Huang, Z. Gu, Y. Zhong, Essential oil composition and antimicrobial activity of *Artemisia dracunculus* L. var. *qinghaiensis* Y. R. Ling (Asteraceae) from Qinghai-Tibet Plateau, *Industrial Crops and Products* 125 (2018) 1-4.
- [23] C.L.C. Albuquerque, M.A.A. Meireles, Defatting of annatto seeds using supercritical carbon dioxide as a pretreatment for the production of bixin: Experimental, modeling and economic evaluation of the process, *The Journal of Supercritical Fluids* 66 (2012) 86-95.
- [24] L.M. Rodrigues, S.C. Alcázar-Alay, A.J. Petenate, M.A.A. Meireles, Bixin extraction from defatted annatto seeds, *Comptes Rendus Chimie* 17(3) (2014) 268-283.
- [25] S.C. Alcázar-Alay, J.F. Osorio-Tobón, T. Forster-Carneiro, C.J. Steel, M.A.A. Meireles, Polymer modification from semi-defatted annatto seeds using hot pressurized water and supercritical CO<sub>2</sub>, *The Journal of Supercritical Fluids* 129 (2017) 48-55.
- [26] F. Zhu, Structures, properties, modifications, and uses of oat starch, *Food Chemistry* 229 (2017) 329-340.
- [27] A. Shah, F.A. Masoodi, A. Gani, B.A. Ashwar, Newly released oat varieties of himalayan region -Techno-functional, rheological, and nutraceutical properties of flour, *LWT - Food Science and Technology* 70 (2016) 111-118.
- [28] S.R. Falsafi, Y. Maghsoudlou, H. Rostamabadi, M.M. Rostamabadi, H. Hamedi, S.M.H. Hosseini, Preparation of physically modified oat starch with different sonication treatments, *Food Hydrocolloids* 89 (2019) 311-320.
- [29] C. Li, S.-G. Oh, D.-H. Lee, H.-W. Baik, H.-J. Chung, Effect of germination on the structures and physicochemical properties of starches from brown rice, oat, sorghum, and millet, *International Journal of Biological Macromolecules* 105 (2017) 931-939.
- [30] G.E. Jacques-Fajardo, R. Prado-Ramírez, E. Arriola-Guevara, E. Pérez Carrillo, H. Espinosa-Andrews, G.M. Guatemala Morales, Physical and hydration properties of expanded extrudates from a blue corn, yellow pea and oat bran blend, *LWT* 84 (2017) 804-814.
- [31] Y.J. Rueda-Ordóñez, K. Tannous, Drying and thermal decomposition kinetics of sugarcane straw by nonisothermal thermogravimetric analysis, *Bioresource Technology* 264 (2018) 131-139.

## Supplementary material

**Table A1.** Mathematical modeling of turmeric using 2 straight-lines spline

Parameter	Value
$b_0$ (g)	$2.22 \times 10^{-16}$
$b_1 = MCER$ (g/min)	0.042
$b_2 = MFER$ (g/min)	-0.042
$tCER$ (min)	2
$RCER$ (kg extract/100kg raw material)	5.49
$Y_{CER}$ (kg extract/kg solvent)	$4.55 \times 10^{-3}$
$R^2$	0.99

**Table A2.** Mathematical modeling of annatto using 3 straight-lines spline

Parameter	Value
$b_0$ (g)	0.31
$b_1 = MCER$ (kg/min)	0.014
$b_2 = MFER$ (kg/min)	-0.011
$b_3$ (kg/min)	$-2.1 \times 10^{-3}$
$tCER$ (min)	22
$tFER$ (min)	135
$RCER$ (kg extract/100kg seeds)	53.02
$RFER$ (kg extract/100kg seeds)	75.89
$Y_{CER}$ (kg extract/kg solvent)	$1.29 \times 10^{-3}$
$Y_{FER}$ (kg extract/kg solvent)	$-2 \times 10^{-4}$
$R^2$	0.99

Table B1. Parameters from SFE in the bench-scale unit applied to turmeric (replicate 1)

t (min)	S/F	P (bar)	Density (g/cm <sup>3</sup> )	Vfm (m <sup>3</sup> )	Mf (g/min)	Mass of CO <sub>2</sub> (g/min)*min	Extract (g)	Accumulated extract (g)	Relative extract (d.b.) (g extract/100 g turmeric)
2	1.2217	0.9315	0.0016786	173.6240	9.23230	18.465	0.7262	0.7262	5.22
4	2.4434	0.9315	0.0016786	173.6350	9.23230	36.929	0.0397	0.7659	5.51
6	3.6651	0.9315	0.0016786	173.6460	9.23230	55.394	0.0145	0.7804	5.61
10	6.1085	0.9315	0.0016786	173.6680	9.23230	92.323	0.0241	0.8045	5.79
15	9.1627	0.9315	0.0016786	173.6955	9.23230	138.484	0.0199	0.8244	5.93
20	12.2170	0.9315	0.0016786	173.7230	9.23230	184.646	0.0146	0.8390	6.03
25	15.2630	0.9310	0.0016777	173.7505	9.22735	230.783	0.0066	0.8456	6.08
30	18.3156	0.9310	0.0016777	173.7780	9.22735	276.919	0.0062	0.8518	6.13
35	21.3682	0.9310	0.0016777	173.8055	9.22735	323.056	0.0046	0.8564	6.16
40	24.4208	0.9310	0.0016777	173.8330	9.22735	369.193	0.0018	0.8582	6.17
45	27.4734	0.9310	0.0016777	173.8605	9.22735	415.330	0.0030	0.8612	6.19
50	30.5260	0.9310	0.0016777	173.8880	9.22735	461.467	0.0027	0.8639	6.21
55	33.5786	0.9310	0.0016777	173.9155	9.22735	507.603	0.0019	0.8658	6.23
60	36.6116	0.9305	0.0016768	173.9430	9.22240	553.715	0.0015	0.8673	6.24

X<sub>0</sub> Turmeric: [g extract/100 g turmeric (d.b.)] 6.25

- Vfm = reading of the volumetric flow meter.
- Initial reading of the volumetric flow meter 173.613 m<sup>3</sup>
- Mf = Mass flow calculation.
- Mass of ground turmeric on a dry basis 13.9048 g.
- Mass of ground turmeric on a wet basis 15.1139 g.
- Residual extract obtained from the cleaning of the bench unit 0.22 kg × 10<sup>-5</sup>
- Moisture of the raw material 8%

Table B2. Parameters from SFE in the bench-scale unit applied to turmeric (replicate 2)

t (min)	S/F	P (bar)	Density (g/cm <sup>3</sup> )	Vfm (m <sup>3</sup> )	Mf (g/min)	Mass of CO <sub>2</sub> (g/min)*min	Extract (g)	Accumulated extract (g)	Relative extract (d.b.) (g extract/100 g turmeric)
2	1.2170	0.9280	0.0016722	174.0000	9.19710	18.394	0.7249	0.7249	5.21
4	2.4341	0.9280	0.0016722	174.0110	9.19710	36.788	0.0351	0.7600	5.47
6	3.6511	0.9280	0.0016722	174.0220	9.19710	55.183	0.0197	0.7797	5.61
10	6.0852	0.9280	0.0016722	174.0440	9.19710	91.971	0.0209	0.8006	5.76
15	9.1278	0.9280	0.0016722	174.0715	9.19710	137.956	0.0140	0.8146	5.86
20	12.1704	0.9280	0.0016722	174.0990	9.19710	183.942	0.0110	0.8256	5.94
25	15.2212	0.9285	0.0016731	174.1265	9.20205	229.952	0.0094	0.8350	6.01
30	18.2654	0.9285	0.0016731	174.1540	9.20205	275.962	0.0059	0.8409	6.05
35	21.3096	0.9285	0.0016731	174.1815	9.20205	321.973	0.0067	0.8476	6.10
40	24.3539	0.9285	0.0016731	174.2090	9.20205	367.983	0.0043	0.8519	6.13
45	27.4128	0.9290	0.0016740	174.2365	9.20700	414.018	0.0042	0.8561	6.16
50	30.4587	0.9290	0.0016740	174.2640	9.20700	460.053	0.0022	0.8583	6.17
55	33.5046	0.9290	0.0016740	174.2915	9.20700	506.088	0.0020	0.8603	6.19
60	36.5723	0.9295	0.0016750	174.3190	9.21250	552.151	0.0027	0.8630	6.21

X<sub>0</sub> Turmeric: [g extract/100 g turmeric (d.b.)] 6.21

- Vfm = reading of the volumetric flow meter.
- Initial reading of the volumetric flow meter 173.989 m<sup>3</sup>
- Mf = Mass flow calculation.
- Mass of ground turmeric on a dry basis 13.9048 g.
- Mass of ground turmeric on a wet basis 15.1139 g.
- Residual extract obtained from the cleaning of the bench unit 0.10 kg × 10<sup>-5</sup>
- Moisture of the raw material 8%

Parameters from SFE in the bench-scale unit applied to annatto seeds are available in:

R.A.C. Torres, D.T. Santos, M.A.A. Meireles, Construction and Validation of an Online Subcritical Adsorption-based Device for Assisting CO<sub>2</sub> Recycling during a Supercritical Fluid Extraction Process The Open Food Science Journal 10 (2018).

- CAPÍTULO 5 – *Discussão geral*

## DISCUSSÃO GERAL

A revisão do **capítulo 2** feita sobre os estudos da influência de vários parâmetros operacionais, como temperatura, pressão e vazão de CO<sub>2</sub>, entre outros, durante o processo de SAF na eficiência de purificação, morfologia das partículas e as principais diferenças sobre os processos patenteados de SAF contribuíram desde um enfoque geral para identificar os processos experimentais de separações físicas desta tese. Assim, os diversos trabalhos experimentais estudados, mostraram que suas adaptações ou modificações feita na unidade de processamento SAF tem certa vantagem com ralação a outras unidades que desenvolvem o mesmo processo.

Isso serviu de estímulo para que o processamento SFE desenvolvido no **capítulo 3** fosse estudado com a necessidade de otimizar as condições de reciclagem de solvente pelo uso de material adsorvente, adaptando certos componentes no equipamento. Uma vez que unidades comerciais semi-industriais dotadas de mecanismo de reciclagem de CO<sub>2</sub> as vezes apresentam alguma limitação em termos de funcionalidade, já que parte do extrato vai para o reservatório do sistema de reciclagem (tanque pulmão), o que limita seu uso permanente. Nesse sentido, o mecanismo de reciclagem da unidade a escala piloto foi otimizado e validado a través de mudanças de peças junto à incorporação de 01 coluna de adsorção (AdC1) utilizando algodão e Celite® como materiais de adsorção e sementes de urucum como matéria-prima.

Incorporar peças e partes numa unidade de processamento semi-industrial pode representar grandes custos de investimento à entidade, não obstante a sugestão de utilizar esses componentes vindos de outras unidades de processamento que no momento não estejam sendo utilizados, pode reduzir significativa esses custos. Assim, por exemplo uma coluna de volume 0,65 L foi emprestada de outra unidade para ser utilizada como coluna de adsorção (AdC1) reduzindo os custos em US \$ 573,36 para operar a unidade de extração de fluido supercrítico com duas colunas de extração (2 x 5 L).

A incorporação do sistema de recirculação junto as mudanças feitas nela (nomeada posteriormente de Purification and Recycling System of CO<sub>2</sub> – PRSCO<sub>2</sub>), assim como na unidade de extração, permitiram atingir altas relações de Solvente/Alimentação de matéria-prima (S/F = 56) utilizando reduzida massa de CO<sub>2</sub>, o que certamente permitiu validar a unidade em escala piloto funcionando com sistema de purificação e reciclo de solvente. Ao mesmo tempo, que o efeito da pressurização/despressurização mostra uma tendência a atingir máximo rendimento de extração (3,09 g extrato/100 g sementes (b.s.)) das sementes de urucum quando comparado com o valor X<sub>0</sub> (2,82 g extrato/100 g sementes (b.s.)) desenvolvido em escala de bancada.

Nesse sentido o foco de otimização através da incorporação e mudança de peças numa unidade de processamento (**capítulo 3**) foi mantido no presente trabalho e permitiu criar um novo processo visto no **capítulo 4**.

O processo de extração com fluido supercrítico combinado com processo de adsorção em meio subcrítico não foi achado na literatura. Da mesma forma, não foram achados relatos no nível industrial da aplicação de esta combinação de processos. Nesse sentido, o presente estudo pode-se constituir na primeira pesquisa com possibilidades de ter boa acolhida no setor industrial, toda vez que o material adsorvente (adsorvente alimentício) resulta num subproduto com agregação de valor, além de obter produtos diversificados dentro da mesma linha de produção.

Os resultados dos testes de adsorção em escala de bancada e o processo de adsorção em escala piloto mostraram eficiência de adsorção de 7.58 Kg de extrato de urucum adsorvido/100 Kg de farelo de aveia e 11.61 Kg de extrato de urucum adsorvido/100 Kg de farelo de aveia, respectivamente. Isso gera uma boa expectativa quanto à aplicação da combinação dos processos extração+adsorção para gerar novos subprodutos ou produtos enriquecidos com frações de extrato. Por outro lado, o critério de reduzir a vazão mássica de CO<sub>2</sub> de 200 g/min a 100 g/min para processar urucum e cúrcuma, respectivamente, obedeceu ao fato da cúrcuma conter o dobro do extrato que o urucum. Com isso, a velocidade intersticial também foi reduzida o que provavelmente tenha limitado o contato do extrato com maior massa de farelo de aveia contida na AdC1. Ou seja, 0.0689 Kg de farelo de aveia (b.s.) adsorveu 0.008 Kg de extrato de urucum e 0.0304 Kg de farelo de aveia (b.s.) adsorveu 0.00597 Kg de extrato de cúrcuma, o qual representa 25.12 Kg e 9.56 Kg de farelo de aveia que adsorveu o extrato/100Kg de farelo de aveia utilizada no processo, para urucum e cúrcuma, respectivamente.

Durante a validação do processo pseudocontínuo junto ao sistema de purificação e reciclagem de CO<sub>2</sub>, as condições de alimentação de CO<sub>2</sub> repurificado (trocador de calor tipo casco e tubo para refrigerar o CO<sub>2</sub> a -5°C, e pressão de 5.5 MPa no interior de tanque pulmão com a temperatura ambiente média de 22°C) permitiram manter aproximadamente 15 L de CO<sub>2</sub> no tanque. Isto é, o CO<sub>2</sub> repurificado no tanque pulmão garante a necessidade mínima de alimentação de CO<sub>2</sub> à bomba, que precisa de 5 MPa para que as RPM necessárias para atingir pressões de processamento de 20 até 25 MPa sejam mantidos embaixo de 110 RPM, que é o ponto a partir do qual se percebe que a bomba realiza maior esforço para atingir as pressões de processamento.

- CAPÍTULO 6 - *Conclusões gerais e sugestões para trabalhos futuros*

## CONCLUSÕES GERAIS

A Tecnologia Supercrítica abrange uma série de processos onde ocorrem separações físicas, a escolha do mais apropriado pode parecer menos complicada quando atrelada ao tipo de produto final que se deseja obter. Nesse sentido, a grande versatilidade desta tecnologia facilita identificar as relações existentes entre os processos, e a forma como elas podem ser enxergadas, de modo tal que os critérios e raciocínios de um processo possam ser aplicados a outros, justificando a escolha em desenvolver diferentes processos nos estudos que possam ser feitos no decorrer da pesquisa. i.e. se na projeção da pesquisa contempla-se a obtenção de um determinado produto, a versatilidade da tecnologia e/ou dos equipamentos deve permitir criar produtos diversificados.

Assim, no **capítulo 1** foi contextualizado a tese com justificativas para o estabelecimento da pesquisa. No **capítulo 2** foi mostrado que o processo SAF é uma técnica para produzir partículas com alto rendimento e pureza de compostos bioativos. Por outro lado, como patentes desenvolvidas usando este tipo de processo são muito escassas, menos atenção é dada ao potencial desta técnica para purificar extratos de plantas com um conteúdo muito complexo de compostos bioativos.

Os procedimentos desenvolvidos em centros de pesquisa, laboratórios ou entidades que permitem o aproveitamento das partes e peças de uma unidade para ser utilizadas em outras unidades segundo a necessidade, certamente torna a pesquisa mais dinâmica e flexível permitindo potencializar seu financiamento. Nessa mesma linha de raciocínio, comprovou-se a eficiência dos resultados preliminares do processo de reciclagem de CO<sub>2</sub> em escala piloto para aplicação na SFE pseudocontinuo, recirculando a mesma quantidade de massa de CO<sub>2</sub> permitindo exceder os valores de S/F em 14 vezes, quando comparado a um processo sem um sistema de reciclagem de CO<sub>2</sub>.

A otimização dos tempos de cada etapa de processamento, desenvolvida para levar em frente o processo pseudocontinuo de purificação/reciclo de CO<sub>2</sub> proposto mostrou que o uso de um terceiro vaso extrator diminuiu o periodo dinâmico de extração de 70 para 25 minutos, mantendo os tempos preestabelecidos para os procedimentos de carga / descarga, pressurização / despressurização e período estático.

A análise por CLAE e CG de ambos os extratos foram coerentes com a literatura e a caracterização do material adsorvente (farelo de aveia) por Calorimetria de varredura diferencial, Difração de raios X, Análise termogravimétrica e Microscopia Eletrônica de Varredura indicaram que a adsorção dos extratos não modificou a estrutura física do farelo de aveia, o que acaba sendo mais uma informação atrativa no sentido de que a suas propriedades

primitivas tais como fonte de carboidratos, fibras, proteínas, ferro, entre outras, são mantidas no subproduto acrescentado pelo fato de ter sido enriquecido com extratos agregando valor comercial no produto.

## SUGESTÕES PARA TRABALHOS FUTUROS

Os resultados mostrados nesta tese estimulam pesquisas para aplicação da metodologia de purificação/reciclo de CO<sub>2</sub> para outras matérias-primas.

A quantidade de massa do farelo de aveia que adsorveu extrato de urucum representa o 25% do total de massa colocado no interior da AdC1 (0.65 mL) utilizando vazão de 200 g CO<sub>2</sub>/min. Recomenda-se para casos semelhantes onde o rendimento de extração da matéria-prima não supere 3 g extrato/100 g matéri-prima utilizar colunas de adsorção com volume menor a 0.65 mL.

Da mesma forma, a foto do farelo de aveia retirada ao finalizar o processamento pseudocontinuo onde se observa mudança de cor produto da adsorção do extrato, mostra o arilo do extrato adsorvido distante à parede da AdC1 utilizada no processo, nesse sentido, recomenda-se utilizar colunas de adsorção que guardem a relação: altura do leito (H<sub>B</sub>) / diâmetro do leito (D<sub>B</sub>) maior que 2.5.

Sugere-se a otimização do processo proposto a partir da adição de uma terceira coluna de extração para tornar à unidade ainda mais versátil e reduzir tempos dinâmicos de extração, assim como obter altos rendimentos de extração e aumento de economia de insumos quando operado em modo pseudocontinuo. Além disso, espera-se que os resultados obtidos neste trabalho sirvam para aplicação de purificação e reciclo de CO<sub>2</sub> para outros processos que usam fluidos supercríticos tais como o antisolvante supercrítico (SAS) e rápida expansão a partir de soluções saturadas (RESS).

*Memórias do doutorado*

## MEMÓRIAS DO DOUTORADO

Ricardo Abel del Castillo Torres ingressou como doutorando na UNICAMP em 2015 através de processo seletivo do Departamento de Engenharia de Alimentos (DEA).

Com auxílio financeiro da Capes no período de março 2015 a fevereiro 2019, cursou as disciplinas TP-159 Tópicos Especiais em Engenharia de Alimentos; QP-268 Planejamento e Otimização de Experimentos; TP-121 Tópicos em Engenharia de Alimentos; TP-199 Seminários, e fez o aproveitamento de estudos da disciplina TP-357 Microencapsulação Aplicada a Alimentos e Nutrientes e participação no Programa de Estágio Docente grupo C (PED C) com atividades de apoio parcial à docência da disciplina TA-331 Termodinâmica, atuando como voluntário entre agosto e dezembro de 2015 (8 h semanais, 0 % carga didática), totalizando 16 créditos.

O doutorando participou em 2018 na qualidade de avaliador de trabalhos científicos inscritos no evento XXVI edição do Congresso Interno de Iniciação Científica da UNICAMP.

As pesquisas referentes ao projeto de doutorado resultou em dois artigos publicados e um manuscrito de artigo a ser publicado, sendo 1 artigo de revisão publicado no periódico Recent Patents on Engineering e 1 artigo experimental publicado no periódico The Open Food Science Journal. Houve também a publicação de 6 trabalhos científicos em anais de eventos na modalidade de resumo, 4 resumos no Convibra Agronomy 2018, 1 resumo no XXVI Congresso Brasileiro de Ciencia e Tecnologia de Alimentos e 1 resumo no III Congresso Óleos e Gorduras – International Meeting on Fats and Oils.

### Artigos completos publicados em periódicos

1. Abel R. C. Torres, Ádina L. Santana, Diego T. Santos and M. Angela A. Meireles, “Perspectives on the Application of Supercritical Antisolvent Fractionation Process for the Purification of Plant Extracts: Effects of Operating Parameters and Patent Survey”, Recent Patents on Engineering (2016) 10: 88.
2. R. Abel C. Torres, Diego T. Santos, M. Angela A. Meireles, “Construction and Validation of an Online Subcritical Adsorption-based Device for Assisting CO<sub>2</sub> Recycling during a Supercritical Fluid Extraction Process”, The Open Food Science Journal (2018) 10: 46.

### Artigo preparado para submissão:

R.A.C. Torres, Á.L. Santana, D.T. Santos, J.Q. Albarelli, M.A.A. Meireles A novel process for CO<sub>2</sub> purification and recycling based on subcritical adsorption of the extracts from annatto and turmeric in oat bran. The Journal of Supercritical Fluids - 2019.

Resumos de trabalhos apresentados em congressos

1. Effects of CO<sub>2</sub> pressurization/depressurization cycle on Annatto seeds oil adsorption during supercritical fluid extraction process with recycling. XXVI CBCTA 2018.
2. Modification of a commercial supercritical fluid extraction pilot unit for assisting CO<sub>2</sub> recycling. Convibra Agronomy 2018.
3. Validation of a Pseudo-continuous process for obtaining food ingredients from plant materials with CO<sub>2</sub> recycling by the aid of supercritical adsorption with oat bran. Convibra Agronomy 2018.
4. Supercritical fluid extraction of emulsion obtained by ultrasound emulsification assisted by nitrogen hydrostatic pressure using novel biosurfactant. Convibra Agronomy 2018.
5. Energetic-economical effects of supercritical antisolvent precipitation process conditions. Convibra Agronomy 2018.
6. Nova proposta de aproveitamento das sementes de urucum utilizando tecnologia supercrítica em diferentes etapas. III Congresso Óleos e Gorduras 2018.

Cabe mencionar que o trabalho apresentado no XXVI Congresso Brasileiro de Ciência e Tecnologia de Alimentos (XXVI CBCTA) foi vencedor do Prêmio Leopold Hartman, na categoria de Óleos e Gorduras, ganhando o 1º lugar dentre os trabalhos apresentados durante o XXVI CBCTA.

## **REFERÊNCIAS**

- F. A. Abdul Kareem, A. M. Shariff, S. Ullah, F. Dreisbach, L. K. Keong, N. Mellon, S. Garg, Experimental measurements and modeling of supercritical CO<sub>2</sub> adsorption on 13X and 5A zeolites. *Journal of Natural Gas Science and Engineering*, 50 (2018)115-127.
- S. Budinis, N. F. Thornhill, Supercritical fluid recycle for surge control of CO<sub>2</sub> centrifugal compressors, *Computers & Chemical Engineering*, 91(2016) 329-342.
- J. L. Gardea-Torresdey, K. J. Tiemann, V. Armendariz, L. Bess-Oberto, R. R. Chianelli, J. Rios, J.G. Parsons, G. Gamez, Characterization of Cr(VI) binding and reduction to Cr(III) by the agricultural byproducts of *Avena monida* (Oat) biomass. *Journal of Hazardous Materials*, 80(1) (2000) 175-188.
- D. Górecka, J. Stachowiak, Sorption of copper, zinc and cobalt by oat and oat products. *Food / Nahrung*, 46(2) (2002) 96-99.
- J. W. King, G. R. List, Supercritical fluid technology in oil and lipid chemistry. The American Oil Chemists Society, 1996. ISBN 0935315713.
- F. S. Souza, M. J. S. Matos, B. R. L. Galvão, A. F. C. Arapiraca, S. N. da Silva, I. P. Pinheiro, Adsorption of CO<sub>2</sub> on biphasic and amorphous calcium phosphates: An experimental and theoretical analysis. *Chemical Physics Letters*, 714 (2019) 143-148.
- C. Chinnarasu, A. Montes, M. T. F. Ponce, L. Casas, C. Mantell, C. Pereyra, E. J. M. de la Ossa, Precipitation of antioxidant fine particles from *Olea europaea* leaves using supercritical antisolvent process, *The Journal of Supercritical Fluids*, 97 (2015) 125- 132.
- G. Brunner, Supercritical fluids: technology and application to food processing, *Journal of Food Engineering*, 67 (2005) 21-33.
- G. Brunner, Gas extraction : an introduction to fundamentals of supercritical fluids and the application to separation processes, Steinkopff ; Springer, Darmstadt: New York,, 1994.
- F. Miguel, A. Martin, T. Gamse, M. J. Cocero, Supercritical anti solvent precipitation of lycopene - Effect of the operating parameters, *Journal of Supercritical Fluids*, 36 (2006) 225-235.
- T. Bruno, C. A. Nieto de Castro, J. F. P. Hamel, A. M. F. Palavra, *Supercritical Fluid Extraction of Biological Products*, John Wiley & Sons, (1993).
- A. Montes, N. Kin, M. D. Gordillo, C. Pereyra, E. J. M. de la Ossa, Polymer-naproxen precipitation by supercritical antisolvent (SAS) process, *The Journal of Supercritical Fluids*, 89 (2014) 58-67.

- P. Imsanguan, S. Pongamphai, S. Douglas, W. Teppaitoon, P. L. Douglas, Supercritical antisolvent precipitation of andrographolide from *Andrographis paniculata* extracts: Effect of pressure, temperature and CO<sub>2</sub> flow rate, *Powder Technology*, 200 (2010) 246-253.
- Y. Bakhbakhi, S. Alfadul, A. Ajbar, Precipitation of Ibuprofen Sodium using compressed carbon dioxide as antisolvent, *European Journal of Pharmaceutical Sciences*, 48 (2013) 30-39.
- A. Bertucco, M. Lora, I. Kikic, Fractional crystallization by gas antisolvent technique: Theory and experiments, *Aiche Journal*, 44 (1998) 2149-2158.
- E. Reverchon, G. Caputo, I. De Marco, Role of phase behavior and atomization in the supercritical antisolvent precipitation, *Industrial & Engineering Chemistry Research*, 42 (2003) 6406- 6414.
- P. G. Debenedetti, J. W. Tom, S. D. Yeo, Rapid expansion of supercritical solutions (RESS): fundamentals and applications, *Fluid Phase Equilibria*, 82 (1993) 311-318.
- E. Weidner, Z. Knez, Z. Novak, Int. Pat. Publ. WO 95/21688. 1995.
- D. Yadav, N. Kumar, Nanonization of curcumin by antisolvent precipitation: Process development, characterization, freeze drying and stability performance, *International Journal of Pharmaceutics*, 477 (2014) 564-577.
- D. Villanueva Bermejo, E. Ibáñez, G. Reglero, C. Turner, T. Fornari, I. Rodriguez-Meizoso, High catechins/low caffeine powder from green tea leaves by pressurized liquid extraction and supercritical antisolvent precipitation, *Separation and Purification Technology*, 148 (2015) 49-56.
- A. Visentin, S. Rodríguez-Rojo, A. Navarrete, D. Maestri, M. J. Cocero, Precipitation and encapsulation of rosemary antioxidants by supercritical antisolvent process, *Journal of Food Engineering*, 109 (2012) 9-15.
- R. Adami, E. Reverchon, E. Jarvenpaa, R. Huopalahti, Supercritical Antisolvent micronization of nalmefene Cl on laboratory and pilot scale, *Powder Technology*, 182 (2008) 105-112.
- P. Kraujalis, P. R. Venskutonis, E. Ibáñez, M. Herrero, Optimization of rutin isolation from *Amaranthus paniculatus* leaves by high pressure extraction and fractionation techniques, *The Journal of Supercritical Fluids*, 104 (2015) 234-242.
- O. J. Catchpole, J. B. Grey, K. A. Mitchell, J. S. Lan, Supercritical antisolvent fractionation of propolis tincture, *The Journal of Supercritical Fluids*, 29 (2004) 97-106.
- C. Chinnarasu, A. Montes, M. T. Fernandez-Ponce, L. Casas, C. Mantell, C. Pereyra, E. J. M. de la Ossa, S. Pattabhi, Natural antioxidant fine particles recovery from *Eucalyptus*

- globulus leaves using supercritical carbon dioxide assisted processes, *The Journal of Supercritical Fluids*, 101 (2015) 161-169.
- B.-C. Liau, C.-T. Shen, F.-P. Liang, S.-E. Hong, S.-L. Hsu, T.-T. Jong, C.-M. J. Chang, Supercritical fluids extraction and anti- solvent purification of carotenoids from microalgae and associated bioactivity, *The Journal of Supercritical Fluids*, 55 (2010) 169-175.
- J. L. Marqués, G. D. Porta, E. Reverchon, J. A. R. Renuncio, A. M. Mainar, Supercritical antisolvent extraction of antioxidants from grape seeds after vinification, *The Journal of Supercritical Fluids*, 82 (2013) 238-243.
- E. de Paz, Á. Martín, H. Every, M. J. Cocero, Production of water- soluble quercetin formulations by antisolvent precipitation and supercritical drying, *The Journal of Supercritical Fluids*, 104 (2015) 281-290.
- T.-L. Huang, J. C.-T. Lin, C.-C. Chyau, K.-L. Lin, C.-M. J. Chang, Purification of lignans from Schisandra chinensis fruit by using column fractionation and supercritical antisolvent precipitation, *Journal of Chromatography A*, 1282 (2013) 27-37.
- E. Haimer, M. Wendland, A. Potthast, U. Henniges, T. Rosenau, F. Liebner, Controlled precipitation and purification of hemicellulose from DMSO and DMSO/water mixtures by carbon dioxide as anti- solvent, *Journal of Supercritical Fluids*, 53 (2010) 121-130.
- M. A. Meneses, G. Caputo, M. Scognamiglio, E. Reverchon, R. Adami, Antioxidant phenolic compounds recovery from Mangifera indica L. by-products by supercritical antisolvent extraction, *Journal of Food Engineering*, 163 (2015) 45-53.
- L. Martin, A. Gonzalez-Coloma, R. Adami, M. Scognamiglio, E. Reverchon, G. Della Porta, J. S. Urieta, A. M. Mainar, Supercritical antisolvent fractionation of ryanodol from Persea indica, *Journal of Supercritical Fluids*, 60 (2011) 16-20.
- C. Chinnarasu, A. Montes, M. T. Fernandez-Ponce, L. Casas, C. Mantell, C. Pereyra, E. J. M. de la Ossa, Precipitation of antioxidant fine particles from Olea europaea leaves using supercritical antisolvent process", *Journal of Supercritical Fluids*, 97 (2015) 125-132.
- Y. Zhang, X. Zhao, W. Li, Y. Zu, Y. Li, K. Wang, Preparation, Characterization, and Dissolution Rate In Vitro Evaluation of Total Panax Notoginsenoside Nanoparticles, Typical Multicomponent Extracts from Traditional Chinese Medicine, Using Supercritical Antisolvent Process, *Journal of Nanomaterials*, (2015).
- E. Reverchon, I. De Marco, Supercritical fluid extraction and fractionation of natural matter, *Journal of Supercritical Fluids*, 38 (2006) 146-166.
- O. J. Catchpole, J. B. Grey, K. A. Mitchell, J. S. Lan, Supercritical antisolvent fractionation of propolis tincture, *Journal of Supercritical Fluids*, 29 (2004) 97-106.

G. Perretti, C. Virgili, A. Troilo, O. Marconi, G. F. Regnicoli, P. Fantozzi, Supercritical antisolvent fractionation of lignans from the ethanol extract of flaxseed, *Journal of Supercritical Fluids*, 75 (2013) 94-100.

Shodhganga, Principles of adorption, 2019.

[http://shodhganga.inflibnet.ac.in/bitstream/10603/22665/8/08\\_chapter3.pdf](http://shodhganga.inflibnet.ac.in/bitstream/10603/22665/8/08_chapter3.pdf). (Accessed 21.01.2019 2019).

D. T. Santos, M. A. A. Meireles, Micronization and encapsulation of functional pigments using supercritical carbon dioxide, *Journal of Food Process Engineering*, 36 (2013) 36-49.

R. A. C. Torres, D. T. Santos, M. A. A. Meireles, Novel Extraction Method to Produce Active Solutions from Plant Materials, *Food and Public Health*, 5 (2015) 38-46.

M. N. Moraes, G. L. Zabot, M. A. A. Meireles, Extraction of tocotrienols from annatto seeds by a pseudo continuously operated SFE process integrated with low-pressure solvent extraction for bixin production, *The Journal of Supercritical Fluids*, 96 (2015) 262-271.

T. Floris, G. Filippino, S. Scugli, M. B. Pinna, F. Argiolas, A. Argiolas, M. Murru, E. Reverchon, Antioxidant compounds recovery from grape residues by a supercritical antisolvent assisted process, *Journal of Supercritical Fluids*, 54 (2010) 165-170.

A. Visentin, M. Cismondi, D. Maestri, Supercritical CO<sub>2</sub> fractionation of rosemary ethanolic oleoresins as a method to improve carnosic acid recovery, *Innovative Food Science & Emerging Technologies*, 12 (2011) 142-145.

A. Gonzalez-Coloma, L. Martin, A. M. Mainar, J. S. Urieta, B. M. Fraga, V. Rodriguez-Vallejo, C. E. Diaz, Supercritical extraction and supercritical antisolvent fractionation of natural products from plant material: comparative results on *Persea indica*, *Phytochemistry Reviews*, 11 (2012) 433-446.

R. A. C. Torres, Purificação de partículas de bixina por precipitação com CO<sub>2</sub> supercrítica como antissolvente a partir de solução de ativos obtida da extração de sementes semi desengorduradas de urucum (*Bixa orellana* L.) assistida por ultrassom, University of Campinas/School of Food Engineering, Campinas, 2015.

Z. Knez, E. Markocic, M. Leitgeb, M. Primožic, M. Knez Hrncic, M. Skerget, Industrial applications of supercritical fluids: A review, *Energy*, 77 (2014) 235-243.

H.-Y. Chin, M.-J. Lee, H.-m. Lin, Vapor-Liquid Phase Boundaries of Binary Mixtures of Carbon Dioxide with Ethanol and Acetone, *Journal of Chemical and Engineering Data*, 53 (2008) 2393-2402.

V. J. Pereira, R. L. Matos, S. G. Cardoso, R. O. Soares, G. L. Santana, G. M. N. Costa, S. A. B. Vieira de Melo, A new approach to select solvents and operating conditions for

- supercritical antisolvent precipitation processes by using solubility parameter and group contribution methods, *The Journal of Supercritical Fluids*, 81 (2013) 128-146.
- C. Zu, X. Zhao, X. Du, "Enhanced water-solubility of Licorice extract microparticle prepared by antisolvent precipitation process, *Advanced Powder Technology*, 25 (2014) 787-794.
- M. Anwar, I. Ahmad, M. H. Warsi, S. Mohapatra, N. Ahmad, S. Akhter, A. Ali, F. J. Ahmad, Experimental investigation and oral bioavailability enhancement of nano-sized curcumin by using supercritical anti-solvent process, *European Journal of Pharmaceutics and Biopharmaceutics*, 96 (2015) 162-172.
- Y. Dong, W. K. Ng, J. Hu, S. Shen, R. B. H. Tan, A continuous and highly effective static mixing process for antisolvent precipitation of nanoparticles of poorly water-soluble drugs, *International Journal of Pharmaceutics*, 386 (2010) 256- 261.
- J. L. Marques, G. Della Porta, E. Reverchon, J. A. R. Renuncio, A. M. Mainar, Supercritical antisolvent extraction of antioxidants from grape seeds after vinification, *Journal of Supercritical Fluids*, 82 (2013) 238-243.
- H. Aro, E. Jarvenpaa, K. Konko, R. Huopalahti, V. Hietaniemi, The characterization of oat lipids produced by supercritical fluid technologies, *Journal of Cereal Science*, 45 (2007) 116-119.
- H. Aro, E. Järvenpää, J. Mäkinen, M. Lauraeus, R. Huopalahti, V. Hietaniemi, The utilization of oat polar lipids produced by supercritical fluid technologies in the encapsulation of probiotics, *LWT - Food Science and Technology*, 53 (2013) 540-546.
- Citation Report: 23 (from All Databases), Online Available:  
[http://apps.webofknowledge.com/CitationReport.do?product=UA&search\\_mode=CitationReport&SID=3FXObzJRT9yFV8YHBPt&page=1&cr\\_pqid=1&viewType=summary](http://apps.webofknowledge.com/CitationReport.do?product=UA&search_mode=CitationReport&SID=3FXObzJRT9yFV8YHBPt&page=1&cr_pqid=1&viewType=summary), Web of Science TM.
- F. V. Correa, S. R. R. Comim, A. M. de Cesaro, A. A. Rigo, M. A. Mazutti, H. Hense, J. V. Oliveira, Phase equilibrium data for the ternary system (propane plus chloroform plus oryzanol), *Journal of Chemical Thermodynamics*, 43 (2011) 34-38.
- C. Chang, T. Huang, C. M. Chang, T. L. Huang, Method for extracting high-purity schizandrin from schisandra fruit, involves applying ethanol solvent to ultrasonically extract schisandra powder, purifying using column and precipitating supercritical carbon dioxide, China (2014).
- C. Chang, Y. Shen, C. M. Chang, Y. C. Shen, Method for preparing purity beta-carotene nano powder from dunaliella salina capable of recycling at least beta-carotene of 36% from dunaliella salina per unit and producing nano particles of beta-carotene of at least 72.9% purity (2013).

- A. Gonzalez-Coloma, Á. Martín, A. M. Mainar, J. S. Urieta, B. M. Fraga, V. Rodrigues-Vallejo, Supercritical extraction and supercritical antisolvent fractionation of natural products from plant material: comparative results on *Persea indica*, *Phytochemistry Reviews*, 11 (2012) 413-431.
- L. Martin, J. L. Marques, A. Gonzalez-Coloma, A. M. Mainar, A. M. F. Palavra, J. S. Urieta, "Supercritical methodologies applied to the production of biopesticides: a review", *Phytochemistry Reviews*, 11 (2012) 413-431.
- A. Martin, F. Mattea, L. Gutierrez, F. Miguel, M. J. Cocero, Co-precipitation of carotenoids and bio-polymers with the supercritical anti-solvent process, *The Journal of Supercritical Fluids*, 41 (2007) 138-147.
- L. Tocchini, A. Z. Mercadante, Extração e determinação, por clae, de bixina e norbixina em coloríficos, *Food Science and Technology*, 21 (2011) 310-313.
- W. Stahl, H. Sies, Antioxidant activity of carotenoids, *Molecular Aspects of Medicine*, 24 (2003) 345-351.
- D. T. Santos, J. Q. Albarelli, M. M. Beppu, M. A. A. Meireles, Stabilization of anthocyanin extract from jabuticaba skins by encapsulation using supercritical CO<sub>2</sub> as solvent, *Food Research International*, 50 (2013) 617-624.
- M. Shahid, Shahid U. I., F. Mohammad, Recent advancements in natural dye applications: a review, *Journal of Cleaner Production*, 53 (2013) 310-331.
- H. Tapiero, D. M. Townsend, K. D. Tew, The role of carotenoids in the prevention of human pathologies, *Biomedicine & Pharmacotherapy*, 58 (2004) 100-110.
- S. M. Rodrigues, V. L. F. Soares, T. M. Oliveira, A. S. Gesteira, W. C. Otoni, M. G. C. Costa, Isolation and Purification of RNA from Tissues Rich in Polyphenols, Polysaccharides, and Pigments of Annatto (*Bixa orellana* L.), *Molecular Biotechnology*, 37 (2007) 220-224.
- M. T. M. G. Rosa, E. K. Silva, D. T. Santos, A. J. Petenate, M. A. A. Meireles, Obtaining annatto seed oil miniemulsions by ultrasonication using aqueous extract from Brazilian ginseng roots as a biosurfactant, *Journal of Food Engineering*, 168 (2016) 68-78.
- W. B. Van Scheppingen, I. A. L. A. Boogers, A. L. L. Duchateau, Study on decomposition products of norbixin during bleaching with hydrogen peroxide and a peroxidase by means of UPLC-UV and mass spectrometry, *Food Chemistry*, 132 (2012) 1354-1359.
- M. A. S. Barrozo, K. G. Santos, F. G. Cunha, Mechanical extraction of natural dye extract from *Bixa orellana* seeds in spouted bed, *Industrial Crops and Products*, 45 (2013) 279-282.
- C. L. C. Albuquerque, M. A. A. Meireles, Defatting of annatto seeds using supercritical carbon dioxide as a pretreatment for the production of bixin: Experimental, modeling and economic evaluation of the process, *The Journal of Supercritical Fluids*, 66 (2012) 86-95.

- M. N. Moraes, G. L. Zabot, M. A. A. Meireles, Applications of Supercritical Fluids in Latin America: Past, Present and Future Trends, *Food and Public Health*, 4 (2014) 162-179.
- J. C. F. Johner, M. A. A. Meireles, Construction of a supercritical fluid extraction (SFE) equipment: validation using annatto and fennel and extract analysis by thin layer chromatography coupled to image, *Food Science and Technology*, 36 (2016) 210-247.
- L. M. Rodrigues, S. C. Alcázar-Alay, A. J. Petenate, M. A. A. Meireles, Bixin extraction from defatted annatto seeds, *Comptes Rendus Chimie*, 17 (2014) 268-283.
- F. Mattea, Á. Martín, A. Matías-Gago, M. J. Cocero, Supercritical antisolvent precipitation from an emulsion:  $\beta$ -Carotene nanoparticle formation, *The Journal of Supercritical Fluids*, 51 (2009) 238-247.
- D. T. Santos, M. A. A. Meireles, Micronization and encapsulation of functional pigments using supercritical carbon dioxide, *Journal of Food Process Engineering*, 36 (2013) 36-49.
- D. Nong, M. Siriwardana, Environmental and economic impacts of a joint emissions trading scheme, *International Journal of Global Energy Issues*, 40 (2017) 184-206.
- J. Royer-Adnot, Y. Le Gallo, Economic Analysis of Combined Geothermal and CO<sub>2</sub> Storage for Small-Size Emitters, *Energy Procedia*, 114 (2017) 7118-7125.
- G. F. Silva, F. M. C. Gamarra, A. L. Oliveira, F. A. Cabral, Extraction of bixin from annatto seeds using supercritical carbon dioxide, *Brazilian Journal of Chemical Engineering*, 25 (2008) 419-426.
- AOAC. Official Methods of Analysis of AOAC International. AOAC International. INTERNATIONAL, A. Gaithersburg, MD, (1997).
- NIST. National Institute of Standards and Technology. 2017. Available at: <http://www.nist.gov>.
- G. L. Zabot, M. N. Moraes, A. J. Petenate, M. A. A. Meireles, Influence of the bed geometry on the kinetics of the extraction of clove bud oil with supercritical CO<sub>2</sub>, *Journal of Supercritical Fluids*, 93 (2014) 56-66.
- J. M. Prado, Estudo do aumento de escala do processo de extração supercrítica em leito fixo. Ph.D thesis, University of Campinas/School of Food Engineering, Campinas, Brazil, 2010.
- S. P. Jesus, M. N. Calheiros, H. Hense, M. A. A. Meireles, A simplified model to describe the kinetic behavior of supercritical fluid extraction from a rice bran oil byproduct, *Food and Public Health*, 3 (2013) 215-222.
- M. A. A. Meireles, Extraction of Bioactive Compounds from Latin American Plants. In: J. Martínez, (Ed.). *Supercritical Fluid Extraction of Nutraceuticals and Bioactive Compounds*: CRC Press - Taylor & Francis Group, LLC, (2008) 243–274.

- M. N. Moraes, G. L. Zabot, M. A. A. Meireles, Extraction of tocotrienols from annatto seeds by a pseudo continuously operated SFE process integrated with low-pressure solvent extraction for bixin production, *Journal of Supercritical Fluids*, 96 (2015) 262-271.
- T. M. Takeuchi, P. F. Leal, R. Favareto, L. Cardozo-Filho, M. L. Corazza, P. T. V. Rosa, M. A. A. Meireles, Study of the phase equilibrium formed inside the flash tank used at the separation step of a supercritical fluid extraction unit, *The Journal of Supercritical Fluids*, 43 (2008) 447-459.
- EXERGY-LLC. Model # 00256-06, Shell & Tube Heat Exchanger. USA, 17/05/2017 2017. Available at: <http://heat-exchangers.exergyllc.com/item/shell-tube-heat-exchangers/35-series-shell-tube-heat-exchangers/00256-06>.
- POLYSCIENCE. Chillers and Coolers. USA, 2017. Available at: <https://polyscience.com/products/chillers/benchtop>.
- POLYSCIENCE. User Guide - Refrigerated Recirculating Chillers. POLYSCIENCE. USA, pp.51, 2016.
- Santos D. T., Albuquerque C. L. C., Meireles M. A. A., *Procedia Food Science*, 1 (2011) 1581 – 1588. [<http://dx.doi.org/10.1016/j.supflu.2003.11.005>]
- R. A. D. C. Torres, Purificação de partículas de bixina por precipitação com CO<sub>2</sub> supercrítico como antissolvente a partir de solução de ativos obtida da extração de sementes semi desengorduradas de urucum (*Bixa orellana* L.) assistida por ultrassom. Master thesis, University of Campinas/School of Food Engineering, Campinas, Brazil, 2015.
- J. M. Del Valle, O. Rivera, M. Mattea, L. Ruetsch, J. Daghero, A. Flores, Supercritical CO<sub>2</sub> processing of pretreated rosehip seeds: effect of process scale on oil extraction kinetics, *The Journal of Supercritical Fluids*, 31 (2004) 159-174.
- J. Q. Albarelli, A. V. Ensinas, M. A. Silva, Product diversification to enhance economic viability of second generation ethanol production in Brazil: the case of the sugar and ethanol joint production, *Chem. Eng. Res. Des.* 92 (2014) 1470–1481.
- S. C. Alcázar-Alay, J. F. Osorio-Tobón, T. Forster-Carneiro, C. J. Steel, M. A. A. Meireles, Polymer modification from semi-defatted annatto seeds using hot pressurized water and supercritical CO<sub>2</sub>, *The Journal of Supercritical Fluids*, 129 (2017) 48-55.
- AOAC. Official methods of analysis of AOAC International 1997
- M. E. M. Braga, P. F. Leal, J. E. Carvalho, M. A. A. Meireles, Comparison of Yield, Composition, and Antioxidant Activity of Turmeric (*Curcuma longa* L.) Extracts Obtained Using Various Techniques, *Journal of Agricultural and Food Chemistry*, 51 (2003) 6604-6611.

- P. I. N. Carvalho, J. F. Osorio-Tobón, M. A. Rostagno, A. J. Petenate, M. A. A. Meireles, Techno-economic evaluation of the extraction of turmeric (*Curcuma longa L.*) oil and ar-turmerone using supercritical carbon dioxide, *The Journal of Supercritical Fluids*, 105 (2015) 44-54.
- V. S. d. Carvalho, K. Tannous, Thermal decomposition kinetics modeling of energy cane *Saccharum robustum*, *Thermochimica Acta*, 657 (2017) 56-65.
- R. N. Cavalcanti, D. T. Santos, M. A. A. Meireles, Non-thermalstabilization mechanisms of anthocyanins in model and foodsystems: an overview, *Food Res. Int.* 44 (2011) 499–509.
- S. R. Falsafi, Y. Maghsoudlou, H. Rostamabadi, M. M. Rostamabadi, H. Hamedi, S. M. H. Hosseini, Preparation of physically modified oat starch with different sonication treatments, *Food Hydrocolloids*, 89 (2019) 311-320.
- R. Gao, H. Liu, Z. Peng, Z. Wu, Y. Wang, G. Zhao, Adsorption of (−)-epigallocatechin-3-gallate (EGCG) onto oat β-glucan, *Food Chemistry*, 132 (2012) 1936-1943.
- Q. Huang, C. H. Niu, A. K. Dalai, Production of anhydrous biobutanol using a biosorbent developed from oat hulls, *Chemical Engineering Journal*, 356 (2019) 830-838.
- P. R. Hussain, S. A. Rather, P. P. Suradkar, Structural characterization and evaluation of antioxidant, anticancer and hypoglycemic activity of radiation degraded oat (*Avena sativa*) β-glucan, *Radiation Physics and Chemistry*, 144 (2018) 218-230.
- G. E. Jacques-Fajardo, R. Prado-Ramírez, E. Arriola-Guevara, E. Pérez Carrillo, H. Espinosa-Andrews, G. M. Guatemala Morales, Physical and hydration properties of expanded extrudates from a blue corn, yellow pea and oat bran blend, *LWT*, 84 (2017) 804-814
- F. Koneski, D. Popovic-Monevska, I. Gjorgoski, J. Krajoska, M. Popovska, I. Muratovska, B. Velickovski, G. Petrushevska, V. Popovski, In vivo effects of geranylgeraniol on the development of bisphosphonate-related osteonecrosis of the jaws, *Journal of Cranio-Maxillofacial Surgery*, 46 (2018) 230-236.
- C. Li, S. G. Oh, D. H. Lee, H. W. Baik, H. J. Chung, Effect of germination on the structures and physicochemical properties of starches from brown rice, oat, sorghum, and millet, *International Journal of Biological Macromolecules*, 105 (2017) 931-939.
- T. Liu, P. Lin, T. Bao, Y. Ding, Q. Lha, P. Nan, Y. Huang, Z. Gu, Y. Zhong, Essential oil composition and antimicrobial activity of *Artemisia dracunculus L. var. qinghaiensis* Y. R. Ling (Asteraceae) from Qinghai-Tibet Plateau, *Industrial Crops and Products*, 125 (2018) 1-4.
- A. Marcuzzi, V. Zanin, E. Piscianz, P. M. Tricarico, J. Vuch, M. Girardelli, L. Monasta, A. M. Bianco, S. Crovella, Lovastatin-induced apoptosis is modulated by geranylgeraniol in a neuroblastoma cell line, *International Journal of Developmental Neuroscience*, 30 (2012) 451-456.

- C. Moreno-Castilla, Adsorption of organic molecules from aqueous solutions on carbon materials, *Carbon*, 42 (2004) 83-94.
- J. F. Osorio-Tobón, P. I. N. Carvalho, M. A. Rostagno, A. J. Petenate, M. A. A. Meireles Extraction of curcuminoids from deflavored turmeric (*Curcuma longa L.*) using pressurized liquids: Process integration and economic evaluation, *The Journal of Supercritical Fluids*, 95 (2014) 167-174.
- J. M. Prado, T. Forster-Carneiro, M. A. Rostagno, L. A. Follegatti-Romero, F. Maugeri Filho, M. A. A. Meireles, Obtaining sugars from coconut husk defatted grapeseed, and pressed palm fiber by hydrolysis with subcriticalwater, *The Journal of Supercritical Fluids*, 89 (2014) 89–98.
- J. M. Prado, I. Dalmolin, N. D. D. Carareto, R. C. Basso, A. J. A. Meirelles, J. Vladimir Oliveira, E. A. C. Batista, M. A. A. Meireles, Supercritical fluid extraction of grape seed: Process scale-up, extract chemical composition and economic evaluation, *Journal of Food Engineering*, 109 (2012) 249-257.
- J. M. Prado, G. H. C. Prado, M. A. A. Meireles, Scale-up study of supercritical fluid extraction process for clove and sugarcane residue, *The Journal of Supercritical Fluids*, 56 (2011) 231-237.
- Y. J. Rueda-Ordóñez, K. Tannous, Drying and thermal decomposition kinetics of sugarcane straw by nonisothermal thermogravimetric analysis, *Bioresource Technology*, 264 (2018) 131-139.
- K. S. Sandhu, P. Godara, M. Kaur, S. Punia, Effect of toasting on physical, functional and antioxidant properties of flour from oat (*Avena sativa L.*) cultivars, *Journal of the Saudi Society of Agricultural Sciences*, 16 (2017) 197-203.
- Á. L. Santana, J. Q. Albarelli, D. T. Santos, R. Souza, N. T. Machado, M. E. Araújo, M. A. A. Meireles, Kinetic behavior, mathematical modeling, and economic evaluation of extracts obtained by supercritical fluid extraction from defatted assaí waste, *Food and Bioproducts Processing*, 107 (2018) 25–35.
- Á. L. Santana, D. T. Santos, M. A. A. Meireles, Perspectives on small-scale integrated biorefineries using supercritical CO<sub>2</sub> as a green solvent, *Current Opinion in Green and Sustainable Chemistry*, 18 (2019) 1-12.
- D. T. Santos, J. Q. Albarelli, M. A. Rostagno, A. V. Ensinas, F. Maréchal, M. A. A. Meireles, New proposal for production of bioactive compounds by supercriticaltechnology integrated to a sugarcane biorefinery, *CleanTechnol. Environ. Policy* 16 (2014) 1455–1468.
- A. Shah, F. A. Masoodi, A. Gani, B. A. Ashwar, Newly released oat varieties of himalayan region -Techno-functional, rheological, and nutraceutical properties of flour, *LWT - Food Science and Technology*, 70 (2016) 111-118.

- I. Shahid ul, L. J. Rather, F. Mohammad, Phytochemistry, biological activities and potential of annatto in natural colorant production for industrial applications – A review, Journal of Advanced Research, 7 (2016) 499-514.
- Shodhganga, Principles of Adsorption (Accessed in 21.01. 2019): Shodhganga: A reservoir of Indian thesis, Available in: [http://shodhganga.inflibnet.ac.in/bitstream/10603/22665/8/08\\_chapter3.pdf](http://shodhganga.inflibnet.ac.in/bitstream/10603/22665/8/08_chapter3.pdf)
- E. K. Silva, G. L. Zabot, M. A. A. Meireles, Ultrasound-assisted encapsulation of annatto seed oil: Retention and release of a bioactive compound with functional activities, Food Research International, 78 (2015) 159-168.
- V. K. Singh, E. A. Kumar, Experimental investigation and thermodynamic analysis of CO<sub>2</sub> adsorption on activated carbons for cooling system, Journal of CO<sub>2</sub> Utilization, 17 (2017) 290-304.
- X. Tang, N. Ripepi, High pressure supercritical carbon dioxide adsorption in coal: Adsorption model and thermodynamic characteristics, Journal of CO<sub>2</sub> Utilization, 18 (2017) 189-197.
- R. A. C. Torres, Á. L. Santana, D. T. Santos, M. A. A. Meireles, Perspectives on the Application of Supercritical Antisolvent Fractionation Process for the Purification of Plant Extracts: Effects of Operating Parameters and Patent Survey, *Recent Patents on Engineering*, 10 (2016) 128.
- R. A. C. Torres, D. T. Santos, M. A. A. Meireles, Construction and Validation of an Online Subcritical Adsorption-based Device for Assisting CO<sub>2</sub> Recycling during a Supercritical Fluid Extraction Process, *The Open Food Science Journal* 10 (2018).
- R. B. Turton, B. Wallace, J. S. Whiting, D. Bhattacharyya, Analysis, Synthesis and Design of Chemical Processes, 3rd ed. Prentice Hall, Upper Saddle River (2009).
- P. C. Veggi, R. N. Cavalcanti, M. A. A. Meireles, Production of phenolic-rich extracts from Brazilian plants using supercritical subcritical extraction: experimental data and economic evaluation, *J. Food Eng.* 13 (2014) 96–109.
- F. Zhu, Structures, properties, modifications, and uses of oat starch, *Food Chemistry*, 229 (2017) 329-340.
- ASAE-Standard, 1998. American Society of Agricultural Engineers, Method of Determining and Expressing Fineness of Feed Materials by Sieving, pp. 447-550.
- Meireles, M.A.A., 2007. Extraction of Bioactive Compounds from Latin American Plants, in: Martinez, J.L. (Ed.), *Supercritical fluid extraction of nutraceuticals and bioactive compounds*. CRC Press-Taylor and Francis Group, Boca Raton.
- Taham, T., Cabral, F.A., Barrozo, M.A.S., 2015. Extraction of bixin from annatto seeds using combined technologies. *The Journal of Supercritical Fluids* 100, 175-183.

Xiang, H., Zhang, L., Xi, L., Yang, Y., Wang, X., Lei, D., Zheng, X., Liu, X., 2018. Phytochemical profiles and bioactivities of essential oils extracted from seven Curcuma herbs. Industrial Crops and Products 111, 298-305.

*Apêndice*

## APÊNDICE A

O APÊNDICE A comprehende os dados experimentais da parte referente ao Capítulo 3. Tanto informações de diâmetro médio da matéria-prima, fotos da condição inicial da UP e do sistema de reciclo, rendimento de extrato e vazão de solvente quanto rotinas de ajuste do modelo *spline* e parâmetros cinéticos são apresentados no presente APÊNDICE.

### A.1 Diâmetro médio para sementes de urucum *in natura*.

*Tabela A. 1. Dados de medição do diâmetro médio geométrico das sementes de urucum.*

Amostra	a	b	c	Média geométrica	Desvio padrão da média	a	b	c	Média geométrica	Desvio padrão da média
						a	b	c		
1	4.75	3.25	2.90	3.55	0.98	5.00	4.00	3.50	4.12	0.76
2	4.90	3.75	2.75	3.70	1.08	5.00	4.00	3.00	3.91	1.00
3	5.25	4.00	3.50	4.19	0.90	4.50	4.00	3.00	3.78	0.76
4	5.00	3.60	3.10	3.82	0.98	5.00	4.00	3.00	3.91	1.00
5	5.00	3.80	2.80	3.76	1.10	4.50	4.00	3.50	3.98	0.50
6	4.90	4.00	2.50	3.66	1.21	5.50	4.00	3.00	4.04	1.26
7	4.75	3.90	2.90	3.77	0.93	4.50	3.50	3.00	3.62	0.76
8	5.10	3.80	2.60	3.69	1.25	5.00	4.00	3.00	3.91	1.00
9	4.75	3.40	3.00	3.65	0.92	4.50	3.50	3.00	3.62	0.76
10	4.25	3.75	2.50	3.42	0.90	4.50	4.00	4.00	4.16	0.29
11	4.50	4.25	2.60	3.68	1.03	5.00	4.00	3.50	4.12	0.76
12	5.00	3.75	3.25	3.94	0.90	5.00	4.00	3.50	4.12	0.76
13	4.75	3.50	3.20	3.76	0.82	5.50	4.00	3.50	4.25	1.04
14	5.00	3.25	2.80	3.57	1.16	4.50	3.00	3.00	3.43	0.87
15	5.00	3.25	2.75	3.55	1.18	5.00	4.00	3.50	4.12	0.76
16	5.10	4.00	2.80	3.85	1.15	5.00	3.50	3.50	3.94	0.87
17	5.00	4.00	2.90	3.87	1.05	5.00	3.50	3.00	3.74	1.04
18	4.75	3.80	3.25	3.89	0.76	4.50	3.50	3.00	3.62	0.76
19	5.10	3.40	3.00	3.73	1.12	5.00	4.00	3.00	3.91	1.00
20	4.80	3.20	2.75	3.48	1.08	4.50	3.50	3.00	3.62	0.76
21	4.50	4.00	3.40	3.94	0.55	5.00	4.00	3.50	4.12	0.76
22	4.50	4.00	3.20	3.86	0.66	4.50	4.00	3.00	3.78	0.76
23	4.75	4.20	3.10	3.95	0.84	5.00	4.00	3.50	4.12	0.76
24	5.00	3.75	2.90	3.79	1.06	4.50	4.00	3.50	3.98	0.50
25	5.00	3.75	3.10	3.87	0.97	5.00	3.50	3.00	3.74	1.04
26	5.00	3.80	3.20	3.93	0.92	4.50	3.50	3.00	3.62	0.76
27	4.75	3.50	2.10	3.27	1.33	4.50	4.00	3.00	3.78	0.76
28	5.75	3.60	3.00	3.96	1.45	5.00	3.50	3.00	3.74	1.04
29	5.00	3.50	2.75	3.64	1.15	5.50	3.50	3.00	3.87	1.32
30	4.75	3.75	2.75	3.66	1.00	5.00	3.50	3.00	3.74	1.04
Geral	4.89	3.72	2.91	<b>3.75</b>	<b>0.99</b>	4.85	3.78	3.20	<b>3.89</b>	<b>0.84</b>

---

A unidade de medida de (a), (b) e (c) estão dadas em mm e elas são os eixos maior (altura), médio (largura) e menor (comprimento), respectivamente.

Média geométrica final (mm)	Desvio padrão da média (mm)
3.82	0.09

## A.2 Estado inicial da UP

A imagem a continuação mostra o estado da UP antes de fazer a instalação e troca de válvulas, troca de peças com desgaste, preenchimento de espaços visando evitar a retenção de extratos no interior das conexões, extensão de tubulações, troca de manômetro, assim como da instalação do sistema de reciclo, entre outras atividades que conduziram à modificação da UP.



Figura A. 1. Estado inicial das colunas de extração.

Observe-se que os manômetros (a) têm o mesmo tamanho. No desenvolvimento do Capítulo 3 um desses manômetros foi trocado por outro que facilita a leitura da exatidão dos valores da escala, da mesma forma a ordem do posicionamento dos isolantes térmicos (b) e das mantas de aquecimento (c) foi invertida (as mantas de aquecimento foram colocadas na parte superior e os isolantes térmicos na parte inferior) com a finalidade de que o acondicionamento térmico interno aconteça junto com o ingresso do CO<sub>2</sub> que é alimentado desde a parte superior

da coluna. A letra (d) sinaliza a localização da válvula de segurança que tem cada coluna de extração.

A Figura A.2 mostra a vista frontal de UP. Em (A), observa-se o mecanismo de interconectividade eletrônica que permite a transmissão de informação entre as partes. Assim (a) é o transmissor de informação entre as partes da UP com o Software instalado no computador (suspendida numa plataforma na parede vista na Figura D.4). A letra (b) é a válvula backpressure eletrônica, (c) é o comando de controle das temperaturas que está interconectado com o transdutor de energia (d) para aquecimento das duas colunas de extração, (c') também é responsável de controlar as temperaturas de (b) e do trocador de calor (e) de preaquecimento de CO<sub>2</sub>. (c'') é o comando de controle das temperaturas que está interconectado com os transdutores de energia (d'') e (d') para aquecimento dos três vasos de separação (VS) (d' VS1 e VS2 e d' para VS3).

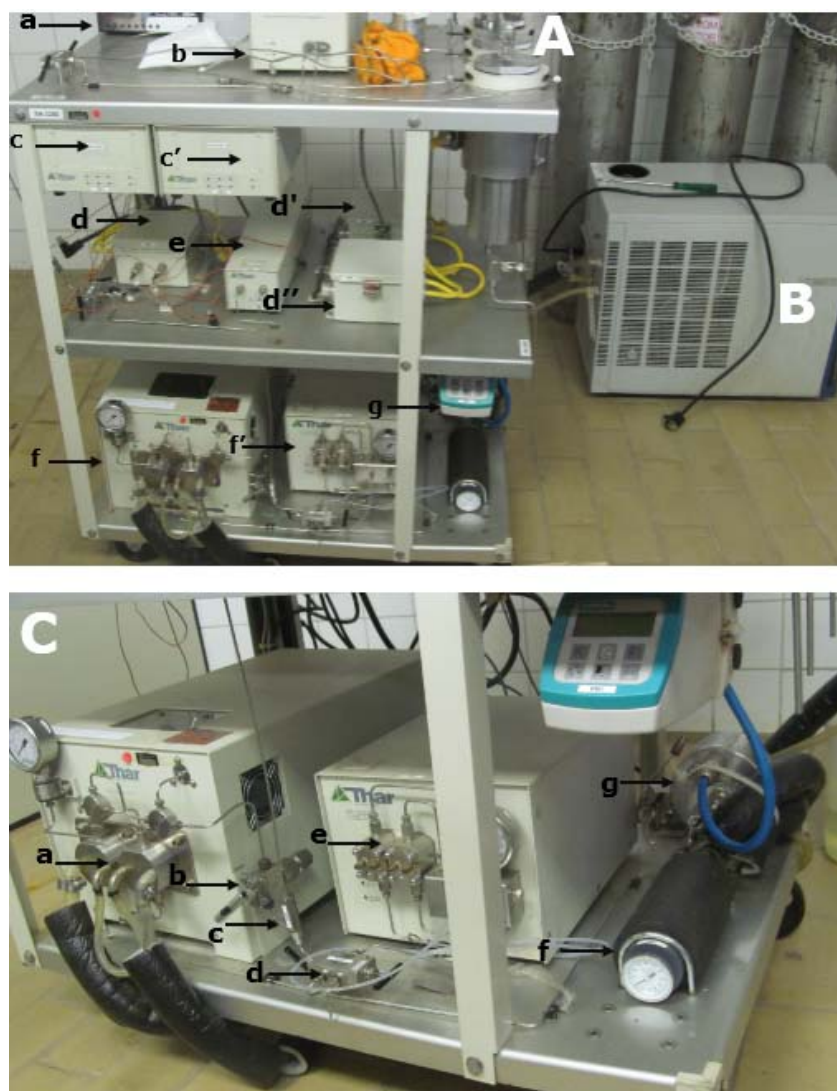


Figura A. 2. (A) Interconectividade eletrônica, (B) Banho de resfriamento da UP e (C) Acionamento mecânico.

O elemento que representa a letra (a) encontra-se conectado diretamente com as bombas de CO<sub>2</sub> (f) e de co-solvente (f') quem transmite as ordens de pressão desde o computador até (f) e (f'). A vazão mássica que ingressa no sistema é registrada pelo totalizador (g) que transmite informação a (f) e que na sequencia ambas informações de vazão (de ingresso e de bombeamento) passam até o Software através de (a).

O responsável de manter o CO<sub>2</sub> à temperatura de resfriamento é o (B), que através do bombeamento da mistura refrigerante mantem ao CO<sub>2</sub> a baixas condições de temperatura baixa (entre -5 e -10 °C).

Na parte (C) da foto, mostra-se os mecanismos de resfriamento dos cabeçotes (a) e (e) para as bombas de CO<sub>2</sub> e de co-solvente, respectivamente. (b) é a válvula de segurança da bomba de CO<sub>2</sub>, que através de um mecanismo de ruptura de disco vence a resistência mecânica do disco liberando CO<sub>2</sub>, isso é esperado que aconteça quando a trajetória à saída da bomba em funcionamento é bloqueada pelo fechamento de alguma válvula localizada posterior a ela. A letra (c) é uma cavidade vazia onde se misturam o CO<sub>2</sub> junto com o co-solvente. A válvula triplo via que alimenta de co-solvente à linha e permite a purga para limpeza ou descompressão da parte da tubulação entre a bomba e a válvula. Finalizando a nomeação das partes da Figura A.2. temos à letra (g) que representa a bobina e a parte mecânica do medidor de vazão coriolis.

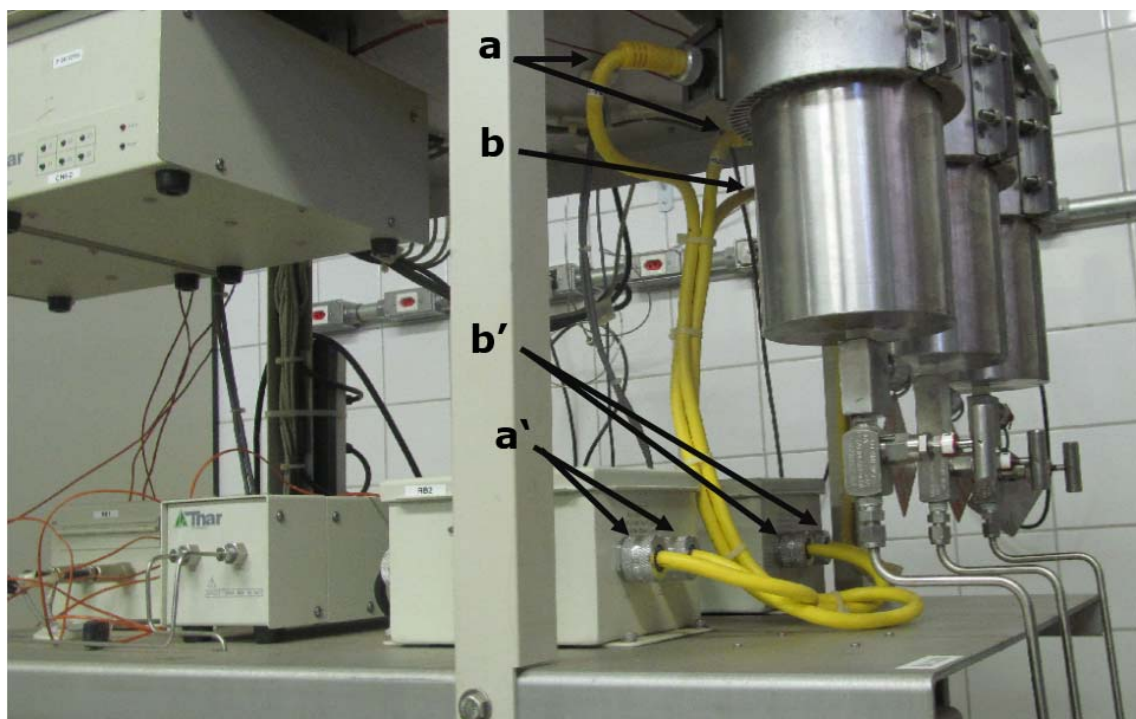


Figura A. 3. Transdutores de energia conectados às mantas de aquecimento dos VS.

Na Figura A.3., mostra-se a conectividade entre os transdutores de energia e as mantas de aquecimento (que são nomeados na próxima figura) dos vasos de separação. A configuração do transdutor mostra que (b') tem a possibilidade de se conectar mais um vaso de separação (que neste caso seria VS4).



Figura A. 4. Configuração das mantas de aquecimento dos VS, válvulas de segurança e termopares.

Na Figura A.4., mostra-se as mantas de aquecimento dos VS (a), elas cobrem aproximadamente uma terceira parte da área lateral de cada vaso o que faz muito provável que a temperatura no interior dos vasos não atinja a programada no software da UP. A letra (b) representa às válvulas de segurança dos vasos. Na lateral externa de cada abraçadeira metálica (c), estão unidas por soldagem as pontas dos termopares (d). Os sensores de temperatura

termopares são responsáveis de transmitir a informação de retorno das condições de temperatura do local até (c°) da Figura A.2.



Figura A. 5. Termopar no VS.

A Figura A.5., mostra as características de conexão do termopar no VS. Ao mesmo tempo, mostra-se o mecanismo de conectividade do sensor de temperatura termopar Tipo K aos sockets plugs macho fêmea. Impresso no VS, encontra-se informação do volume (1 L), assim como do efeito gerado no interior do VS quando a mistura solvente + extrato ingressa no seu interior (VS tipo ciclone). É muito provável que pelo tipo de contato que acontece entre a mistura com a parede interna superior do VS, a manta de aquecimento tenha sido projetada para cobrir só a terceira parte da área lateral do VS. Futuros estudos com sensores de temperatura no interior dos VS podem dar uma melhor resposta a nosso parecer.

### **A.3 Estado inicial do sistema de reciclo da UP**

A Figura A.6 mostra alguns detalhes do estado inicial do sistema de reciclo da UP, a partir do qual foram realizadas as mudanças e adaptações de diversas válvulas e conexões, assim como das colunas de adsorção.



Figura A. 6. Estado inicial do sistema de reciclo antes das mudanças.

As letras a) e m) representam o mesmo manômetro, a) mostra a localização do manômetro dentro do conjunto de partes e m) mostra o vazamento de glicerina. b) é a cabine do conector de cabos do sensor de nível de CO<sub>2</sub>, c) é o tanque pulmão (TP) com capacidade para 15 L, d) entrada de CO<sub>2</sub> no TP, e) recobrimento do isolante (lâ de vidro), f) válvula de alívio, g) receptor de sinal do nível de CO<sub>2</sub>, h) válvula antiretorno para alimentação de CO<sub>2</sub> puro, i) acesso para CO<sub>2</sub> reciclado, j) isolante térmico (espuma elastomérica) que recobre a coluna de condensação do CO<sub>2</sub>, k) e l) são as saídas e entradas do líquido refrigerante; respectivamente, que fazem a troca térmica com o CO<sub>2</sub> e o levam até temperaturas negativas segundo o programado no banho de resfriamento, n) são as conexões da marca Swagelok que foram trocadas por conexões da marca Detroit (compradas no fornecedor Fopil da cidade de Campinas) por motivos de existência no estoque, o) válvula de purga de alta pressão, p) válvula

de bloqueio com conexões da Swagelok que também foi trocada, q) acesso alternativo localizado no topo do TP que pode ser utilizado para instalar sensores de temperatura ou de pressão.

#### A.4 Dados das cinéticas de extração e determinação do valor médio de X<sub>0</sub>

A determinação do rendimento global de extrato (óleo) de urucum já reportada em outros estudos (Albuquerque and Meireles, 2012; Moraes et al., 2015; Rodrigues et al., 2014; Silva et al., 2008; Taham et al., 2015), assim, todos eles servem de referência para observar a proximidade do valor obtido em nosso estudo, mesmo que os lotes da matéria-prima e procedências sejam distintas.

Tabela A. 2. Dados ponderados para a cinética de extração 1 (de urucum) no Spe-ed e determinação de X<sub>0</sub>.

X <sub>0</sub> Urucum	Data:	13/02/2017	Massa resíduo (g)	0,0382	Umidade m-p	11,61%	Tempo OEC	360
Massa em base úmida (g)	17,5007	TV Início (m <sup>3</sup> )	163,466	T (°C)	40	P (MPa)	20	
Massa em base seca (g)	15,4689	VV(m <sup>3</sup> /min)	0,007	VM (g/min)	11,0430	T banho (°C)	-10	
t (min)	S/F	P saída (bar)	Densidade (g/cm <sup>3</sup> )	TV (m <sup>3</sup> )	VM (g/min)	Massa CO <sub>2</sub> (g/min)* min	Extrato (g)	Acumulado (g)
2	1,3292	0,9320	0,0015816	163,479	10,28040	20,561	0,1277	0,1277
4	2,8628	0,9320	0,0015816	163,494	11,86200	44,285	0,0333	0,1610
6	4,2943	0,9320	0,0015816	163,508	11,07120	66,427	0,0237	0,1847
10	7,1571	0,9320	0,0015816	163,536	11,07120	110,712	0,0161	0,2008
15	10,7356	0,9320	0,0015816	163,571	11,07120	166,068	0,0108	0,2116
20	14,3142	0,9320	0,0015816	163,606	11,07120	221,424	0,0106	0,2222
25	18,5884	0,9315	0,0015799	163,648	13,27116	287,780	0,0136	0,2358
30	21,5503	0,9315	0,0015799	163,677	9,16342	333,597	0,0107	0,2465
35	25,0229	0,9315	0,0015799	163,711	10,74332	387,314	0,0114	0,2579
40	28,5976	0,9315	0,0015799	163,746	11,05930	442,610	0,0084	0,2663
45	32,1723	0,9315	0,0015799	163,781	11,05930	497,906	0,0040	0,2703
50	35,7470	0,9315	0,0015799	163,816	11,05930	553,203	0,0026	0,2729
55	39,3217	0,9315	0,0015799	163,851	11,05930	608,499	0,0077	0,2806
60	42,8963	0,9315	0,0015799	163,886	11,05930	663,796	0,0043	0,2849
70	50,0457	0,9315	0,0015799	163,956	11,05930	774,389	0,0082	0,2931
80	57,1951	0,9315	0,0015799	164,026	11,05930	884,982	0,0079	0,3010
90	64,3445	0,9315	0,0015799	164,096	11,05930	995,575	0,0075	0,3085
100	71,4939	0,9315	0,0015799	164,166	11,05930	1106,168	0,0070	0,3155
110	78,5412	0,9315	0,0015799	164,235	10,90131	1215,181	0,0091	0,3246
120	85,6906	0,9315	0,0015799	164,305	11,05930	1325,774	0,0153	0,3399
140	99,9893	0,9315	0,0015799	164,445	11,05930	1546,960	0,0164	0,3563
160	114,2881	0,9315	0,0015799	164,585	11,05930	1768,146	0,0145	0,3708
180	128,5869	0,9310	0,0015799	164,725	11,05930	1989,332	0,0039	0,3747
210	150,0351	0,9310	0,0015799	164,935	11,05930	2321,111	0,0053	0,3800
240	171,4833	0,9310	0,0015799	165,145	11,05930	2652,890	0,0047	0,3847
270	192,7238	0,9300	0,0015782	165,355	11,04740	2984,312	0,0039	0,3886
300	214,1489	0,9300	0,0015782	165,565	11,04740	3315,734	0,0030	0,3916
330	235,5740	0,9300	0,0015782	165,775	11,04740	3647,156	0,0012	0,3928
360	256,9991	0,9300	0,0015782	165,985	11,04740	3978,578	0,0002	0,3930

X<sub>0</sub> Urucum : [g extrato/ 100 g sementes b.s.]

2,79

Tabela A. 3. Dados ponderados para a cinética de extração 2 (de urucum) no Spe-ed e determinação de  $X_0$ .

$X_0$ Urucum		Data:	14/02/2017	Massa resíduo (g)	0,0186	Umidade m-p	11,61%	Tempo OEC	360
Massa em base úmida(g)			17,5008	TV Início (m <sup>3</sup> )	165,985	T (°C)	40	P (MPa)	20
Massa em base seca (g)			15,4690	VV(m <sup>3</sup> /min)	0,007	VM (g/min)	11,17301	T banho (°C)	-10
t (min)	S/F	P saída (bar)	Densidade (g/cm <sup>3</sup> )	TV (m <sup>3</sup> )	VM (g/min)	Massa CO <sub>2</sub> (g/min)* min	Extrato (g)	Acumulado (g)	Massa acumulada (g óleo/100 g sementes)
2	1,4299	0,9315	0,0015799	165,999	11,05930	22,119	0,1459	0,1459	0,94
4	2,8628	0,9320	0,0015816	166,013	11,07120	44,261	0,0218	0,1677	1,08
6	4,2942	0,9320	0,0015816	166,027	11,07120	66,403	0,0147	0,1824	1,18
10	7,1570	0,9320	0,0015816	166,055	11,07120	110,688	0,0232	0,2056	1,33
15	10,7356	0,9320	0,0015816	166,090	11,07120	166,044	0,0164	0,2220	1,44
20	14,3141	0,9320	0,0015816	166,125	11,07120	221,400	0,0123	0,2343	1,51
25	17,8926	0,9320	0,0015816	166,160	11,07120	276,756	0,0113	0,2456	1,59
30	21,4711	0,9320	0,0015816	166,195	11,07120	332,112	0,0104	0,2560	1,65
35	25,0497	0,9320	0,0015816	166,230	11,07120	387,468	0,0063	0,2623	1,70
40	28,6282	0,9320	0,0015816	166,265	11,07120	442,824	0,0072	0,2695	1,74
45	32,3452	0,9365	0,0015884	166,300	11,11880	498,418	0,0077	0,2772	1,79
50	35,9391	0,9365	0,0015884	166,335	11,11880	554,012	0,0045	0,2817	1,82
55	39,5330	0,9365	0,0015884	166,370	11,11880	609,606	0,0032	0,2849	1,84
60	43,1269	0,9365	0,0015884	166,405	11,11880	665,200	0,0089	0,2938	1,90
70	50,3147	0,9365	0,0015884	166,475	11,11880	776,388	0,0044	0,2982	1,93
80	58,2213	0,9365	0,0015884	166,552	12,23068	898,695	0,0042	0,3024	1,95
90	65,4091	0,9365	0,0015884	166,622	11,11880	1009,883	0,0039	0,3063	1,98
100	72,5969	0,9365	0,0015884	166,692	11,11880	1121,071	0,0157	0,3220	2,08
110	79,7847	0,9365	0,0015884	166,762	11,11880	1232,259	0,0144	0,3364	2,17
120	87,0656	0,9370	0,0015901	166,832	11,13070	1343,566	0,0169	0,3533	2,28
140	101,4567	0,9370	0,0015901	166,972	11,13070	1566,180	0,0079	0,3612	2,33
160	115,8477	0,9370	0,0015901	167,112	11,13070	1788,794	0,0038	0,3650	2,36
180	130,0994	0,9365	0,0015884	167,252	11,11880	2011,170	0,0075	0,3725	2,41
210	151,6629	0,9365	0,0015884	167,462	11,11880	2344,734	0,0077	0,3802	2,46
240	174,3559	0,9360	0,0015884	167,683	11,70121	2695,770	0,0077	0,3879	2,51
270	194,8925	0,9360	0,0015884	167,883	10,58933	3013,450	0,0126	0,4005	2,59
300	217,1747	0,9360	0,0015884	168,100	11,48943	3358,133	0,0114	0,4119	2,66
330	238,4826	0,9355	0,0015867	168,310	11,10690	3691,340	0,0062	0,4181	2,70
360	260,0230	0,9350	0,0015867	168,520	11,10690	4024,547	0,0033	0,4214	2,72
X <sub>0</sub> Urucum : [g extrato/ 100 g sementes b.s.]								2,84	

Tabela A. 4. Dados ponderados para a cinética de extração 3 (de urucum) no Spe-ed e determinação de  $X_0$ .

$X_0$ Urucum		Data:	15/02/2017	Massa resíduo (g)	0,0229	Umidade m-p	11,61%	Tempo OEC	360
Massa em base úmida(g)			17,5006	TV Início (m³)	168,52	T (°C)	40	P (MPa)	20
Massa em base seca (g)			15,4688	VV(m³/min)	0,007	VM (g/min)	11,13070	T banho (°C)	-10
t (min)	S/F	P saída (bar)	Densidade (g/cm³)	TV (m³)	VM (g/min)	Massa CO₂ (g/min)* min	Extrato (g)	Acumulado (g)	Massa acumulada (g óleo/100 g sementes)
2	1,4437	0,9400	0,0015952	168,534	11,16640	22,333	0,1453	0,1453	0,94
4	2,8875	0,9400	0,0015952	168,548	11,16640	44,666	0,0224	0,1677	1,08
6	4,3312	0,9400	0,0015952	168,562	11,16640	66,998	0,0150	0,1827	1,18
10	7,2187	0,9400	0,0015952	168,590	11,16640	111,664	0,0246	0,2073	1,34
15	10,8280	0,9400	0,0015952	168,625	11,16640	167,496	0,0166	0,2239	1,45
20	14,4373	0,9400	0,0015952	168,660	11,16640	223,328	0,0135	0,2374	1,53
25	18,0467	0,9400	0,0015952	168,695	11,16640	279,160	0,0126	0,2500	1,62
30	21,6560	0,9400	0,0015952	168,730	11,16640	334,992	0,0110	0,2610	1,69
35	25,2653	0,9400	0,0015952	168,765	11,16640	390,824	0,0085	0,2695	1,74
40	28,8747	0,9400	0,0015952	168,800	11,16640	446,656	0,0075	0,2770	1,79
45	32,4840	0,9400	0,0015952	168,835	11,16640	502,488	0,0072	0,2842	1,84
50	36,0933	0,9400	0,0015952	168,870	11,16640	558,320	0,0063	0,2905	1,88
55	39,7027	0,9400	0,0015952	168,905	11,16640	614,152	0,0056	0,2961	1,91
60	43,3120	0,9400	0,0015952	168,940	11,16640	669,984	0,0070	0,3031	1,96
70	50,5307	0,9400	0,0015952	169,010	11,16640	781,648	0,0069	0,3100	2,00
80	57,7493	0,9400	0,0015952	169,080	11,16640	893,312	0,0068	0,3168	2,05
90	64,9680	0,9400	0,0015952	169,150	11,16640	1004,976	0,0055	0,3223	2,08
100	72,1867	0,9400	0,0015952	169,220	11,16640	1116,640	0,0098	0,3321	2,15
110	79,3207	0,9395	0,0015935	169,290	11,15450	1228,185	0,0079	0,3400	2,20
120	86,5317	0,9395	0,0015935	169,360	11,15450	1339,730	0,0092	0,3492	2,26
140	100,9537	0,9395	0,0015935	169,500	11,15450	1562,820	0,0068	0,3560	2,30
160	115,3756	0,9395	0,0015935	169,640	11,15450	1785,910	0,0064	0,3624	2,34
180	129,7976	0,9395	0,0015935	169,780	11,15450	2009,000	0,0077	0,3701	2,39
210	151,4305	0,9395	0,0015935	169,990	11,15450	2343,635	0,0091	0,3792	2,45
240	173,0634	0,9390	0,0015935	170,200	11,15450	2678,270	0,0096	0,3888	2,51
270	194,4886	0,9385	0,0015918	170,410	11,14260	3012,548	0,0099	0,3987	2,58
300	216,0985	0,9380	0,0015918	170,620	11,14260	3346,826	0,0084	0,4071	2,63
330	237,7083	0,9380	0,0015918	170,830	11,14260	3681,104	0,0054	0,4125	2,67
360	259,0412	0,9375	0,0015901	171,040	11,13070	4015,025	0,0021	0,4146	2,68

$X_0$  Urucum : [g extrato/ 100 g sementes b.s.]

2,83

### A.5 Curvas de extração de urucum

As curvas de extração conduzem a obter as estimativas iniciais dos parâmetros  $b_0$ ,  $b_1$ ,  $b_2$ ,  $b_3$ ,  $t_{CER}$  e  $t_{FER}$ . Para o caso do presente estudo são parâmetros médios das cinéticas desenvolvida em três réplicas. Todas elas necessárias para calcular os valores de  $t_{CER}$  e  $t_{FER}$  da curva de extração utilizando um método numérico interativo.

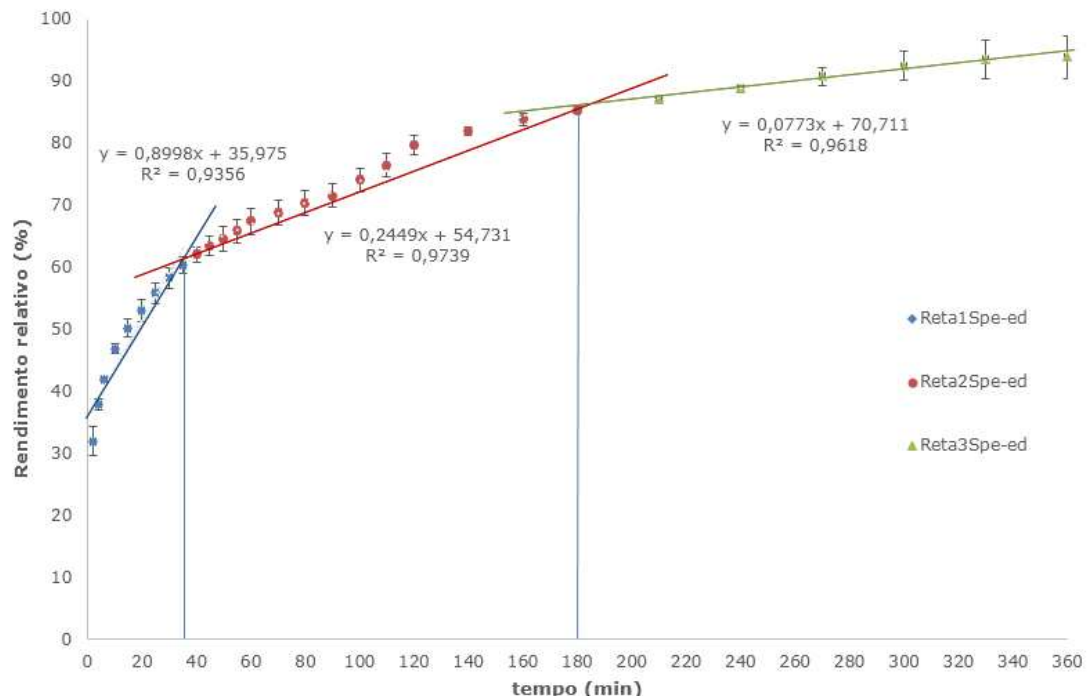


**Figura A. 7.** Cinética média para o ajuste usando spline para urucum.

A informação de partida para o ajustes realizados pelo programa SAS aos dados cinéticos de urucum presentes nesta seção (utilizados no capítulo 3) estão plotados na Figura A.7 e apresentados na Tabela A.5.

**Tabela A.5.** Dados organizados para análises no SAS para urucum (usados no capítulo 3).

Tempo	UnidadeSpe_edSFE
2	32.01
4	37.93
6	42.01
10	46.90
15	50.24
20	53.02
25	55.89
30	58.34
35	60.34
40	62.11
45	63.55
50	64.58
55	65.84
60	67.38
70	68.87
80	70.31
90	71.61
100	74.09
110	76.49
120	79.65
140	82.03
160	83.92
180	85.38
210	87.06
240	88.74
270	90.76
300	92.50
330	93.48
360	93.91

As estimativas iniciais dos parâmetros a seguir foram obtidas das equações das três retas vistas na Figura A.7., assim como os valores de  $t_{CER}$  e  $t_{FER}$ .

**Tabela A. 6.** Resultados obtidos a partir dos valores médios das cinéticas no Spe-ed para urucum (usados no capítulo 3).

Valores dos parâmetros	b0	b1	b2	b3	$t_{CER}$	$t_{FER}$
Valores da Estimativa						
Inicial	35.98	0.90	0.24	0.08	35.00	180.00
Valores Calculados no						
SAS	34.31	0.95	0.21	0.05	26.17	143.50

Tabela A.7. Resultado obtidos para os parâmetros cinéticos para urucum (usados no capítulo 3).

$t_{CER}$ (min)	$M_{CER}$ (g/min)	$R_{CER}$ (%)	$Y_{CER}$ (g ext/g CO <sub>2</sub> )
26.17	0.0041	59.17	0.00088
$t_{FER}$ (min)	$M_{FER}$ (g/min)	$R_{FER}$ (%)	$Y_{FER}$ (g ext/g CO <sub>2</sub> )
143.50	0.0022	83.81	0.00022

```
/*
 *-----*/
/* Departamento de Engenharia de Alimentos - DEA / Unicamp      */
/* Ajuste das curvas experimentais no SAS                         */
/* Ricardo Abel del Castillo Torres - LASEFI                      */
/*                                                               */
/* -----*/
/* --[Cabeçalho]-----*/
Options NoDate NoNumber PS=100 LS=100 FormDLim='-' ;
Title'Cinética de extração Urucum Unidade Spe_ed: 20 MPa/40oC CO2';
FootNote;
```

```
DATA DADOSNLIN;
INPUT TEMPO UnidadeSpe_edSFE;
CARDS;
2    32.01
4    37.93
6    42.01
10   46.90
15   50.24
20   53.02
25   55.89
30   58.34
35   60.34
40   62.11
45   63.55
50   64.58
55   65.84
60   67.38
70   68.87
80   70.31
90   71.61
100  74.09
110  76.49
120  79.65
140  82.03
160  83.92
```

```

180  85.38
210  87.06
240  88.74
270  90.76
300  92.50
330  93.48
360  93.91
;
PROC PRINT DATA = DADOSNLIN;
RUN;

PROC NLIN DATA = DADOSNLIN;
TITLE 'UnidadeSpe_edSFE NLIN';
PARMS b0 = 35.98
      b1 = 0.90 /*---termo de primeira ordem do período tcer---*/
      b2 = 0.24 /*---termo de primeira ordem do período tfer---*/
      b3 = 0.08 /*---termo de primera ordem do período difusional---*/
      C1 = 35 /*---tcer---*/
      C2 = 180; /*---tfer---*/
      INT = MIN(Tempo,C1);
      AL1 = MAX(Tempo-C1,0);
      AL2 = MAX(Tempo-C2,0);
      AL3 = MAX(Tempo-C2,0);

MODEL UnidadeSpe_edSFE = b0 + b1*INT + b2*(AL1-AL2) + b3*AL3;
Output out = a p=UnidadeSpe_edSFE_hat r=Mres;
Axis order = (0 to 100 by 10);
run;

```

## Resultados obtidos do SAS

---

Cinética de extração Urucum Unidade Spe\_ed: 20 MPa/40oC CO<sub>2</sub>

Obs	Unidade Spe_ed	
	TEMPO	SFE
1	2	32.01
2	4	37.93
3	6	42.01
4	10	46.90
5	15	50.24
6	20	53.02
7	25	55.89
8	30	58.34
9	35	60.34
10	40	62.11
11	45	63.55
12	50	64.58
13	55	65.84
14	60	67.38
15	70	68.87
16	80	70.31
17	90	71.61
18	100	74.09
19	110	76.49
20	120	79.65
21	140	82.03
22	160	83.92
23	180	85.38
24	210	87.06
25	240	88.74
26	270	90.76
27	300	92.50
28	330	93.48
29	360	93.91

---

UnidadeSpe\_edSFE NLIN

Procedimiento NLIN

Variable dependiente UnidadeSpe\_edSFE

Método: Gauss-Newton

Iter	Fase iterativa						
	b0	b1	b2	b3	C1	C2	Suma de cuadrados
0	35.9800	0.9000	0.2400	0.0800	35.0000	180.0	3656.1
1	35.9965	0.7598	0.1852	0.0502	34.3567	159.5	72.1693
2	35.1010	0.8530	0.2024	0.0524	28.8110	143.6	59.1814
3	34.3066	0.9494	0.2080	0.0524	25.8041	143.5	50.8267
4	34.3066	0.9494	0.2080	0.0524	26.1725	143.5	49.1830

NOTA: Convergence criterion met.

Resumen de estimación	
Método	Gauss-Newton
Iteraciones	4
R	0
PPC	0
RPC(C1)	0.014277
Objeto	0.032341
Objetivo	49.18297
Observaciones leídas	29
Observaciones usadas	29
Observaciones ausentes	0

Fuente	Cuadrado				
	DF	Suma de cuadrados	de la media	Approx F-Valor	Pr > F
Modelo	5	8404.3	1680.9	786.04	<.0001
Error	23	49.1830	2.1384		
Total correcto	28	8453.5			

Parámetro	Approx			
	Estimación	Std Error	Approximate 95% Confidence Limits	
b0	34.3066	0.9820	32.2752	36.3379
b1	0.9494	0.0693	0.8061	1.0928
b2	0.2080	0.0118	0.1836	0.2325
b3	0.0524	0.00773	0.0364	0.0684
C1	26.1725	1.7947	22.4600	29.8851
C2	143.5	8.7842	125.3	161.6

	Approximate Correlation Matrix						
	b0	b1	b2	b3	C1	C2	
b0	1.0000000	-0.8265558	0.0000000	0.0000000	0.3884985	-0.0000000	
b1	-0.8265558	1.0000000	-0.0000000	-0.0000000	-0.7528838	0.0000000	
b2	0.0000000	-0.0000000	1.0000000	0.0000000	-0.4175496	-0.6069515	
b3	0.0000000	-0.0000000	0.0000000	1.0000000	-0.0000000	-0.6378150	
C1	0.3884985	-0.7528838	-0.4175496	-0.0000000	1.0000000	0.1694534	
C2	-0.0000000	0.0000000	-0.6069515	-0.6378150	0.1694534	1.0000000	

### A.6 Características do leito

A Tabela A.8 mostra os cálculos realizados para a análises das característica do leito, onde VI é a velocidade intersticial do solvente no leito. As letras desde a A até o E, são as mesmas da Tabela 3 do Capítulo 2.

Tabela A. 8. Dados calculados a partir das características do leito.

Processo	Massa (Kg) (b.u.)	$V (m^3)$ $\times 10^{-3}$	$\rho_a$ ( $Kg/m^3$ )	$\rho_r$ ( $Kg/m^3$ )	$\varepsilon = 1 - \frac{\rho_a}{\rho_r}$	HB/DB	VI (m/min)	$Q_{CO_2}$ (kg/min)
1_X0	0,0175007		700,03		0,48	4,18	44	0,01
2_X0	0,0175008	0,025	700,03		0,48	4,18	44	0,01
3_X0	0,0175006		700,02		0,48	4,18	44	0,01
A	3,5200	5	704,00		0,48	4,46	28	0,20
B	1,5009	2	750,46		0,44	1,90	30	0,20
C	1,5007	2	750,33	1350,00	0,44	1,90	30	0,20
D	3,6647	5	732,94		0,46	4,46	30	0,20
	3,5712	5	714,24		0,47	4,46	29	0,20
E	3,4760	5	695,20		0,49	4,46	28	0,20
	3,4207	5	684,13		0,49	4,46	27	0,20

A figura a seguir mostra a descrição do leito extrator utilizados para realizar as cinéticas de extração e a determinação de  $X_0$ . O valor de  $H_B$  (altura do leito) para os leitos das letras A, D e E foi 0.47 m e 0.20 m para as letras B e C.

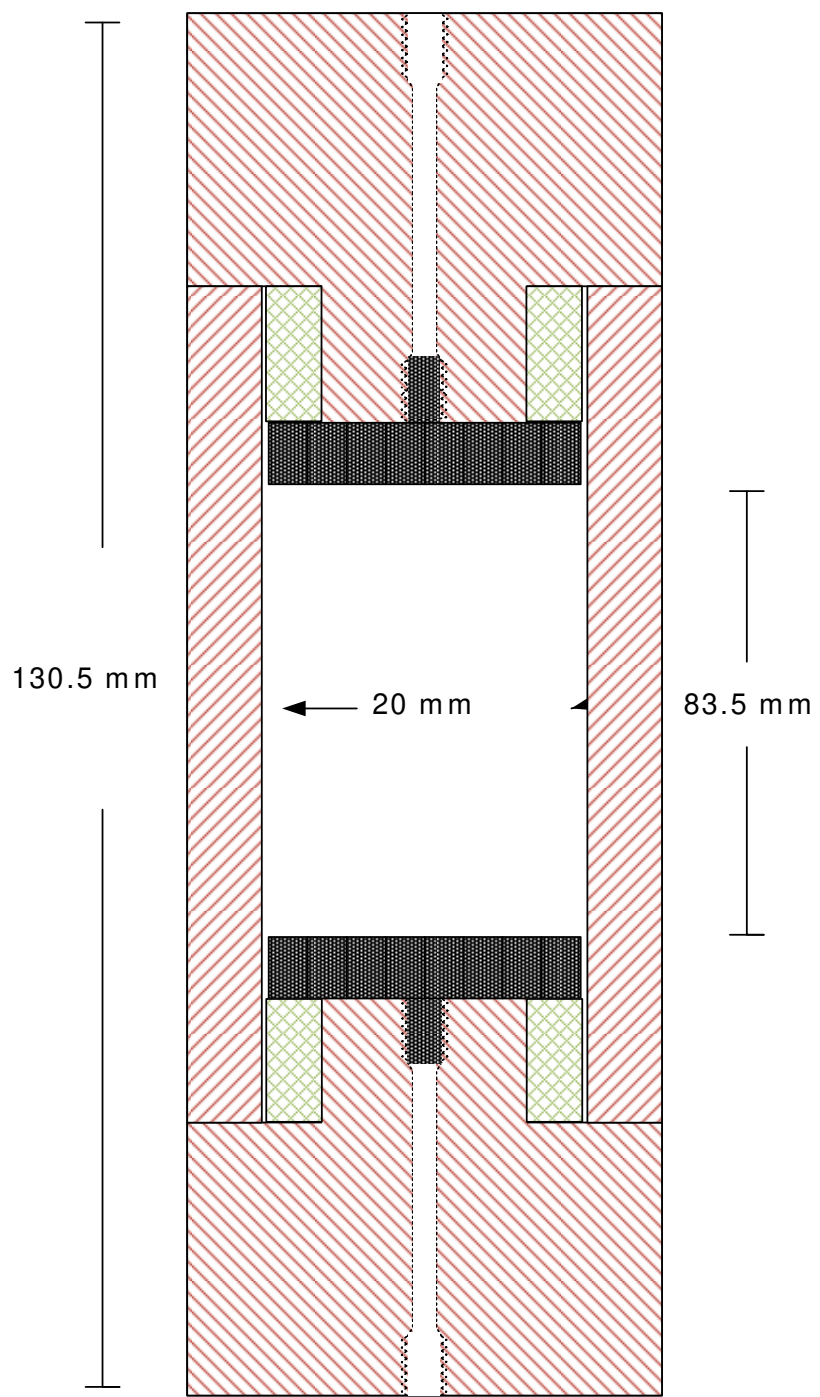


**Figura A. 8.** Desenho da coluna de 25 mL utilizada da determinação das cinéticas de extração.

## APÊNDICE B

O APÊNDICE B comprehende os dados experimentais do Capítulo 4. Informações de despressurização do leito empacotado junto à massa de CO<sub>2</sub>, assim como a despressurização dos vasos de fracionamento também junto à massa de CO<sub>2</sub>, fotos das válvulas backpressure manuais conectadas à bomba de líquido utilizada para a limpeza e fotos das características visuais do farelo de aveia e das conexões do equipamento são apresentados neste APÊNDICE.

### B.1 Massa de CO<sub>2</sub> calculada durante a despressurização do leito com urucum

Na Tabela B.1 mostra-se o cálculo da massa de CO<sub>2</sub> durante a despressurização do leito empacotado com 3 kg de urucum (o volume vazio foi preenchido com pérolas de vidro).

*Tabela B. 1. Massa de CO<sub>2</sub> calculada durante a despressurização do leito empacotado desde 20 MPa até pressão ambiente*

Despressurização da C1: Urucum		P = 20 MPa	TV Início (m <sup>3</sup> )	0,011	
Data:	15/04/2017	T = 22°C	T banho (°C)	-10	
t (min)	P saída (bar)	Densidade (g/cm <sup>3</sup> )	TV (m <sup>3</sup> )	VM (g/min)	Massa CO <sub>2</sub> (g/min)* min
2	0,9325	0,0016804	0,0166	4,70512	9,410
4	0,9325	0,0016804	0,0232	5,54532	20,501
6	0,9320	0,0016795	0,0308	6,38210	33,265
10	0,9320	0,0016795	0,0499	8,01961	65,344
15	0,9315	0,0016786	0,073	7,75513	104,119
20	0,9315	0,0016786	0,097	8,05728	144,406
25	0,9310	0,0016777	0,122	8,38850	186,348
30	0,9310	0,0016777	0,146	8,05296	226,613
35	0,9310	0,0016777	0,171	8,38850	268,555
40	0,9285	0,0016731	0,195	8,03088	308,710
45	0,9290	0,0016740	0,219	8,03520	348,886
50	0,9290	0,0016740	0,244	8,37000	390,736
55	0,9290	0,0016740	0,269	8,37000	432,586
60	0,9295	0,0016750	0,293	8,04000	472,786
80	0,9295	0,0016750	0,389	8,04000	633,586
100	0,9295	0,0016750	0,484	7,95625	792,711
120	0,9295	0,0016750	0,583	8,29125	958,536
140	0,9300	0,0016759	0,679	8,04432	1119,422
160	0,9300	0,0016759	0,767	7,37396	1266,901
180	0,9305	0,0016768	0,863	8,04864	1427,874
200	0,9305	0,0016768	0,965	8,55168	1598,908
220	0,9310	0,0016777	1,098	11,15671	1822,042
240	0,9310	0,0016777	1,235	11,49225	2051,887
260	0,9310	0,0016777	1,336	8,47239	2221,334
270	0,9310	0,0016777	1,376	6,71080	2288,442
275	0,9310	0,0016777	1,382	2,01324	2298,509
280	0,9310	0,0016777	1,383	0,3355	2300,186

## B.2 Massa de CO<sub>2</sub> calculada durante a despressurização dos vasos de fracionamento

Na Tabela B.2., mostra-se o cálculo da massa de CO<sub>2</sub> a partir da despressurização dos vasos de separação (VS). Elas foram pressurizados desde 8,0 MPa, 6,5 MPa e 5,5 MPa até a pressão ambiente, para VS1, VS2 e VS3, respectivamente.

*Tabela B. 2. Massa de CO<sub>2</sub> calculada durante a despressurização dos vasos de fracionamento*

Despressurização Vasos de Fracionamento			P (MPa)	8, 6,5 e 5,5	
Data:		15/04/2017	T (°C)	22	
TV Início (m <sup>3</sup> )		1,382	T banho (°C)	-10	
t (min)	P saída (bar)	Densidade (g/cm <sup>3</sup> )	TV (m <sup>3</sup> )	VM (g/min)	Massa CO <sub>2</sub> (g/min)* min
2	0,9310	0,0016777	1,385	2,5166	5,033
4	0,9310	0,0016777	1,39	4,1942	13,422
6	0,9310	0,0016777	1,396	5,0331	23,488
10	0,9310	0,0016777	1,409	5,4525	45,298
20	0,9310	0,0016777	1,44	5,2009	97,307
30	0,9310	0,0016777	1,47	5,0331	147,638
40	0,9310	0,0016777	1,501	5,2009	199,646
50	0,9310	0,0016777	1,533	5,3686	253,333
60	1,9310	0,0017845	1,571	6,7811	321,144
70	2,9310	0,0017845	1,608	6,6027	387,170
80	3,9305	0,0017845	1,647	6,9595	456,766
85	4,9305	0,0017845	1,664	6,0673	487,102
90	5,9305	0,0017845	1,671	2,4983	499,594
95	5,9305	0,0017845	1,672	0,3569	501,378

### B.3 Massa de CO<sub>2</sub> calculada durante a despressurização do leito com cúrcuma

Na Tabela B.3., mostra-se o estimativa da despressurização do leito. Ela foi empacotada com 2 kg de cúrcuma e posteriormente o volume vazio foi preenchido com pérolas de vidro, após atingir 25 MPa, a coluna foi despressurizada

*Tabela B. 3. Massa de CO<sub>2</sub> calculada durante a despressurização da C1 utilizando cúrcuma.*

Despressurização da C1: Cúrcuma		P (MPa)	25	TV Início (m <sup>3</sup> )	3,235
Data:	05/06/2017	T (°C)	22	T banho (°C)	-10
t (min)	P saída (bar)	Densidade (g/cm <sup>3</sup> )	TV (m <sup>3</sup> )	VM (g/min)	Massa CO <sub>2</sub> (g/min)* min
2	0,9360	0,0016867	3,24	4,21675	8,434
4	0,9360	0,0016867	3,249	7,59015	23,614
6	0,9360	0,0016867	3,259	8,43350	40,481
10	0,9360	0,0016867	3,281	9,27685	77,588
15	0,9360	0,0016867	3,305	8,09616	118,069
20	0,9360	0,0016867	3,331	8,77084	161,923
25	0,9360	0,0016867	3,356	8,43350	204,091
30	0,9360	0,0016867	3,382	8,77084	247,945
35	0,9360	0,0016867	3,407	8,43350	290,112
40	0,9285	0,0016731	3,435	9,36936	336,959
45	0,9290	0,0016740	3,468	11,04840	392,201
50	0,9290	0,0016740	3,497	9,70920	440,747
55	0,9290	0,0016740	3,525	9,37440	487,619
60	0,9295	0,0016750	3,557	10,72000	541,219
80	0,9295	0,0016750	3,655	8,20750	705,369
100	0,9295	0,0016750	3,752	8,12375	867,844
120	0,9295	0,0016750	3,848	8,04000	1028,644
140	0,9295	0,0016750	3,954	8,87750	1206,194
160	0,9300	0,0016759	4,049	7,96053	1365,405
180	0,9300	0,0016759	4,160	9,30124	1551,430
200	0,9305	0,0016768	4,264	8,71936	1725,817
220	0,9305	0,0016768	4,365	8,46784	1895,174
240	0,9305	0,0016768	4,475	9,22240	2079,622
260	0,9305	0,0016768	4,575	8,38400	2247,302
270	0,9310	0,0016777	4,601	4,36202	2290,922
275	0,9310	0,0016777	4,607	2,01324	2300,988
280	0,9310	0,0016777	4,608	0,3355	2302,666

#### B.4 Orientação para a limpeza das válvulas backpressure

Na Figura B.1 e B.2., indica-se que a limpeza das válvulas backpressure (válvulas manuais) merece uma atenção particular devido a que o passo do líquido limpador (etanol por exemplo) precisa vencer uma pressão mínima de 0,3 MPa para permitir fluir através dele. Para uma adequada limpeza das válvulas backpressure é conveniente iniciar a limpeza desde terceira válvula correspondente ao vaso de fracionamento 3 (VS3) que foi aquele que regulou a pressão mais baixa de fracionamento. Logo o líquido limpador continua o seu passo pelas outras duas válvulas na sequência de pressão ascendente como foi utilizada no processamento. No momento da limpeza pode-se inverter a posição das válvulas VS1 com a VS3.



*Figura B. 1. Conexão entre válvulas backpressure para limpeza*



*Figura B. 2. Conexão da bomba de líquido com a válvula backpressure.*

### B.5 Coluna utilizada durante os testes de adsorção

A Figura B3 mostra as dimensões da coluna utilizada na unidade Spe-ed para os testes de adsorção, neste caso foram três colunas: 01 de capacidade de 25 mL (utilizada como coluna de extração) e 02 de capacidade de 5 mL (uma utilizada como vaso de separação de extrato e a outra utilizada como coluna de adsorção recheada com farelo de aveia).

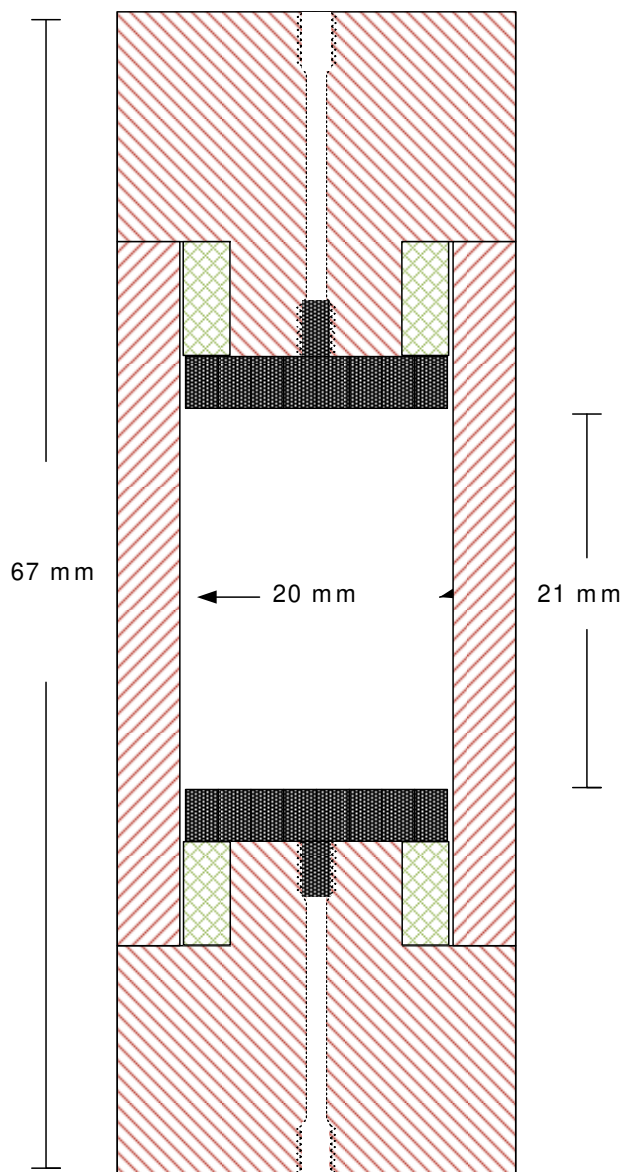


Figura B. 3. Coluna utilizada nos testes de adsorção (5 mL)

## B.6 Diâmetro médio geométrico das partículas de cúrcuma

A relação das massas de cúrcuma retida segundo o processo de peneiramento é mostrada na seguinte tabela.

*Tabela B. 4. Dados de peneiramento de cúrcuma moída.*

Réplica 1					
Peneira – mesh	Abertura (mm)	Massa peneira (g)	Massa peneira+MP(g)	Massa retida (g)	Retido (%)
Fundo	0,00	466,65	469,20	2,55	10,20
1 - 100	0,15	368,30	376,45	8,15	32,60
2 - 80	0,18	314,68	320,49	5,81	23,24
3 - 48	0,30	433,64	438,39	4,75	19,00
4 - 24	0,71	462,00	462,99	0,99	3,96
5 - 18	1,00	394,12	396,51	2,39	9,56
6 - 8	2,38	482,09	482,42	0,33	1,32
Réplica 2					
Peneira - mesh	Abertura (mm)	Massa peneira (g)	Massa peneira+MP(g)	Massa retida (g)	Retido (%)
Fundo	0,00	466,66	468,23	1,57	6,28
1 - 100	0,15	368,32	377,01	8,69	34,76
2 - 80	0,18	314,67	320,87	6,20	24,80
3 - 48	0,30	433,65	438,50	4,85	19,40
4 - 24	0,71	462,02	462,98	0,96	3,84
5 - 18	1,00	394,08	396,52	2,44	9,76
6 - 8	2,38	482,07	482,35	0,28	1,12
Réplica 3					
Peneira – mesh	Abertura (mm)	Massa peneira (g)	Massa peneira+MP(g)	Massa retida (g)	Retido (%)
Fundo	0,00	466,70	469,03	2,33	9,32
1 - 100	0,15	368,34	376,74	8,40	33,60
2 - 80	0,18	314,72	320,68	5,96	23,84
3 - 48	0,30	433,64	438,38	4,74	18,96
4 - 24	0,71	461,97	462,81	0,84	3,36
5 - 18	1,00	394,05	396,46	2,41	9,64
6 - 8	2,38	482,11	482,38	0,27	1,08

\*Massa de cúrcuma: 25g. Tempo de peneiramento: 15 min. Relação vibração/tempo: 10

A determinação do diâmetro médio geométrico das partículas círcuma foi calculado de acordo com o método recomendado pela ASAE-Standard (1998) utilizando a Equação a seguir:

$$d_{mp} = \text{Exp} \left[ \frac{\sum_{i=1}^n (w_i \log(d_i \cdot d_{i+1})^{0.5})}{\sum_{i=1}^n w_i} \right] \quad (\text{B1})$$

*Tabela B. 5. Diâmetro médio de partícula para círcuma.*

$D_{mp}$ (mm)	$\sum w_i$	$(d_i \times d_{i+1})^{0.5}$	$\log (d_i \times d_{i+1})^{0.5}$	$w_i$	$w_i \times \log (d_i \times d_{i+1})^{0.5}$	$\sum (w_i \times \log (d_i \times d_{i+1})^{0.5})$
0.632	24.6	---	---	---	---	-11.3164
		0.1643	-0.7843	8.15	-6.3922	
		0.2312	-0.6360	5.81	-3.6951	
		0.4592	-0.3380	4.75	-1.6055	
		0.8426	-0.0744	0.99	-0.0736	
		1.5427	0.1883	2.39	0.4500	
<hr/>						
$D_{mp}$ (mm)	$\sum w_i$	$(d_i \times d_{i+1})^{0.5}$	$\log (d_i \times d_{i+1})^{0.5}$	$w_i$	$w_i \times \log (d_i \times d_{i+1})^{0.5}$	$\sum (w_i \times \log (d_i \times d_{i+1})^{0.5})$
0.615	24.7	---	---	---	---	-12.0101
		0.1643	-0.7843	8.69	-6.8157	
		0.2312	-0.6360	6.2	-3.9431	
		0.4592	-0.3380	4.85	-1.6393	
		0.8426	-0.0744	0.96	-0.0714	
		1.5427	0.1883	2.44	0.4594	
<hr/>						
$D_{mp}$ (mm)	$\sum w_i$	$(d_i \times d_{i+1})^{0.5}$	$\log (d_i \times d_{i+1})^{0.5}$	$w_i$	$w_i \times \log (d_i \times d_{i+1})^{0.5}$	$\sum (w_i \times \log (d_i \times d_{i+1})^{0.5})$
0.625	24.7	---	---	---	---	-11.5895
		0.1643	-0.7843	8.4	-6.5883	
		0.2312	-0.6360	5.96	-3.7905	
		0.4592	-0.3380	4.74	-1.6021	
		0.8426	-0.0744	0.84	-0.0625	
		1.5427	0.1883	2.41	0.4538	

O diâmetro médio das partículas ( $D_{mp}$ ) de círcuma colocado dentro da C1 e C2 teve  $0.624 \pm 0.010$  mm.

### B.7 Diâmetro médio geométrico das partículas de farelo de aveia

A relação das massas de farelo de aveia retida segundo o processo de peneiramento é mostrada na seguinte tabela.

*Tabela B. 6. Dados de peneiramento de farelo de aveia.*

Réplica 1					
Peneira - mesh	Abertura (mm)	Massa peneira (g)	Massa peneira+MP(g)	Massa retida (g)	Retido (%)
Fundo	0.00	466.66	467.39	0.73	2.92
1 - 100	0.15	368.33	369.25	0.92	3.68
2 - 80	0.18	314.70	315.82	1.12	4.48
3 - 48	0.30	433.65	438.78	5.13	20.52
4 - 24	0.71	461.99	472.01	10.02	40.08
5 - 18	1.00	394.10	400.62	6.52	26.08
6 - 8	2.38	482.08	482.63	0.55	2.20
Réplica 2					
Peneira - mesh	Abertura (mm)	Massa peneira (g)	Massa peneira+MP(g)	Massa retida (g)	Retido (%)
Fundo	0.00	466.68	467.42	0.74	2.96
1 - 100	0.15	368.31	369.25	0.94	3.76
2 - 80	0.18	314.68	315.77	1.09	4.36
3 - 48	0.30	433.64	438.73	5.09	20.36
4 - 24	0.71	462.01	471.90	9.89	39.56
5 - 18	1.00	394.09	400.80	6.71	26.84
6 - 8	2.38	482.09	482.61	0.52	2.08
Réplica 3					
Peneira - mesh	Abertura (mm)	Massa peneira (g)	Massa peneira+MP(g)	Massa retida (g)	Retido (%)
Fundo	0.00	466.69	467.40	0.71	2.84
1 - 100	0.15	368.32	369.27	0.95	3.80
2 - 80	0.18	314.70	315.77	1.07	4.28
3 - 48	0.30	433.65	438.75	5.10	20.40
4 - 24	0.71	461.99	471.89	9.90	39.60
5 - 18	1.00	394.07	400.82	6.75	27.00
6 - 8	2.38	482.10	482.62	0.52	2.08

\*Massa de farelo de aveia: 25g. Tempo de peneiramento: 15 min. Relação vibração/tempo: 10

A determinação do diâmetro médio geométrico das partículas de farelo de aveia foi calculado de acordo com o método recomendado pela ASAE-Standard (1998) utilizando a Equação a seguir:

$$d_{mp} = \text{Exp} \left[ \frac{\sum_{i=1}^n (w_i \log(d_i \times d_{i+1})^{0.5})}{\sum_{i=1}^n w_i} \right] \quad (\text{B1})$$

*Tabela B. 7. Diâmetro médio de partícula para farelo de aveia.*

$D_{mp}$ (mm)	$\sum w_i$	$(d_i \times d_{i+1})^{0.5}$	$\log (d_i \times d_{i+1})^{0.5}$	$w_i$	$w_i \times \log (d_i \times d_{i+1})^{0.5}$	$\sum (w_i \times \log (d_i \times d_{i+1})^{0.5})$
0.898	24.99	---	---	---	---	-2.6853
		0.1643	-0.7843	0.92	-0.7216	
		0.2312	-0.6360	1.12	-0.7123	
		0.4592	-0.3380	5.13	-1.7339	
		0.8426	-0.0744	10.02	-0.7452	
		1.5427	0.1883	6.52	1.2276	
0.900	24.98	---	---	---	---	-2.6230
		0.1643	-0.7843	0.94	-0.7373	
		0.2312	-0.6360	1.09	-0.6932	
		0.4592	-0.3380	5.09	-1.7204	
		0.8426	-0.0744	9.89	-0.7355	
		1.5427	0.1883	6.71	1.2634	
0.901	25.00	---	---	---	---	-2.6147
		0.1643	-0.7843	0.95	-0.7451	
		0.2312	-0.6360	1.07	-0.6805	
		0.4592	-0.3380	5.10	-1.7238	
		0.8426	-0.0744	9.90	-0.7363	
		1.5427	0.1883	6.75	1.2709	

O diâmetro médio das partículas ( $D_{mp}$ ) de farelo de aveia colocado dentro das colunas de adsorção teve  $0.899 \pm 0.001$  mm.

## APÊNDICE C

### C.1 Dados da cinética de extração e determinação de X<sub>0</sub> da cúrcuma

As Tabelas C.1. e C.2. mostram a cinética de extração de cúrcuma na unidade comercial Spe-ed.

**Tabela .C.1.** Dados ponderados para a cinética de extração 1 (de cúrcuma) na unidade Spe-ed e determinação de X<sub>0</sub>.

X <sub>0</sub> Cúrcuma		Massa resíduo: 0.0022 g		Data: 01/03/2017		Umidade m-p 8.00%		Tempo OEC 60	
Massa em base úmida(g)		15.1139		TV Início (m <sup>3</sup> )		173.613		T (°C)	
Massa em base seca (g)		13.9048		VV(m <sup>3</sup> /min)		0.0055		VM (g/min)	
t (min)	S/F	P saída (bar)	Densidade (g/cm <sup>3</sup> )	TV (m <sup>3</sup> )	VM (g/min)	Massa CO <sub>2</sub> (g/min)* min	Extrato (g)	Acumulado (g)	Massa acumulada (g óleo/100 g cúrcuma)
2	1.2217	0.9315	0.0016786	173.6240	9.23230	18.465	0.7262	0.7262	5.22
4	2.4434	0.9315	0.0016786	173.6350	9.23230	36.929	0.0397	0.7659	5.51
6	3.6651	0.9315	0.0016786	173.6460	9.23230	55.394	0.0145	0.7804	5.61
10	6.1085	0.9315	0.0016786	173.6680	9.23230	92.323	0.0241	0.8045	5.79
15	9.1627	0.9315	0.0016786	173.6955	9.23230	138.484	0.0199	0.8244	5.93
20	12.2170	0.9315	0.0016786	173.7230	9.23230	184.646	0.0146	0.8390	6.03
25	15.2630	0.9310	0.0016777	173.7505	9.22735	230.783	0.0066	0.8456	6.08
30	18.3156	0.9310	0.0016777	173.7780	9.22735	276.919	0.0062	0.8518	6.13
35	21.3682	0.9310	0.0016777	173.8055	9.22735	323.056	0.0046	0.8564	6.16
40	24.4208	0.9310	0.0016777	173.8330	9.22735	369.193	0.0018	0.8582	6.17
45	27.4734	0.9310	0.0016777	173.8605	9.22735	415.330	0.0030	0.8612	6.19
50	30.5260	0.9310	0.0016777	173.8880	9.22735	461.467	0.0027	0.8639	6.21
55	33.5786	0.9310	0.0016777	173.9155	9.22735	507.603	0.0019	0.8658	6.23
60	36.6116	0.9305	0.0016768	173.9430	9.22240	553.715	0.0015	0.8673	6.24
X <sub>0</sub> Cúrcuma : [g extrato/ 100 g cúrcuma b.s.]								6.25	

**Tabela .C.2.** Dados ponderados para a cinética de extração 2 (de cúrcuma) na unidade Spe-ed e determinação de  $X_0$ .

$X_0$ Cúrcuma		Massa resíduo: 0.001 g		Data: 01/03/2017		Umidade m-p		8.00%	Tempo OEC	60
Massa em base úmida(g)		15.1139		TV Início (m <sup>3</sup> )		173.989		T (°C)	60	P (MPa)
Massa em base seca (g)		13.9048		VV(m <sup>3</sup> /min)		0.0055		VM (g/min)	9.2125	T banho (°C)
t (min)	S/F	P saída (bar)	Densidade (g/cm <sup>3</sup> )	TV (m <sup>3</sup> )	VM (g/min)	Massa CO <sub>2</sub> (g/min)* min	Extrato (g)	Acumulado (g)	Massa acumulada (g óleo/100 g cúrcuma)	
2	1.2170	0.9280	0.0016722	174.0000	9.19710	18.394	0.7249	0.7249	5.21	
4	2.4341	0.9280	0.0016722	174.0110	9.19710	36.788	0.0351	0.7600	5.47	
6	3.6511	0.9280	0.0016722	174.0220	9.19710	55.183	0.0197	0.7797	5.61	
10	6.0852	0.9280	0.0016722	174.0440	9.19710	91.971	0.0209	0.8006	5.76	
15	9.1278	0.9280	0.0016722	174.0715	9.19710	137.956	0.0140	0.8146	5.86	
20	12.1704	0.9280	0.0016722	174.0990	9.19710	183.942	0.0110	0.8256	5.94	
25	15.2212	0.9285	0.0016731	174.1265	9.20205	229.952	0.0094	0.8350	6.01	
30	18.2654	0.9285	0.0016731	174.1540	9.20205	275.962	0.0059	0.8409	6.05	
35	21.3096	0.9285	0.0016731	174.1815	9.20205	321.973	0.0067	0.8476	6.10	
40	24.3539	0.9285	0.0016731	174.2090	9.20205	367.983	0.0043	0.8519	6.13	
45	27.4128	0.9290	0.0016740	174.2365	9.20700	414.018	0.0042	0.8561	6.16	
50	30.4587	0.9290	0.0016740	174.2640	9.20700	460.053	0.0022	0.8583	6.17	
55	33.5046	0.9290	0.0016740	174.2915	9.20700	506.088	0.0020	0.8603	6.19	
60	36.5723	0.9295	0.0016750	174.3190	9.21250	552.151	0.0027	0.8630	6.21	

$X_0$  Cúrcuma : [g extrato/ 100 g cúrcuma b.s.] 6.21

## APÊNDICE D

### Procedimentos operacionais de unidade piloto Thar Technologies junto a PRSCO<sub>2</sub>

#### D.1 Etapa 1: Pré-extração

- 1 Verificar a disponibilidade de CO<sub>2</sub> (1 da Figura 2 do Capítulo 4) para o desenvolvimento do processo, assim como também a entrega do Laudo<sup>1</sup> técnico na hora da compra e recepção dos cilindros.
- 2 Preparar a matéria-prima: limpeza, moagem, determinação de diâmetro médio, umidade, etc.
- 3 Verificar a disponibilidade de material de recheio quando usarem matéria-prima ocupando volume menor que a capacidade da Coluna de Extração (C, ela pode ser C1 ou C2, segundo o que esteja sendo utilizado no momento), tais como pérolas de vidro, bucha ou tarugo de teflão.

<sup>1</sup> Documento entregado pelo provedor referente ao parecer técnico do produto (i.e. grau de pureza, data e nº de lote de produção, entre outras informações)

4 Verificar a disponibilidade de frascos coletores de extratos, assim como de células de nylon com comprimento maior à altura e diâmetro igual do que a C. Elaborar um registro com os dados da massa de cada um de estes elementos.

#### D.2 Etapa 2: Pressurização do tanque pulmão (TP)

1 Conectar as partes do TP junto à UP na sequência (válvulas e indicadores de pressão e temperatura entre os componentes estão incluídos, ver Figura D1): Cilindro de CO<sub>2</sub> (1), filtro de linha para CO<sub>2</sub> (3), novamente outro filtro de linha (3), trocador de calor com tubo interno em espiral (5), Totalizador de Vazão Mássica (TVM) (6), Bomba de CO<sub>2</sub> (7), Trocador de calor para CO<sub>2</sub> (8), válvula de três vias (9), condensador tipo casco e tubo do TP (16) e TP (17). Manter fechada somente a válvula de saída do TP.

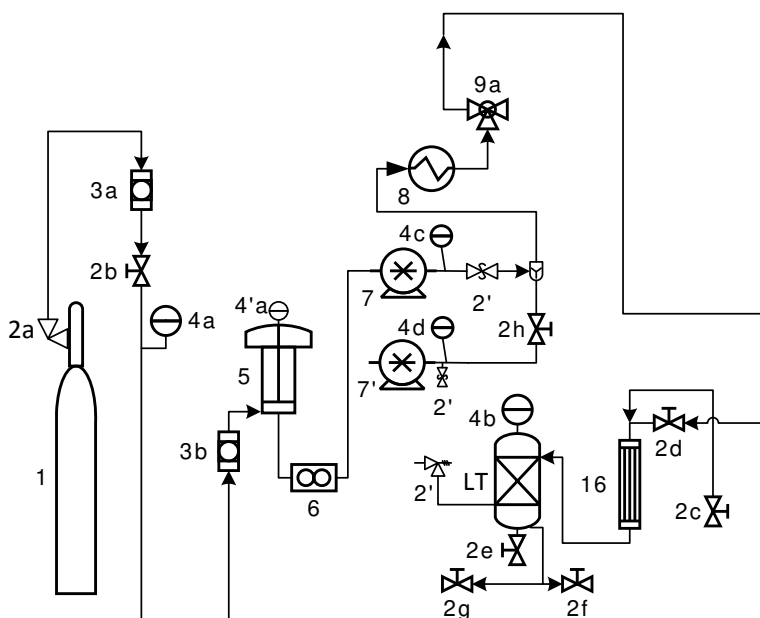


Figura D. 1. Pressurização do tanque pulmão (Storage Tank - LT).

- 2 Verificar nos componentes que constituem a UP a informação de tensão elétrica à qual devem ser ligados<sup>2</sup>.
- 3 Ligar o banho de resfriamento<sup>3</sup> (letra f da Figura D.2.), primeiro ative o passe de energia apertando o botão da parte posterior do banho e após ver a luz acesa na parte dianteira aperte o

<sup>2</sup> Observar que plugues com pinos de diâmetro maior se correspondem também a tomadas com diâmetro maior e de maior corrente elétrica. Plugues com pinos de menor diâmetro não necessariamente se correspondem a tomadas com menor corrente elétrica. Qualquer que for o caso, verifique sempre no equipamento a informação de tensão elétrica recomendada antes de conectar o plugue na tomada.

<sup>3</sup> Recomendações do fabricante: Não restrinja o fluxo de ar na parte dianteira, traseira ou lateral do banho. Quando operado a temperaturas menores a 15 °C, o líquido refrigerante deve ser uma mistura de água (50%) e etileno glicol (50%). Não utilize cloro. Não utilize água deionizada pura, ao menos que o banho esteja equipada com a opção especial. Não utilize líquido inflamável.

botão POWER (após 30 segundos a bomba irá recircular o líquido refrigerante caracterizado pelo incremento de som). O refrigerante do banho irá acondicionar a temperatura das partes internas do trocador de calor com tubo interno em espiral (5), do cabeçote da Bomba de CO<sub>2</sub> (7) e do condensador do TP (16). Verificar que a temperatura<sup>4</sup> programada seja -5 °C.

4 Ligar as tomadas da UP e do computador. Ativar o passe de energia na terminal (letra c, Figura D.2.) da Bomba de CO<sub>2</sub> apertando o botão localizado na parte posterior da Bomba.

5 Abrir o software de controle da UP, escrever nos espaços de Login e Senha a palavra Admin. Na aba “View” selecionar “CO<sub>2</sub> Pump”.

6 Assim que a temperatura do banho atinja a programada, inicie a alimentação de CO<sub>2</sub> abrindo a válvula do cilindro, o CO<sub>2</sub> irá passar pelos componentes indicados no passo 1 até chegar ao TP<sup>5</sup>.

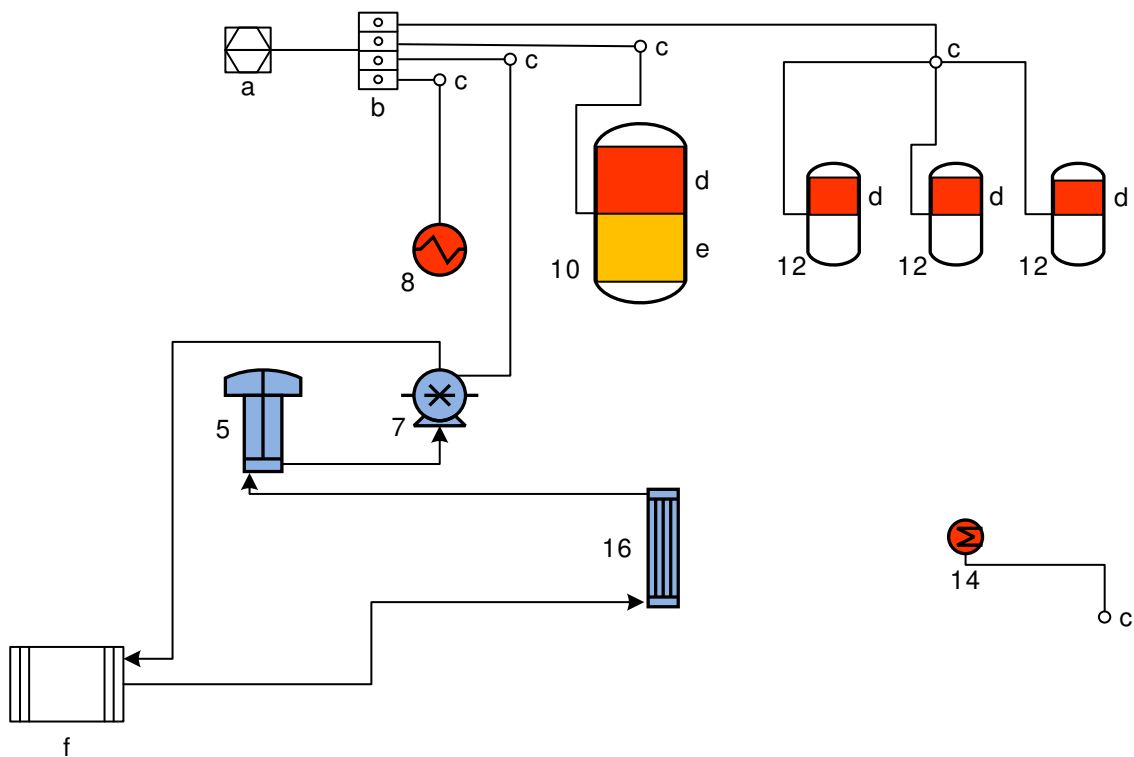


Figura D. 2. Sistema de aquecimento e resfriamento<sup>6</sup>.

<sup>4</sup> Aperte o botão giratório até conseguir intermitênciam no ponto decimal aceso e gire-o para programar temperaturas de -5 até -10 °C, normalmente, tempos entre 10 a 13 min são necessários.

<sup>5</sup> Pode ser que não se observe mudança na tela do TVM, no manômetro da Bomba de CO<sub>2</sub> e do TP por obstrução em alguma parte da tubulação, devido ao congelamento da água arrastrada desde o cilindro de CO<sub>2</sub> (1), pela falta de purga na lavagem do TP (17) ou das tubulações de entrada e saída dele. Qualquer que for o caso, desligue o banho. Elimine as obstruções por ação da despressurização, desapertando as conexões por setores. Posteriormente, ligue o banho e espere que atinja a temperatura programada para dar continuidade com a alimentação de CO<sub>2</sub>.

<sup>6</sup> A Figura D.2., está constituída pelos seguintes componentes: a Computador, b Quadro de terminais, c Terminal de circuito, d Resistência elétrica com cerâmica refratada, e Isolante de lã de vidro, f Banho de refrigeração (temperatura programada -5°C). 5 Trocador de calor com tubo em espiral para resfriamento de CO<sub>2</sub>, 7 Bomba, 8 Trocador de calor para aquecimento de CO<sub>2</sub>, 10 Coluna de extração, 12 Coluna de separação, 14 Trocador de calor com resistência elétrica para aquecer a válvula micrométrica, 16 Condensador tubular com passagens múltiplas.

7 Fique atento aos valores da pressão e da vazão mássica vistas na janela “CO<sub>2</sub> Pump” do computador (Figura D.3.) e no TVM (6 da Figura D.1.), assim como nos manômetros da Bomba de CO<sub>2</sub> e do TP (letras a e b, respectivamente da Figura D.4.), todas elas têm que mostrar um valor superior do que zero. Neste passo, pelo menos os valores da vazão mássica visto na janela “CO<sub>2</sub> Pump” e no TVM têm que ser iguais ou próximas entre elas<sup>7</sup>. Se após realizar o passo 5 não se visualiza mudança nos valores da janela “CO<sub>2</sub> Pump”, feche e abra novamente esta janela, se isso não for suficiente, reinicie o software fechando-o e abrindo-o novamente tendo em consideração as indicações dos passos 4 e 5.

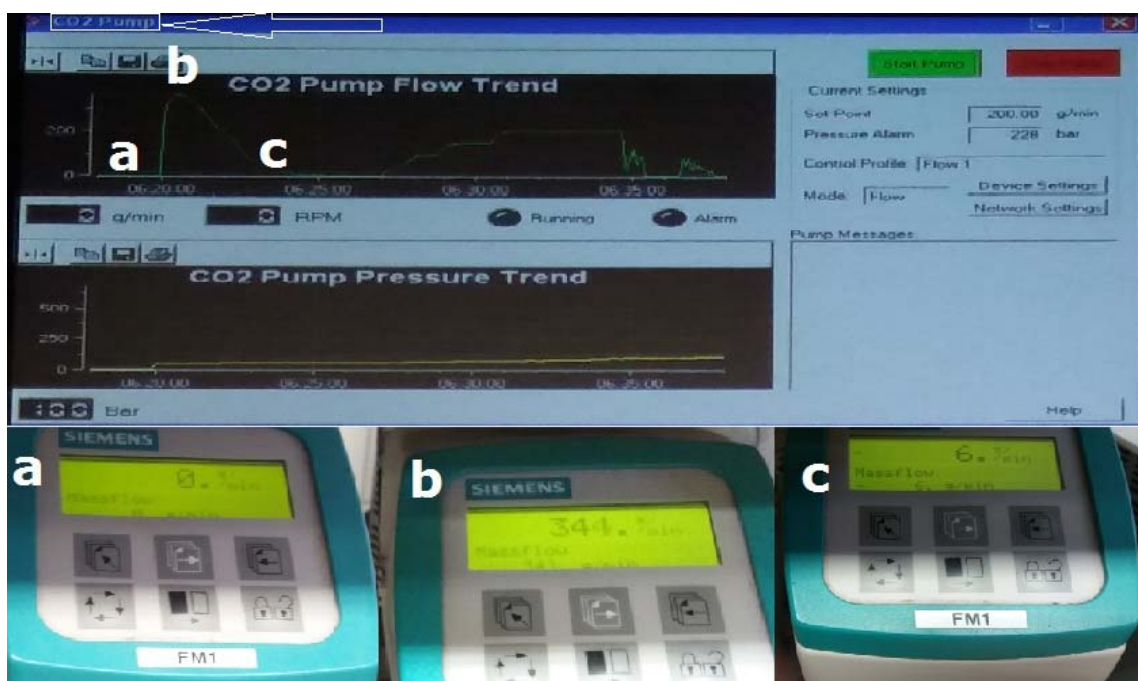


Figura D. 3. "CO<sub>2</sub> Pump" da tela do computador junto à mudança nos valores do Totalizador de vazão<sup>8</sup>.

8 Esperar o equilíbrio da pressão. Para isso observe o TVM, quando o valor da vazão zerar significa que as pressões entre o cilindro de CO<sub>2</sub> e o TP estão equilibradas (Figura D.3.).

9 Pelo software conduzir a pressurização de alimentação dentro do TP com aumentos gradativos da vazão. Para isso, na aba “View” selecionar “CO<sub>2</sub> Pump”, pelo menu “Device

<sup>7</sup> Vazões mássicas superiores do que 250 g/min visto no TVM durante o primeiro minuto é um indicativo que todas as válvulas o CO<sub>2</sub> estão abertas e que a alimentação está chegando até o TP. Verificar que não exista vazamento nas conexões.

<sup>8</sup> A Figura D.3., mostra na parte superior a janela ‘CO<sub>2</sub> Pump’ do computador e na parte inferior mostra a mudança na tela do “Totalizador de vazão mássica (TVM)”. As letras a, b e c se corresponde tanto com á informação observada na parte superior e inferior da Figura. Assim por exemplo, quando a alimentação de CO<sub>2</sub> ao Tanque Pulmão e iniciada pelo passo 6, a vazão de CO<sub>2</sub> vai desde 0 g/min (letra a) até 344 g/min (letra b), e a vazão vai descendo (letra c) até atingir o equilíbrio indicado no passo 8. A janela “CO<sub>2</sub> Pump” também mostra a evolução no tempo da vazão de CO<sub>2</sub> descrita pela linha contínua.

“Settings” no parâmetro “Pressure Alarm” colocar o valor da pressão superior<sup>9</sup> a 60 bar e através do parâmetro “Set Point” conduzir a pressurização com aumentos gradativos da vazão até atingir uma pressão entre 55 e 60 bar visto no manômetro do TP<sup>10</sup>. Os valores acima de 110 RPM visto na janela “CO<sub>2</sub> Pump” é um indicativo de que é necessário trocar o cilindro de CO<sub>2</sub> por outro com maior massa do que o anterior<sup>11</sup>. Feito isso pode dar continuidade com a alimentação de CO<sub>2</sub> até o TP atingir a pressão já indicada.

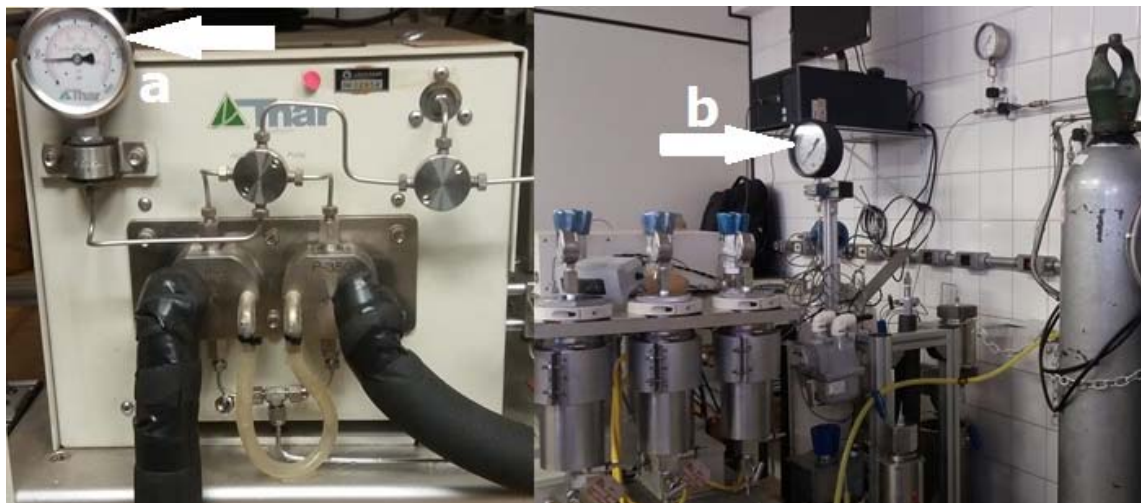


*Figura D. 4. Manômetros da Bomba de CO<sub>2</sub> (a) e do Tanque Pulmão (b).*

10 Assim atingido a pressão desejada (menor que 70 bar<sup>12</sup>) pare o bombeamento de CO<sub>2</sub> clicando na opção “Stop pump” da janela “CO<sub>2</sub> Pump” e feche a válvula de entrada de CO<sub>2</sub> do TP (ela está instalada na parte superior do condensador, letra a da Figura D.5.). Feito isso pode voltar as conexões no modo de Extração conforme encontrados antes de realizar o passo 1 (para isso pode voltar na Figura 2 do Capítulo 4).

<sup>9</sup> A bomba de CO<sub>2</sub> atinge um pressão máxima de 370 bar que é possível programar no “CO<sub>2</sub> Pump”, é recomendável que a máxima condição de pressão considerada como variável de processo (pressão de extração) seja 340 bar.

<sup>10</sup> Este é um indicativo que aproximadamente 12.5 Kg de CO<sub>2</sub> já foi alimentado dentro do TP.

<sup>11</sup> Para um maior aproveitamento do consumo de CO<sub>2</sub>, quando o TP estiver vazio inicie a alimentação dentro dele utilizando cilindros de CO<sub>2</sub> que apresentem baixa pressão. Lembre-se de dar uma olhada no laudo da compra dos cilindros de CO<sub>2</sub>, se o laudo mostrar presença de água no cilindro de CO<sub>2</sub> igual o acima de 0.15% descarte o cilindro de CO<sub>2</sub> quando ele atingir uma pressão igual o menor que 30 bar.

<sup>12</sup> Se a programação do processo de extração dinâmica não for acontecer após o acondicionamento do TP e das colunas de adsorção, é preferível pressurizar o TP até 60 bar. Pois a expansão do CO<sub>2</sub> pode acontecer durante o intervalo de tempo fruto do equilíbrio térmico entre o TP e o ambiente circundante. Acima de 80 bar a válvula de segurança irá liberar CO<sub>2</sub> para fora do TP.



*Figura D. 5. Válvula de entrada de CO<sub>2</sub> do TP e conexões superior e inferior da AdC1.*

11 É provável que neste ponto você deseje finalizar a sua jornada de trabalho, caso contrário, continue com o passo 1 da seguinte etapa.

12 Desligue o banho de resfriamento, aperte o botão POWER e após 30 segundos desative a energia apertando o botão da parte posterior, feche a janela “CO<sub>2</sub> Pump” e desative a energia na terminal da Bomba de CO<sub>2</sub> apertando o botão localizado na parte posterior. Feche o software de controle da UP e após desligar o computador desligue todos os plugues das tomadas de energia elétrica.

### D3. Etapa 3: Condicionamento das colunas AdC1 e AdC2

1 A AdC1 de 0.65 L (letra a da Figura D.6.) é o ponto de início do Sistema de Purificação e Reciclo de CO<sub>2</sub> (PRSCO<sub>2</sub>) e permite a sua purificação<sup>13</sup> durante o Período Dinâmico de Extração (PDE). Com a tampa inferior fechada, o material adsorvente<sup>14</sup> (de massa, diâmetro médio, umidade e densidade aparente conhecida, etc.) é colocado dentro da AdC1, coloque e feche a tampa superior e faça os ajustes nas conexões (letras b e c da Figura D.5.) com as tubulações de saída (parte superior) e de entrada (parte inferior).

2 A AdC2 de 0.40 L (letra b da Figura D.6.) é utilizado para despressurizar as colunas de extração (C1 e C2) e aproveitar o extrato ainda solubilizado no CO<sub>2</sub> após o tempo dinâmico de extração. Com a tampa inferior fechada, 250 g de material adsorvente é introduzido no interior da AdC2, coloque e feche a tampa superior e faça os ajustes nas conexões.

---

<sup>13</sup> Coletas de CO<sub>2</sub> tomadas a partir da válvula de purga localizada na base do TP, permitiram observar a ausência de extrato durante o reciclo e na finalização do processo como todo.

<sup>14</sup> Aproximadamente 25% de 300 g de farelo de aveia foram necessários para purificar o CO<sub>2</sub> durante o processo pseudocontínuo na AdC1.



*Figura D. 6. Colunas de adsorção utilizadas no processamento pseudocontínuo, AdC1 (a) e AdC2 (b).*

3        Dois subprodutos que adsorveram diferentes concentrações de extrato são gerados na AdC1 e na AdC2.

4        Se desejar calcular a massa de CO<sub>2</sub> despressurizado a partir da C1 (10 da Figura D.7.) que será liberado no ambiente, conecte a parte da mangueira unindo a tubulação de saída da válvula micrométrica (15) (ou de expansão) com o conector de entrada do Totalizador de Vazão Volumétrico (TVV) (6'), depois conecte a parte maior da mangueira com o conector de saída do TVV que leva o fluido expandido até o exterior do laboratório.

5        Verifique que o volume de água no interior do trocador de calor da válvula micrométrica (14) atinja no máximo 1 cm antes de chegar ao topo da tampa do trocador.

#### D.4 Etapa 4: Extração SFE

1        Ligar o banho de resfriamento (letra f da Figura D.2.), primeiro ative o passe de energia apertando o botão da parte posterior do banho e após ver a luz acesa na parte dianteira aperte o botão POWER (após 30 segundos a bomba irá recircular o líquido refrigerante caracterizado pelo incremento de som). O refrigerante do banho irá acondicionar a temperatura do CO<sub>2</sub> no seu passo pelo trocador de calor com tubo interno em espiral, pelo cabeçote da Bomba de CO<sub>2</sub> e pelo condensador do TP. Programe<sup>15</sup> a temperatura de resfriamento.

2        Empacotar a matéria-prima na C1 ou C2 ou em ambos ("a" e "b" da Figura D.7.) segundo a necessidade de matéria-prima a processar.

3        Conferir se todas as tubulações estão devidamente conectadas.

---

<sup>15</sup> Aperte o botão giratório até conseguir intermitência no ponto decimal acesso e gire-o para programar temperaturas negativas de 5 até 10 °C. Pode ser que a Bomba de CO<sub>2</sub> mostre cavitação durante o processamento por obstrução da tubulação que se encontra dentro do trocador de calor com tubo interno em espiral devido ao congelamento da água presente no cilindro de CO<sub>2</sub>, água presente na matéria-prima, pela falta de purga na lavagem do TP ou pelo arrastre de extrato. Qualquer que for o caso, desligue o banho na hora de fazer as purgas e posteriormente intente manter a temperatura programada em 5 °C negativos.

4 Ligar as tomadas da UP e do computador. Aperte o botão localizado na parte posterior de cada uma das terminais (letras a, b e c da Figura D.2.) para permitir o passe de energia nas respectivas terminais da “CO<sub>2</sub> Pump”, de temperatura para “Heater Controller 1” e “Heater Controller 2” e do “Pressure Regulator”.

5 Abrir o software de controle da UP, escrever nos espaços de Login e Senha a palavra Admin.

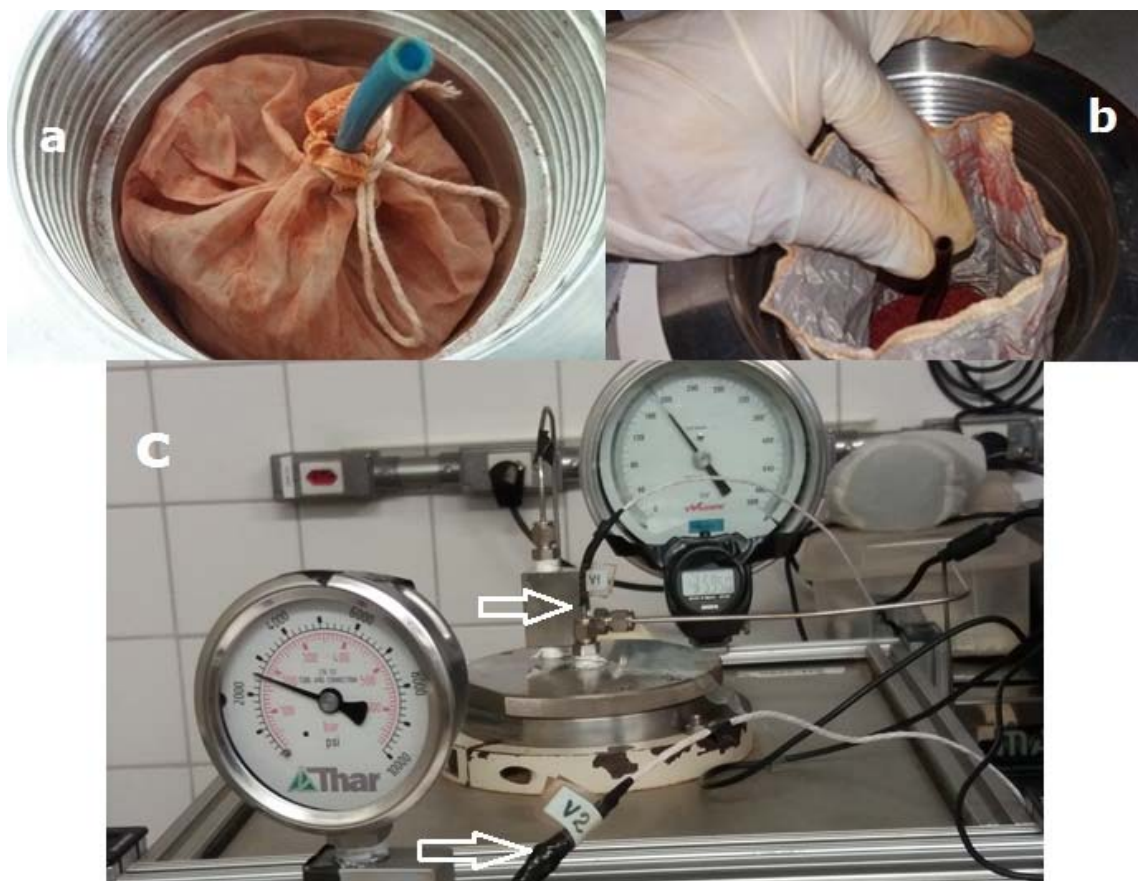


*Figura D. 7. Empacotamento das C1 e C2 e indicação dos sensores de temperatura<sup>16</sup>.*

6 Na aba “View” selecionar “Heater Controller 1” (janela “c” da Figura D.8) e ajustar as temperaturas pelo menu “Device Settings” no parâmetro “Temp. Set Point”. Aqui são ajustadas as temperaturas das mantas de aquecimento<sup>17</sup> (letra d Figura D.2.) da C1 (Zone 1 e Zone 2), da C2 (Zone 3 e Zone 4) e do trocador de calor (Zone 5) para pré-aquecimento do CO<sub>2</sub> à

<sup>16</sup> Na Figura D.7., as letras (a) e (b) mostram as mangueiras (pneumática reta de TPU-poliuretano termoplástico-elastomérico) onde foram colocados os termopares (c). Cada mangueira foi posicionada no eixo da coluna de extração (o extremo inferior da mangueira se situa no centro da coluna). Para manter retas as mangueiras, os termopares foram colocadas inicialmente durante a carga com a matéria-prima.

<sup>17</sup> O aquecimento da manta de cada coluna de extração é controlada pelas respostas dos termopares V1-TS1, V1-TS2 e V2-TS1, V2-TS2 para a C1 e C2, respectivamente.

temperatura de extração. Para aplicar as mudanças, aperte os botões na seguinte sequência: “Apply”, “Ok” e “On”.

7 Na aba “View” selecionar “Heater Controller 2” (janela “d” da Figura D.8) e ajustar as temperaturas pelo menu “Device Settings” no parâmetro “Temp. Set Point” dos vasos de separação 1, 2 e 3, para a Zone 1, 2 e 3, respectivamente. Aplique as mudanças apertando os botões “Apply”, “Ok” e “On”.

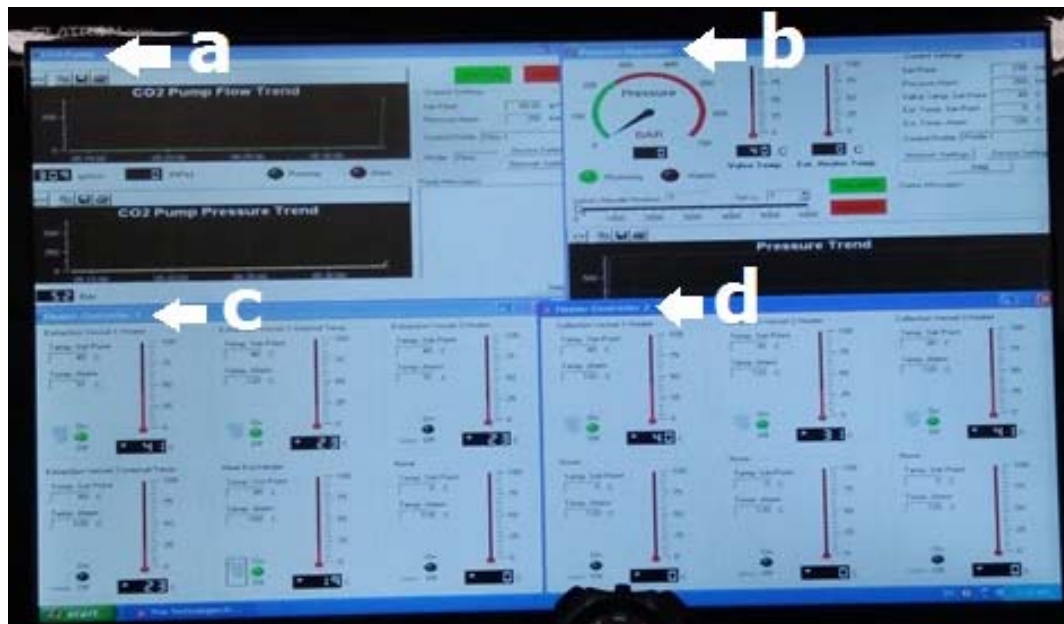


Figura D. 8. Tela do computador mostrando as 04 janelas operando durante SFE.

8 Fechar as três válvulas manuais backpressure que controlam a pressão nos vasos de separação e verificar que a válvula de bloqueio de entrada do reciclo do TP também este fechada.

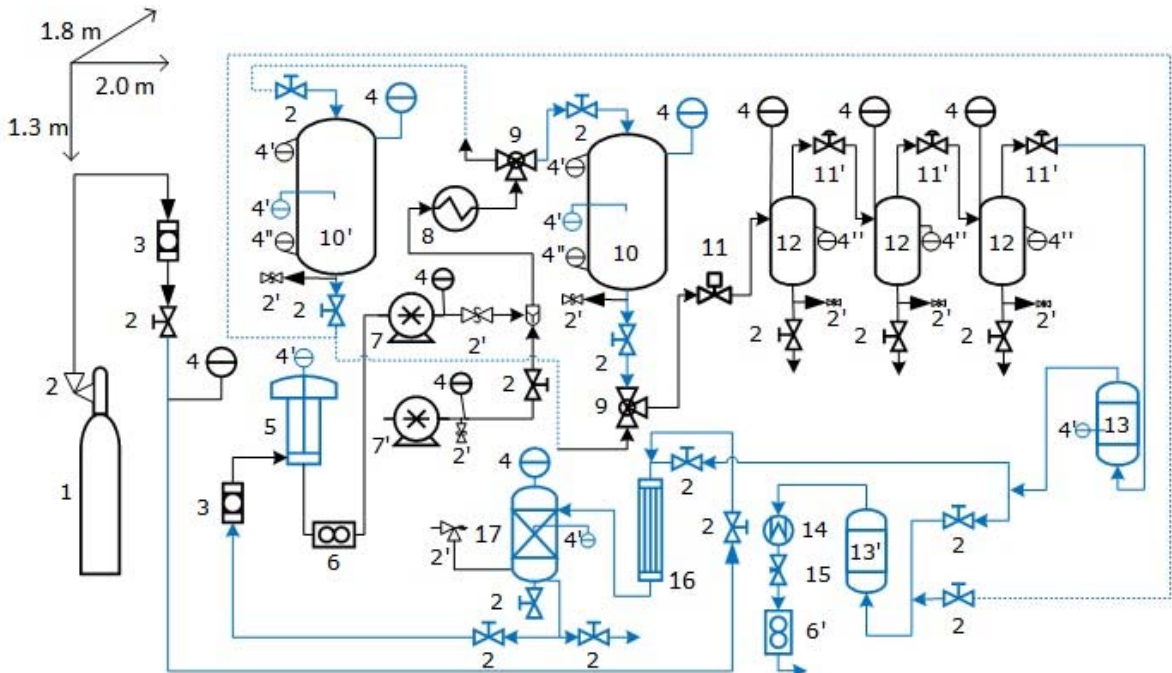


Figura D. 9. Unidade de processamento em escala piloto.

A Figura D.9., está constituído pelos seguintes componentes: (1) cilindro de CO<sub>2</sub>, (2) válvula de bloqueio e (2') válvula de segurança, (3) filtro de linha, (4) manômetro. Indicador de temperatura: (4') interna e (4'') externa, (5) trocador de calor com tubo em espiral para resfriar CO<sub>2</sub>, (6) medidor de vazão mássica, (7) bomba de CO<sub>2</sub>, (7') bomba de co-solvente, (8) trocador de calor para aquecimento de CO<sub>2</sub>, (9) válvula triplo via, (10) coluna de extração. Válvula backpressure: (11) automatizada e (11') manual, (12) vaso de separação, (13) coluna de adsorção 1 (AdC1 = 0.65 L), (13') coluna de adsorção 2 (AdC2 = 0.4 L), (14) traçador de calor com resistência elétrica, (15) válvula micrométrica, (16) condensador de casco e tubo, (17) tanque pulmão.

9 Na aba “View” selecionar “Pressure Regulator” (janela “b” da Figura D.8) e feche “Backpressure valve” que controla a pressão na C1. Para isso, pelo menu “Device Settings” colocar 50 bar acima da pressão de extração no parâmetro “Pressure Alarm” e no parâmetro “Set Point” colocar uma pressão 20 bar acima da pressão de extração. No parâmetro “Valve Heater Set Point” colocar o valor da temperatura de extração. Aplique as mudanças apertando os botões “Apply”, “Ok” e “Start ABPR”.

10 Verificar que todas as válvulas de conduzem o CO<sub>2</sub> desde o TP até a “Backpressure valve” estejam abertas, com exceção da válvula da Bomba de Co-Solvente (7'). Abrir a alimentação de CO<sub>2</sub> proveniente do TP. Esperar o equilíbrio da pressão entre os valores vistos nos manômetros do TP e da C1. Para isso, também pode acompanhar observando a mudança do valor da vazão no TVM, quando a vazão zerar as pressões no interior da C1 e do TP atingiram o equilíbrio.

11 Pressurizar até a pressão do processo<sup>18</sup>. Para isso, na aba “View” selecionar “CO<sub>2</sub> Pump” (janela “a” da Figura D.8), pelo menu “Device Settings” no parâmetro “Pressure Alarm” colocar o valor da pressão de extração<sup>19</sup> (pressão do processo) e através do parâmetro “Set Point” conduzir a pressurização com aumentos gradativos da vazão<sup>20</sup>. Aplique as mudanças apertando os botões “Apply”, “Ok” e “Start Pump”<sup>21</sup>. A bomba irá automaticamente parar após atingir o valor programado na “Pressure Alarm”<sup>22</sup>.

12 Iniciar o controle do Tempo Estático (TE). Durante o TE a pressão na C pode cair. Nesse caso, reiniciar a bomba selecionando “CO<sub>2</sub> Pump” e dando um clic no “Start Pump”<sup>23</sup>.

13 Para iniciar o Período Dinâmico de Extração (PDE), também chamado de tempo dinâmico de extração, no “Pressure Regulator” ajustar o parâmetro “Set Point” para a pressão de extração e no parâmetro “Pressure Alarm” para 10 bar acima da pressão de extração. E no “CO<sub>2</sub> Pump” ajustar o parâmetro “Pressure Alarm” para 30 bar acima da pressão de extração<sup>24</sup> e no parâmetro “Set Point” colocar a vazão (gCO<sub>2</sub>/min) de processamento.

14 Se necessário, CO<sub>2</sub> puro deve ser alimentado durante o processo para manter a pressão na C<sup>25</sup>.

15 Conduza o fracionamento do extrato com valores de pressão em cascada dentro dos vasos de separação 1, 2 e 3, identificadas como VS1, VS2 e VS3, respectivamente. Para isso, assim que atingido a pressão desejada dentro do VS1 inicie a abertura da backpressure manual. Da mesma forma, atingido o valor da pressão desejada no VS2 abra a respectiva backpressure

<sup>18</sup> Pode ser que a Bomba de CO<sub>2</sub> (7) mostre cavitação durante o processamento por obstrução de alguma parte da tubulação que se encontra antes dela, por congelamento da água presente na matéria-prima ou pelo arrastre de extrato. Qualquer que for o caso, desligue a bomba e o banho e feche as duas válvulas de três vias (9). Elimine a obstrução, para isso, por cada seção de tubulação, desaperte as conexões para liberar o CO<sub>2</sub> pressurizado. Passe mais CO<sub>2</sub> por aquela parte ou seção para purgar e eliminar por completo a obstrução. Faça o mesmo por cada setor até ter a certeza que não exista mais obstruções. Posteriormente, ligue o banho (espere até atingir a temperatura programada), volte às válvulas na posição antes do incidente e ligue a bomba.

<sup>19</sup> A bomba de CO<sub>2</sub> atinge um pressão máxima de 370 bar que é possível programar no “CO<sub>2</sub> Pump”, é recomendável que a máxima condição de pressão considerada como variável de processo (pressão de extração) seja 340 bar.

<sup>20</sup> Ex. Pode iniciar programando 20 gCO<sub>2</sub>/min e assim que atingir esse valor pode passar para 40, depois para 60, e assim sucessivamente até atingir o máximo valor de 280 gCO<sub>2</sub>/min.

<sup>21</sup> Uma vez que a bomba estiver em funcionamento (quando apertar o botão “Start Pump”) o aumento gradativo pode ser conduzido apertando unicamente o botão “Apply”.

<sup>22</sup> Caso seja necessário, pode-se programar desde 4 até 6 bar a mais no “Pressure Alarm” para atingir o valor da pressão de extração dentro da C durante o tempo estático.

<sup>23</sup> Se por ventura a Bomba de CO<sub>2</sub> não desligar automaticamente quando atingir 10 bar acima da pressão programada, dê um clic no “Stop Pump” e volte a dar um clic no “Star Pump” quando a pressão cair para pressurizar novamente a C. Lembre-se sempre de ficar atento nas suas condições de processamento.

<sup>24</sup> **IMPORTANTE**, se por acaso acontecer vazamento ou algum outro tipo de anomalia observada no equipamento, **PRIMEIRO** aperte o botão “Stop Pump”, depois feche ou abra as válvulas segundo seja o casso e proceda a fazer os ajustes necessárias até resolver a anomalia. Feito as correções, volte as válvulas à posição antes do imprevisto e continue o processo apertando o botão “Start Pump”.

<sup>25</sup> Importante manter o valor da pressão dentro do TP abaixo do valor da pressão do VS3 (terceiro separador), preferentemente, mantenha entre eles uma diferença no mínimo de 5 bar.

manual, assim que atingir a pressão desejada dentro do VS3 abra a respectiva válvula manual backpressure junto com a válvula de bloqueio de entrada do reciclo do TP<sup>26</sup>. Se necessário, repita o passo 14.

16 Se necessário, coletas periódicas de extrato por cada separador podem ser realizadas durante o PDE<sup>27</sup>. Para isso, a válvula localizado na base de cada separador tem que se abrir lentamente a os poucos para evitar espichar o extrato fora do frasco coletor.

17 Para finalizar o PDE<sup>28</sup>, no “CO<sub>2</sub> Pump” aperte o botão “Stop Pump” e feche a válvula de bloqueio do TP que é utilizada para alimentar o CO<sub>2</sub> à UP (também chamada de “válvula de saída do TP”).

18 Proceda a despressurizar parcialmente a C através do “Pressure Regulator”, pelo menu “Device Settings” colocar no parâmetro “Set Point” valores desde 3 até 5 bar menores que o valor observado no manômetro da C e até que a pressão no manômetro do TP atinja um valor de pressão entre 70 e 80 bar.

19 Feche as válvulas de entrada e saída da C, a válvula triplo via que alimenta a “Backpressure valve”, as backpressure manuais dos vasos de separação VS1, VS2 e VS3 e também a válvula de bloqueio do TP que permite o ingresso ou de entrada de CO<sub>2</sub> durante o reciclo (durante o Período Dinâmico de Extração (PDE), esta válvula pode ser chamada também como “válvula de entra do TP”).

20 Desligue o banho de resfriamento, aperte o botão POWER e após 30 segundos desative o passe de energia apertando o botão da parte posterior.

21 Despressurize a Bomba de CO<sub>2</sub> e a parte da tubulação que chega até a válvula de bloqueio de alimentação (válvula de saída) de CO<sub>2</sub> do TP, para isso, solte o conector que une a válvula triplo via com a tubulação de entrada de CO<sub>2</sub> da C. Abra a válvula triplo via pelo lado que acabou de soltar.

<sup>26</sup> Neste preciso instante uma fração dos compostos do extrato que são solúveis no CO<sub>2</sub> nas condições de P e T do VS3 são carregados até a AdC1, onde se espera aconteça a purificação do CO<sub>2</sub> (já foi testado Salvado de Aveia com ótimos resultados). Se for necessário e se dispor do material suficiente, é possível rearranjar esta parte do reciclo para instalar uma bateria de AdC (Colunas de Adsorção) para testar diferentes matérias adsorventes antes de pressurizar o sistema.

<sup>27</sup> Após iniciado o PDE, para matérias-primas com rendimento global de extrato acima de 8% e com curtos períodos de Taxa de Extração Constante (CER), pode realizar a primeira coleta em no máximo dentro de 15 min. Para tal, já foram utilizados com sucesso frascos coletores de 100 mL de capacidade, tipo “frasco reagente graduado com tampa azul e dispositivo anti gotas”.

<sup>28</sup> Dependendo do critério utilizado para a finalização, como por exemplo: quando atingido o valor de S/F (S representa a massa de CO<sub>2</sub> utilizada no PDE, ou seja a “vazão mássica (gCO<sub>2</sub>/min) que passou pelo leito empacotado (C) durante um certo tempo (“x”min) de processamento e F representa massa de matéria-prima (g M-P) carregada na C), quando atingido ou superada a interface entre o t<sub>CER</sub> (duração do período da taxa de extração constante) e o t<sub>FER</sub> (duração do período da taxa de extração decrescente) ou quando atingido o esgotamento do leito (observado através do acompanhamento das coletas periódicas)

22 Desligue o trocador de calor (Zone 5), para isso, no “Heater Controller 1” na seção do “Heat Exchanger” aperte o botão na opção “Off”.

23 Pode realizar a coleta de extrato dos vasos de separação<sup>29</sup>, lembre-se que a válvula localizado na base de cada vaso de separação tem que ser aberta lentamente a os poucos. Assim que perceber que a coleta foi concluída<sup>30</sup> feche estas três válvulas e no “Heater Controller 2” aperte o botão na opção “Off” para desligar as mantas de aquecimento dos vasos de separação 1, 2 e 3. Depois, conecte uma mangueira no bico de saída de cada separador e estenda-o até fora do laboratório para realizar a completa despressurização.

24 Despressurize a parte da tubulação existente entre a válvula triplo via e a “Backpressure valve”. Para isso, no “Pressure Regulator”, pelo menu “Device Settings” colocar no parâmetro “Set Point” um valor de pressão até 5 bar menor que aquele registrado no “Set Point”, dê um clic no botão “Apply” toda vez que deseje aplicar a mudança. Aperte o botão “Stop ABPR” após aplicar o valor de 0 (zero) e este esteja registrado na mudança.

25 Complete a despressurização da C<sup>31</sup> até o valor da pressão atingir 0 (zero) bar, para isso, ligue o trocador de calor da válvula de expansão de CO<sub>2</sub>, depois solte o conector que une a tubulação de saída da C com a válvula triplo via. Utilize este mesmo conector para unir a tubulação de saída da C com a parte da tubulação que chega até a válvula de bloqueio da AdC2. Feito a conexão, abra as válvulas de saída da C e a válvula de bloqueio da AdC2.

26 Despressurize a AdC1, para isso, feche a válvula de bloqueio da AdC2 e abra a válvula de bloqueio que conecta a AdC1 com a AdC2.

27 Desligue a manta de aquecimento da C, para isso, no “Heater Controller 1” nas seções “Extraction Vessel 1 (ou 2) Heater” e “Extraction Vessel 1 (ou 2) Internal Temp.” aperte o botão na opção “Off”.

28 Abra as tampas dos separadores e observe o estado do interior delas, se for necessário faça a coleta do extrato que ficou nas paredes.

29 Retire a tampa superior da C, a seguir retire a lâmina circular sinterizada localizado na tampa<sup>32</sup>. Realize o desempacotamento da matéria-prima processada na C1 ou C2, e registre a massa assim que atinja o equilíbrio térmico com o ambiente.

<sup>29</sup> Utilize frascos coletores de massa conhecida. Papel-alumínio pode ser utilizado para proteger o extrato da ação da luz. Pesagens periódicas da massa dos extratos coletados podem ser realizadas até atingir massas constantes.

<sup>30</sup> Caracterizado pela saída unicamente de CO<sub>2</sub> congelado ou pela ausência de extrato.

<sup>31</sup> Dependendo do material utilizado para a adsorção do extrato ainda solubilizado no interior das colunas de extração (C1 ou C2), para o aproveitamento dele durante a despressurização da C, um subproduto enriquecido com esse extrato pode ser obtido neste passo. Pressões entre 80 e 100 bar dentro da C, podem levar tempos de despressurização entre 15 e 25 min onde que a vazão mássica aproximada é 84 gCO<sub>2</sub>/min.

<sup>32</sup> Se for necessário limpar, coloque as peças à espera do passo 9 na etapa “limpeza das partes da UP”.

30 É muito provável que neste ponto você deseje finalizar a sua jornada de trabalho, caso contrário, passe ao ponto 1 da etapa “Limpeza das partes da UP”.

31 Para finalizar esta Etapa, feche a janelas de “CO<sub>2</sub> Pump”, “Pressure Regulator” “Heater Controller 1” e “Heater Controller 2”. Aperte o botão localizado na parte posterior de cada uma das terminais para cortar o passe de energia e feche o software de controle da UP. Após desligar o computador desligue todas as tomadas de energia elétrica.

#### **D.5 Etapa 5: Procedimento alternativo a partir do passo 19 da D.4 Etapa 4**

19 Feche as válvulas triplo via que alimenta à “Backpressure valve” e à válvula de bloqueio de entrada de CO<sub>2</sub> no reciclo do TP.

20 Desligue o banho de resfriamento, aperte o botão POWER e após 30 segundos desative o passe de energia apertando o botão da parte posterior.

21 Ligue o trocador de calor da válvula de expansão<sup>33</sup> de CO<sub>2</sub>.

22 Se desejar, pode realizar o cálculo da quantidade de massa<sup>34</sup> de CO<sub>2</sub> que será liberado no ambiente, para isso, conecte a parte da mangueira unindo a tubulação de saída da válvula de expansão com o conector de entrada do Totalizador de Vazão Volumétrico (TVV), depois conecte a parte maior da mangueira com o conector de saída do TVV que leva o fluido expandido até o exterior do laboratório.

23 Abra a válvula triplo via que alimenta à “Backpressure valve”, a continuação abra a válvula de bloqueio que conecta a AdC1 com a AdC2<sup>35</sup> e seguindo o procedimento de despressurização do passo 18 (D.4 Etapa 4) acompanhe também a despressurização do VS1, VS2 e VS3 manipulando as suas respectivas válvulas “backpressure”, mantendo no possível as pressões às quais foram processadas.

24 Inicie a coleta de extrato por cada separador assim que atingir 14 bar (200 psi) nos manômetros de cada um deles, abrindo lentamente as válvulas localizadas na base do VS1, VS2 e VS3.

25 No “Pressure Regulator”, quando já tiver colocado o valor de 0 (zero), pelo menu “Device Settings” no parâmetro “Set Point” e após concluída a coleta aperte o botão “Stop ABPR”. No “Heater Controller 2” aperte o botão na opção “Off” para desligar as mantas de aquecimento do VS1, VS2 e VS3. Desligue o trocador de calor da válvula de expansão de CO<sub>2</sub>.

<sup>33</sup> Verifique que o nível do volume de água no interior atinja no máximo 1 cm antes de chegar ao topo da tampa.

<sup>34</sup> Utilizando os dados da densidade de CO<sub>2</sub> a partir de NIST, 2017. National Institute of Standards and Technology.

<sup>35</sup> Farelo de Aveia também foi utilizado dentro da AdC2.

26 No “Heater Controller 1” aperte o botão na opção “Off” para desligar a manta de aquecimento da C e do trocador de calor (Zone 5, segundo visto na tela do computador). A continuação, efetuar os passos 28, 29, 30 e 31 descrito em D.4 Etapa 4.

#### **D.6 Etapa 6: Limpeza da unidade piloto**

1 Ligar as tomadas da UP e do computador. Ativar o passe de energia nos terminais da “Bomba de Co-Solvente”, da “Backpressure valve” e do “Heater Controller 1” apertando o botão localizado na parte posterior de cada um deles.

2 Abrir o software de controle da UP, escrever nos espaços de Login e Senha a palavra Admin.

3 Conecte e abra as duas válvulas triplo via (aquela que alimenta à C e aquela que alimenta à “Backpressure valve”)<sup>36</sup>, com a parte da tubulação conectado à válvula de entrada da AdC2. Antes desconecte-o da AdC2.

4 Feche a válvula de segurança da Bomba de CO<sub>2</sub>.

5 Ajuste a temperatura do trocador de calor (Zone 5) para pré-aquecimento das soluções de limpeza (água, etanol, água:etanol ou outros recomendados na utilização da Bomba de Co-Solvente<sup>37</sup>) à temperatura maior ou igual do recinte processo de extração que foi realizado. Para isso, na sequência dê um clic na aba “View”, “Heater Controller 1”, “Device Settings” e no parâmetro “Temp. Set Point” faça as mudanças necessárias. Para aplicar as mudanças, aperte os botões na seguinte sequência: “Apply”, “Ok” e “On”.

6 Abra a válvula da Bomba de Co-Solvente e pressurize o conjunto das partes (neste caso a pressurização inicia desde a Bomba de Co-Solvente e finaliza na “Backpressure valve”). Para isso, na aba “View” selecionar “Pump Co Solvent”, pelo menu “Device Settings” colocar nos parâmetros “Set Point” e “Pressure Alarm” os valores da vazão mássica<sup>38</sup> e da pressão<sup>39</sup>, respectivamente. Com o “Pressure Regulator”, pelo menu “Device Settings” no parâmetro “Set Point” acompanhe a pressurização colocando valores gradativos de pressão menores que a programada na “Pump Co Solvent”. Em ambas as janelas, dê um clic no botão “Apply” toda vez que deseje aplicar a mudança nos parâmetros. A solução irá limpar as partes até chega ao

<sup>36</sup> Preferentemente realize a união dos conectores pelas quais o extrato passou através deles.

<sup>37</sup> Segundo as recomendações pelo fabricante da bomba, recomenda os seguintes solventes: acetonitrilo, etanol, metanol, dióxido de carbono, álcool isopropílico, clorofórmio e cloreto de metileno.

<sup>38</sup> O máximo valor que pode ser programado corresponde 50 gSolvente/min. Utilize um reservatório com solvente na quantidade maior à que será bombeada durante a limpeza, isso evitará a cavitação da bomba por falta solvente.

<sup>39</sup> A máxima pressão que já foi testada correspondeu a 370 bar.

VS1. Faça o mesmo procedimento para limpar as tubulações que conectam as C e outros setores de tubulação pelas quais o extrato tenha passado<sup>40</sup>.

7 Despressurizar através do “Pressure Regulator”, pelo menu “Device Settings” no parâmetro “Set Point” coloque valores gradativos menores que aquelas programadas na “Pump Co Solvent” até atingir 0 (zero) bar, dar um clic no botão “Apply” para aplicar as mudanças.

8 Na “Pump Co Solvent”, pelo menu “Device Settings” diminuir gradativamente até atingir o valor 0 (zero) nos parâmetros “Set Point” (g/min) e “Pressure Alarm” (bar). Finalmente, dê um clic nos botões “Stop ABPR” e “Stop Pump”.

9 Proceda a limpar as tampas e o interior do VS1, VS2 e VS3. Evite que a solução de limpeza atinja os dois orifícios localizada a 3.5 cm do topo de cada separador<sup>41</sup>. Proteja as mantas de aquecimento dos separadores de possíveis vazamentos, para isso, utilize uma fita ou película impermeabilizante com ação aderente na parte superior das mantas. Além das soluções de limpeza, pode utilizar panos de tecido branco ou guardanapo de papel, assim como de alguns litros de água até observar que a limpeza foi suficiente. No final, após o passo da água, faça fluir ar comprimido pelas partes por onde passou as soluções de limpeza.

10 Rearranje a posição das tubulações do setor entre as válvulas Backpressure dos separadores<sup>42</sup>, aqui a parte da tubulação do passo 3 será utilizado para unir a válvula da Bomba de Co-Solvente com o extremo da tubulação da válvula Backpressure do VS1. Aplique o procedimento de pressurização do passo 6, complemente a pressurização fechando manualmente e de forma gradual a válvula Backpressure do VS3. Acompanhe a pressurização observando o incremento da pressão no manômetro da Bomba de Co-Solvente e na janela da “Pump Co Solvent”.

11 Despressurize as tubulações e o setor das válvulas Backpressure dos vasos de separação abrindo a Backpressure do VS3 e finalize o processo seguindo o procedimento do passo 8.

<sup>40</sup> Proceda a pressurizar ou despressurizar sempre com aumento ou diminuição gradativa. Atingido o equilíbrio da pressão, aplique as mudanças para os próximos níveis de valores. Se pretende pausar o processo por longos períodos de tempo é melhor deixar as partes e os componentes despressurizados. No final, passe sempre água e por último ar comprimido.

<sup>41</sup> Cada vaso de separação (VS1, VS2 e VS3) tem volume de 1 L.

<sup>42</sup> Se o extrato obtido no VS1 e/ou no VS2 tiver uma textura viscosa tipo das ceras, pode trocar a colocação da válvula Backpressure do VS1 pelo VS3, com a finalidade de passar a solução limpadora primeiro pela Backpressure do VS3, VS2 e por último pela Backpressure do VS1.

12 Retire a tampa inferior da C, a seguir retire a lâmina circular sinterizada localizado na tampa inferior<sup>43</sup> para ser colocado dentro do banho de ultrassom<sup>44</sup>.

13 Limpar a parede interna da C, com guardanapo de papel e com jatos de solução de limpeza saídos da pisseta.

14 Retire a parte da tubulação que conecta o cabeçote da Bomba de CO<sub>2</sub> com o totalizador de massa tipo coriolis (Totalizador de Vazão Mássica (TVM)). Observe a cor das soluções de limpeza<sup>45</sup> após a passagem delas através da parte da tubulação, se a cor das soluções de limpeza na saída da parte que está sendo limpado for diferente com a cor das soluções alimentada; então, isso é um claro indicio que parte do extrato foi arrastrado pelo CO<sub>2</sub> pelo interior da bomba durante o processo de extração. Se for assim, procure assistência no manual de uso da bomba Thar para realizar a manutenção preventiva.

#### **D7. Etapa 7: Limpeza do tanque pulmão**

1 Com as válvulas de bloqueio fechadas de saída e de entrada do TP (manipuladas nos passos 17 e 19, na etapa de Extração com CO<sub>2</sub> supercrítico), desconecte o extremo da tubulação que está unida ao filtro de linha localizado antes do TVM.

2 Conectar o extremo da tubulação do passo anterior com a tubulação que conecta a válvula micrométrica<sup>46</sup> ou com a tubulação que conecta a válvula micrométrica (alternativamente pode utilizar uma válvula de abertura maior ou backpressure) para proceder com a despressurização do TP.

3 Tirar as duas conexões laterais e a porca localizada no centro do topo do TP assim que observar o valor 0 (zero) no manômetro do TP.

4 Cobrir com fita ou película impermeabilizante com ação aderente as duas partes que ficaram abertas na lateral do TP.

5 Cobrir com material impermeabilizante o isolante térmico do TP.

---

<sup>43</sup> A fixação da lâmina circular sinterizada na tampa é produzida pelo giro no sentido anti-horário. O contrário acontece girando no sentido horário.

<sup>44</sup> A lâmina circular sinterizada é colocado dentro de um recipiente que contem num primeiro momento água com sabão líquido (0.95:0.05, v/v), num segundo momento só água, depois só etanol e por fim novamente água. Os tempos e a troca das soluções vai depender da facilidade com a qual o resíduo está sendo eliminando.

<sup>45</sup> Segundo as especificações de fabricante da Bomba, NÃO pode ser utilizada as seguintes soluções: Aquo Regia, Bromo, Cloro Anidro, Cloreto de cobre, Cloreto férrico, Cloreto ferroso, Freon 12, Guanidina, Ácido hidrobromico, Ácido clorídrico, Ácido Hidrofluorico, Ácido Hydrofluorsilicic, Peróxido de hidrogênio, Iodo e Cloreto de mercúrio.

<sup>46</sup> Se quiser calcular a quantidade de CO<sub>2</sub> que se encontra dentro do TP, é preferível utilizar a válvula micrométrica para o melhor controle da vazão. Verifique as conexões das mangueiras de entrada e saída do TVV (consulte o passo 4 da etapa Acondicionamento das Colunas de Adsorção 1 e 2 (AdC1 e AdC2). Verifique também, o nível da água no trocador de calor para aquecimento da válvula.

6 Colocar aproximadamente 100 mL de sabão líquido neutro no interior do TP, colocar um funil no topo e encher com água. Agitar a solução no interior do TP com ar comprimido. Para isso, introduzir o extremo da mangueira que transporta o ar comprimido até o fundo do interior do TP.

7 Conectar no extremo da válvula da base uma peça de mangueira pela qual as soluções de limpeza irão passar desde o TP até o exterior do laboratório. Abra a válvula de ar comprimido e deixe sair pelo topo, pela válvula da base<sup>47</sup> (localizada no centro), pela válvula de saída e pela válvula de purga do TP as bolhas de sabão da lavagem.

8 Tirar o excedente de bolhas de sabão enchendo de água o TP a quantidade de vezes que precisar e purgar o TP como feito no passo anterior.

9 Utilizar jatos de etanol na parede interna do TP e no final encher novamente com água. Após isso, purgar o TP.

10 Secar as partes e o interior utilizando ar comprimido.

11 Desconectar as conexões inferior e superior da coluna de condensação, passar as soluções de limpeza através deles e no final repita o passo 9.

12 Unir todas as conexões da forma como as deixou após o passo 1 e mantenha fechada todas as válvulas com exceção da válvula de entrada do TP.

13 Pressurizar o TP até uma pressão entre 5 e 10 bar, para isso abrir a válvula do cilindro de CO<sub>2</sub> e a válvula anti-retorno localizado na lateral superior da coluna de condensação, acompanhe a pressurização no manômetro do TP.

14 Purgar o interior do TP, para isso, abrir todas as válvulas unidas a ele.

15 Repetir os passos 13 e 14 pelo menos duas vezes antes de pressurizar o TP para o desenvolvimento dos novos PDE.

#### **D8. Etapa 8: Limpeza de AdC1 e AdC2**

1 Desconectar (para ambas as AdC) a união que conectam as tubulações tanto de saída quanto de entrada, das tampas superior e inferior, respectivamente.

2 Tirar a tampa superior da AdC1. Num beker de massa conhecida e ajudado com uma espátula, colocar dentro do beker o material adsorvente que não sofreu alteração de cor. Levar à balança para determinar a massa e a continuação, retirar completamente a fração do material adsorvente que ficou na AdC1.

---

<sup>47</sup> Para agilizar a purga da lavagem e após ter passado parte das soluções de limpeza através da válvula localizada na base do TP é possível tirar esta válvula para colocar no seu lugar só a mangueira que levará até o esgoto (localizado no exterior do laboratório) as soluções da lavagem.

3 Tire a tampa inferior, mas antes colocar uma bandeja na parte inferior da AdC1 onde será colocado a tampa e recolher parte do material adsorvente que ficou retida entre as zonas de difícil acesso.

4 Novamente, levar até a balança e com os dados registrados do antes e do depois do processo, faça os cálculos do balaço de massa.

5 Utilizar as soluções de lavagem para colocar as tampas no banho de ultrassom e utilize a pisseta para aplicar jatos durante a limpeza da AdC1.

6 Passar as soluções de limpeza através das tubulações que foram desconectadas da coluna AdC1. No final faça fluir ar comprimido através das peças e partes que foram lavadas.

7 Remover a tampa da coluna AdC2. Em um bécker vazio de massa conhecida faça a coleta do material adsorvente. Para isso, colocar a bandeja e o bécker justo embaixo da AdC2, utilizar uma barra para fazer a pressão de encima para abaixo do material adsorvente para que este possa ser coletado. Com os dados obtidos, realizar o balaço de massa.

8 Aplicar os passos 5 e 6 para a AdC2.

9 Empacar o material adsorvente tirado das AdC para posterior extração e quantificação dos compostos adsorvidos. Com isso o balanço de massa fica melhor apresentado.

10 Realizar as conexões de tal forma que as AdC possam ser utilizadas nos novos processamentos.

## APÊNDICE E

### E.1 Tampa e interior da AdC1

No presente apêndice se mostra alguns detalhes que caracterizaram o processamento pseudocontínuo em escala piloto junto ao PRSCO<sub>2</sub>.

A Figura E.1., mostra a configuração e as partes da tampa superior da AdC1. Ela tem as seguintes partes: parte maior da tampa (a), filtro com poros de 0.5μm (b), anel (c) que prende a parte (a) com a (b) e anel de vedação (d)



*Figura E. 1. Configuração da tampa superior da AdC1.*

A Figura E.2., mostra a configuração interior da AdC1, nela é possível observar o sensor de temperatura colocado no eixo da AdC1. A ponta do sensor também foi posicionado no centro com relação à altura da coluna. A relação H<sub>B</sub>/D<sub>B</sub> é igual a 2.49.



*Figura E. 2. Configuração interna da AdC1.*

## E.2 Desmontagem da tampa da AdC1 e farelo de aveia após processo pseudocontínuo



*Figura E. 3. Desmontagem da tampa superior da AdC1.*

Na Figura E.3., mostra-se a desmontagem da tampa superior da AdC1. Na letra (a), observa-se a utilização de duas chaves de boca, na letra (b) foi utilizada uma espátula para ajudar a levantar levemente a tampa, na letra (c) foi utilizado um pincel para limpar a superfície em contato com o farelo e na letra (d) foi verificado a limpeza nas bordas internas da tampa.



*Figura E. 4. Massa de farelo de aveia após processo pseudocontínuo.*

Na Figura E.4. mostra-se a massa de farelo de aveia após processo pseudocontínuo posicionada no topo da AdC1 (Fig. E.4a), o farelo de aveia sem mudança de cor (Fig. E.4b) foi retirada utilizando uma espátula. Após observar mudança de cor no farelo (Fig. E.4c), a pesagem da massa foi realizada. Com isso foi calculada a eficiência de adsorção do farelo expressado em kg extrato adsorvido/ 100 kg de farelo de aveia.

### E.3 Extrato adsorvido no farelo de aveia e mistura das frações de farelo de aveia

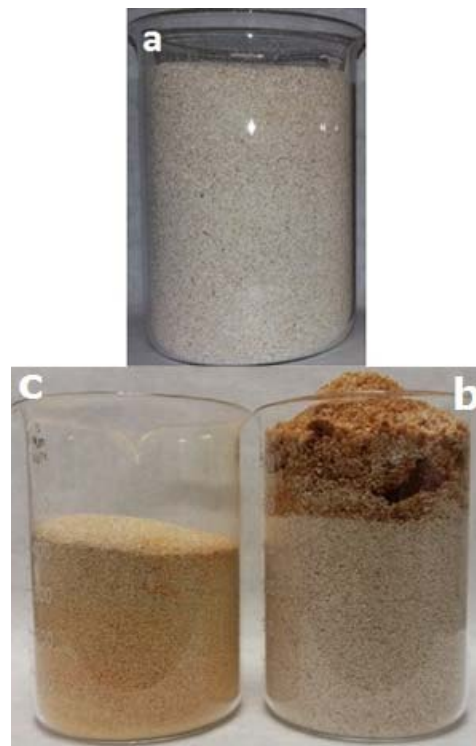


*Figura E. 5. Extrato adsorvido no farelo de aveia.*

Na Figura E.5., observa-se o extrato adsorvido junto à mudança de cor no farelo de aveia utilizada no processamento de urucum. Farelo inicial (a) e farelo após o processo retirado da AdC1 (b) e da AdC2 (c).



*Figura E. 6. Farelo de aveia após misturar as frações pertencentes a cada AdC.*

A Figura E.6., mostra-se o farelo de aveia homogeneizado (mistura de ambas frações com e sem mudança de cor para o caso da AdC1). As letras “A” e “B” mostram o farelo de aveia após processamento pseudocontínuo do urucum das AdC1 e AdC2, respectivamente.

**E.4 Extrato à saída da AdC2 durante a despressurização das C1 e C2 e coluna de adsorção 2 (AdC2) com e sem farelo de aveia**

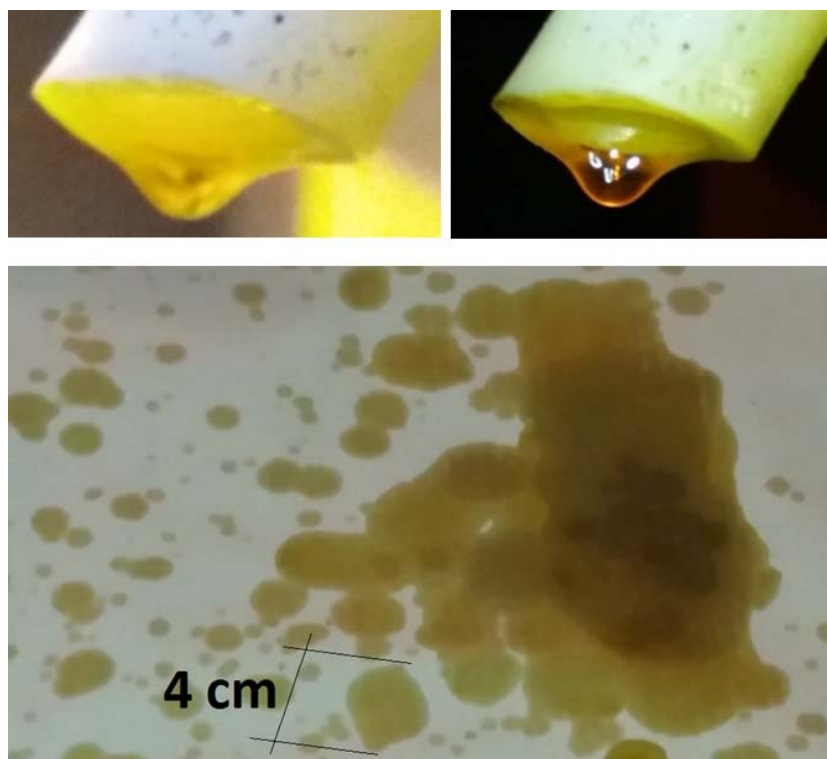


*Figura E. 7. Extrato após o passo pela AdC2 durante a despressurização de C1 e C2.*

A Figura E.7., mostra o extrato de urucum à saída da AdC2 durante a despressurização da coluna de extração (1 e 2) no desenvolvimento do processamento pseudocontínuo.



*Figura E. 8. Coluna de adsorção 2.*

A Figura E.8. se mostra a coluna de adsorção 2 (AdC2). Em (a), mostra-se o posicionamento das ferramentas para o ajuste ou desajuste da tampa da base da coluna, em (b) mostra-se a coluna carregada com o farelo de aveia.

### E.5 Válvula de purga do Tanque pulmão



*Figura E. 9. Válvula de purga do TP.*

A Figura E.9. se mostra a válvula de purga conectada na base do tanque pulmão, a mesma que é utilizada para o controle e verificação da aparente pureza de CO<sub>2</sub> durante e ao término do processo.

### E.6 Limpeza das válvulas backpressure



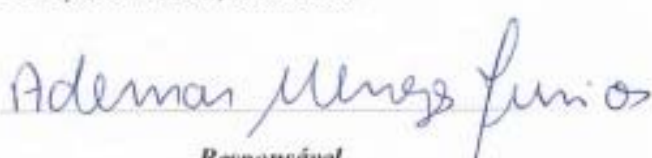
*Figura E. 10. Limpeza das válvulas backpressure.*

A Figura E.10., mostra que o conteúdo de cada beker vai se tornando cada vez mais claro sinalizando o final da limpeza das partes internas das válvulas backpressure. Essa atividade é repetida todas as vezes ao finalizar cada processo. Quando projetada o processamento com uma diferente matéria-prima, o equipamento em conjunto é submetido a duas extrações com o intuito de habituar as partes internas do equipamento em contato com a nova matéria-prima.

*Anexos*

## ANEXO A

### A.1 Laudo Técnico - Cúrcuma moída.

		<b>Sítio da Mata</b> <b>Laudo Técnico</b> <small>Rodovia Cajuru   Cassia dos Coqueiros   Fone/Fax: (16) 2133.4466 Nº Inscr. Prod.: 024.308.176</small>	
<b>Produto:</b>	<b>Cúrcuma - Pó</b>	<b>-CURCUMA RIZOMA PO</b>	
<b>Nome Científico 1:</b> Curcuma longa L. <b>Nome Científico 2:</b> <b>Família:</b> Zingiberaceae <b>Origem (país):</b> Brasil <b>Parte Utilizada</b> Rizomas <b>Características Macro e/ou Microscópicas:</b> Planta herbácea, aromática de folhas grandes. Flores amareladas, pequenas dispostas em espiga comprida. As raízes terminam em rizomas, quando cortadas mostram cor vermelho alaranjada. Cheiro forte agradável e sabor aromático e picante.			
<b>Referência Bibliog.:</b> T. de Fitomedicina, pg. 439 e Farmacopéia dos E. U. do Br., 1ª Ed., pg. 1037			
<b>Lote</b>	CUR111116SDM	<b>Cor:</b> Laranja	
<b>Colheita:</b>	11/11/2016	<b>Validade:</b>	11/11/2019
<b>Descontaminação:</b>	Congelamento por 10 dias		
<b>Mét. de Secagem:</b>	À sombra		
<b>Umidade:</b>	8%		
<b>Odor e Sabor:</b>	Característico da Planta		
<b>Obs.:</b>	Por se tratar de insumo de origem vegetal, poderão ocorrer leves variações em sua cor, odor e sabor.		
 <b>Responsável</b> Ademar Menezes Jr. Ademar Menezes Junior - CREA: 5060000803 Eng. Agrônomo - (16) 2133.4455			

## ANEXO B

### B.1 Determinação da densidade por picnometria de gás hélio - Urucum e Cúrcuma.



Central Analítica - Instituto de Química - UNICAMP

**CA 163/17**

### **RESULTADO DE ANÁLISE CA 163/17**

<b>Empresa</b>	Fundação de Amparo à Pesquisa do Estado de São Paulo
<b>Endereço</b>	Rua Pio XI, 1500 - Alto da Lapa CEP: 05468-901 - São Paulo/SP
<b>A/C</b>	Ricardo Abel Del Castillo Torres
<b>E-mail</b>	<a href="mailto:delcastilloabel@hotmail.com">delcastilloabel@hotmail.com</a>
<b>Telefone</b>	(19) 9-9689-8807

#### **1. OBJETIVO**

Determinação da densidade por picnometria de gás hélio.

#### **2. AMOSTRAS**

As amostras foram recebidas em 12 de Abril de 2017 a temperatura ambiente. A amostragem foi de responsabilidade do cliente e as identificações das amostras estão apresentadas na Tabela 1.

Tabela 1 - Legenda de identificações das amostras.

Central Analítica	Cliente
AM 0776/17	Sementes de urucum
AM 0777/17	Cúrcuma moída

#### **3. MÉTODO DE ANÁLISE**

As amostras foram analisadas em picnômetro de gás hélio conforme manual de operação do equipamento.

Equipamento: Picnômetro automático Quantachrome Ultrapyc 1200e.

#### **4. RESULTADOS**

Os resultados obtidos estão resumidos na Tabela 2.

Tabela 2 - Resultado obtido na análise.

Amostras	Densidade (g/cm <sup>3</sup> ) <sup>1</sup>
Sementes de urucum	1,35 ( $\pm$ 0,01)
Cúrcuma moída	1,46 ( $\pm$ 0,01)

<sup>1</sup> Resultados expressos como média e estimativa do desvio padrão de dez determinações.



**Obs.1:** Os resultados referem-se exclusivamente à análise em amostras entregues pelo cliente à Central Analítica - IQ/UNICAMP.

**Obs.2:** Fica o cliente notificado que o uso do nome do Instituto de Química da UNICAMP e a reprodução deste resultado de análise somente podem ser feitos sob prévia autorização.

**Obs.3:** O conteúdo e as conclusões aqui apresentadas são de responsabilidade exclusiva do(s) autor(es) e não representam a opinião da Universidade Estadual de Campinas nem a compromete.

Campinas 27 de Abril de 2017.

A handwritten signature in blue ink that reads "Sabrina Barboza Rosa".

Assinado de forma digital por Sabrina Barboza Rosa  
Dados: 2017.04.27 15:44:22 -03'00'

Sabrina Barboza Rosa  
Química Responsável - Signatária Autorizada  
CRQ: 04263563 - 4<sup>a</sup> Região

Central Analítica  
Universidade Estadual de Campinas  
Instituto de Química - CP 6154 - 13084-971 - Campinas, SP  
Fone: (019) 3521-0219  
E-mail: ca@iqm.unicamp.br

B.2 Determinação da densidade por picnometria de gás hélio – Farelo de aveia.



Central Analítica - Instituto de Química - UNICAMP

CA 371/17

## RESULTADO DE ANÁLISE CA 371/17

**Empresa** FEA - Faculdade de Engenharia de Alimentos - UNICAMP

**Endereço** Rua Monteiro Lobato, 80 - Barão Geraldo  
CEP: 13083-862 - Campinas/SP

**A/C** Ricardo Abel Del Castillo Torres

**E-mail** [delcastilloabel@hotmail.com](mailto:delcastilloabel@hotmail.com)

**Telefone** (19) 3521-0100

### 1. OBJETIVO

Determinação da densidade por picnometria de gás hélio.

### 2. AMOSTRAS

As amostras foram recebidas em 24 de Julho de 2017 a temperatura ambiente. A amostragem foi de responsabilidade do cliente e as identificações das amostras estão apresentadas na Tabela 1.

Tabela 1 - Legenda de identificações das amostras.

Central Analítica	Cliente
AM 1733/17	Pérola de Vidro -24/07/2017
AM 1734/17	Farelo De Aveia

### 3. MÉTODO DE ANÁLISE

As amostras foram analisadas em picnômetro de gás hélio conforme manual de operação do equipamento.

Equipamento: Picnômetro automático Quantachrome Ultrapyc 1200e.

### 4. RESULTADOS

Os resultados obtidos estão resumidos na Tabela 2.

Tabela 2 - Resultados obtidos nas análises.

Amostras	Densidade (g/cm <sup>3</sup> ) <sup>1</sup>
Pérola de Vidro - 24/07/2017	2,50 ( $\pm$ 0,01)
Farelo De Aveia	1,35 ( $\pm$ 0,01)

<sup>1</sup> Resultados expressos como média e estimativa do desvio padrão de dez determinações.



**Obs.1:** Os resultados referem-se exclusivamente à análise em amostras entregues pelo cliente à Central Analítica - IQ/UNICAMP.

**Obs.2:** Fica o cliente notificado que o uso do nome do Instituto de Química da UNICAMP e a reprodução deste resultado de análise somente podem ser feitos sob prévia autorização.

**Obs.3:** O conteúdo e as conclusões aqui apresentadas são de responsabilidade exclusiva do(s) autor(es) e não representam a opinião da Universidade Estadual de Campinas nem a compromete.

Campinas 09 de Agosto de 2017.

A handwritten signature in black ink, appearing to read "Ana Rosa" or "Sabrina Barboza Rosa".

Sabrina Barboza Rosa  
Química Responsável - Signatária Autorizada  
CRQ: 04263563 - 4ª Região

Assinado de forma digital por  
Sabrina Barboza Rosa  
Dados: 2017.08.09 16:10:43 -03'00'

Central Analítica  
Universidade Estadual de Campinas  
Instituto de Química - CP 6154 - 13084-971 - Campinas, SP  
Fone: (019) 3521-0219  
E-mail: ca@iqm.unicamp.br